THE STRATIGRAPHY AND EMPLACEMENT OF THE ANTRIM LAVA GROUP, NORTHERN IRELAND

by

ADAM BERESFORD-BROWNE

A thesis submitted to the University of
Birmingham for the degree of
DOCTOR OF PHILOSOPHY

School of Geography, Earth & Environmental Sciences
College of Life and Environmental Sciences
University of Birmingham
December 2023

For my Mum, Francesca, who raised me to believe that anything is possible if you are prepared to work for it

ACKNOWLEDGEMENTS

Huge thanks to the tax-paying public of the UK for allowing UKRI, NERC, CENTA and BGS to fund and support this research.

I want to thank my internal supervisors, Dr Carl Stevenson and Dr Sebastian Watt for conceiving the project and working with me to get the necessary funding. Thanks also to Carl for his tireless enthusiasm for my research, calm advice, boundless encouragement and inevitable hand-holding during the tough times; and to Seb for his ability to get to the heart of an issue and help me see things from multiple sides (rather than just the obvious or easy one!).

To my external supervisor, Dr Rob Raine, I can only say thank you for your patience, understanding, accommodation and insightful sharing of your considerable knowledge of the geology of Antrim and all the work that has ever been carried out on those rocks! Our time spent in the core stores of Belfast or the Antrim countryside are some of the fondest memories I hold from this research.

To Professor David Jolley I owe a huge debt of gratitude. He enthusiastically engaged with my research after I discovered the fluvial interbed at Ross's Quarry, and put his time, energy, and research money into uncovering the palynological information locked away in those, and other, Antrim sediments. Without David's palynological expertise and enthusiasm for more samples, this would have been a much shorter thesis and all the poorer for it. A true mentor and friend, thank you. I hope that this is only the start of our journey.

ACKNOWLEDGEMENTS

To Dr Elliott Carter, here's to a cracking bit of shared fieldwork and huge respect to you for all of the laboratory work you undertook during the trying COVID times to get the WD-XRF results. Our next paper awaits!

Dr Mike Simms has been a stalwart friend and fieldwork companion. His fresh viewpoint and willingness to discuss abstract concepts in the field gave me the support and headspace I really needed.

A huge cheers to Dr Dougal Jerram for being a sound voice of geological reason when I got lost in the academia of it all. His knowledge of igneous processes and volcanicity always shed new light on the problems with which I was wrestling.

Thanks to Dr John Millett for his patience and guidance with all matters geochemical, WellCAD™ and geophysical. A selfless gentleman who always tried to make time for me even when under the combined pressures of work deadlines and new baby. Thank you, sir!

Thanks to the kind assistance of Mr Gordon Best, Regional Director of the Mineral Products Association (Northern Ireland) Ltd., all 9 quarry operators agreed to permit access. Mr Russell Drew, the contact at Whitemountain Quarry, offered access to Cam and Blackmountain Quarries, bringing the number of planned quarry visits to 11. During fieldwork in Northern Ireland, Mr John McReynolds of Croaghan Quarry invited me to visit the nearby quarry at Macosquin giving a final total of 12 quarries to visit.

ACKNOWLEDGEMENTS

Love and thanks to Dr Tim Cunningham, Amy Kelly, Sidonie Beresford-Browne and all my friends for their love, kindness, early morning coffee chats and late night music sessions over the past four years.

TABLE OF CONTENTS

TABLE OF CONTENTS

TABLE OF CONTENTS

TABLE OF CONTENTS

LIST OF FIGURES

LIST OF FIGURES

LIST OF FIGURES

LIST OF TABLES

LIST OF TABLES

FOREWORD

As a professional geologist with two decades of international experience behind me, I had some preconceptions about how large igneous provinces are formed. Specifically, I had imagined them to consist of unimaginably spectacular and widespread volcanic activity continuing over significant lengths of time.

When I started reading around the subject of Antrim Lava Group and the North Atlantic Igneous Province, I found myself imagining the peaceful rolling chalk hills of early Paleogene Ireland venting steam, being ripped apart, yielding to a wildly dangerous, volcanic landscape full of burning vegetation and smoke, with glowing fountains of basaltic rock and rivers of lava as far as the eye can see. These first impressions were based on an initial understanding of the two, long periods of volcanic emplacement responsible for the Lower and Upper Basalt Formations, separated in time by a long period of peace and quiet in subtropical conditions, represented in the geological record as the Interbasaltic Formation.

This model persisted until well into the first year of my research, when it started to become evident that much of the time represented within the Antrim Lava Group was locked away among the palaeosols, boles, laterites and other interbeds located between lava flows. It also became clear that the single, long period of 'interbasaltic' quiescence that I had read about was instead full of volcanic activity, with flood basalt effusions, intermediate magma intrusions, and acid lava surface volcanoes with clouds of ash and tuff spewing from classic, explosive volcanism.

Some time was spent investigating the 'minor' flood basalt events in recent history, specifically those around 934 AD and 1783 AD, located respectively at Eldgjá and Laki

in Iceland. These provided some insight into the rate of lava production that can occur from fissure effusion volcanism. Based on upper estimates of the volume of the Antrim Lava Group, extrapolation of these effusion rates suggested that it could have been possible to erupt all of the component basaltic lavas in under 1300 years, possibly even as little as 40 years! Obviously, from all of the dating work already done, we know that the Antrim Lava Group formed over several million years so this was another strong piece of (admittedly anecdotal) evidence that for most of the time, there were no volcanic eruptions taking place. Quite different to the imagined scene of persistent hellfire and smoke borne from initial reading.

I started reading around the area of research before enrolling at the University of Birmingham, but it wasn't until I started that I finished formulating the plan of how to execute the investigation. After reviewing the available data and research tools at my disposal I created the research plan, and the details of the methods employed are explained in **Chapter 2**.

Like many other workers before, examination of the stratigraphy of the Antrim Lava Group was focused on looking for what separated the component igneous units so we could easily distinguish between them at outcrop, in borehole core, by geochemical data, etc. Near the conclusion of my research, I came to realise that this mindset had blinkered me to the implications of accepting that the igneous units were more alike than they were different, essentially only differing geochemically due to the location and temperature of the source melt zone(s), the time spent between their source melt zone(s) and the surface, and the cooling situation in which they found themselves once

at the surface. The key part of this was the assimilation of continental crust and residence time encouraging the processes of fractional crystallisation and magmatic evolution, which most notably led to the very different geochemistry of the Causeway Tholeiite Member basalts (some of which are basaltic andesite) when compared to lavas of the Lower and Upper Basalt Formations. Thanks to the borehole core and data generated by Lonmin (NI) Plc and curated by GSNI, I was able to examine near-complete sequences of the Antrim Lava Group basalt flows by their geochemistry; a first in the history of research in this field. My findings from geochemical investigations, greatly assisted by collaborations with Dr Elliot Carter and Dr John Millett, are presented in **Chapter 3**.

In close collaboration with Professor David Jolley, we were able to examine the palynology of many interbeds located between the basalt flows of the Antrim Lava Group, and thereby gain insights into the ecology, environment and climate that developed during these periods of volcanic quiescence. We confirmed that hiatuses of reasonable length occurred before and after the emplacement of the Causeway Tholeiite Member, recorded by the presence of interbasaltic sedimentary units that were found, examined and sampled at outcrop in Ross's Quarry near Ballycastle, County Antrim. On this topic, we submitted a paper for the Geological Society of London special publication 547, edited for this thesis and presented here as **Chapter 4**.

From the outset, I had issues with some of the stratigraphic nomenclature of the Antrim Lava Group. I did not agree with using the word 'basalt' in the Upper and Lower Basalt Formations, nor did I approve the use of the word 'tholeiite' in the Causeway

Tholeiite Member. As my work continued, and I came to realise that the Interbasaltic Formation was, for the most part, composed of basalts and their derivatives, I began to have a real problem with the phrase 'Interbasaltic Formation'. Originally correctly applied to describe the weathered lithologies of economic interest that were literally between basalt flows, it somehow evolved to become the blanket term for a wide variety of lithologies that were effused, erupted, emplaced, eroded, weathered, deposited or otherwise formed over a significant swath of geological time. I share my thoughts on this as topically relevant in **Chapters 5, 6 and 7**.

The need to constrain the tempo of volcanic activity was addressed by a number of methods, including examination of weathered flow tops in previously unexamined borehole cores, review of age dating data of NAIP rocks, and flow volumes from modern corollaries. The work and findings are presented in **Chapter 5**.

Continuing on from the work on modern corollaries in Chapter 5, **Chapter 6** takes a closer look at how the recent volcanic activity of Iceland might provide significant clues as to the processes involved during the emplacement of the Antrim Lava Group.

In carrying out this research I hope to have contributed positively to the understanding of the Antrim Lava Group stratigraphy and emplacement, as well as adding to the knowledge of the British & Irish Paleogene Igneous (sub)Province and the wider North Atlantic Igneous Province. The summary discussion and concluding section of my research thesis are contained within **Chapter 7**.

CHAPTER 1 – INTRODUCTION

1.1 Synopsis

This thesis presents the work undertaken between October 2019 and December 2023 by Adam Beresford-Browne at the University of Birmingham, funded by the National Environment Research Council (NERC) Doctoral Training Programme, CENTA. The main aim of the research was to examine the stratigraphic relationships and emplacement timing and mechanisms of the igneous and sedimentary rocks of the Antrim Lava Group (ALG) in Northern Ireland, one component of the British & Irish Paleogene Igneous Province (BIPIP) which locally represents a sub-province of the much larger North Atlantic Igneous Province (NAIP). The NAIP was primarily active during the Paleocene and Eocene epochs of the Paleogene period, from the start of the Danian age (c.66 Ma), through the Selandian and Thanetian ages, to the end of the Ypresian age (c.48 Ma).

The research primarily focused on examining geological and geochemical data from ALG borehole core samples held at the Geological Survey of Northern Ireland (GSNI) in Belfast, Northern Ireland. Additionally, palynological sampling and analysis of the interbeds between the basalt lava flows provided key information on the contemporaneous climate and ecology of the ALG, and enabled evaluation of the timespan between successive flood basalt events.

Palynological samples revealed new information about the palaeoenvironment showing that the climate was more temperate than previously thought. This has led to new understandings in this work about the traditionally accepted evolution of ‘laterite’ in the ALG. Namely, these interbeds have more diverse origins, including weathered

basalt horizons and sedimentary deposits (fluvial, lacustrine, bogland). Volcanostratigraphic analysis using outcrop facies and geochemistry has shown a number of significant differences in the ALG to the north and south of the Tow Valley Fault, including the absence of the Causeway Tholeiite Member to the south of the fault. This is consistent with a model of syn-tectonic emplacement of the ALG. This research also looks to modern equivalents, specifically the recent flood basalt eruptions of Iceland, as a potential corollary to the ALG, in order to improve our understanding of emplacement mechanisms and the volcanic tempo of the ALG.

1.2 Research project outline

This chapter first presents the overall rationale behind the project, including the aims, objectives and thesis structure, before going on to present the geological background to the study region.

2.1 Research aims and objectives

The key aim of this research is to take advantage of a unique set of borehole data from the Antrim Lava Group (ALG), alongside a range of geochemical, stratigraphic, and environmental observations, to reinvestigate the stratigraphy, emplacement mechanisms and volcanic timing of the Antrim Lava Group, a well-preserved episode within the North Atlantic Igneous Province (NAIP).

The same is achieved through the following objectives:

- A detailed stratigraphic investigation based on geology, geochemistry, and palynology;

- Estimate tempo of eruption rate based on basaltic weathering profiles;
- Examine syn-tectonic emplacement timings through detailed volcanostratigraphic correlations across key tectonic structures; and
- Determine palaeoenvironmental setting during ALG emplacement.

The stratigraphic information used to achieve the research aims was found in Lonmin (NI) Plc borehole data and at field exposures. From these, samples were taken to study the geochemistry and palynology. Geochemical profiles were analysed and used alongside lithological logs and logs from key exposed sections to define a new stratigraphy. The temporal information held within the weathered horizons (which represent hiatuses) in this work provided the basis for estimating the tempo of ALG volcanism. This was done by comparing the timing of loosely comparative basaltic traps that have been active in human history, giving access to anecdotal and temporal constraints.

Following the regional stratigraphic work, detailed volcanostratigraphic analysis uses a combination of outcrop facies and geochemical signatures to provide better correlations across the ALG.

1.3 Research context: Large Igneous Provinces

Locked in the geological past of planet Earth lies evidence of volcanic episodes that seem so much larger, more catastrophic and longer-lasting than anything humankind has experienced that they are initially hard to comprehend. These massive emplacements of volcanic and plutonic rock, evidence of which can be found all over the world, are termed Large Igneous Provinces (LIPs; Coffin & Eldholm, 1991). Although

many types of LIP have been identified, they often comprise thousands of cubic kilometres of relatively fluid, basaltic lavas that flowed from numerous fissures and vents to bury valleys and lowlands under kilometres of volcanic rock. Unsurprisingly, LIPs have been connected to several of the planet's mass extinctions, notably the Emeishan flood basalts with the end-Guadalupian extinction (~259 Ma), the Siberian Traps with the end-Permian extinction (~252 Ma), and the Central Atlantic Magmatic Province with the end-Triassic extinction (~201 Ma) (Green et al., 2022; Wignall, 2001; Ernst & Youbi, 2017). However, the link between flood basalts and mass extinctions remains a topic of debate (Green et al., 2022; Henehan & Witts, 2023).

1.3.1. LIP Distribution

Large igneous provinces (LIPs) are massive emplacements of volcanic and plutonic rock that are found all over the Earth (Figure 1.1; Bryan & Ferrari, 2013) and have been recognised on the Earth's moon and planet Mercury (Taylor & McLennan, 2005).

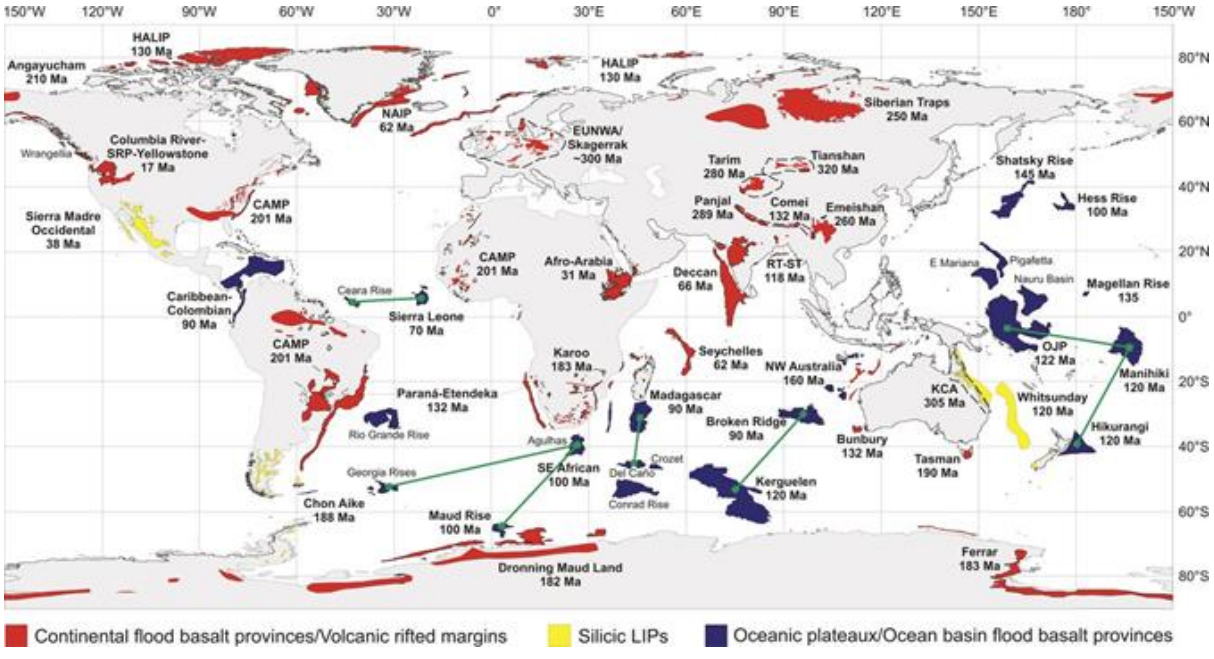

Figure 1.1 Global distribution of large igneous provinces (LIPs) since c. 320 Ma (Bryan & Ferrari, 2013).

Table 1.1 Large igneous provinces (LIPs) with suggested hotspot links (Bryan & Ferrari, 2013).

Province	Region	Hotspot
Columbia River Basalt	Northwestern USA	Yellowstone hotspot
Ethiopia-Yemen Flood Basalts	Ethiopia, Yemen	*Not identified*
North Atlantic Igneous Province	Northern Canada, Greenland, the Faeroe Islands, Norway, Ireland and Scotland	Iceland hotspot
Deccan Traps	India	Réunion hotspot
Rajmahal Traps	Eastern India	Ninety East Ridge
Kerguelen Plateau	Indian Ocean	Kerguelen hotspot
Ontong-Java Plateau	Pacific Ocean	Louisville hotspot
Paraná and Etendeka traps	Brazil–Namibia	Tristan hotspot
Karoo-Ferrar Province	South Africa, Antarctica, Australia & New Zealand	Marion Island
Caribbean large igneous province	Caribbean-Colombian oceanic plateau	Galápagos hotspot
Mackenzie Large Igneous Province	Canadian Shield	Mackenzie hotspot

The generally accepted theory regarding terrestrial LIPs is that they result from the arrival of a mantle plume under the lithosphere, which spreads out after impact and causes significant partial melting of the upper mantle and lower lithosphere primarily by the two key mechanisms of temperature increase or pressure decrease. The arrival of a mantle plume is accompanied by thermal and mechanical uplift. Often, there follows a period of extreme flood volcanics that can persist for several million years. A summary of LIP data is presented in Tables 1.1 and 1.2.

Table 1.2 Age, duration and volume of selected large igneous provinces (LIPs) (Bryan & Ferrari, 2013).

Name	Location	Age start (Ma)	Age end (Ma)	Area (km^2)	Max thickness (km)	Estimated volume (km^3)
Columbia River Basalts	America	17	14	163,700	1.8	174,300
Ethiopia-Yemen	Africa	31	25	600,000	*uncertain*	350,000

NAIP	North Atlantic	62	54	1,300,000	*uncertain*	6,600,000
Antrim Lava Group	NAIP	62	58	4,000	0.8	1,280
Deccan Traps	India	66.25	65	500,000	2.0	1,000,000
Siberian Traps	North Asia	252	250	2,000,000	2.0	4,000,000
Emeishan Traps	China	265	259	250,000	5.5	300,000

1.3.2 Continental Flood Basalts

At the inception of Continental Flood Basalt Provinces (CFBP) volcanism, relatively low-volume transitional-alkaline eruptions forcibly erupt into exposed cratonic basement lithologies, sediments, and in some cases, water. Distribution of initial volcanism is strongly controlled by the arrangement of pre-existing topography, the presence of water bodies and local sedimentary systems, but is primarily controlled by existing lithospheric and crustal weaknesses and concurrent regional stress patterns. (Jerram & Widdowson, 2005).

The main phase of volcanism is typically characterised by a culmination of repeated episodes of large-volume tholeiitic flows that predominantly generate large tabular flows and flow fields from several spatially restricted eruption sites and fissures. These tabular flows build a thick lava flow stratigraphy in a relatively short period (c. 1–5 My) (Jerram & Widdowson, 2005). See Figure 1.1 for locations of key examples.

1.4 The North Atlantic Igneous Province

The birth of the North Atlantic Ocean is connected to an LIP event, which took place in the early Paleogene period (Wilkinson et al., 2017), between c. 70 and 50 million years

ago (Ma). Before its birth, the embryonic North Atlantic existed as an epeiric sea in the Rockall Trough between the landmasses of what we know as Rockall Bank and the UK (Nielsen et al., 2007, Figure 1.2). Recorded in the geological history of Baffin Island, Greenland, Faroe Islands, Ireland and Scotland by thousands of metres of volcanic rock, this regional LIP is known as the North Atlantic Igneous Province (NAIP), adding an estimated 6.6 million km^3 of material to the crust and extruding approximately 1.8 million km^3 of basaltic rock (Eldholm & Grue, 1994) with associated differentiates and anatectic melts (Saunders et al., 1997). The volcanic and tectonic onset of the NAIP was heralded by rifting and the emplacement of numerous dyke swarms. Long before the North Atlantic started opening (~55 Ma) there were significant episodes of effusive volcanism from 61.5 Ma (Cooper et al, 2021), possibly earlier. Eruptions of flood basalts from fissures and vents occurred in Greenland, Ireland and Scotland around this time; the exact sequence of events is still being pieced together. The key sub-provinces of the NAIP are Greenland (East Greenland, West Greenland), Faroes, Northern Ireland (Antrim), Scottish/Hebridean Islands (primarily Skye, Mull, Arran). These have been extensively researched, from Greenland (e.g. Larsen at al., 1998; Brooks, 2011) through the Faroe Islands (e.g. Søager & Holm, 2009; Jolley et al., 2021) and Ireland (e.g. Patterson & Mitchell, 1955; Walker, 1959; Old, 1975) over to Scotland (e.g. Ridley, 1971; Morrison, 1978; Ganerød et al., 2008). Spanning an area of approximately 1.3 million km^2, most of the remaining, younger basalts of the NAIP now lie under the deep waters of the North Atlantic (Figure 1.3).

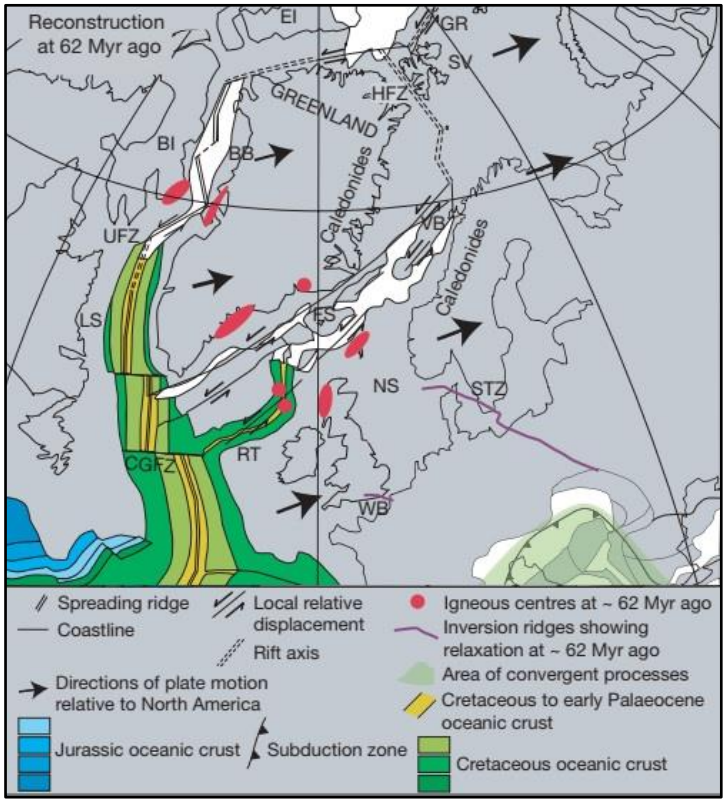

Figure 1.2. Modified reproduction of Figure 1 from Neilson et al., 2007, showing the palaeogeographic setting of the wider research area c. 62 Ma. BB, Baffin Bay; BI, Baffin Island; CGFZ, Charlie–Gibbs fracture zone; EI, Ellesmere Island; FS, Faroe–Shetland trough; GR, future Gakkel rift; HFZ, Hornsund fault zone; LS, Labrador Sea; NS, North Sea basin; VB, Vøring basin; RT, Rockall trough; SV, Svalbard; UFZ, Ungava fault zone; WB, Weald–Boulonnais area.

A significant proportion of NAIP rocks remain above sea level on the North American and European continents (Figures 1.2 and 1.3) in the following major subprovinces:

- Canada
- Greenland
- Faroe Islands
- Ireland (Northern Ireland)
- Scotland (Hebrides)

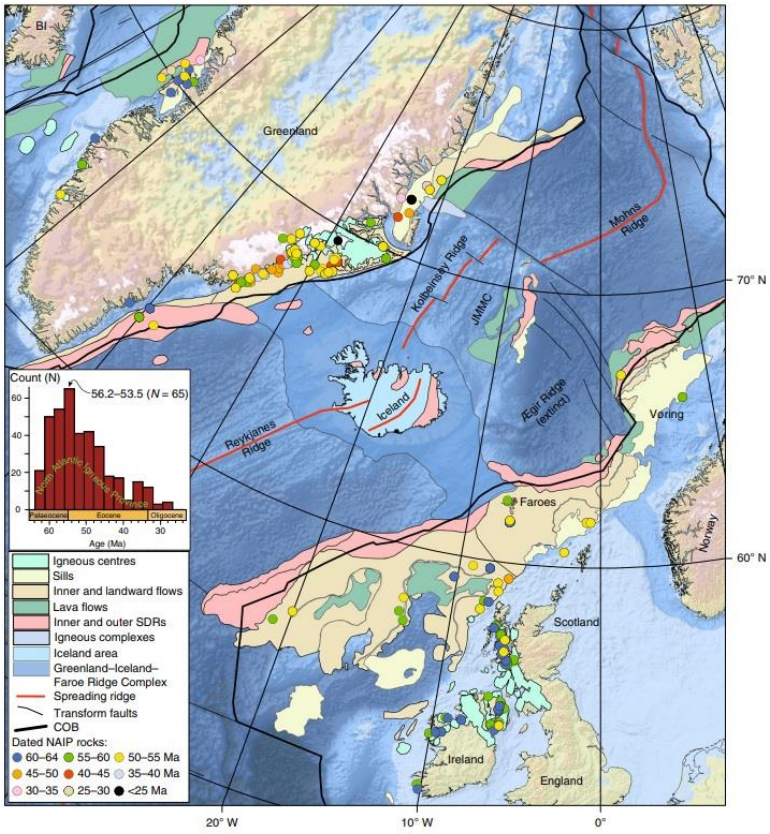

Figure 1.3. Direct reproduction of Figure 1 from Steinberger et al. (2019) showing the geology and modern extent of the North Atlantic Igneous Province (NAIP). Note the vast proportion of NAIP igneous rocks lie submerged off the continental shelves of the European and North American plates.

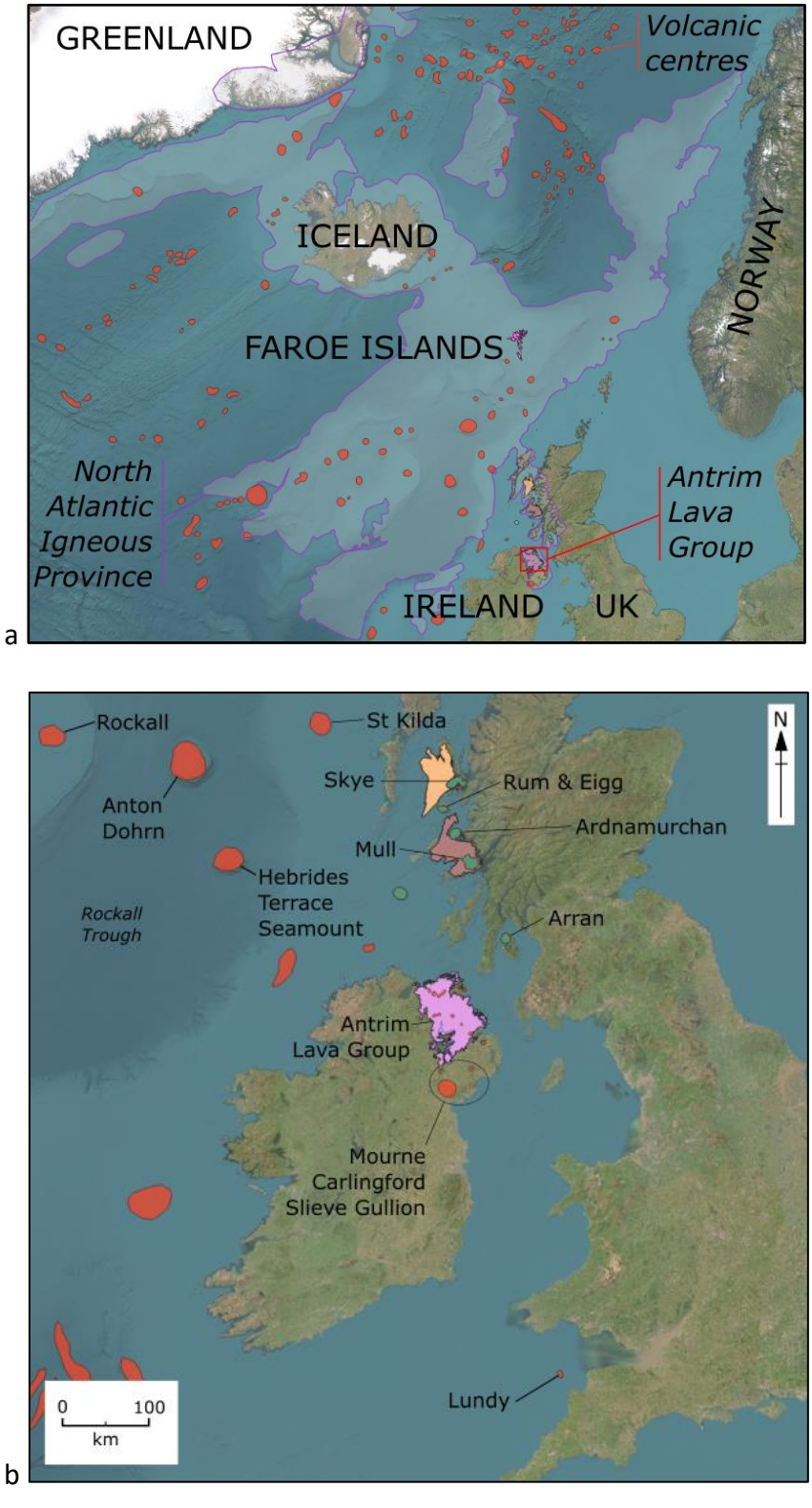

Figure 1.4. (a) outline of the NAIP showing ALG setting. Red polygons indicate volcanic centres (á Horni et al., 2017).

(b) Relevant sub-provinces of the North Atlantic Igneous Province. Green and red polygons indicate NAIP

igneous/volcanic centres (á Horni et al., 2017). The lava fields of Antrim (pink), Mull (brown) and Skye (yellow) are also shown.

The volcanic sub-provinces of England, Ireland and Scotland are grouped together into the British & Irish Paleogene Igneous Province (BIPIP), which primarily comprise the following **lava fields** and *igneous centres/intrusive complexes* (or ***both***):

- Ireland / Northern Ireland
    - ***Antrim Lava Group***
    - *Mourne*
    - *Carlingford*
    - *Slieve Gullion*
- Scotland (Hebrides)
    - ***Mull***
    - ***Skye***
    - *Arran*
    - *Muck*
    - *Eigg*
    - *Ardnamurchan*
    - *Rum & Eigg*
    - *St. Kilda*
- Other
    - *Rockall* (Rockall Bank, UK)
    - *Anton Dohrn* (Rockall Trough, UK)
    - *Lundy* (Bristol Channel, UK)

As can be seen in Figure 1.4, there are significantly more igneous centres than those listed above, but these are outside the scope of this research. The specific body of work carried out on each of the sub-provinces of the NAIP varies from one location to the next, and only recently has there been interest in tying these threads into a cohesive story. While significant work has been carried out on the geochemistry of the Antrim Lava Group (ALG), more remains to be done to understand the volcanostratigraphy and emplacement timing of the ALG flood basalts of northeast Ireland, and that research forms the central theme of this work.

1.5 The Antrim Lava Group

This work will focus on the Antrim Lava Group (ALG), which is a group of Paleogene lithologies found in the counties of Antrim, Derry, Tyrone, Armagh and Down in Northern Ireland, UK (Figure 1.6). The ALG primarily consists of a variety of basaltic igneous rocks, with subdominant intermediate and acidic intrusions and lavas (Old, 1975; Lyle & Thompson, 1983; Lyle, 1985) interspersed with weathered lavas and ash tuffs, and a variety of sedimentary units and well-developed palaeosols (Cole, 1912; Eyles, 1952; Hill et al, 2000; Hill et al, 2001; Beresford-Browne et al, 2023).

The various lithologies of the ALG were emplaced or formed over several million years, thought to have begun with the development of the North Atlantic spreading margin in the Rockall Trough during the Danian age (c. 64 Ma; Figures 1.1 and 1.4; Wilkinson et al., 2017). This also heralded the onset of extrusive volcanic activity of the NAIP (Wilkinson et al., 2017; Jolley et al., 2021) which persisted until the mid-Ypresian age (c. 48 Ma) when NAIP flood basalt volcanic activity essentially ceased (Figure 1.5;

Wilkinson et al., 2017). The relevant section of the stratigraphic chart is presented in Figure 1.7.

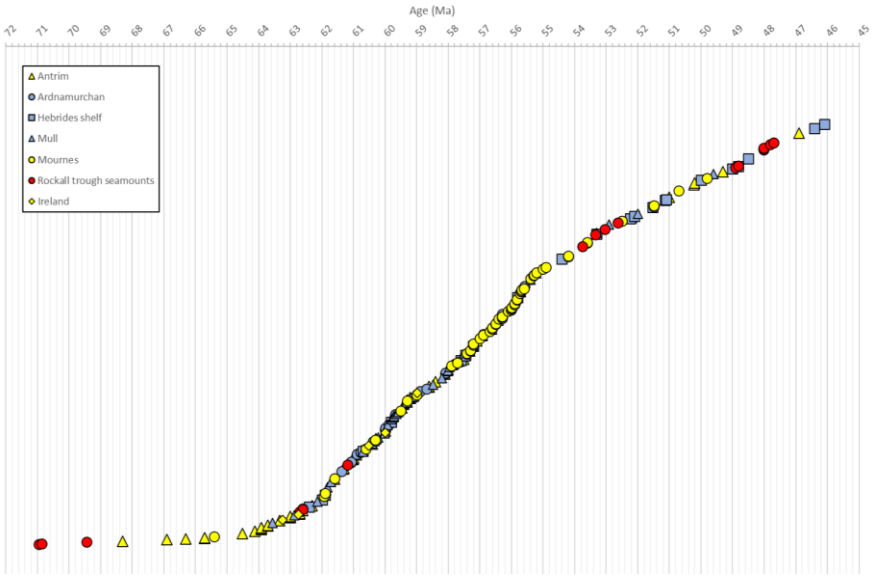

Figure 1.5. Data from Wilkinson et al., 2017 replotted to illustrate near-continual volcanic activity in the BIPIP from ~64 to 48 Ma.

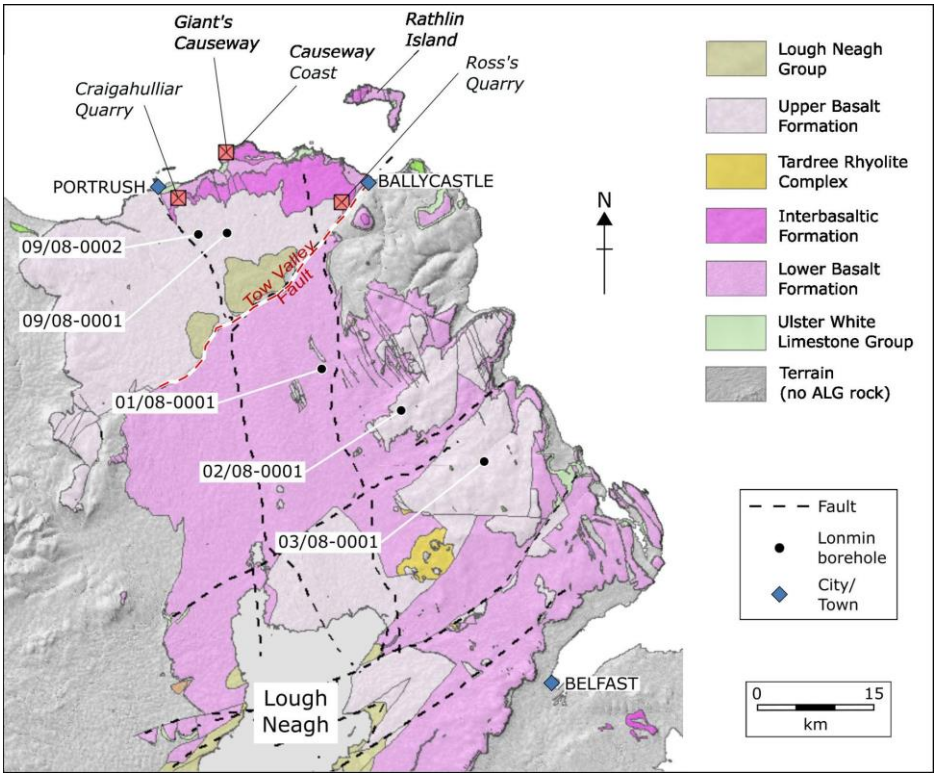

Figure 1.6. The Antrim Lava Group outcrop and research area (based on data from GSNI). Key locations and geological features are annotated. Some fault lines were interpreted by the author based on TELLUS data provided by GSNI.

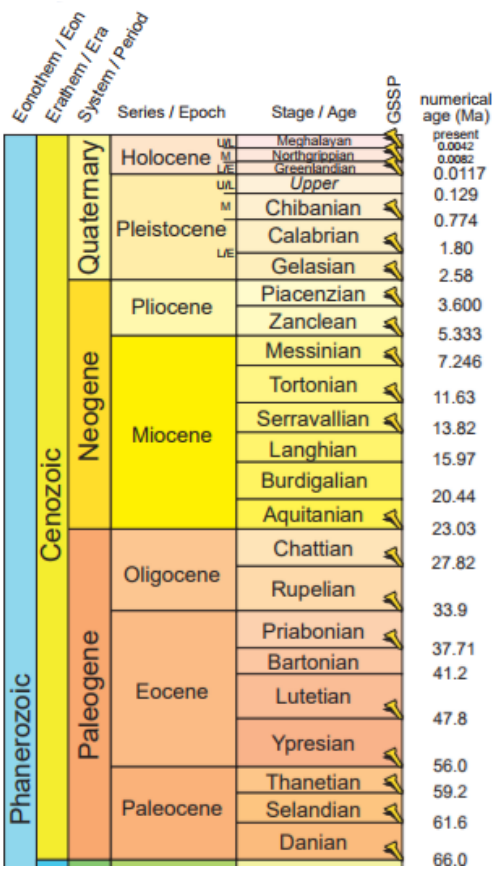

Figure 1.7. Direct reproduction of the chronostratigraphic chart detailing the Cenozoic era (credit: International Commission on Stratigraphy)

More recently, work to review the abundance and quality of dating work done on the NAIP including the ALG (Wilkinson et al., 2017) has revealed a more continuous sequence of LIP volcanism than previously understood, starting as early as 81 Ma in offshore Shetlands (c. 81-79 Ma, Fitch et al., 1988), 71 Ma in the Rockall Trough (O'Connor et al., 2000) and the central Eastern coast of Greenland (c. 71–67 Ma, Roddick, et al., 1989), 68.3 Ma in the BIPIP (Coleraine, Northern Ireland, Evans et al., 1973), and continuing up to c. 13.6 Ma (East Greenland, Storey et al., 2004). The

relevance and implications of this for the timing and emplacement of the Antrim Lava Group will be applied to discussions in later chapters.

Current thinking tells us that the pre-volcanic topography and landscape of the Antrim locality was mainly one of low relief hills formed of Cretaceous marine sedimentary units of the Ulster White Limestone Group (UWLG; Simms, 2000; Mitchell et al., 2004). In parts where the limestone had been eroded, or higher areas where it had not been deposited, the bedrock was pre-Paleogene (e.g. Dalradian metasedimentary units of shale and slate; Mitchell et al., 2004). Recent developments regarding the onset of BIPIP volcanic activity (Wilkinson et al., 2017) and palaeontological dating of the youngest formations of the UWLG (Hopson, 2005) both occurring in the mid- to late-Maastrichtian age suggest that the boundary between the deposition and diagenesis of some of the UWLG and the onset of NAIP volcanic activity may be more blurred and complex than previously understood. Future models for this period need to build in the combined, incompatible features of karst weathering features on the pre-volcanic UWLG landscape (Simms, 2000) alongside ocean acidification associated with the NAIP chemically affecting these marine sediments (Lindgreen et al., 2011), the development and remobilisation of the enigmatic 'Clay with Flints' unit (Patterson & Mitchell, 1955; Mitchell et al., 2004; Cooper et al., 2017), and the volcanic shattering of UWLG rocks in Whiterocks, Antrim, Northern Ireland (Mitchell et al., 2004). A detailed examination of this falls outside the scope of this research but suitable attention will be paid in later chapters where appropriate.

1.6 The Antrim Plateau and the topography of the ALG

The extant Paleogene lavas and associated rocks of the ALG form a physiogeographical feature in Northern Ireland called the Antrim Plateau. The plateau is resplendent with spectacular cliffs and escarpments around much of the perimeter, and predominantly low-lying featureless land towards the centre. Approximately rectangular in its 3,940 km^2 extent, elongate along the north-south axis and rotated ~35° anticlockwise from north, the elevation of the Antrim Plateau falls from the edges towards the interior (Figure 1.8) from ~390 mASL in the northwest to less than 15 mASL down the central axis (Bann River), to as much as 540-550 mASL in the east (the topographic highs of Slievenanee and Trostan).

The notably flat stretch of land down the central north-south axis of the Antrim Plateau is due in part to both post-volcanic emplacement subsidence and the erosional actions of glaciers flowing northwards from the Lough Neagh depocentre (Mitchell et al., 2004). The generally flat to undulating area is strewn with glaciomorphological features such as drumlins, roche moutonnée and erratics, many of which delineate the direction of glacial movement (Figure 1.8). There are some exceptions to the flat morphology of the central plateau, including remnant volcanic centres or dolerite plugs like Doonbought, Knocklayd, Tardree and Slemish which stand proud of the landscape having partly withstood the force of glacial erosion (Carter, 1982; Mitchell et al., 2004).

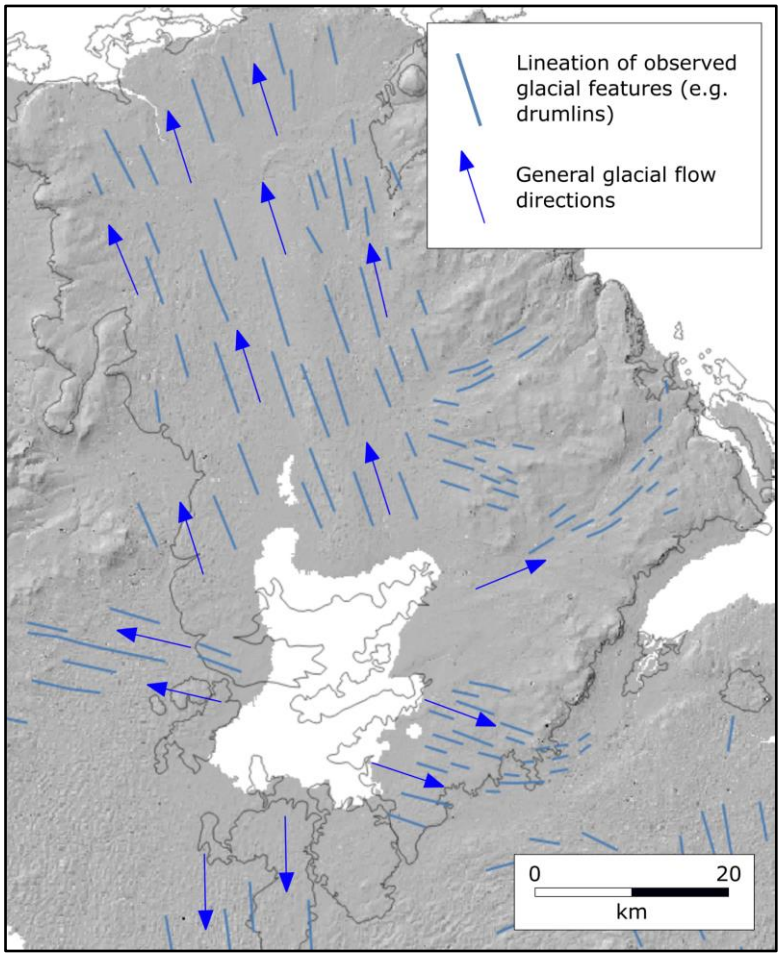

Figure 1.8. Shaded relief terrain model of the Antrim plateau showing the extent of the Antrim Lava Group and the Scrabo Hill intrusion inferred by the author from TELLUS data (black outline), Lough Neagh (white), the lineation of observed glacial features (identified by the author) and general glacial flow directions (Mitchell et al., 2004).

The edge of the plateau in the southwest quarter does not present an escarpment (as seen almost all around the rest of the plateau). This is almost entirely due to the presence of the Lough Neagh depocentre and the significant subsidence that has occurred in that area since the Eocene epoch (Mitchell et al., 2004).

1.7 Age of the ALG

Wilkinson *et al*. (2017) provided the most comprehensive review of age dating from the NAIP including the ALG. This review demonstrates how poorly constrained dates for the ALG are with considerable overlap in the upper and lower boundaries of the constituent units. After removing potentially unreliable K-Ar dates, the span of the ALG from this work is generally accepted to be 64.12 to 50.22 Ma with the bulk of activity occurring between 64.12 and 58.40 Ma (Wilkinson *et al*., 2017). Large areas south of the Antrim Plateau are now denuded and expose feeder dykes at or near the surface. Based on the ages of dykes, there may be significant sequences of basalt in the so-called interbasaltic phase.

1.8 Stratigraphy of the ALG

The literature tells us that the Antrim Lava Group (ALG) is primarily composed of two significant formations of basaltic lava flows that built up over the course of volcanic activity in the region, c. 62 to 57 Ma, and that these lava flows are generally phyric tholeiitic basalts with olivine phenocrysts visible in hand specimen, particularly within the Upper Basalt Formation. The **Lower Basalt Formation** (LBF) and the **Upper Basalt Formation** (UBF) are separated by a disconformity (at least two disconformities to the north of the Tow Valley Fault) representing as-yet unspecified lengths of time. Based on their observed stratigraphic relationships with the LBF and UBF lavas, a number of formally identified geological units are positioned within the stratigraphic span of this unconformity; primarily:

- the Tardree Rhyolite Complex,

- the Causeway Tholeiite Member (formerly the Middle Basalts), and
- the Ballypalady Plant Bed (and nearby Templepatrick rhyolite).

Additional geological units have been observed (some during this research) but are yet to be formally identified and positioned within the stratigraphy of Northern Ireland, namely:

- Rhyolitic volcanic centres, e.g.
    - NIRE 08/08-0001 located 4 km north of Rasharkin
    - NIRE 09/08-0002 located 6.5 km east of Coleraine
- Sedimentary sequences, e.g.
    - fluvial deposit discovered among basalt lava flows at Ross's Quarry 4.5 km southwest of Ballycastle (approximately coeval with Ballylagan Member of the Interbasaltic Formation?)
    - lacustrine deposits discovered among basalt lava flows at Ross's Quarry 4.5 km southwest of Ballycastle (approximately coeval with Port na Spaniagh Member of the Interbasaltic Formation?)

Collectively, the units of this condensed section with disconformities are termed the **Interbasaltic Formation**. To summarise, the ALG comprises three main stratigraphic units:

- the Lower Basalt Formation (LBF),
- the Interbasaltic Formation (IBF), and
- the Upper Basalt Formation (UBF).

To the north of the Tow Valley Fault, the Interbasaltic Formation is subdivided into the Port Na Spaniagh Member (PSM), the Causeway Tholeiite Member (CTM), and the Ballylagan Member (BLM). The Causeway Tholeiite Member has yet to be identified to the south of the Tow Valley Fault, and so the Tardree Rhyolite Complex is identified as its southerly counterpart within that hiatus. However, since the 'interbasaltic' hiatus may have been a million years or more, much work remains to be done to more carefully constrain and define the stratigraphy of this complex period of Earth's history.

Despite the body of investigative work that has already focussed on the ALG basalts, much is still unclear about the specific timing and periodicity of its component eruptions, and whether the individual flows were erupted from discrete point sources (i.e. volcanoes) or over large areas via a network of fissures. Some basaltic units of the ALG have been misidentified due to the level of similarities between the Lower and Upper Basalt Formation, despite the eruptions that extruded these basalts likely being separated in time by a million years or more.

From as early as 1786, the igneous origins of the Antrim basalts were proposed (Hamilton). Portlock (1843) and Hull (1878) concurred with this general hypothesis, although much argument persisted over the fine details. The work of Tomkeieff (1940) brought fresh interest to the geological questions that remained unanswered, leading Patterson (1955) to first identify, or at least formerly classify, three discrete units; namely the Lower, Middle, and Upper Basalt Series. Other workers (Levlie et al, 1972) took a more petrological approach to nomenclature, referring to Patterson's Middle Basalt Series as the 'Tholeiitic Basalts'. Old (1975) replaced Patterson's Lower and Upper Basalt Series with the Lower and Upper Basalt Formations, and gave name to

the Causeway Tholeiite Member of the Interbasaltic Formation (previously the Tholeiitic Basalts or the Middle Basalt Series).

Attempts to further our understanding of the Antrim basalts using geochemical analysis had some success (e.g. Patterson & Swaine, 1955) and this was continued by Lyle (1980, 1984, 1985, 1988, 2001; & Patton, 1989; & Preston, 1993) who more fully examined the petrochemistry of the basalts and intermediate lavas of the Lower and Upper Basalt Formations, as well as the Causeway Tholeiite Member of the Interbasaltic Formation.

There are currently no subdivisions of the LBF or UBF, which was one of the primary starting aims of this research. Previous work, including unpublished MSc and PhD theses (Gould, 2004; Brooks, 2016), focused on various geological aspects to find markers for stratigraphic correlation, including interbasaltic zircons, bulk geochemistry, mineralogy, petrology, age dating, etc. Yet despite similar investigations that focused on interbeds of the Inner Hebrides (Emeleus et al., 1996), very little published work has focused on using interbed palynology for stratigraphic determination or regional correlation of the Antrim Lava Group (Bell & Jolley, 1997). These techniques, in conjunction with high-precision WD-XRF analysis of over 200 basalt samples, were applied here with the aim of finding markers for correlation. Each technique alone can only offer so much. Our aim was to blend the results of various techniques into a coherent sequence and thus more accurately determine the spatial and chronological relationships between flows of the Lower and Upper Basalt Formations within the Antrim Lava Group and the wider BIPIP.

In this work we have taken a holistic approach to understanding the first phase of NAIP volcanism, using localised knowledge gained from examining the ALG and applying it to the broader setting. Due to its position on a spreading ridge with some level of mantle plume interaction, we will also look to recent (<3 Ma) tectonic and volcanic activity in Iceland as a guide to understanding the mechanisms of volcanic tempo, and fissure location and propagation that might help to improve our understanding of the same processes that may have been active during the emplacement of the ALG, BIPIP and NAIP.

The stratigraphy of the ALG has evolved over several generations of work, yet significant gaps remain. In particular, the detailed stratigraphy across the plateau is unclear, the timing and tempo of emplacement are uncertain, and up with this we shall not put.

1.8.1 Stratigraphic Units

Forming the Antrim Plateau, the ALG consists of up to 104 individual flood basalt lava flows (Thompson, 1979), along with lesser intermediate and acidic volcanic intrusions and deposits, piled up into thicknesses reaching almost 900 m near Ballymacilroy (Thompson, 1979).

The previously accepted volcanic activity responsible for the emplacement of the Lower Basalt, Interbasaltic and Upper Basalt formations of the ALG was historically understood to have occurred in three discrete steps, the middle of which until now was reported to be a period of significant quiescence despite experiencing notable flood basalt and associate volcanic activity:

Step 1 saw abundant mafic volcanism from ~62 Ma (Lower Basalt Formation, LBF),

Step 2 between ~61 and 60 Ma was relatively quiet in terms of mafic volcanism (although some still occurred, i.e. the Causeway Tholeiite Member) and is represented instead by more evolved acidic volcanic events such as the Tardree Rhyolite, then

Step 3 saw a return to prolific mafic volcanism ~60 Ma, which is understood to have ended ~58 Ma.

The ALG rocks follow the series: tholeiitic basalt - tholeiitic basaltic andesite - tholeiitic andesite - dacite - rhyolite (Lyle & Thompson, 1983). The ALG comprises a variety of Paleogene lithologies, which we will present here in greater detail. The currently identified and accepted components of the Antrim Lava Group are listed below.

'Clay with Flints'

At the base of the Antrim Lava Group across much of the Antrim Plateau, between the pre-existing underlying bedrock units and the basaltic lavas of the Antrim Lava Group, there is a horizon of flinty clay which appears to have been formed by at least two different processes; (1) by in situ weathering of UWLG rocks, or (2) by repositioning of the same rocks by subsequent transport methods (e.g. fluvial transport, ploughing by lava flows, etc.) (Cooper et al, 2017). The thickness of this deposit varies across the Antrim plateau but is generally less than 2 metres thick. The unit is known as the 'Clay with Flints' but it is not the same 'Clay with Flints' unit found in the south of the United Kingdom. The unit is still the focus of study due to outstanding questions about its

precise relationship to the UWLG, the Antrim Lava Group and palaeoclimatic conditions affecting its formation.

Explosive onset volcanics

Across the area underlying the main basalt sequences of the Antrim Lava Plateau there are remnants of shattered bedrock and hydrothermal/volcanic vents (Whiterocks, Portrush), very large blocks of bedrock relocated 'upsequence' (The Gobbins, Islandmagee), and thick ash deposits (Carrick-a-rede, Ballintoy). These geological artifacts point towards a period of volcanic activity of a powerful and violent nature, widely accepted as being linked to the inception of Continental Flood Basalts (Jerram & Widdowson, 2005), likely involving the explosive potential of acidic magma and copious volumes of water. Some workers have attributed this volcanism to the presence of a caldera off the northern coast, defined by an approximate and incomplete ring of small islands, but this has yet to be fully investigated or presented to the scientific community. As yet, no thorough investigations have been carried out to determine the scope, nature and extent of this early explosive volcanic phase of the Antrim Lava Group.

Lower Basalt Formation

The first phase of flood basalt volcanism comprised highly fluid basic lavas that flooded the palaeolandscape of Antrim. These lavas were classified as olivine basalts of the Hebridean Plateau Magma Type by Patterson & Mitchell (1955), which suggests a petrological linkage between the Antrim lavas and those of Mull and Skye.

The currently accepted age of emplacement for the Lower Basalt Formation is ~62.5 to 61 Ma.

Port na Spaniagh Member. This unit is predominantly the product of deeply weathered basalts of the Lower Basalt Formation interspersed with lacustrine sedimentary units. After emplacing the last main lavas of the Lower Basalt Formation, there followed a significant quiescence, during which time the youngest Lower Basalt Formation lavas were subjected to prolonged weathering and alteration. The precise length of time represented by that hiatus is still under research and debate, which may be the focus of future work.

The Port na Spaniagh Member has identifiable lithomarge, laterite, palaeosol and sedimentary units, in addition to remnant basalt artefacts.

The age of formation of the Port na Spaniagh Member is poorly constrained by it's stratigraphic position between the later flows of the Lower Basalt Formation (from some of which it is formed) below and the Causeway Tholeiite Member lava flows above. To date, no robust age dating has been carried out on the Port na Spaniagh Member, but it is now rightly placed within the Lower Basalt Formation (Figure 1.9).

Interbasaltic Formation

The lithological description of the Interbasaltic Formation is "bauxite-clay with subsidiary weathered rock" (www.bgs.ac.uk). However, the formation comprises much more than this, including tholeiitic flood basalts (e.g. Patterson & Swaine, 1955), rhyolitic volcanic deposits (e.g. Old, 1975), as well as fluvial and lacustrine sedimentary

sequences (e.g. Cole *et al.*, 1912; Patterson, 1955; Old, 1975; Beresford-Browne *et al.*, 2023).

The Middle Basalts (now the Causeway Tholeiite Member) were originally defined to the north of the Tow Valley Fault by the presence of thick, lateritic horizons underneath and above the lavas, which stratigraphically separated them from the Lower and Upper Basalt Formations.

The main, currently recognised component members of the Interbasaltic Formation include:

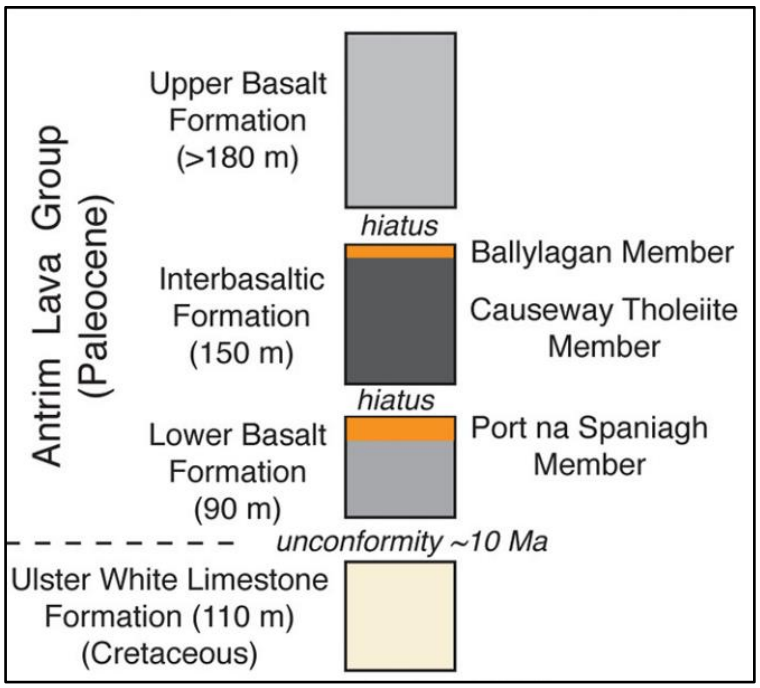

Figure 1.9. Stratigraphic grouping and nomenclature of the Antrim Lava Group to the north of the Tow Valley Fault (reproduced directly from Simms, 2021.

Causeway Tholeiite Member. The Causeway Tholeiite Member comprises up to nine observable flows (Lyle & Preston, 1993) of quartz-normative basalt, stratigraphically positioned between the two main flood basalt sequences of the Lower and Upper

Basalts. Thus far this geological unit has only been identified to the north of the Tow Valley Fault, sitting between the Port na Spaniagh and Ballylagan Members.

Ballylagan Member. After the Causeway Tholeiite / Middle Basalts were emplaced, a second significant hiatus was noted (Patterson, 1950) by the presence of this weathered horizon atop lavas of the Causeway Tholeiite Member.

The age of formation of the Ballylagan Member is poorly constrained by its stratigraphic position between the later flows of the Causeway Tholeiite Member (from some of which it is formed) below and the early lava flows of the Upper Basalt Formation above. To date, no robust age dating has been carried out on the Ballylagan Member.

The fluvial sedimentary unit discovered by the author at Ross's Quarry (proposed name: the Craignagat Member) also sits above basalts of the CTM and below those of the UBF so is likely to have formed within the same period as the Ballylagan Member seen at the Causeway Coast and Ballylagan Lake.

Upper Basalt Formation

The second phase of flood basalt volcanism emplaced olivine-normative basalt lavas. The earliest age date from Wilkinson et al.'s (2017) review is 59.99 ±0.32 Ma which overlaps with dates for the Lower Basalt and Interbasaltic formations. The duration of the Upper Basalt Formation, and when this phase of volcanism ended, is not yet constrained.

2.1 **Introduction**

This chapter presents a detailed account of data sources, including lists of all boreholes as well as natural and quarried field outcrop locations. I also present the list of samples taken for a range of analyses, including pXRF (handheld/portable X-Ray Fluorescence), WD-XRF (high precision, laboratory XRF), palynological study, and petrological examination. Where appropriate, the analytical strategy including decisions around further analyses, targeted geochemical analyses, and availability of geophysical data will also be explained.

2.2 **Geological Survey of Northern Ireland borehole logs and samples**

Datasets from 19 Lonmin boreholes (prefix NIRE) were made available for this research. Lonmin (NI) Plc drilled numerous boreholes across Northern Ireland between 2012 and 2013; 19 of which encountered Paleocene igneous rocks of the Antrim Lava Group (Figure 2.1).

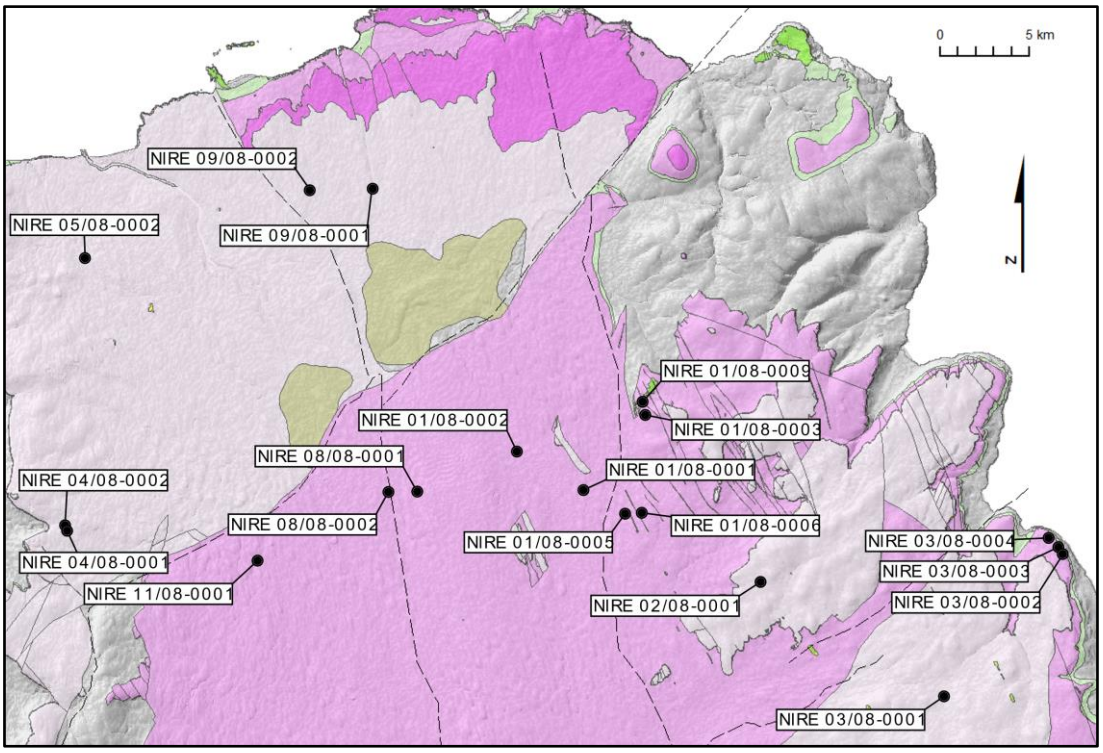

Figure 2.1. Location of inspected NIRE boreholes in Northern Ireland

The borehole datasets included boxed core samples, wellside logs, and spreadsheets containing pXRF, trace element and magnetic susceptibility data (Table 2.1).

Table 2.1. NIRE borehole data made available by GSNI

Borehole ID	Easting	Northing	Elevation	Log	pXRF	Trace elements	Core	Mag Sus
NIRE 01/08-0001	306212	417691	95.8	Yes	Yes	-	Yes	Yes
NIRE 01/08-0002	302489	419822	90.7	Yes	Yes	-	Yes	Yes
NIRE 01/08-0003	309689	421897	235.0	Yes	-	Yes	Yes	Yes
NIRE 01/08-0005	308528	416359	122.2	Yes	Yes	-	Yes	Yes
NIRE 01/08-0006	309473	416438	182.8	Yes	Yes	-	Yes	Yes
NIRE 01/08-0009	309509	422616	255.0	Yes	-	Yes	Yes	Yes
NIRE 02/08-0001	316129	412540	259.9	Yes	Yes	-	Yes	Yes
NIRE 03/08-0001	326391	406143	218.3	Yes	Yes	-	Yes	Yes
NIRE 03/08-0002	333053	414144	200.8	Yes	Yes	-	Yes	Yes
NIRE 03/08-0003	332828	414530	191.4	Yes	Yes	-	Yes	Yes
NIRE 03/08-0004	332255	414987	142.9	Yes	Yes	-	Yes	Yes
NIRE 04/08-0001	277233	415430	225.0	Yes	Yes	-	Yes	Yes
NIRE 04/08-0002	277179	415701	227.5	Yes	-	Yes	Yes	Yes
NIRE 05/08-0002	278240	430729	106.0	Yes	-	Yes	Yes	Yes
NIRE 08/08-0001	296903	417587	116.0	Yes	-	Yes	Yes	Yes
NIRE 08/08-0002	295284	417562	58.5	Yes	-	Yes	Yes	Yes
NIRE 09/08-0001	294362	434582	47.7	Yes	Yes	-	Partial	Yes
NIRE 09/08-0002	290853	434532	78.2	Yes	Yes	-	Yes	Yes
NIRE 11/08-0001	287917	413754	79.0	Yes	Yes	-	Yes	Yes

The provided data gave stratigraphic information of the Antrim Lava Group encountered within the boreholes (Table 2.2). The Lonmin borehole logs provided by GSNI are in Appendix K.

Handheld pXRF geochemistry

The Lonmin XRF geochemical datasets provided by GSNI include sample points (minimum 66, maximum 352) from 13 boreholes with an average spacing of between 0.98 and 3.22 m (Table 2.3).

Table 2.2. Antrim Lava Group information from NIRE borehole data (rhyolite only)*

Borehole ID	Easting	Northing	Elevation	UBF top depth	IBF top depth	LBF top depth	Unit under ALG	CWF thickness	ALG thickness	Flow count
NIRE 01/08-0001	306212	417691	95.8	-	-	-	*Not logged*	-	162.3	*
NIRE 01/08-0002	302489	419822	90.7	-	-	12	Dalradian	1.08	283.54	37
NIRE 01/08-0003	309689	421897	235.0	-	-	8.95	Dalradian	2.6	36.65	6
NIRE 01/08-0005	308528	416359	122.2	-	-	3.16	Cretaceous UWLG	1.58	210.84	34
NIRE 01/08-0006	309473	416438	182.8	-	-	6	Cretaceous UWLG	0.2	231.55	36
NIRE 01/08-0009	309509	422616	255.0	-	-	8.87	Dalradian	4.88	33.23	5
NIRE 02/08-0001	316129	412540	259.9	5.8	50.32	71.8	Cretaceous UWLG	0.98	417.62	64
NIRE 03/08-0001	326391	406143	218.3	9.2	97.4	131.46	Cretaceous UWLG	5.64	377.44	67
NIRE 03/08-0002	333053	414144	200.8	6	-	-	Cretaceous UWLG	0.42	75.8	29
NIRE 03/08-0003	332828	414530	191.4	6.2	-	-	Cretaceous UWLG	1.18	98.39	49
NIRE 03/08-0004	332255	414987	142.9	6.2	-	-	Cretaceous UWLG	2.92	109.22	25
NIRE 04/08-0001	277233	415430	225.0	3.5	-	-	Cretaceous UWLG	1.27	111.87	20
NIRE 04/08-0002	277179	415701	227.5	1.65	-	-	Cretaceous UWLG	1.23	107.17	6
NIRE 05/08-0002	278240	430729	106.0	3.7	-	-	Cretaceous UWLG	2.23	100.8	17
NIRE 08/08-0001	296903	417587	116.0	-	-	6.41	Cretaceous UWLG	0.99	151.79	25
NIRE 08/08-0002	295284	417562	58.5	-	-	14.94	Cretaceous UWLG	0.46	68.57	13
NIRE 09/08-0001	294362	434582	47.7	3.1	278.15	292.7	Cretaceous UWLG	2.59	432.85	79
NIRE 09/08-0002	290853	434532	78.2	8.12	108.22	162.94	*Not logged*	-	244.28	84
NIRE 11/08-0001	287917	413754	79.0	-	-	6	Dalradian	0.25	116.45	51

Handheld magnetic susceptibility

The Lonmin magnetic susceptibility datasets provided by GSNI include sample points (minimum 27, maximum 855) from 13 boreholes with an average spacing of between 0.48 and 2.59 m (Table 2.4).

Table 2.3. List of pXRF data analysis sample distribution in NIRE boreholes

Borehole ID	Sample points	Average spacing between sample points (m)
NIRE 01/08-0001	87	1.62
NIRE 01/08-0002	155	1.83
NIRE 01/08-0005	66	3.22
NIRE 01/08-0006	108	2.15
NIRE 02/08-0001	352	1.21
NIRE 03/08-0001	113	3.35
NIRE 03/08-0002	66	1.15
NIRE 03/08-0003	89	1.11
NIRE 03/08-0004	91	1.20
NIRE 04/08-0001	113	0.98
NIRE 09/08-0001	335	1.29
NIRE 09/08-0002	243	1.00
NIRE 11/08-0001	105	1.13

Table 2.4. List of magnetic susceptibility data analysis sample distribution in NIRE boreholes

Borehole ID	Sample points	Average spacing between sample points (m)
NIRE 01/08-0001	280	0.52
NIRE 01/08-0002	538	0.51
NIRE 01/08-0003	60	0.49
NIRE 01/08-0005	81	2.59
NIRE 01/08-0006	444	0.51
NIRE 01/08-0009	63	0.45
NIRE 02/08-0001	415	0.99
NIRE 03/08-0001	380	0.97
NIRE 03/08-0002	27	2.00
NIRE 03/08-0003	39	2.00
NIRE 03/08-0004	44	2.00
NIRE 04/08-0001	215	0.50
NIRE 04/08-0002	214	0.49
NIRE 05/08-0002	193	0.50
NIRE 08/08-0001	301	0.48
NIRE 08/08-0002	139	0.50
NIRE 09/08-0001	855	0.50
NIRE 09/08-0002	481	0.50
NIRE 11/08-0001	245	0.48

Borehole core

Approximately 3.5 km of borehole core samples were donated to GSNI in organised core trays (Figure 2.2a, b & c). Lonmin borehole logs, logged by Lonmin staff in 2012/13, were provided by GSNI in PDF files, author-annotated versions of which are presented in Appendix K. In addition, two of the boreholes that encountered recognisable sequences of

Lower Basalt, Interbasaltic and Upper Basalt Formation rocks were re-logged as part of this work. These are presented in Appendix L. Most boreholes proved basalt flows with interbeds (see Table 2.2) except borehole NIRE 01/08-0001 which proved only rhyolite.

a

Antrim Lava Group basalt

Shattered UWL, 'Clay with Flints', basalt

Ulster White Limestone

b

c

Figure 2.2a. NIRE 03/08-0001 core samples laid out for inspection and sampling at GSNI core stores, Belfast, Northern Ireland. b. Contact between Ulster White Limestone Group and Antrim Lava Group in NIRE 03/08-0001 with 'Clay with Flints' Formation in zone of contact. c. NIRE 03/08-0001 core samples from Lower (LBF) to Upper Basalt Formations (UBF), presenting weathered basalts of the 'Interbasaltic' Formation (IBF).

Other borehole data (provided by GSNI)

Borehole logs from an additional 40 boreholes were made available for this research, all of which encountered Paleocene igneous rocks of the Antrim Lava Group. In addition to borehole logs, a few also came with **geophysical logs** and complete geological reports (Table 2.5).

*Table 2.5. Borehole records held by GSNI. Annotations as follows: underlined = report included; bold = **geophysical data included**.*

BOREHOLE ID	Easting	Northing	Elevation	Unit under ALG	Basalt flow count	ALG thickness
Port More No.1	306897	443525	103.0	Cretaceous UWLG		57.04
Ballycastle	311048	440700		Cretaceous UWLG		63.09
B'leese Nurseries	283536	436810		Cretaceous UWLG		115.30
B'leese House	283566	436840		Cretaceous UWLG		64.10
Portstewart No.1	281339	436779		Cretaceous UWLG		77.77
Upton Park No.2	322957	386644		Terminated in ALG		211.68
Washing Bay	289964	366071		Terminated in ALG		235.70
Aughrimderg	287978	368413		Cretaceous UWLG		302.00
Holmlea	305492	412976		Terminated in ALG		54.30
Inshamph	310784	411447		Terminated in ALG		100.30
Site A Woodside Rd Ind Est	313968	404332		Terminated in ALG		147.10
Greenmount Hill Farm, Glenwhirrey	327850	400030		Terminated in ALG		76.00
Ballymullock Reservoir	337589	403606		Terminated in ALG	8	49.23
Maxwells Quarry No.1	286395	383976	96.0	Cretaceous UWLG		
Maxwells Quarry No.2	286414	384083	92.0	Cretaceous UWLG		2.00
Maxwells Quarry No.3	286414	384168	91.0	Cretaceous UWLG		1.00
Maxwells Quarry No.4	286465	384139	93.0	Cretaceous UWLG		22.00

BOREHOLE ID	Easting	Northing	Elevation	Unit under ALG	Basalt flow count	ALG thickness
Maxwells Quarry No.5	286439	384258	98.0	Terminated in ALG		
Maxwells Quarry No.6	286444	384299	104.0	Cretaceous UWLG		20.25
Maxwells Quarry No.7	286980	384399	110.0	Cretaceous UWLG		64.60
Maxwells Quarry No.8	286602	384109	125.0	Terminated in ALG		10.50
Maxwells Quarry No.9	286426	383939	103.0	Cretaceous UWLG		21.00
SIte B Carn, Portadown	303005	357048	25.0	Terminated in ALG		155.00
Glendinning 2	308076	359441	22.0	Cretaceous UWLG		65.50
Creamline Dairy	308611	357244	62.0	Cretaceous UWLG		105.77
Glen Eyre Nursing Home	303545	353777	43.0	Mudstone (Dalradian?)		89.00
Ballinlea No.1	303765	439317	87.6	Cretaceous UWLG		130.00
Dernagh No.2	285382	367053	45.0	Cretaceous UWLG		206.35
Dernagh No.1	285444	367067	45.0	Cretaceous UWLG		127.69
Mire House	286100	366328	23.0	Cretaceous UWLG		212.45
Ballytober Fynegold Petroleum	332737	404944	286.6	Cretaceous UWLG		100.00
Salmon No.1	330000	412900	27.0	Cretaceous UWLG	28	101.50
Annaghmore No.1	299658	387857	16.2	Cretaceous UWLG		350.43
Balymacilroy	305731	397597	73.5	Cretaceous UWLG	104	773.19
Ballynamullan	300150	387045	21.6	Cretaceous UWLG		462.30
Ballynure	337736	395467	172.6	Cretaceous UWLG		163.00
Langford Lodge	309089	374836	22.0	Cretaceous UWLG		794.00
Rathlin Island	313912	451570	103.0	Cretaceous UWLG		107.50
Corbally Reservoir	288031	438806		Cretaceous UWLG		201.17

2.3 **Basalt geochemistry**

Geochemical data generated by Lonmin were provided by GSNI for this work. The details of the samples are provided above including scanned pXRF data. Further samples were analysed at Trinity College Dublin (TCD) using WD-XRF analytical methods. Data generated by the two XRF methods were compared in order to test the validity and usefulness of the pXRF data as a chemostratigraphic tool. This was done by taking specific samples from basalt flow cores throughout boreholes NIRE 02/08-0001 and NIRE 09/08-0001, analysing them at the GSNI Core Stores using pXRF equipment provided by GSNI, before boxing up and sending the samples to the laboratory at TCD to be analysed by WD-XRF (Wavelength Dispersive X-ray Fluorescence).

Additional samples for geochemical analysis were obtained from quarries and field locations (Table 2.6). Of the 218 samples taken from borehole core and field outcrop, a total of 173 samples were considered to be fresh basalt. 4 samples were taken from a sedimentary interbed at Ross's Quarry, and a further 15 samples were interpreted as being pegmatitic, doleritic, or from a basaltic dyke.

Table 2.6. Samples taken for geochemical analysis of basalt flows

Location	Sample ID
Ballycastle Quarry	BA1
	BA2a
	BA2b
	BA3
	BA4
	BA5
	BA6
	BA7
	BA8
	BA9
	BA10

Location	Sample ID
Corkey Quarry	CO1
	CO2
	CO3
	CO4
	CO5
	CO6
	CO7
	CO8
	CO9
	CO10
	CO11

Location	Sample ID
Garron stream section	GS1a
	GS1b
	GS1c
	GS1d
	GS2
	GS3a
	GS3b
	GS4
	GS5
	GS6
	GS7

Location	Sample ID
	BA11
	BA12
	BA13
Binevenagh	BI1
	BI2
	BI3
	BI4
	BI5
	BI6
	BI7
	BI8
	BI9a
	BI9b
	BI9c
	BI10
	BI11
	BI12
	BI13
Ballymena Quarry	BM1
	BM2
	BM3
	BM4
Blackmountain Quarry	BMQ1
	BMQ2
	BMQ3
	BMQ4
	BMQ5
Clinty Quarry	CL1
	CL2
	CL3
	CL4
	CL5
	CL6
	CL7
	CL8
	CL9
	CL10
	CL11
	CL12
	CL13
	CL14

Location	Sample ID
	CO12
	CO13
	CO14
	CO15
	CO16
	CO17
Craigall Quarry	CRA1
	CRA2
	CRA3
	CRA4
	CRA5
	CRA6
	CRA7
	CRA8
	CRA9
Croaghan Quarry	CRO1a
	CRO1b
	CRO2a
	CRO2b
	CRO3
	CRO4
Craig's Quarry	CRQ1
	CRQ2
	CRQ3
	CRQ4
	CRQ5
	CRQ6
	CRQ7
	CRQ8
	CRQ9
	CRQ10
	CRQ11
	CRQ12
	CRQ13
	CRQ14
	CRQ15
	CRQ16
	CRQ17
	CRQ18

Location	Sample ID
	GS8
	GS9
	GS10
Knockloughrim Quarry	KN1
	KN2
	KN3
	KN4
	KN5
	KN6a
	KN6b
	KN7
	KN8
	KN9
	KN10
	KN11
	KN12
	KN13
	KN14
	KN15
	KN16
	KN17
Macosquin Quarry	MA1
	MA2
Slemish	SL1
	SL2a
	SL2b
	SL3
Big Collin	TD1
Whitemountain Quarry	WM1
	WM2
	WM3
	WM4a
	WM4b
	WM4c
	WM4d
	WM5
Cam Quarry	CAM1
	CAM2
	CAM3
	CAM4

Of the remaining 199 basalt samples, 26 were examined during the sample preparation process and found to be altered to a noticeable extent. The extent of alteration was then assigned a numerical value between 1 (unaltered, fresh) and 5 (deeply weathered) to better manage, interrogate and interpret the resulting geochemical data.

Limitations to the data

- Lonmin scanned pXRF nominally every metre or so, whereas I needed to focus on specific horizons
- pXRF datasets for the various boreholes were not consistent with each other (see Table 2.10)

Figure 2.3. Olympus Vanta pXRF workstation set up at GSNI core stores, Belfast, NI

The pXRF equipment used was an Olympus Vanta Delta Premium (Figures 2.3 & 2.4) equipped with a gold anode. The pXRF unit was operated in conjunction with a desktop, shielded sample box (Figure 2.3) to free up the operator during the 120 second scan cycle and also minimise the risk of accidental exposure to X-rays during analysis.

Figure 2.4. Olympus Vanta pXRF unit in charging dock. Analytical Blank and Standard samples to lower left of image

Unlike ED-XRF (Energy Dispersive X-ray Fluorescence), which is designed to analyze groups of elements simultaneously, WD-XRF uses crystals to disperse the fluorescence spectrum into individual wavelengths of each element, providing high resolution and low background spectra for accurate determination of elemental concentrations (ThermoFisher Scientific). The elemental range for ED-XRF, sodium to uranium, has an energy resolution of ~150 eV. The elemental range for WD-XRF, beryllium to uranium, has an energy resolution of ~15-150 eV.

Figure 2.5. Basalt samples from NIRE 02/08-0001 and NIRE 09/08-0002, bagged and labelled after being scanned with pXRF ready for shipping to Dr Elliot Carter, TCD, Ireland

Boreholes NIRE 02/08-0001 and NIRE 09/08-0001 were chosen for further analysis because they not only had significant lengths of Antrim basalts from Lower and Upper Basalt Formations but also had representative rocks from the Interbasaltic Formation. This not only gave access to a full sequence of ALG rocks for analysis, but also gave confidence as to whether the basalts were of the Lower or Upper Basalt Formation due to absolute stratigraphic control of sampling. Unfortunately, the borehole core from NIRE 09/08-0001 below 257.10 mbgl could not be located by GSNI staff. This was significant because the Causeway Tholeiite Member commenced at 257 mbgl, meaning that only the Upper Basalt Formation was sampled.

Borehole NIRE 02/08-0001 was logged from 12th to 14th October 2020. Samples were collected for pXRF and WD-XRF analysis, presented in Table 2.7.

Table 2.7. Sample information for borehole NIRE 02/08-0001

Borehole ID	Sample ID	Start Depth (m)	End Depth (m)	Length (m)	Approx Core Amount	Core Diameter (m)	Est Volume (m^3)	Est Weight (kg)
02/08-0001	ABB001	8.32	8.52	0.20	0.25	0.060	0.00014	0.426
02/08-0001	ABB002	13.41	13.51	0.10	0.50	0.060	0.00014	0.426
02/08-0001	ABB003	20.22	20.44	0.22	0.50	0.048	0.00020	0.599
02/08-0001	ABB004	29.03	29.19	0.16	0.50	0.048	0.00014	0.436
02/08-0001	ABB005	35.10	35.30	0.20	0.50	0.048	0.00018	0.545
02/08-0001	ABB006	46.68	46.83	0.15	0.50	0.048	0.00014	0.409
02/08-0001	ABB007	76.52	76.66	0.14	0.50	0.048	0.00013	0.381
02/08-0001	ABB008	81.35	81.48	0.13	0.50	0.048	0.00012	0.354
02/08-0001	ABB009	91.11	91.22	0.11	0.50	0.048	0.00010	0.300
02/08-0001	ABB010	114.16	114.28	0.12	0.50	0.048	0.00011	0.327
02/08-0001	ABB011	126.23	126.35	0.12	0.50	0.048	0.00011	0.327
02/08-0001	ABB012	133.73	133.87	0.14	0.50	0.048	0.00013	0.381
02/08-0001	ABB013	164.02	164.20	0.18	0.50	0.048	0.00016	0.490
02/08-0001	ABB014	174.54	174.75	0.21	0.50	0.048	0.00019	0.572
02/08-0001	ABB015	192.13	192.23	0.10	0.50	0.048	0.00009	0.272
02/08-0001	ABB016	203.72	203.91	0.19	0.50	0.048	0.00017	0.518
02/08-0001	ABB017	206.70	206.91	0.21	0.50	0.048	0.00019	0.572
02/08-0001	ABB018	231.15	231.35	0.20	0.50	0.048	0.00018	0.545
02/08-0001	ABB019	250.43	250.60	0.17	0.50	0.048	0.00015	0.463
02/08-0001	ABB020	266.28	266.43	0.15	0.50	0.048	0.00014	0.409
02/08-0001	ABB021	278.25	278.40	0.15	0.50	0.048	0.00014	0.409
02/08-0001	ABB022	291.52	291.75	0.23	0.50	0.048	0.00021	0.627
02/08-0001	ABB023	312.62	312.76	0.14	0.50	0.048	0.00013	0.381
02/08-0001	ABB024	322.70	322.87	0.17	0.50	0.048	0.00015	0.463
02/08-0001	ABB025	327.75	327.90	0.15	0.50	0.048	0.00014	0.409
02/08-0001	ABB026	333.80	333.95	0.15	0.50	0.048	0.00014	0.409
02/08-0001	ABB027	348.30	348.46	0.16	0.50	0.048	0.00014	0.436
02/08-0001	ABB028	358.30	358.50	0.20	0.50	0.048	0.00018	0.545
02/08-0001	ABB029	368.15	368.30	0.15	0.50	0.048	0.00014	0.409
02/08-0001	ABB030	376.15	376.30	0.15	0.50	0.048	0.00014	0.409
02/08-0001	ABB031	381.20	381.34	0.14	0.50	0.048	0.00013	0.381
02/08-0001	ABB032	394.28	394.42	0.14	0.50	0.048	0.00013	0.381
02/08-0001	ABB033	403.75	403.90	0.15	0.50	0.048	0.00014	0.409
02/08-0001	ABB034	409.57	409.71	0.14	0.50	0.048	0.00013	0.381
02/08-0001	ABB035	416.67	416.85	0.18	0.50	0.048	0.00016	0.490
02/08-0001	ABB036	423.73	423.89	0.16	0.50	0.048	0.00014	0.436
02/08-0001	ABB037	426.51	426.66	0.15	0.50	0.048	0.00014	0.409
02/08-0001	ABB038	432.58	432.70	0.12	0.50	0.048	0.00011	0.327

Borehole NIRE 09/08-0001 was logged on 15th October and 2nd to 3rd November 2020.

Samples were collected for pXRF and WD-XRF analysis, presented in Table 2.8.

Studies on the successful application of pXRF to science have been carried out (e.g. Young et al., 2012; Young et al., 2016) and show that the equipment and methodology are suitable subject to the known limitations (e.g. poor reading of Mg, unable to read Na, etc.).

Table 2.8. Sample information for borehole NIRE 09/08-0001

Borehole ID	Sample ID	Start Depth (m)	End Depth (m)	Length (m)	Approx Core Amount	Core Diameter (m)	Est Volume (m^3)	Est Weight (kg)
09/08-0001	ABB901	18.00	18.10	0.10	0.50	0.060	0.00014	0.426
09/08-0001	ABB902	26.50	26.65	0.15	0.50	0.060	0.00021	0.639
09/08-0001	ABB903	41.50	41.60	0.10	0.50	0.060	0.00014	0.426
09/08-0001	ABB904	48.50	48.60	0.10	0.50	0.060	0.00014	0.426
09/08-0001	ABB905	54.10	54.20	0.10	0.50	0.060	0.00014	0.426
09/08-0001	ABB906	66.10	66.20	0.10	0.50	0.060	0.00014	0.426
09/08-0001	ABB907	75.50	75.60	0.10	0.50	0.060	0.00014	0.426
09/08-0001	ABB908	80.00	80.15	0.15	0.50	0.060	0.00021	0.639
09/08-0001	ABB909	88.40	88.50	0.10	0.50	0.060	0.00014	0.426
09/08-0001	ABB910	93.00	93.10	0.10	0.50	0.060	0.00014	0.426
09/08-0001	ABB911	99.10	99.20	0.10	0.50	0.060	0.00014	0.426
09/08-0001	ABB912	108.50	108.60	0.10	0.50	0.060	0.00014	0.426
09/08-0001	ABB913	115.65	115.75	0.10	0.50	0.060	0.00014	0.426
09/08-0001	ABB914	122.20	122.30	0.10	0.50	0.060	0.00014	0.426
09/08-0001	ABB915	124.20	124.30	0.10	0.50	0.060	0.00014	0.426
09/08-0001	ABB916	128.75	128.85	0.10	0.50	0.060	0.00014	0.426
09/08-0001	ABB917	140.20	140.30	0.10	0.50	0.060	0.00014	0.426
09/08-0001	ABB918	192.85	192.95	0.10	0.50	0.060	0.00014	0.426
09/08-0001	ABB919	198.30	198.40	0.10	0.50	0.060	0.00014	0.426
09/08-0001	ABB920	204.20	204.30	0.10	0.50	0.060	0.00014	0.426
09/08-0001	ABB921	207.70	207.80	0.10	0.50	0.060	0.00014	0.426
09/08-0001	ABB922	213.90	214.00	0.10	0.50	0.060	0.00014	0.426
09/08-0001	ABB923	217.55	217.65	0.10	0.50	0.060	0.00014	0.426
09/08-0001	ABB924	220.55	220.65	0.10	0.50	0.060	0.00014	0.426
09/08-0001	ABB925	226.40	226.50	0.10	0.50	0.060	0.00014	0.426
09/08-0001	ABB926	235.50	235.70	0.20	0.50	0.060	0.00028	0.851
09/08-0001	ABB927	242.95	243.05	0.10	0.50	0.060	0.00014	0.426
09/08-0001	ABB928	251.10	251.20	0.10	0.50	0.060	0.00014	0.426
09/08-0001	ABB929	257.40	257.50	0.10	0.50	0.060	0.00014	0.426

Table 2.9. Minimum and maximum data values for specific elements measured using pXRF for NIRE borehole core.

	Ti (ppm)		Fe (ppm)		Cr (ppm)		Ni (ppm)		Zr (ppm)	
Borehole ID	min	max	min	max	min	max	min	max	min	max
01/08-0001	54.0	229.0	4,680.0	14,228.0	0.0	21.0	0.0	29.0	93.0	121.0
01/08-0002	1,591.3	38,983.9	43,475.9	152,914.7	0.0	5,017.8	0.0	1,161.3	8.3	179.4
01/08-0005	3,479.0	38,007.0	35,449.0	330,973.0	0.0	2,239.0	0.0	987.0	51.8	430.0
01/08-0006	1,634.5	38,875.1	40,111.7	164,363.7	0.0	3,060.1	0.0	1,025.7	19.4	296.8
02/08-0001	0.0	30,058.0	459.0	428,657.0	0.0	1,650.0	0.0	669.0	0.0	440.0
03/08-0001	0.0	44,750.0	3,251.0	332,210.0	0.0	2,706.0	0.0	894.0	10.5	699.0
03/08-0002	182.0	15,060.0	1,027.0	103,953.0	0.0	1,756.0	0.0	775.0	2.8	194.0
03/08-0003	170.0	13,869.0	471.0	106,380.0	6.4	1,852.0	18.0	751.0	1.7	198.0
03/08-0004	0.0	18,116.0	807.0	133,452.0	0.0	1,900.0	0.0	951.0	0.0	307.0
04/08-0001	4,333.0	10,964.0	10,240.0	117,610.0	125.0	1,597.0	107.0	635.0	51.9	216.0
09/08-0001	0.0	56,290.0	1,539.0	265,297.0	0.0	948.0	0.0	791.0	5.0	537.0
09/08-0002	190.0	58,839.0	2,827.0	1,430,101.0	0.0	1,136.0	0.0	664.0	4.6	884.0
11/08-0001	4,157.0	16,401.0	11,215.0	130,418.0	22.0	1,385.0	0.0	524.0	72.1	522.0

Table 2.10. Elements measured by pXRF equipment on each borehole (BH) core. Note the inconsistency in data availability.

BH ID	Elements determined by pXRF																																
01/08-0001	Ag	As	Bi	Ca	Cd	Cl	Co	Cr	Cu	Fe	Hg	K	Mn	Mo	Ni	P	Pb	Rb	S	Sb	Se	Sn	Sr	Th	Ti	U	V	W	Y	Zn	Zr			
01/08-0002	Ag	Al	As	Bi	Ca	Cd	Cl	Co	Cr	Cu	Fe	Hg	K	Mg	Mn	Mo	Ni	P	Pb	Rb	S	Sb	Se	Si	Sn	Sr	Th	Ti	U	V	W	Y	Zn	Zr
01/08-0005	Ag	As	Ba	Ca	Cd	Cl	Co	Cr	Cu	Fe	Hg	I	K	Mn	Mo	Ni	P	Pb	Rb	S	Sb	Se	Sn	Sr	Ti	Zn	Zr							
01/08-0006	Ag	Al	As	Bi	Ca	Cd	Cl	Co	Cr	Cu	Fe	Hg	K	Mg	Mn	Mo	Ni	P	Pb	Rb	S	Sb	Se	Si	Sn	Sr	Th	Ti	U	V	W	Y	Zn	Zr
02/08-0001	Ag	As	Ba	Ca	Cd	Cl	Co	Cr	Cu	Fe	Hg	I	K	Mn	Mo	Ni	P	Pb	Rb	S	Sb	Se	Sn	Sr	Ti	Zn	Zr							
03/08-0001	Ag	As	Ba	Ca	Cd	Cl	Co	Cr	Cu	Fe	Hg	I	K	Mn	Mo	Ni	P	Pb	Rb	S	Sb	Se	Sn	Sr	Ti	Zn	Zr							
03/08-0002	Ag	As	Ba	Ca	Cd	Cl	Co	Cr	Cu	Fe	Hg	I	K	Mn	Mo	Ni	P	Pb	Rb	S	Sb	Se	Sn	Sr	Ti	Zn	Zr							
03/08-0003	Ag	As	Ba	Ca	Cd	Cl	Co	Cr	Cu	Fe	Hg	I	K	Mn	Mo	Ni	P	Pb	Rb	S	Sb	Se	Sn	Sr	Ti	Zn	Zr							
03/08-0004	Ag	As	Ba	Ca	Cd	Cl	Co	Cr	Cu	Fe	Hg	I	K	Mn	Mo	Ni	P	Pb	Rb	S	Sb	Se	Sn	Sr	Ti	Zn	Zr							
04/08-0001	Ag	As	Ba	Ca	Cd	Cl	Co	Cr	Cu	Fe	Hg	I	K	Mn	Mo	Ni	P	Pb	Rb	S	Sb	Se	Sn	Sr	Ti	Zn	Zr							
09/08-0001	Ag	As	Ba	Ca	Cd	Cl	Co	Cr	Cu	Fe	Hg	I	K	Mn	Mo	Ni	P	Pb	Rb	S	Sb	Se	Sn	Sr	Ti	Zn	Zr							
09/08-0002	Ag	As	Ba	Ca	Cd	Cl	Co	Cr	Cu	Fe	Hg	I	K	Mn	Mo	Ni	P	Pb	Rb	S	Sb	Se	Sn	Sr	Ti	Zn	Zr							
11/08-0001	Ag	As	Ba	Ca	Cd	Cl	Co	Cr	Cu	Fe	Hg	I	K	Mn	Mo	Ni	P	Pb	Rb	S	Sb	Se	Sn	Sr	Ti	Zn	Zr							

Geochemical analyses of the NIRE borehole core samples already analysed by pXRF analysis at the GSNI Core Stores in Belfast was subsequently carried out by Dr Elliot Carter, Trinity College Dublin, using WD-XRF equipment.

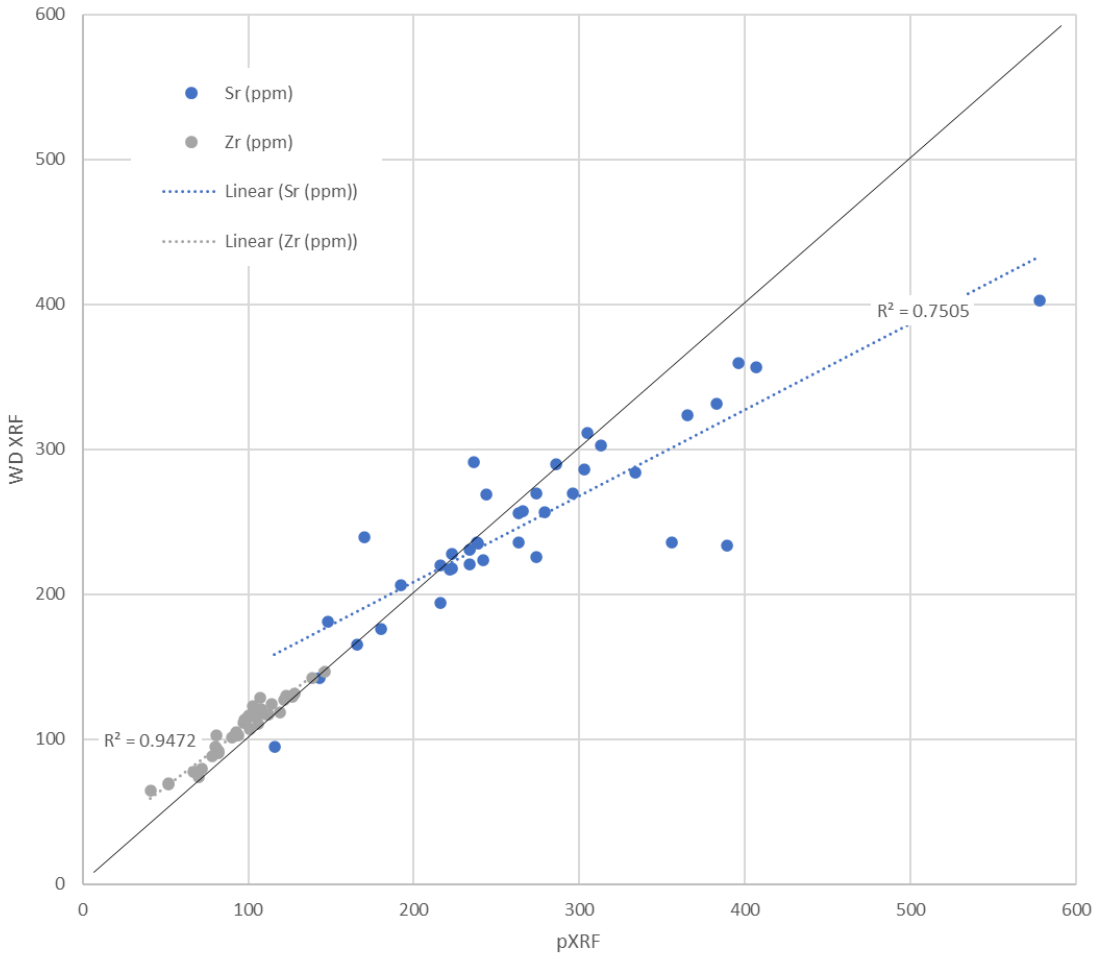

Figure 2.6. Comparative plot of Sr and Zr values determined by handheld pXRF and WD-XRF

WD-XRF data were compared to pXRF data on the 281 and 981 samples. Results for individual elements were directly compared to assess the reliability of pXRF data for the purposes of this research. Figure 2.6 shows the correlation between pXRF and WD-XRF for Sr and Zr. The graph shows that Zr data has excellent correlation and is therefore reliable (R^2 = 0.9472). Sr also has a good but weaker correlation (R^2 = 0.7505) with some outliers, which we have not removed. These pXRF over-reads may be due to the fact that the pXRF tool

scans an area of heterogenous whole rock whereas WD-XRF is carried out on finely-ground, homogenised samples.

Figure 2.7 shows the correlation between pXRF and WD-XRF for Cr and Ni. In this plot, the correlation for Ni is excellent (R^2 = 0.9173), as is the correlation for Cr (R^2 = 0.9297), but with regular under-readings by pXRF.

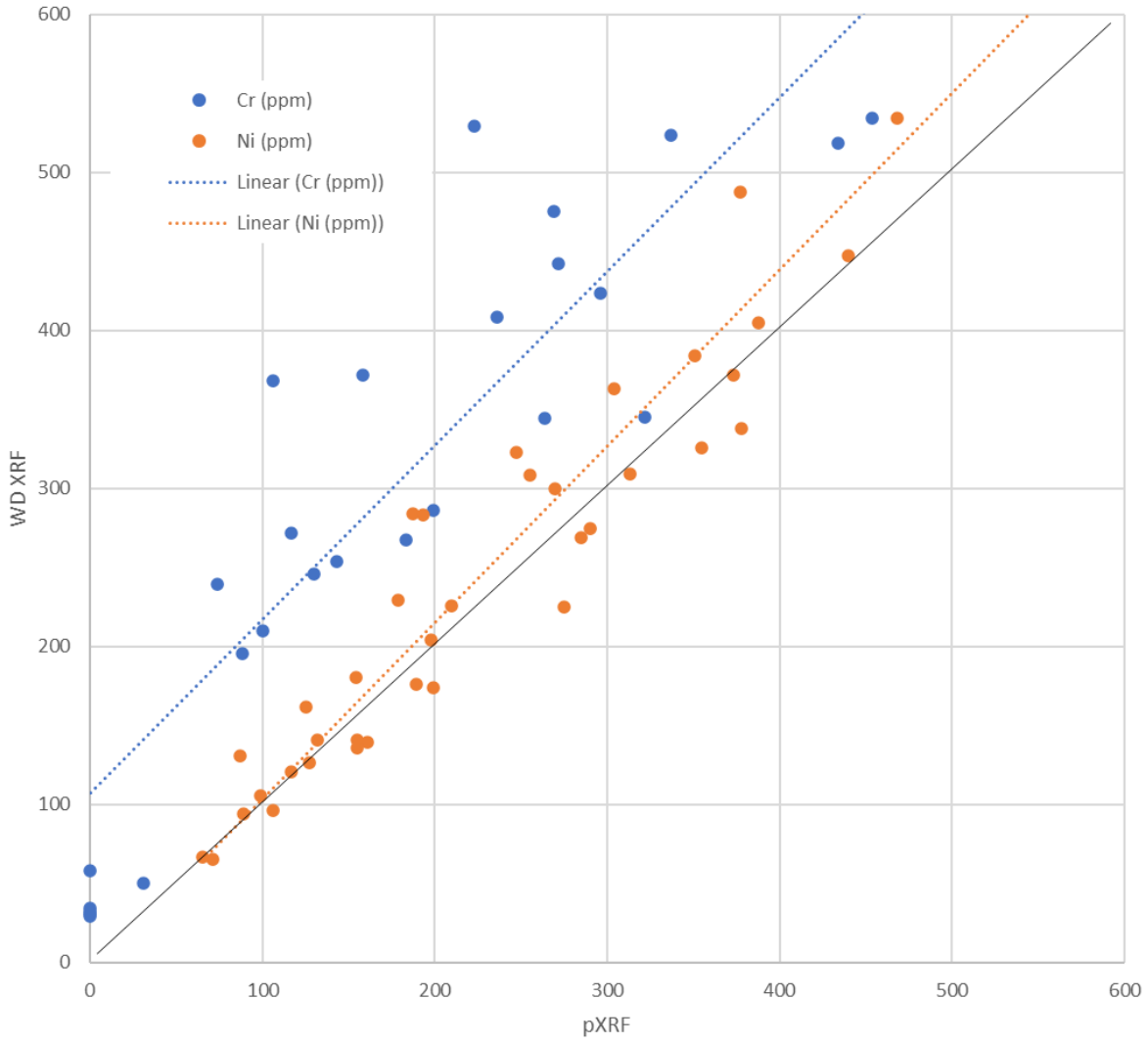

Figure 2.7. Comparative plot of Cr and Ni values determined by handheld pXRF and WD-XRF with associated trendlines and 1:1 line for comparison

Figure 2.8 shows the correlation between pXRF and WD-XRF for Fe. In this plot, the correlation is fine (R^2 = 0.7340).

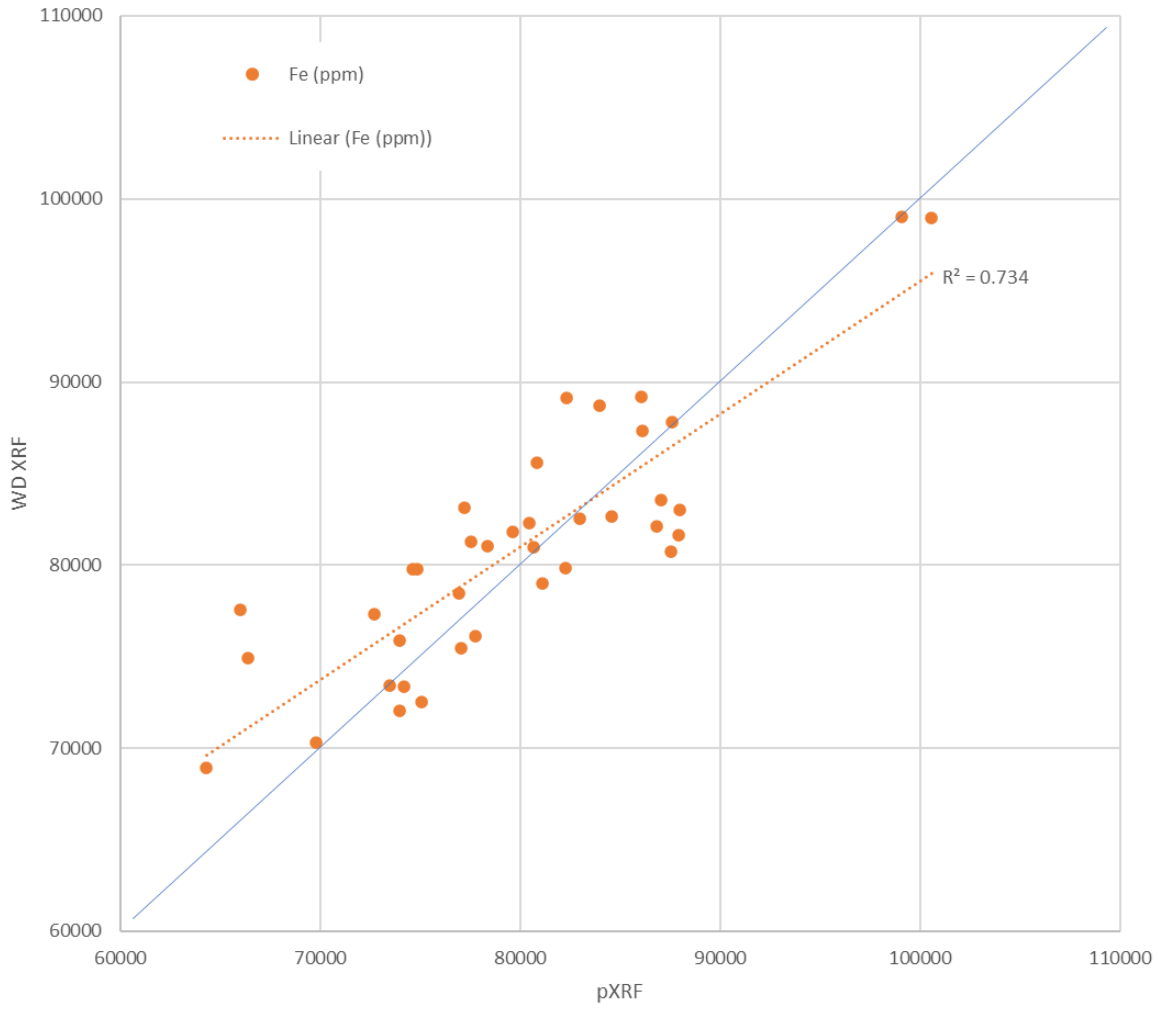

Figure 2.8. Comparative plot of Fe values determined by handheld pXRF and WD-XRF with trendline and 1:1 line for comparison

Figure 2.9 shows the correlation between pXRF and WD-XRF for Ti. In this plot, the correlation is good (R^2 = 0.8214) with slight under-reads for lower values (<4000 ppm).

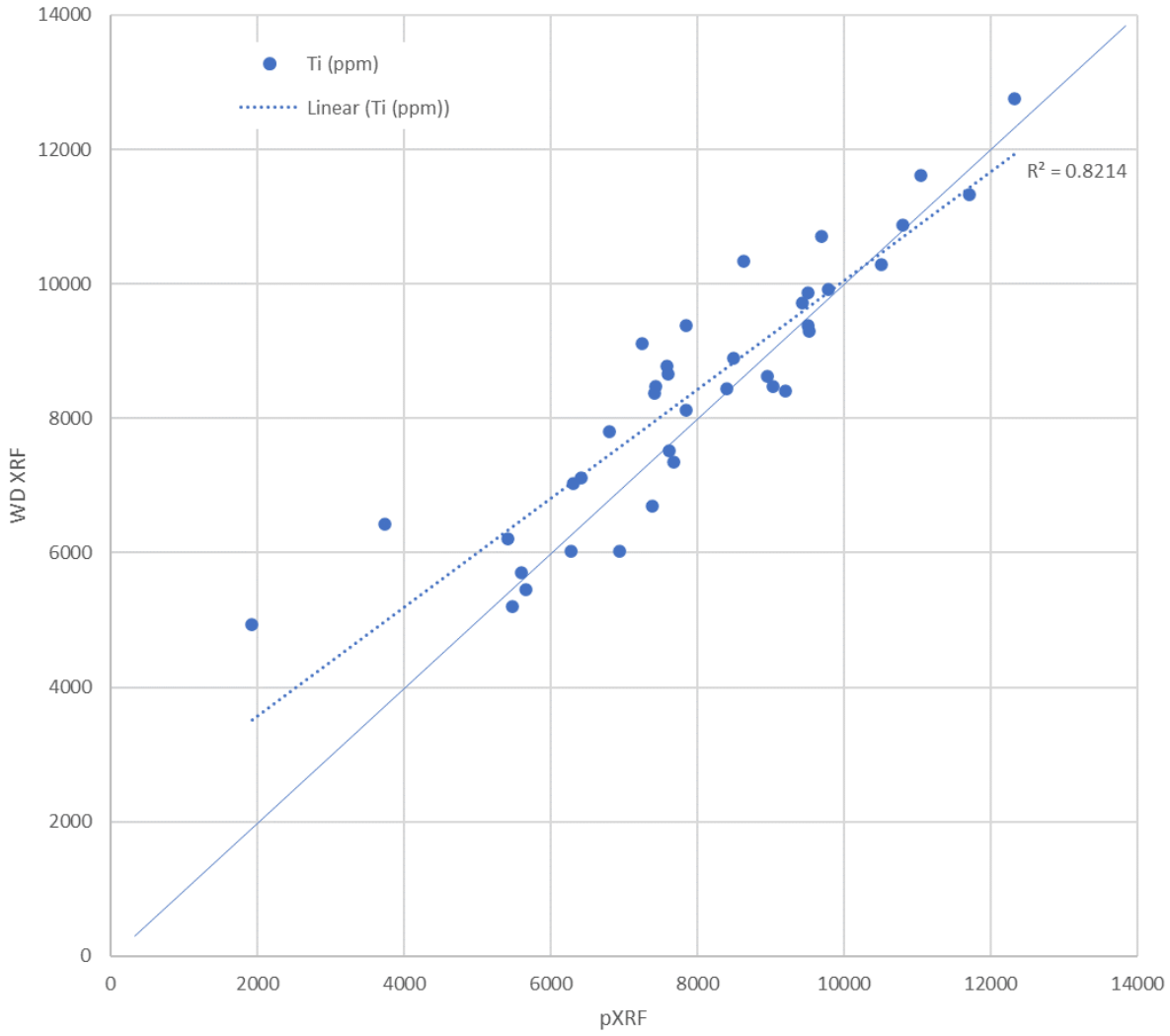

Figure 2.9. Comparative plot of Ti values determined by handheld pXRF and WD-XRF with trendline and 1:1 line for comparison

In addition to the comparative cross-plots, the WD-XRF data for boreholes NIRE 09/08-0001 and NIRE 02/08-0001 were plotted in WellCAD™ over the geochemical data from the same samples done by pXRF. The resulting plots have an extremely strong correlation, despite discrepancies in the absolute values (Appendix F). This means that the overall geochemical trends can be accurately determined by pXRF, especially when using ratios.

2.4 **Interbed geochemistry and palynology**

Further to the basalt lava flow samples, additional samples were collected from interbed horizons in boreholes NIRE 02/08-0001 and NIRE 09/08-0001 and several quarries and field locations for geochemical and palynological analysis (Fig. 2.10; Tables 2.11, 2.12, 2.13, 2.14).

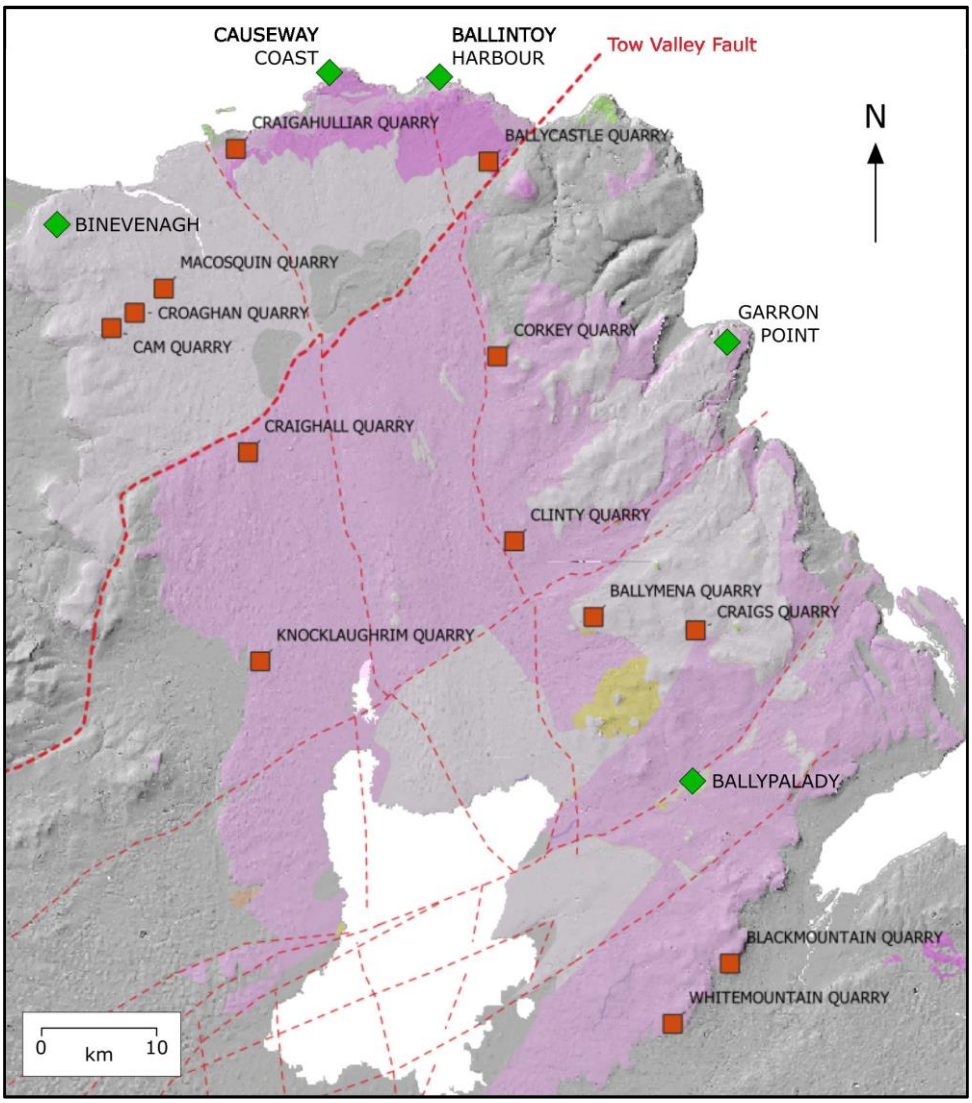

Figure 2.10. Map showing field locations (green diamonds) and quarries (red squares). Dashed red lines show faults.

Table 2.11. Interbed samples from NIRE 02/08-0001 and NIRE 09/08-0001

Location	Easting	Northing	Depth	ID	Comment
NIRE 09/08-0001	294362	434582	9.8-9.85	ABC008	clay/tuff?
NIRE 09/08-0001	294362	434582	103-103.02	ABC010	clay vein
NIRE 09/08-0001	294362	434582	144.6-144.63	ABC011	clay horizon?
NIRE 09/08-0001	294362	434582	245	ABC012	?
NIRE 09/08-0001	294362	434582	253.9	ABC013	clay/ash
NIRE 09/08-0001	294362	434582	254.1	ABC014	organic material
NIRE 09/08-0001	294362	434582	254.25-254.4	ABC015	laterite/palaeosol
NIRE 09/08-0001	294362	434582	254.5	ABC016	laterite/palaeosol
NIRE 09/08-0001	294362	434582	254.75	ABC017	palaeosol?
NIRE 09/08-0001	294362	434582	255	ABC018	palaeosol?
NIRE 09/08-0001	294362	434582	255.2	ABC019	?
NIRE 09/08-0001	294362	434582	255.5	ABC020	?
NIRE 09/08-0001	294362	434582	255.9	ABC021	palaeosol/basalt?
NIRE 09/08-0001	294362	434582	257.25	ABC022	palaeosol/basalt?
NIRE 09/08-0002	290853	434532	132.5	ABC023	lignite?
NIRE 09/08-0002	290853	434532	133.1	ABC024	sediment/lignite?
NIRE 09/08-0002	290853	434532	133.35	ABC025	clay
NIRE 09/08-0002	290853	434532	133.7	ABC026	lignite?
NIRE 09/08-0002	290853	434532	134.1	ABC027	clay
NIRE 09/08-0002	290853	434532	134.9	ABC028	clay
NIRE 09/08-0002	290853	434532	137.7	ABC029	red laterite
NIRE 02/08-0001	316129	412540	45.5-45.7	ABL001	lignite
NIRE 02/08-0001	316129	412540	49.8-50	ABL002	lignite
NIRE 02/08-0001	316129	412540	48.5	ABL003	lignite
NIRE 02/08-0001	316129	412540	84.9-85.2	ABC001	clay/tuff?
NIRE 02/08-0001	316129	412540	377.1	ABC002	clay/tuff?
NIRE 02/08-0001	316129	412540	377.28	ABC003	clay
NIRE 02/08-0001	316129	412540	399.5	ABC004	palaeosol?
NIRE 02/08-0001	316129	412540	404.8	ABC005	carbonaceous material
NIRE 02/08-0001	316129	412540	424.05	ABC006	carbonaceous material
NIRE 02/08-0001	316129	412540	328.75-328.8	ABC007	soil/clay?

Table 2.12. Interbed samples from visited quarries and field locations (greyed samples were unviable for analysis)

Location	Easting	Northing	Sample ID	Comment
Whitemountain Quarry	323575	367790	LAT001	laterite
Craig's Quarry	325455	400025	LAT002	L3
Craig's Quarry	325455	400025	LAT003	L1
Craig's Quarry	325455	400025	LAT004	L2
Clinty Quarry	310615	407330	LAT005	L1
Clinty Quarry	*310615*	*407330*	*LAT006*	*L2*
Clinty Quarry	310615	407330	LAT007	L3
Corkey Quarry	309250	422470	LAT008	odd unit over Clay with Flints
Ballycastle Quarry	308513	438418	LAT009	red laterite between basalt flows f1-f2
Ballycastle Quarry	308513	438418	LAT010	burned unit between basalt flows f1-f2
Croaghan Quarry	279590	426035	LAT011	laterite 'dome'
Binevenagh	268724	430196	LAT012	between B1 and B0
Binevenagh	268724	430196	LAT013	top of package 6
Cam Quarry	277700	424790	LAT014	L1

Location	Easting	Northing	Sample ID	Comment
Cam Quarry	277700	424790	LAT015	L2
Macosquin Quarry	281975	428020	LAT016	L1 (between f1 and f2)
Craigall Quarry	*288865*	*414600*	*LAT017*	*L3*
Craigall Quarry	288865	414600	LAT018	L3
Craigall Quarry	288865	414600	LAT019	L3
Knocklaughrim Quarry	289850	397485	LAT020	basal laterite
Ballymena Quarry	317094	401111	LAT021	L2
Ballymena Quarry	*317094*	*401111*	*LAT022*	*L1*

The interbed samples presented above were sent to MB Stratigraphy for sample preparation involving crushing, demineralisation, sieving and mounting on glass slides before being sent to the University of Aberdeen for palynological analysis (see Chapter 4 for a detailed description of preparation and analysis). The analytical process revealed the presence or absence of palynospores within the samples, which in turn were identified to aid with environmental, ecological and climatic interpretation.

2.5 **Fieldwork**

Outline

The following field trips were made to Northern Ireland during this research (Table 2.13).

Table 2.13. Field trip timing and duration

Trip #	Start date	End date	Duration	Comment
1	Nov 2019	Nov 2019	3 days	GSNI orientation
2	Oct 2020	Nov 2020	1 month	Fieldwork
3	Oct 2021	Oct 2021	1 week	Fieldwork
4	Apr 2022	May 2022	10 days	Fieldwork
5	Feb 2023	Feb 2023	5 days	Fieldwork

Quarries

The primary reason for choosing to visit quarries to inspect and sample the Antrim Lava Group was to avoid sampling the natural outcrops of Northern Ireland. Responsible

geological sampling should always aim to leave no trace, and thereby avoid causing any upset to local residents or visitors to the area. Additionally, permissions to access private land would need to be obtained in writing, a process that would not have fit within the planned schedule. Active quarries also have H&S regulations in place, be more likely to respond to access requests, and also have fresher basalt surfaces for inspection.

According to GSNI data there are 221 active quarries across Northern Ireland, of which 64 are within the area of interest, i.e. encounter the Antrim Lava Group. 36 are listed as active, 26 as inactive, and 2 have the unknown status "H". After considering their location, excavated lithologies and spatial distribution, I chose the following 11 quarries to approach for permission and assigned each a factor of perceived importance relative to the research goals. Namely, this process identified quarries close to Lonmin (NI) Plc boreholes to enable comparative analysis, or quarries at a reasonable distance from those boreholes to provide wider coverage.

Importance	Name	Postcode
Critical	Craighall Quarry	BT51 5XR
Critical	Corkey Quarry	BT44 9JQ
High	Robinson Quarry Masters (Craig's)	BT42 4RE
High	Clinty Quarries	BT43 6SS
High	Knocklaughrim Quarry	BT45 8QA
High	Ballycastle Quarry	BT54 6JE
High	Croaghan Quarry	BT51 4PS
Helpful	Northstone Ballymena Quarry	BT42 4RB
Helpful	Whitemountain Quarry	BT28 3QY

Field locations

Four field locations were visited; the Giant's Causeway, Ballintoy Harbour, Binevenagh and Garron Point (Figure 2.11a, b, c & d). The Giant's Causeway exposes LBF and IBF (CTM and

Port na Spaniagh) and at Ballintoy the stratigraphic equivalents are potentially exposed. The aim was to test this correlation geochemically. The escarpment at Binevenagh exposes multiple basalt flows and palaeosol interbeds. The stream section exposed at Garron Point reveals multiple basalt flows in volcanostratigraphic succession. Fieldwork at these sites involved sampling and field mapping.

Figure 2.11. Field locations visited. a. Garron Point. b. Ballintoy Harbour. c. Causeway Coast. d. Binevenagh


b


c

2.6 Geophysics

GSNI provided geophysical data in *.las format for nine boreholes across the study area, including Annaghmore, Ballymacilroy, Ballynamullan, Ballynure, Ballytober, Drumcross, Killary Glebe, Port More, Salmon Hatchery. The data types included a selection of downhole measurements including caliper, gamma ray, velocity, neutron density, and porosity. The geophysical data were uploaded to WellCAD™ and are presented in Appendix N.

CHAPTER 3 – ANTRIM LAVA GROUP GEOCHEMISTRY

3.1 Introduction

The geochemistry of the Antrim Lava Group has long been the subject of scientific investigations (Patterson & Swaine, 1955; Patterson & Mitchell, 1955; Walker, 1959; Lyle & Thompson, 1983; Kitchen, 1984; Lyle, 1985; Francis et al., 1986; Lyle, 1988; Lyle & Patton, 1989), which have generally agreed that the major and minor element geochemistry of the Lower and Upper Basalt Formations are too similar to provide any significant tools for distinguishing between them. Efforts to identify trends or signatures from the isotopic and trace / rare earth element composition of the lavas yielded useful information about their likely source zones and the condition of the lower crust at the time of melt generation, and some fractionation trends were tentatively identified (Lyle, 1988) but not such a distinct signal that a random basalt sample from the ALG could be analysed in the laboratory and then assigned with reasonable confidence to either the Lower or Upper Basalt Formation. Geochemical investigations of the volcanostratigraphy of other NAIP subprovinces have used basalt geochemistry to identify magmatic signatures of flow groups, thereby offering the potential to correlate lavas across a larger area than defined by each flow within a flow field (e.g. Millet et al, 2017).

3.2 Limitations

As already mentioned in Chapter 2, using pXRF tools for precise fieldwork currently has some key drawbacks:

- no compositional data for sodium;
- compositional data for magnesium is recognised to be of low quality
- compositional data for potassium sporadically returns a zero result
- inconsistent geochemical datasets between Lonmin boreholes

- the variable error margin for elements can be larger than the result such that it can render the data unusable for correlation;

To fully utilise the potential of the available pXRF data we had to be sure which elements, if any, could be used with a degree of confidence. To that end, the pXRF and WD-XRF data were generated on identical samples and the resulting cross-plots are presented further in this chapter. The limitation here is that finding a geochemical toolkit had to account for the weaknesses inherent in pXRF data, without losing confidence in the final data analysis in the process. This involved finding the set of elements that could be reliably analysed by the handheld XRF tool that offered some geochemical insights that could be applied to this research.

3.3 Methods

This chapter primarily presents the analysis of the whole rock geochemical data collected by pXRF from the Lonmin borehole cores and field outcrop samples. These data were investigated in an attempt to identify basaltic flow groups based on geochemically similar packages of adjacent flows and non-basaltic horizons (e.g. sedimentary deposits) and deeply weathered igneous rock (hereafter collectively referred to as interbeds).

The bulk of the available portable/handheld XRF (pXRF) data was gathered by Lonmin staff and provided for this research by GSNI (1923 sample points from 13 boreholes). As the focus of this research moved towards closer examination of the interbeds, several cores were re-analysed to gather geochemical information from specific horizons that had been previously overlooked.

This novel dataset, the first of its kind for the Antrim Lava Group, afforded geochemical information on a resolution hitherto unavailable for this kind of research. Here we present

an analysis of pXRF geochemical data measured from the Lonmin borehole core by Lonmin staff and by using GSNI equipment. In addition, a selection of field samples were analysed for comparison.

The chosen pXRF geochemical data (Ti, Fe, Cr, Ni, Zr, and Rb/Sr) were plotted vertically in WellCAD™ (software manufactured by Advanced Logic Technology) alongside graphic logs of the stratigraphy from the geological logs. The top part of an example is shown in Figure 3.1, while the entire series of plots can be found in Appendix A.

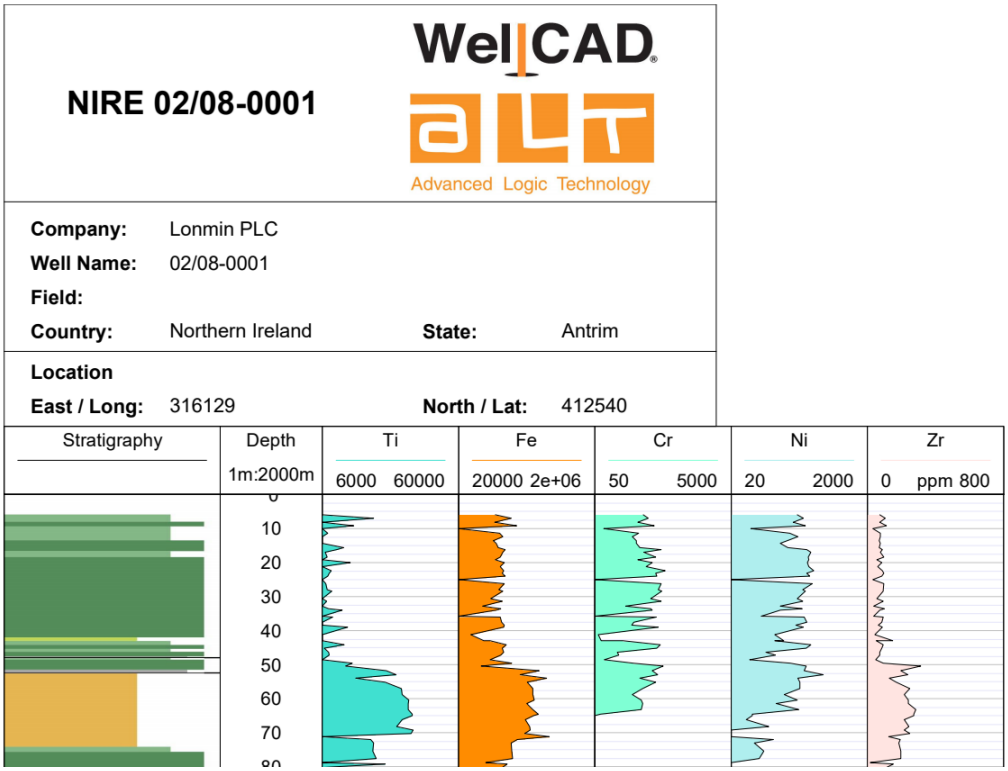

Figure 3.1. An example of the plotting of geochemical and stratigraphic data in WellCAD™

Chemostratigraphy examines chemical variations within (usually barren) sedimentary sequences in order to establish chemical stratigraphy and stratigraphic relationships for correlation (Berger & Vincent, 1981; Ramkumar, 2015). This geological tool can broadly be applied to extrusive igneous systems because magma tends to chemically evolve over time and lava flows generally follow the law of superposition (Millett et al., 2017). The notable

exception to this rule is that magma has the capacity to intrude, inflate and assimilate existing strata and earlier lava flows, thus potentially creating chronological inaccuracies within the overall process. Bearing this in mind, and with a keen eye on the petrology, petrography and structure of the lavas, we aim to tentatively observe geochemical signatures throughout a lava pile to assess overall trends in lava geochemistry and thereby potentially reveal geochemical flow groups that can be correlated. This correlation could in theory be used to map individual lava flows, but given the relative chemical homogeneity of basaltic lavas, our focus here is on correlating packages of lavas with similar geochemical characteristics, rather than individual flows. The underlying assumption is that magmas erupted at a similar time or during the same phase of activity will be geochemically similar. This assumption may break down over large spatial scales but is something that can be tested here given our independent stratigraphic constraints on the major divisions of the ALG. For example, in other large igneous provinces lava flows have been traced for several hundreds of kilometres. The Frenchman Springs Member of the Wanapum Basalt (Columbia River Basalt Group) has been traced over 750 km, largely by virtue of that flow being areally extensive and having a distinctive geochemical signature (Martin et al, 2013).

The key aims of examining the geochemical data of the Antrim Lava Group rocks are:

1. The identification of sedimentary and deeply weathered rocks, i.e. interbeds;
2. To understand the geochemical signature(s) of basalts and basaltic flow groups in order to define packages for correlation;
3. to understand how the ALG evolved over time and between the currently defined LBF, Interbasaltic Formation/Causeway Tholeiite Member, and UBF.

In Chapter 2, the acceptably robust relationship between portable XRF data and laboratory WD-XRF data was shown. The following plots, etc. make use of both pXRF and WD-XRF data sets as required.

3.4 Results

3.4.1 Whole rock geochemistry of the Antrim Lava Group

The basalts of the upper and lower ALG are traditionally regarded as hypersthene/olivine-normative basalts of Hawaiian alkalic or tholeiitic type (e.g Lyle, 1979; Lyle 1985). The basalts within the Interbasaltic Formation have been classified as quartz-normative basalts of tholeiite type (e.g Lyle, 1979). The data presented here are generally in agreement with preceding work (Figure 3.2a and b).

The presence of basaltic andesite in the Causeway Tholeiite Member (Figure 3.2a & c) has already been noted by Francis et al. (2009).

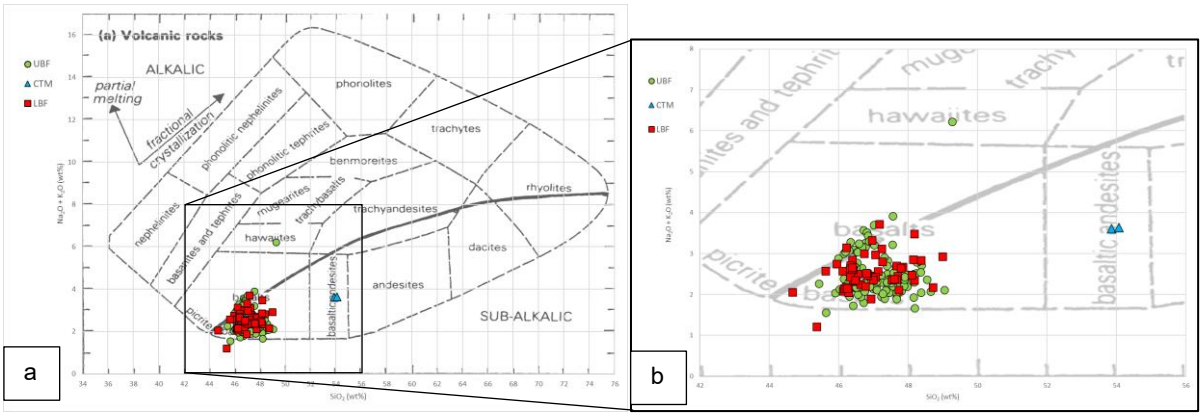

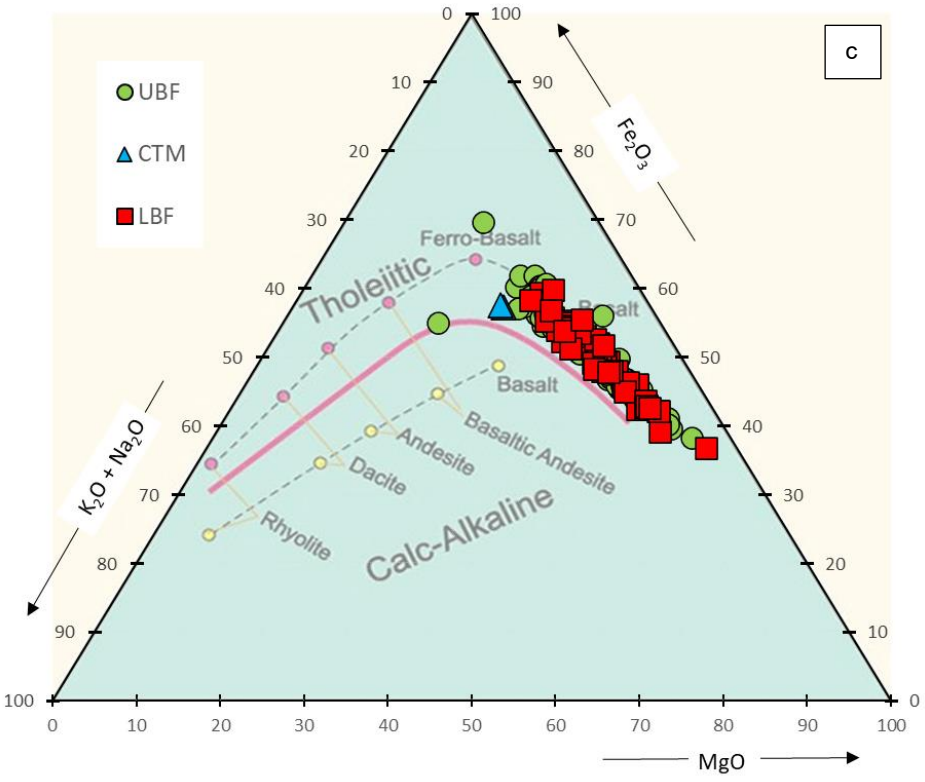

Figure 3.2a. Total alkalis vs silica (TAS) diagram showing WD-XRF data from Lonmin core and outcrop samples. data credit: Dr Elliot Carter, post-doctoral researcher at TCD). b. Expanded detail from TAS diagram in Figure 3.2a. c. AFM diagram showing WD-XRF data from the same Lonmin core and outcrop samples.

The basalt samples responsible for the geochemical data plotted in Figure 3.2 were collected from quarries and field locations by Dr Elliot Carter, and from borehole cores NIRE 02/08-0001 and NIRE 09/08-0001 (see Figure 2.1) by Adam Beresford-Browne. The plotted data were generated by WD-XRF analysis carried out at Trinity College, Dublin by Dr Elliot Carter. The majority of continental flood basalts (CFBs) are quartz tholeiites with SiO_2 values between 49 and 55% (La Bas et al., 1986; Middlemost, 1994), so it is noteworthy that nearly all of our samples (97.7%) have less than 49% SiO_2, and plot close to the boundary with picritic basalt (ultramafic) type on the TAS figure (Figure 3.2a and c), as this deviation from 'normal' CFB composition doesn't seem to have been discussed in much detail to date. This would interest those researching the temperature and mechanics of the NAIP source melt

zone, as picritic basalts suggest higher temperature source melts, but that largely falls outside the scope of this work. Our interest would be constrained to finding information on the pulsing of magma or melting (Jones et al., 2019) that might add another thread of data to our model of emplacement timing. The principal observation from Figure 3.3 is that the UBF is systematically shifted to slightly higher SiO_2 values than the LBF; a trend we examine further with trace element data below. Although Figure 3.3 is just based on borehole samples, where the relative stratigraphic division into lower and upper units is clear, a similar pattern is observed when the same data are plotted to include field samples based on their assigned stratigraphy.

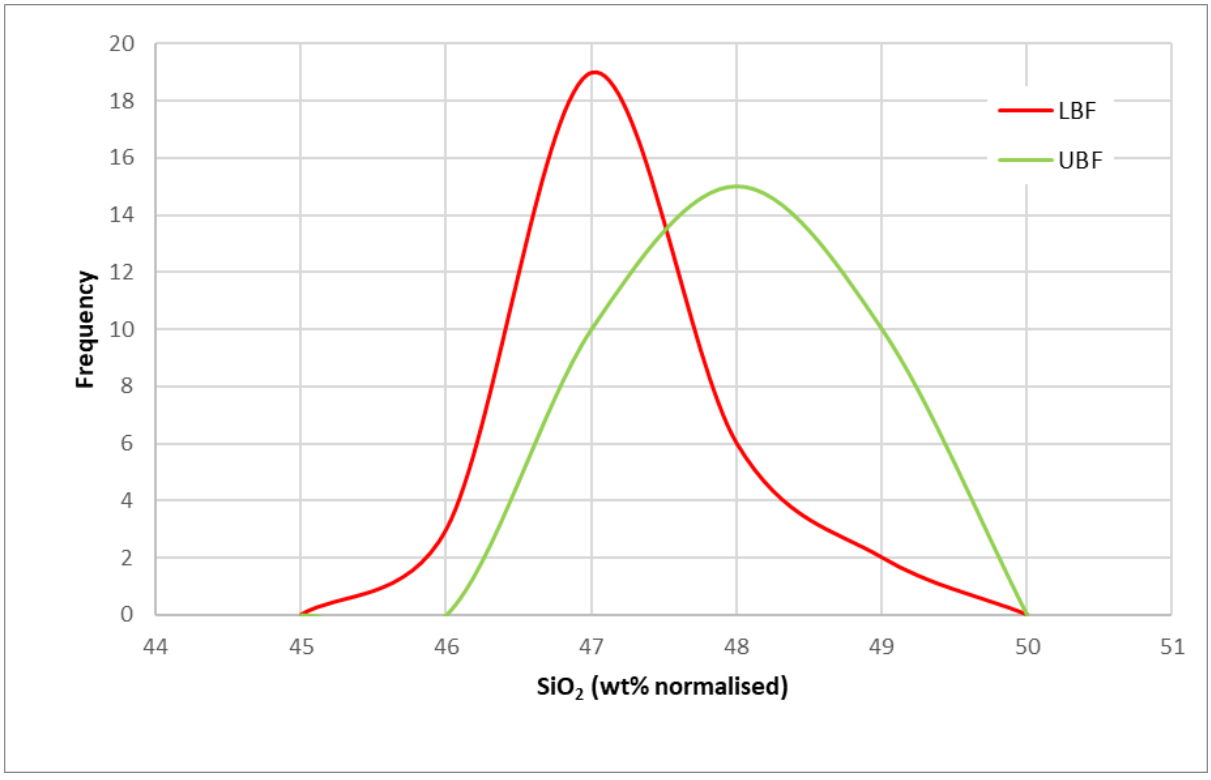

Figure 3.3. The distribution of SiO_2 values in fresh borehole core samples. n = 65 (data credit: Dr Elliot Carter, TCD). Here we only plot data for two key boreholes (NIRE 02/08-0001 and NIRE 09/08-0001), where the stratigraphic division into UBF and LBF is as unequivocal as possible within the current understanding of emplacement.

3.4.2 CIPW Norm Calculations

Using an online CIPW Norm Calculation tool (at internet: CIPW Norm Calculation (smith.edu)) we have calculated the normative mineralogy for averaged fresh basalt sample values generated by WD-XRF on the borehole core and quarry outcrop samples (Table 3.1). The Causeway Tholeiite Member is clearly distinctive in terms of normative quartz. The normative mineral values for the UBF and LBF are almost identical, with the marked exception of normative quartz being an order of magnitude higher in the Upper Basalt Formation.

Table 3.1 CIPW norm results

Upper Basalt Formation (n = 120)		**Causeway Tholeiite Member (n = 2)**		**Lower Basalt Formation (n = 52)**	
Plagioclase		**Plagioclase**		**Plagioclase**	
- anorthite	33.5 %	- anorthite	25.4 %	- anorthite	32.4 %
- albite	19.2 %	- albite	23.4 %	- albite	18.5 %
Pyroxene		**Pyroxene**		**Pyroxene**	
- Hypersthene	20.8 %	- Diopside	11.9 %	- Hypersthene	22.5 %
Hematite	12.4 %	Quartz	11.9 %	Hematite	12.6 %
Pyroxene		Hematite	11.7 %	**Pyroxene**	
- Diopside	8.2 %			- Diopside	8.2 %
Titanite	2.9 %	**Pyroxene**		Titanite	3.4 %
		- Hypersthene	7.2 %		
K-Feldspar		**K-Feldspar**		**K-Feldspar**	
- Orthoclase	1.6 %	- Orthoclase	5.1 %	- Orthoclase	1.6 %
Quartz	0.7 %	Titanite	2.5 %	Ilmenite	0.4 %
Ilmenite	0.4 %	Ilmenite	0.4 %	Apatite	0.4 %
Apatite	0.4 %	Apatite	0.4 %	Quartz	0.04 %

3.5 pXRF analysis of ALG samples

Only a limited number of elements were found to be reliable following our comparison of pXRF and WD-XRF data (Chapter 2). Of the elements found to be reliably measured using pXRF, we found that Zr and Ti values obtained by WD-XRF showed the greatest degree of variation down borehole (i.e. through the lava pile). Despite having lower reliability, K values also showed a significant variation down borehole that appeared related to other elemental

shifts, rather than scatter. In addition, elemental plots of K and Ti against depth from NIRE 02/08-0001 and NIRE 09/08-0001 improved the variations between Lower and Upper Basalt Formations but the signal is not particularly clear. The ratio of K to Ti produced a more convincing suggestion of the difference between the basalts of the Lower Basalt Formation and the Upper Basalt Formation. An elemental plot of Zr against depth shows a distinct drop as we move from the Lower to the Upper Basalt Formation, similar to that of Ti. As they both show a similar trend, we used the product of Ti and Zr to amplify the drop in concentrations from Lower to Upper Basalt Formations; however, this parameter does not reveal interbeds to an observable resolution (Figure 3.4).

Figure 3.4 Summary geochemical data vs depth for NIRE 09/08-0001 (north of the Tow Valley Fault) plotted using WellCAD™. The Interbasaltic Formation is highlighted by the orange box. Stratigraphy key in Appendix A.

The ratio of Ba to Sr reveals interbeds and weathered horizons but does not show a significant difference between Lower and Upper Basalt Formations. The ratio of Zr to K/Ti reveals interbeds at a higher resolution than that shown by the ratio of Ba to Sr, and also suggests a clear difference between the values in the Lower and Upper Basalt Formations (Zr/KTi column in Figures 3.4 and 3.5).

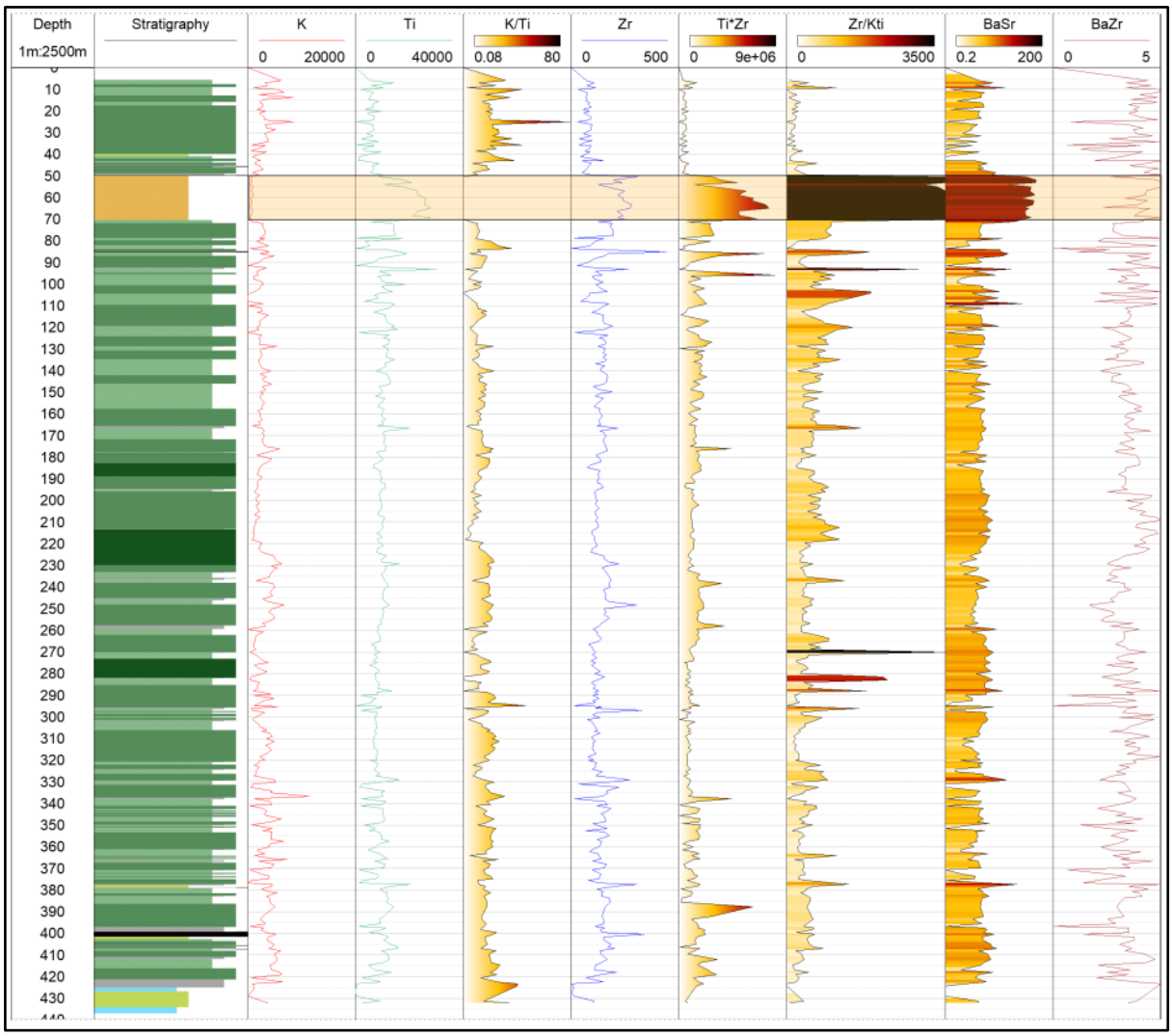

Figure 3.5 Summary geochemical data vs depth for NIRE 02/08-0001 (south of the Tow Valley Fault) plotted using WellCAD™. The Interbasaltic Formation is highlighted by the orange box. Stratigraphy key in Appendix A.

The ratio of Ba to Zr can be used as a proxy for isotopic signatures for crustal contamination of NAIP magmas (Fitton et al., 1998; Kerr, 1995). Ba/Zr values greater than 1-2 may suggest crustal contamination. With few exceptions we can surmise that almost all of the analysed ALG basalts have Ba/Zr ratio values greater than 3 so may well indicate significant levels of crustal contamination. Certain horizons have a Ba/Zr ratio <1, which could suggest minimal crustal contamination but as many of these horizons coincide with apparent or identified interbeds (i.e. deeply weathered) it is not possible to draw any firm conclusions. A more targeted study into this relationship is required in order to more fully explore the possibility of whether uncontaminated magma occasionally had a pathway from source to surface during the emplacement of the ALG basalts.

3.6 Geochemical signature shift from LBF to UBF

In this section, we present a geochemical methodology that is applicable in the field by which a group of basalt flows can be assigned to either the Lower or Upper Basalt Formation with some confidence.

Using the elemental concentrations obtained by WD-XRF we tested the hypothesis that there could be systematic chemostratigraphic differences within the ALG, and found that across the hiatus responsible for the rocks of the Interbasaltic Formation there was a recognisable and significant change in the K, Ti and Zr signal from the Lower Basalt Formation to the Upper Basalt Formation lavas (Figure 3.6).

Using data from the two boreholes (Figure 3.6) with robust stratigraphic controls and WD-XRF the ratio of (Zr*Ti)/K shows a systematic distinction between the LBF (higher values) and UBF (lower values). This ratio was extended to our pXRF datasets to test if the pattern remained robust as a tool for stratigraphic discrimination despite the noted variation in the

reliability of K values obtained by pXRF. As shown in Figure 3.7, across all of the boreholes analysed by pXRF methods, the same signal is observed.

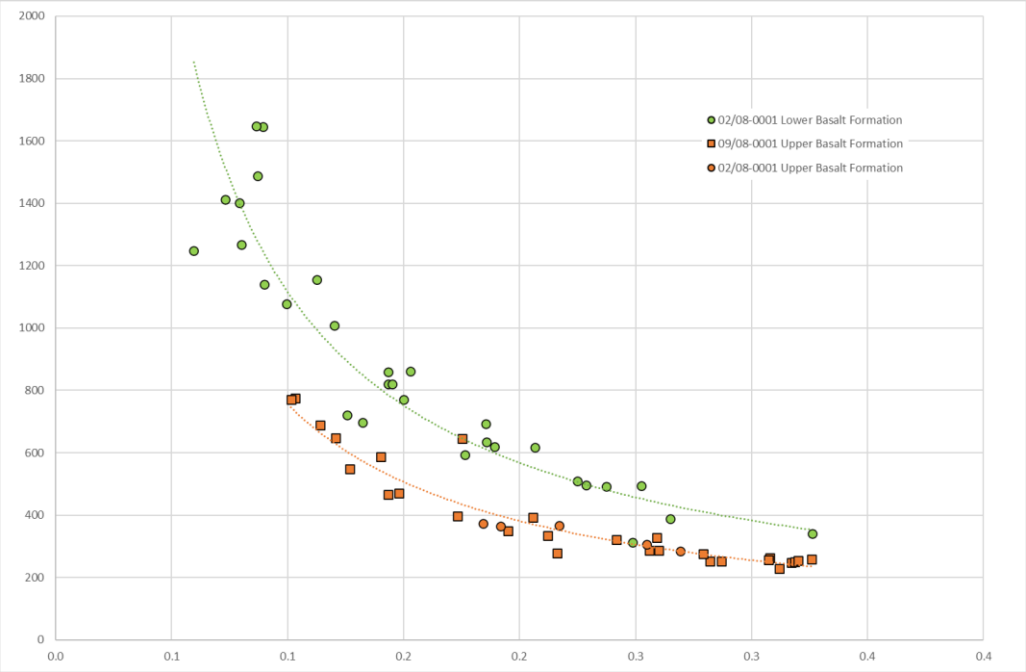

Figure 3.6. Signal variation between Lower Basalt Formation and Upper Basalt Formation lavas using WD-XRF data from NIRE 02/08-0001 and NIRE 09/08-0001. Both boreholes have a well-developed, thick, weathered horizon attributed to the hiatus responsible for the Interbasaltic Formation laterites to the north of the Tow Valley Fault.

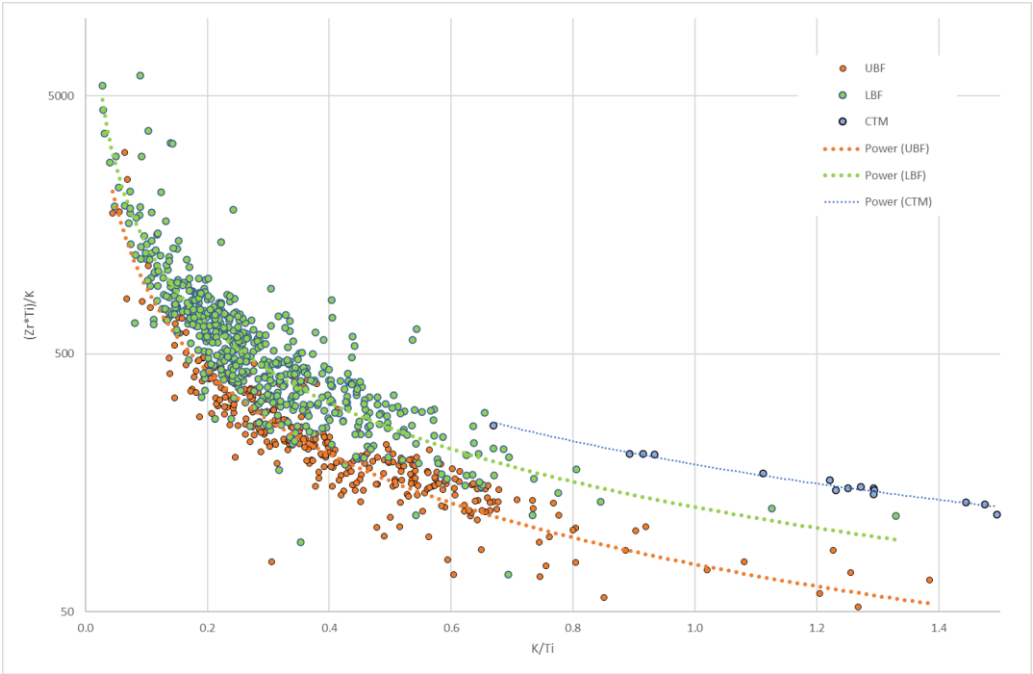

Figure 3.7. Signal variation between the Lower Basalt and Upper Basalt Formations using pXRF data from all NIRE boreholes based on pre-existing stratigraphic assignations. Note the string of data points with high K/Ti values that plot in the Lower Basalt field despite being assigned as Upper Basalt Formation, potentially indicating misidentification.

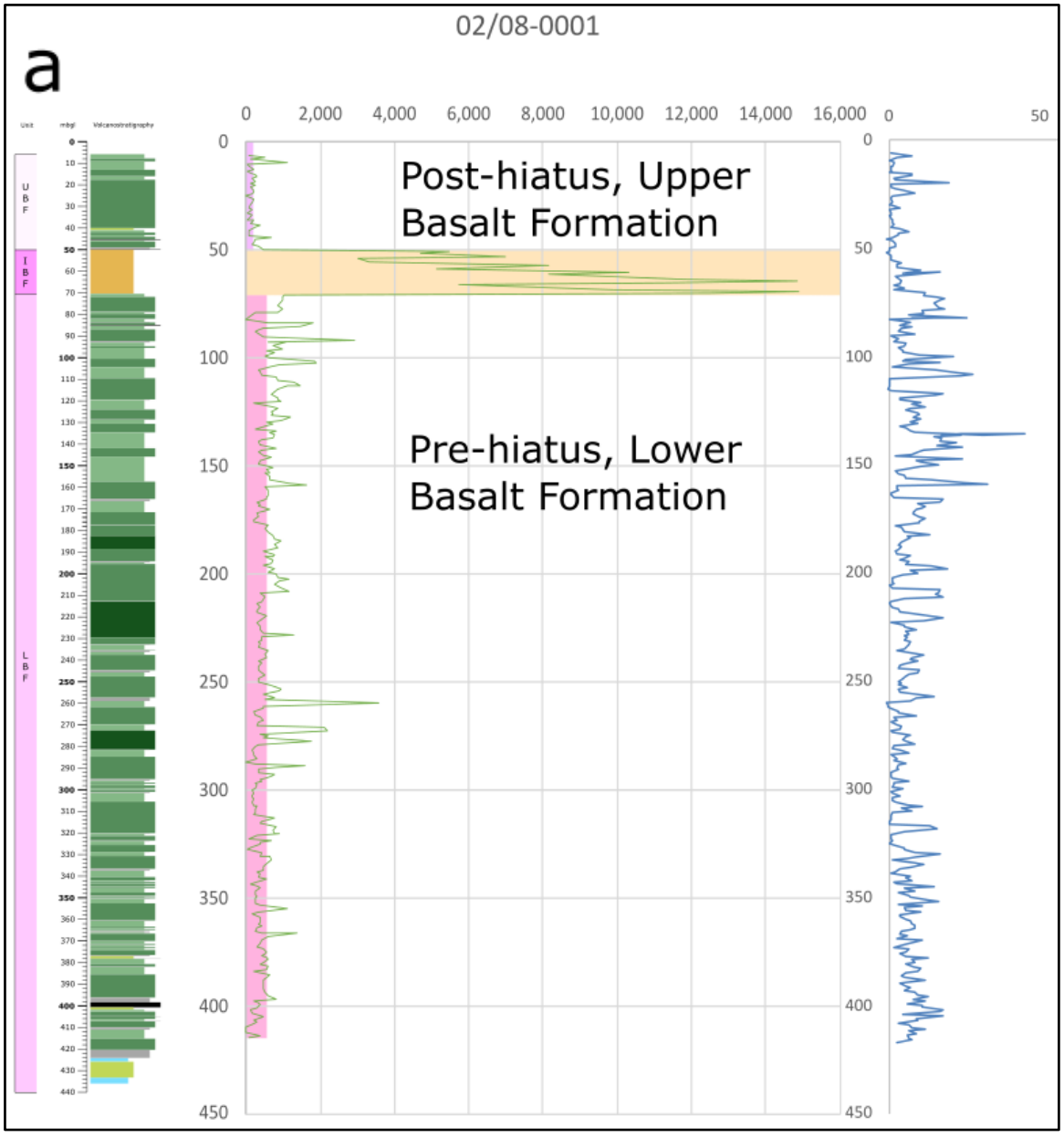

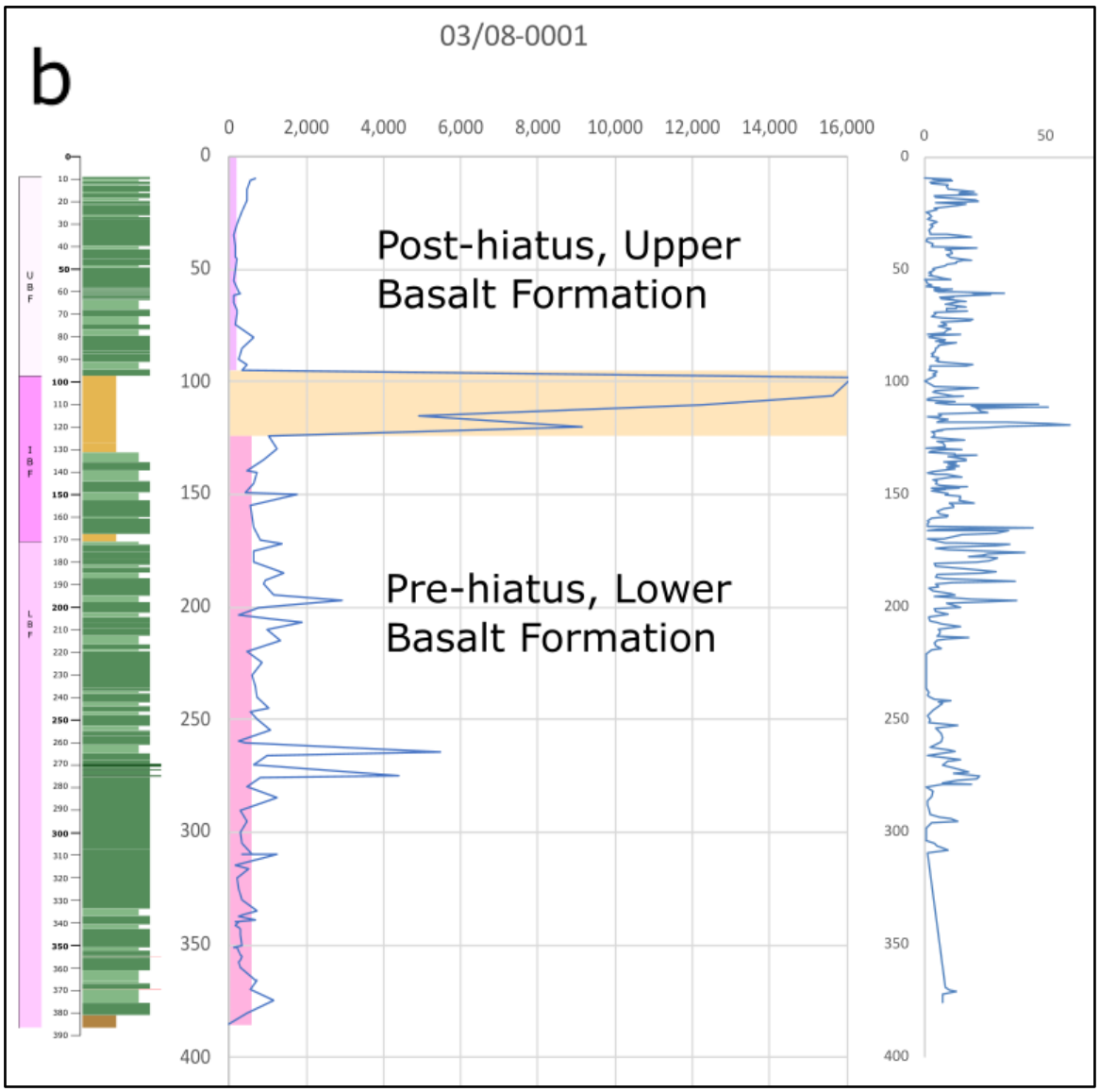
b
03/08-0001
0
2,000
4,000
6,000
8,000
10,000
12,000
14,000
16,000
0
50
0
50
100
150
200
250
300
350
400
Post-hiatus, Upper Basalt Formation
Pre-hiatus, Lower Basalt Formation
UBF
IBF
LBF

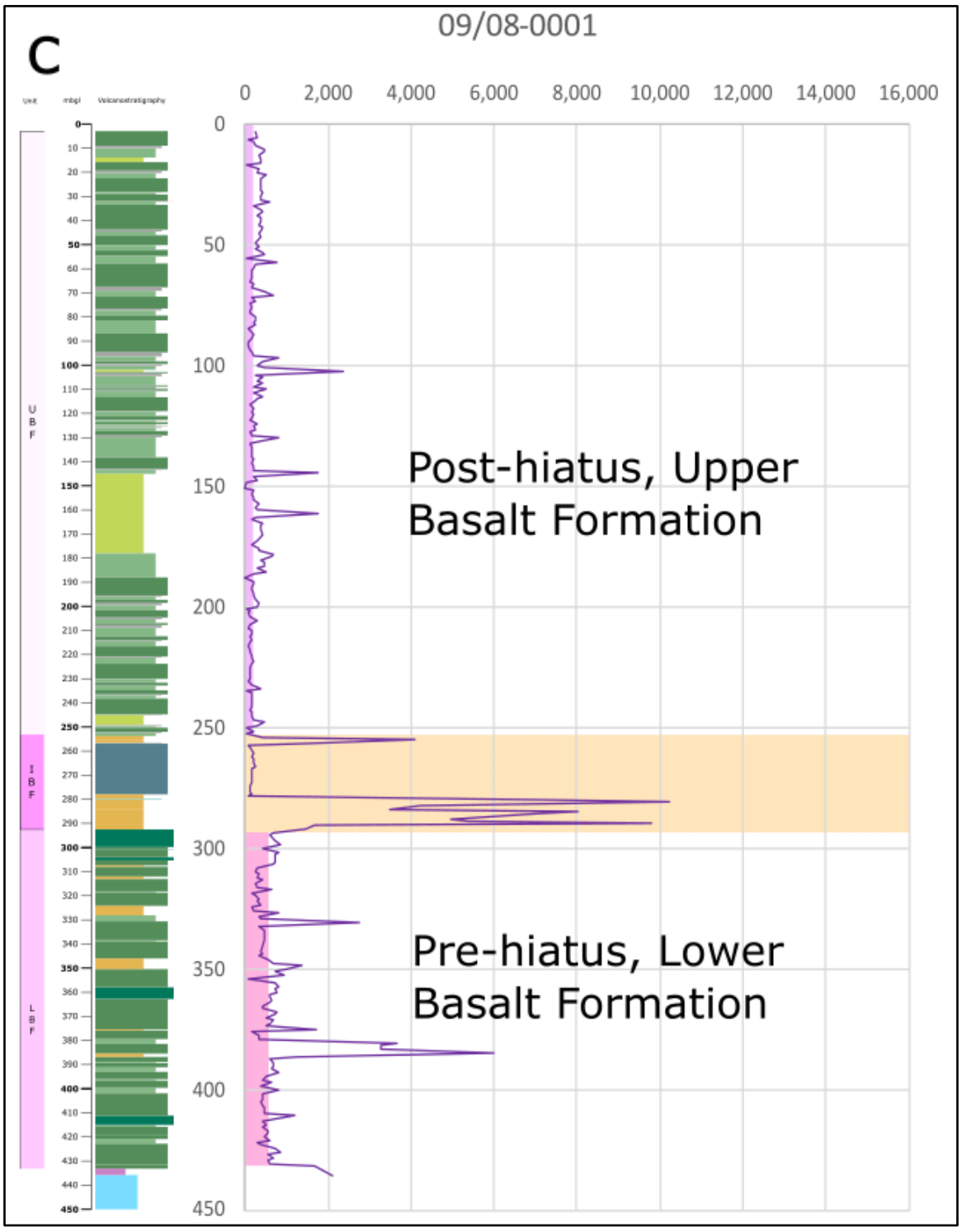
C
09/08-0001
0
2,000
4,000
6,000
8,000
10,000
12,000
14,000
16,000
Post-hiatus, Upper Basalt Formation
Pre-hiatus, Lower Basalt Formation
UBF
IBF
LBF

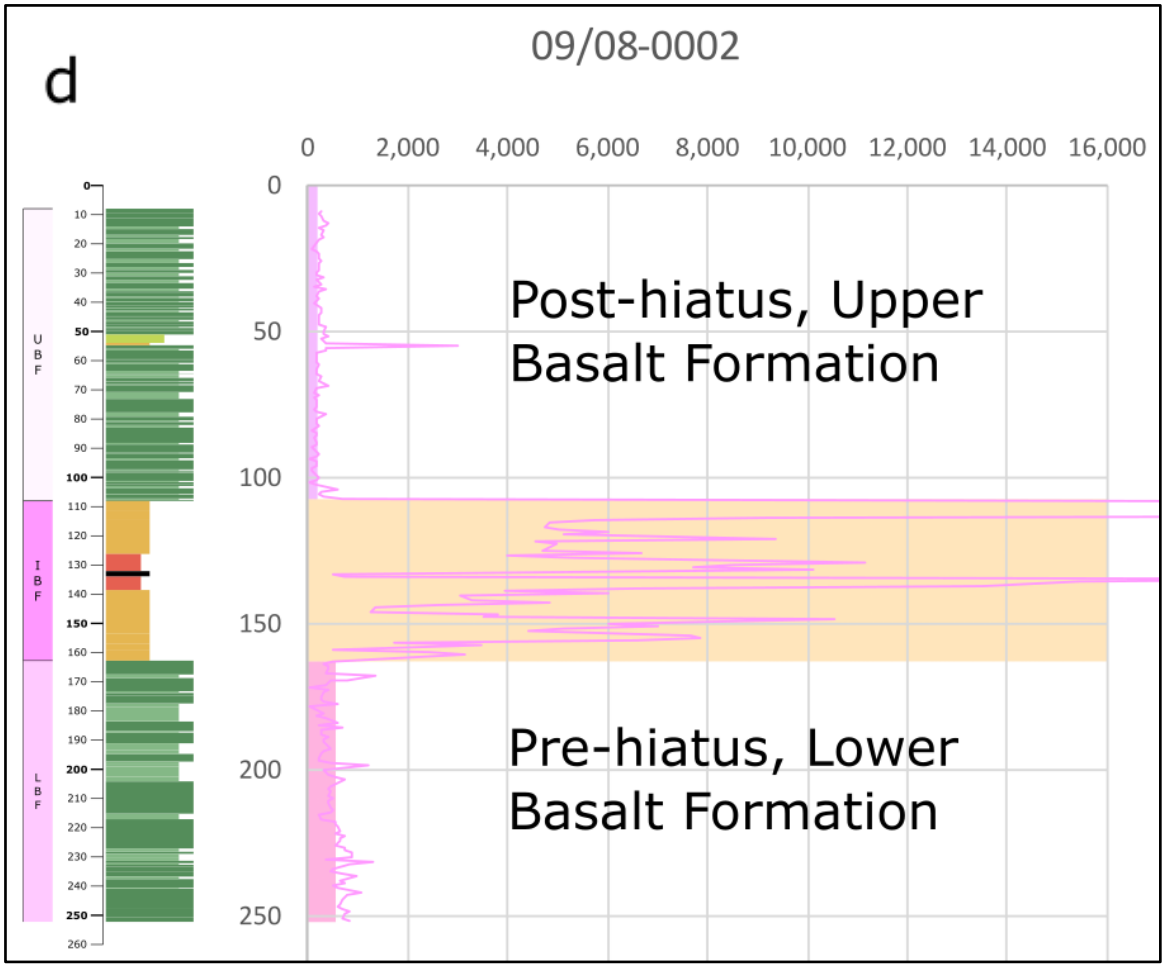

*Figure 3.8 Downhole plots for NIRE boreholes with identified Interbasaltic Formation strata, showing pXRF (Zr*Ti)/K signal change from LBF to UBF. The average values for LBF and UBF are represented by the pink blocks behind the green data plot. Magnetic Susceptibility readings are shown in the blue plot on the right. The horizontal pale yellow box denotes the interbasaltic period. (a) NIRE 02/08-0001. (b) NIRE 03/08-0001. (c) NIRE 09/08-0001. (d) NIRE 09/08-0002.*

This method also allows us to test the stratigraphic placement of sections that are missing robust stratigraphic control, e.g. those to the south of the Tow Valley Fault, especially those with no proximity to the thick lateritic horizons indicative of the Interbasaltic Formation (e.g. NIRE 02/08-0001 and 03/08-0001 in Figures 3.8a and b). Based on this we agree that the basalts of NIRE 11/08-0001 (Figure 3.9) are consistent with being of the Lower Basalt Formation, although no significant interbeds indicative of the Interbasaltic Formation were identified in this borehole core.

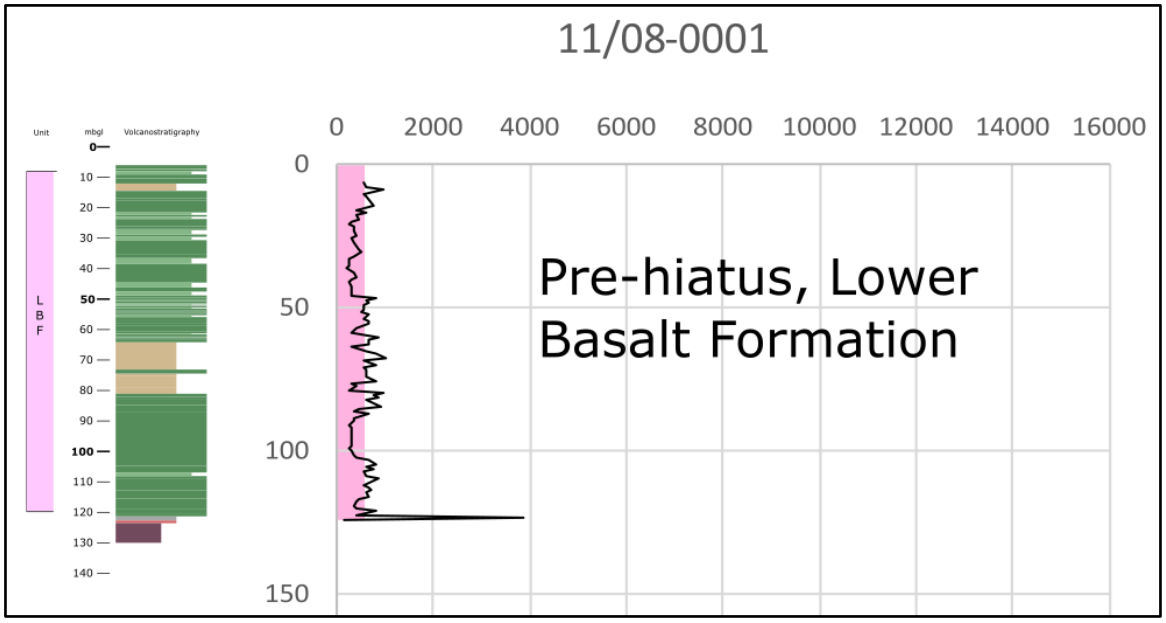

Figure 3.9. Ratio of Zr/(K/Ti) for NIRE 11/08-0001 showing a signal indicative of the Lower Basalt Formation (annotation).

3.7 Discussion

From geochemical data gathered across the NAIP (georoc.mpch-mainz.gwdg.de, 2023), there seems to be region-wide evidence of a drop in basalt Ti concentration related to the development of the North Atlantic spreading ridge and associated volcanic activity, from high (>1.5 wt%) to low (<1.5 wt%), as evidenced in Greenland and the Faroe Islands (Rohrman, 2022). Can this trend be identified within the basalts of the ALG? And if so, does the trend link neatly with the lengthy hiatus responsible for the rocks of the Interbasaltic Formation?

Initially, the WD-XRF geochemical data were plotted using standard, published cross-plots as a base reference. These included TAS and AFM diagrams already presented, as well as a host of other plots from publications on the topic of basalt geochemistry, including:

Zr v Ba, Zr v K2O, Zr v Nb, Zr v Cr

SiO2 v K2O

MgO v SiO2, MgO v Al2O3, Mgo v CaO, MgO v Total Fe

The process of identifying geochemical signatures within basalt flows and flow groups continued with a visual assessment of the data when plotted. Various cross-plots were built using Orange software (Python script GUI) to drill down into the underlying data to seek trends and patterns (e.g. Figure 3.10 below).

Figure 3.10 presents a plot of vanadium (ppm) against TiO_2 (wt%) with location labels and the data points colour-coded by their currently accepted stratigraphic formation. There is an immediately recognisable trend of low V, low Ti among the UBF samples and the reverse among those of the LBF. There are several samples that plot 'out of position' in regards to this trend, and given the regional shift from high Ti to low Ti across the lengthy hiatus in volcanic activity we might suppose that the samples from Garron Point, and Cam and Croaghan quarries (prefixed GS, CAM and CRO in the upper right quadrant of the plot) should be assigned to the Lower Basalts since they are all plotting well above 1.5 wt% TiO_2. However, the data plot reveals that these samples do not plot in sequence from high to low TiO_2 when put in stratigraphical order. This could mean that the geochemical story of the magma feeding the ALG was significantly different from that/those of Greenland and the Faroe Islands or that some basalts that were logged as flows in stratigraphic sequence were actually emplaced later as sills. Alternatively, it could point towards the effusion of lavas in smaller flow groups with their own, discrete geochemical trends.

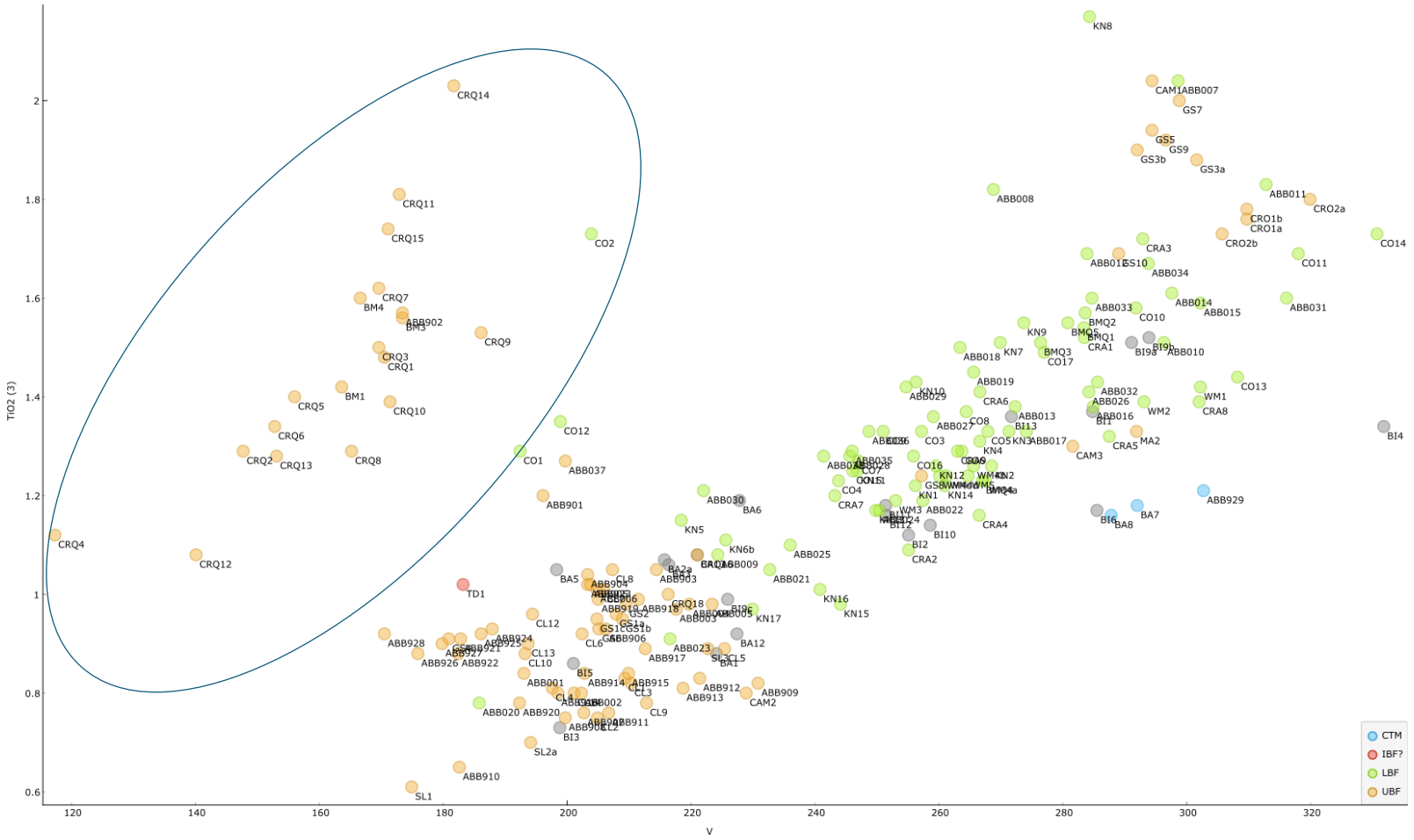

Figure 3.10. An example cross-plot of WD-XRF data using Orange software, highlighting the flexibility and investigative potential of the process. CTM = Causeway Tholeiite Member, IBF? = Interbasaltic Formation assumed, LBF = Lower Basalt Formation, UBF = Upper Basalt Formation. Samples in the blue oval are discussed in the text.

Interestingly, Figure 3.10 also shows the samples from Craig's Quarry and Blackmountain Quarry (within the blue oval) as plotting in a markedly different field to the rest of the sample locations. Three samples from Corkey Quarry along with a sample each from boreholes NIRE 02/08-0001 and 09/08-0001 plot toward that area. The strong trend shown may indicate a separate fractionation trend or evidence of crustal contamination but again the samples do not plot in a recognisable order compared to their stratigraphic positions in the field. We examined data plots for each borehole, in turn, using WellCAD software donated by ALT to identify patterns and trends within the plotted data visually.

More broadly, workers have attempted to use basalt geochemistry as a diagnostic indicator of their tectonic setting (Xia & Li, 2019), noting that we should be cautious if only using geochemistry to differentiate between continental intraplate basalts since contamination by continental crust or lithosphere can impart signatures akin to subduction settings, i.e. low Nb, low Ta and low Ti. Crustal contamination has also been noted to cause low Nb/La ratios of less than one (Xia et al., 2008).

With regards to the TAS plot, which showed many ALG basalts as being of ultramafic type, it is worth noting that these ultramafics are dispersed throughout the sequence with no obvious trend, which may be indicative of pulsing within the mantle plume that fed the system, *sensu* Jones et al. (2019).

One of the key similarities between the Lower and Upper Basalt Formations revealed by this research is that they are almost equally non-uniform. The variation in petrology and geochemistry between flows and flow groups is at times quite remarkable, whether in the Lower or Upper Basalt Formation. Of the 32 flows of the Lower Basalt Formation analysed by WD-XRF on samples from NIRE 02/08-0001 and NIRE 09/08-0001, 19 were clearly phyric and 5 were clearly aphyric. Of the 34 flows of the Upper Basalt Formation analysed by WD-

XRF on samples from NIRE 02/08-0001 and NIRE 09/08-0001, 21 were clearly phyric and 6 were clearly aphyric. Further understanding of the emplacement mechanisms is required in order to more fully appreciate how these features formed. The potential for exactly this is explored in later sections when we consider Icelandic eruptions and the range of basaltic lavas being erupted from fissure volcanism and how this has helped to model the volcanic plumbing under Iceland.

Anaerobic conditions are suggested by MIA results.

By applying calculations for the Mafic Index of Alteration to our WD-XRF data we found that the results suggested using the equation for reducing conditions since the results from the oxidising conditions equation suggested that the observably fresh basalt samples were more weathered than they appeared.

The equations for calculating the MIA under oxidising and reducing conditions are presented here:

$$MIA_{(Ox)} = 100 \times [(Al_2O_3 + Fe_2O_3)/(Al_2O_3 + Fe_2O_3 + MgO + CaO + Na_2O + K_2O)]$$

$$MIA_{(Re)} = 100 \times [(Al_2O_3)/(Al_2O_3 + Fe_2O_3 + MgO + CaO + Na_2O + K_2O)]$$

Using $MIA_{(Ox)}$ on 174 samples yielded a range of values from 45.10 to 68.47, with an average of 56.11. The observable samples were not considered to be as deeply (chemically) weathered as these values suggest and so the MIA equation for reducing conditions was applied.

Using $MIA_{(Re)}$ on 174 samples yielded a range of values from 22.05 to 37.22, with an average of 31.64. These values are more acceptable when compared to the observable sample integrity. Neither surface waters nor phreatic groundwaters would offer the reducing conditions required to explain these data. Palynological data point towards fairly shallow, anoxic lakes periodically covered with algal blooms. The generally very fine grade of sediments lining the bottom of these lakes would

have quickly gone from aerobic to anoxic within a few centimetres of depth. Anoxic groundwater generally requires a confined aquifer system so these large, shallow lakes may have been acting as confining layers for the groundwater system(s) below.

CHAPTER 4 – PALYNOLOGY OF THE ANTRIM LAVA GROUP

This chapter has been adapted from the following publication:

Depositional system and plant ecosystem responses to long-term low tempo volcanism, the Interbasaltic Formation, Antrim Lava Group.

Adam Beresford-Browne[1], David Jolley[2], John Millett[2,3] Carl Stevenson[1], Sebastian Watt[1], Rob Raine[4], Elliot Carter[5]

1. University of Birmingham, UK. 2. University of Aberdeen, UK. 3. VBER, Norway. 4. Geological Survey of Northern Ireland, UK. 5. Trinity College Dublin, Ireland. *correspondence (geologist@postmaster.co.uk)

This paper was first published in Geological Society of London Special Publication 547, 2023 "The Impacts of Igneous Systems on Sedimentary Basins and their Energy Resources". As lead author, the PhD candidate conceived and led the study. The main secondary contribution was from Professor David Jolley, who led the palynological analysis. All other co-authors contributed in other, more minor ways, as well as contributing to the final editing and writing of the paper.

4.1 Introduction

The predominantly basaltic rocks of the Antrim Lava Group in Northern Ireland were erupted during the formation of the North Atlantic Igneous Province (NAIP) and covered much of northeast Ireland during the Paleocene (Figure 4.1). Available chronostratigraphical evidence indicates that the Antrim Lava Group mainly erupted during the Danian and Selandian stages of the Paleocene (63.24–60 Ma, Wilkinson et al., 2017), part of Phase 1 of North Atlantic rifting (Knox & Morton, 1988; Jolley et al., 2021). The Antrim Lava Group is divided into three formations; the oldest and youngest of these, respectively termed the Lower and Upper Basalt formations (Patterson, 1955; Old, 1975), comprise olivine-normative basalt. Positioned stratigraphically between these lavas are the sedimentary and varied extrusive igneous rocks of the Interbasaltic Formation (Cole, 1912; Patterson, 1955; Old, 1975). This formation includes a series of quartz-normative tholeiitic basalts, termed

the Causeway Tholeiite Member, present predominantly (if not exclusively) to the north of the Tow Valley Fault, as well as several dacitic intrusions and rhyolitic lavas occurring across the lava plateau, e.g. the Tardree Rhyolite (Figure 4.1).

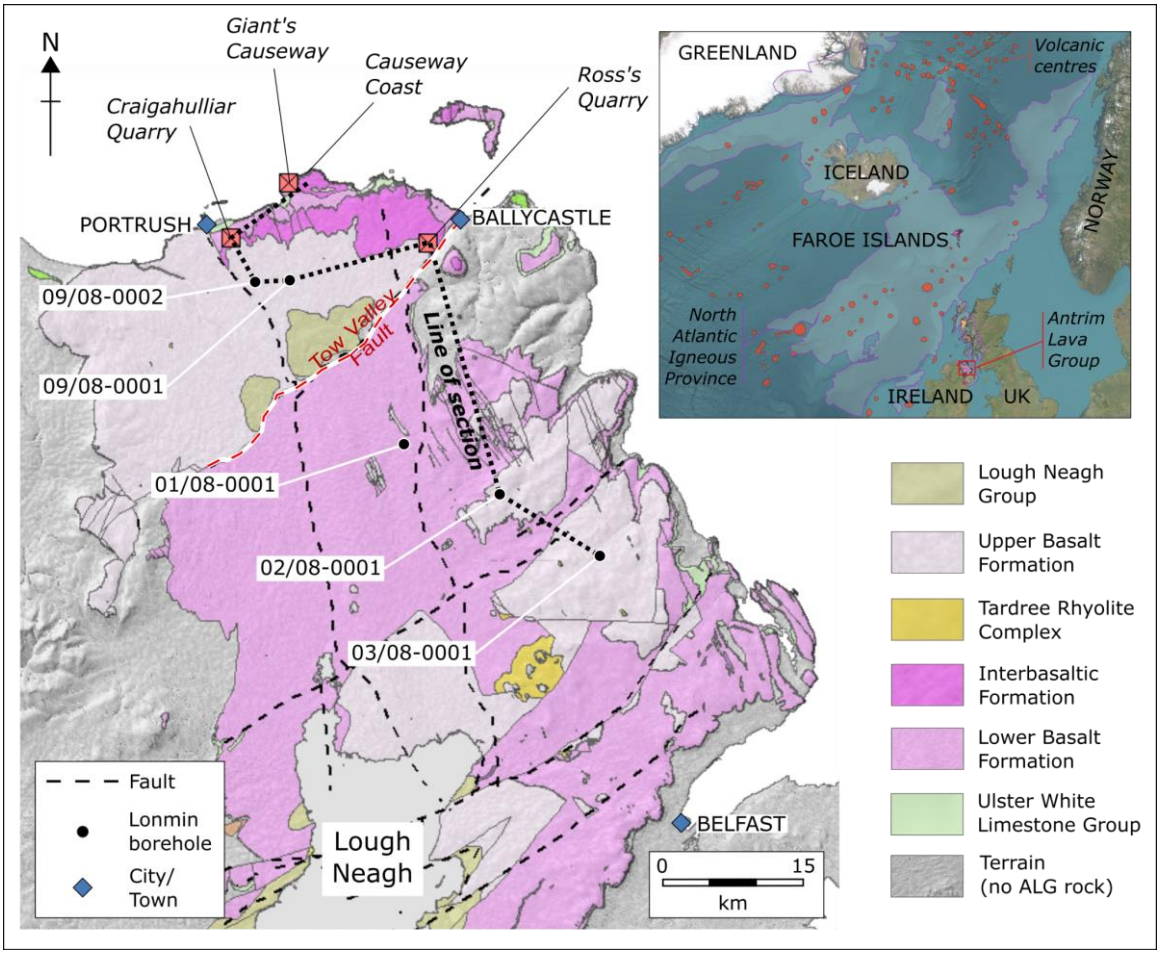

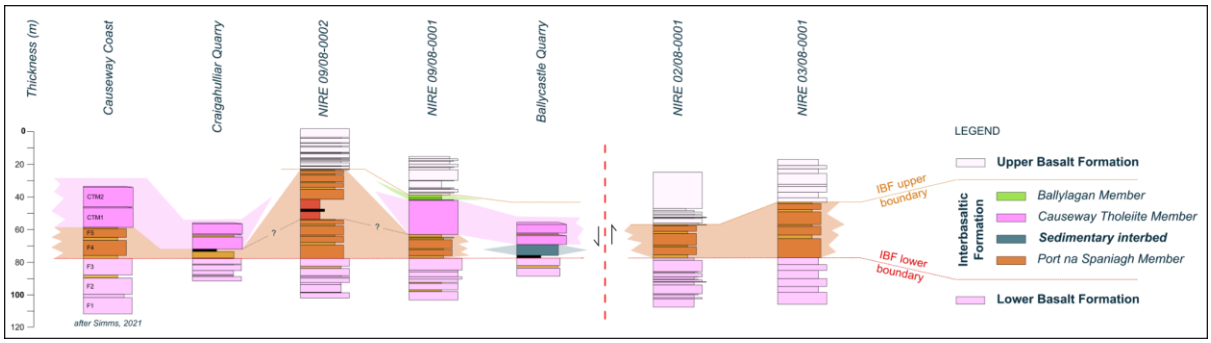

Figure 4.1 (a) Map of the Antrim Lava Group. The inset map shows the location of the ALG, NAIP sub-provinces, and the NAIP outline (Horni et al., 2017) within the wider setting, and (b) lithological sections of the studied boreholes and field locations.

In the long-standing but now revised Antrim Lava Group lithostratigraphy (cf. Figure 4.1 in Simms, 2021) the Interbasaltic Formation included the Port Na Spaniagh Member (containing weathered Lower Basalts, now placed at the top of the LBF by Simms, 2021) and the Ballylagan Member (containing weathered Causeway Tholeiites), respectively identified by their position below and above the Causeway Tholeiite Member (Patterson, 1955) (Figure 4.1). However, the current absence of identified Causeway Tholeiite Member outcrops south of the Tow Valley Fault, makes it difficult to correlate these other members beyond their type localities.

The Antrim Lava Group forms one part of the British & Irish Paleogene Igneous Province (BIPIP), along with the similar volcanic regions of Skye, Mull and Arran on the west side of Scotland (collectively the Hebridean Igneous Subprovince). However, unlike the lava successions of Mull and Skye NAIP volcanics (Bailey et al., 1924; Anderson & Dunham, 1966), the thick, heterolithic volcanic and sedimentary rocks of the ALG Interbasaltic Formation suggests a significant hiatus or change in the nature of volcanism during emplacement. These rocks have been the focus of much academic and economic interest for well over a century. Prominent amongst this early work is that of Cole et al., (1912), who reviewed the economic resources of the aluminium and iron-rich lateritic horizons that are recorded in the Interbasaltic Formation interval. Workers have variably described the reddened horizons in the Antrim Lava Group as either a ‘laterite’, ‘bole’ or ‘lithomarge’ (Mallet, 1881; Cole et al, 1912; Eyles, 1952; Lyle & Preston, 1993; Simms, 2021), although not always in a consistent way. Where discussed, the presence of these interbeds was taken as indirect evidence of a subtropical climate, since such a climate is widely associated elsewhere with the production of laterites and lateritic soils (e.g., the red clays of East Africa (Muff, 1908); Deccan Traps, India (Ghosh et al., 2006)). The presence of extensive and sometimes thick laterites in the

Antrim Lava Group, along with the occurrence of commercially viable bauxites (Cole, 1912), implied formation under extended periods of weathering, which would be required to transform the original basalt lavas and other volcanic products from parent rock to weathered deposits.

Here, we have applied the generic term '**interbed**' throughout the Antrim Lava Group to refer to any lithological unit that was formed or deposited during periods of quiescence between episodes of effusive volcanism, including deep weathering and the onset of soil formation and/or lateritisation. Additionally, we have avoided using the terms 'interbasaltic' or 'intrabasaltic' to describe these strata in the same manner as some previous NAIP studies (e.g., Jolley, 1997; Passey & Jolley, 2009; Williamson & Bell, 2012) as their use here could cause confusion with the Interbasaltic Formation stratigraphic unit of the Antrim Lava Group.

A number of volcanic and sedimentary rock successions are broadly coeval with the well-developed interbed horizons of the late Lower Basalt Formation and Interbasaltic Formation; specifically intermediate lavas and intrusives (Patterson, 1951; Walker, 1960; Lyle & Thompson, 1983) and acidic volcanic centres such as the Tardree Rhyolite Complex (Old, 1975; Ganerod et al., 2011) and the rhyolitic centre identified by Lonmin borehole NIRE 01/08-0001 (Figure 4.1) which proved 145.3 m vertical thickness of porphyritic and tuffaceous rhyolite under 17 m of overburden. These varied lithologies occur above, between and below the often columnar jointed lava flows of the Causeway Tholeiite Member (Eyles, 1950; Lyle, 2000) and throughout the Antrim Lava Group. This heterolithic succession suggests formation, either by weathering or sedimentary processes, over an extended time period in varied environments. Examining the record of spatial and temporal environmental change within the uppermost Lower Basalt Formation and the Interbasaltic

Formation helps constrain the dominant lava field processes and tempo of eruptive activity. Environmental indicators aid with the identification and interpretation of interbeds, allowing some determination of eruptive hiatuses across the plateau as well as providing a sense of their duration. Identifying the locality and duration of these hiatuses helps to determine if these are local and asynchronous features, or consistent with dominant vent positions and their migration. Timescale information from both weathering patterns and environmental or depositional reconstructions also provides a route to evaluating the overall rate of lava emplacement in the Antrim Lava Group.

As mentioned above, the terms laterite, lateritic, lithomarge, and bole have been widely used to describe interbeds (Eyles, 1952; Patterson & Mitchell, 1955; Old, 1975; Hill *et al*, 2000; Hill *et al*, 2001) as well as in the wider NAIP (Bell *et al*., 1996), although not always consistently. These terms allude to the composition and method of deposition or formation of the strata, which may include both sediment input and in-situ weathering or a combination thereof. Applied to the Antrim Lava Group, the term 'lithomarge' refers to an advanced stage of weathering in the sequence; basalt –> saprolite –> lithomarge –> laterite –> duricrust (Hill et al., 2001). Early workers were divided as to the nature of the formation of the red interbeds of Antrim; some argued that they were lacustrine in origin (Hull, 1874; Mallet, 1881; Cole et al., 1912), noting the presence of plant remains as additional evidence for this (Tate & Holden, 1870). Other workers saw them as advanced palaeosol artefacts, e.g. Muff (1908) compared the red bole interbeds of Antrim with the 'red clay' of East Africa (Kenya), claiming them to be identical at outcrop and very similar in chemistry. However, those 'red clay' soils were forming on sloping land surfaces where they were experiencing "alternate soaking by rain and [drying by] solar evaporation", and since lakes cannot form on a sloping topography some other mechanism is suggested. The point at which the

laterite, lithomarge and bole horizons of Antrim were accepted as being indicative of a subtropical weathering process is unclear, but the red interbeds of the Antrim Lava Group have mostly been interpreted as deriving from a subtropical climate (e.g. Mallet, 1881; Cole et al, 1912; Scrivenor, 1937; Eyles, 1952; Evans et al., 1973; Lyle, 1988; Lyle & Preston, 1993; Hill et al., 2000; Simms, 2021).

The interbeds found throughout the Antrim Lava Group are key to understanding the palaeoenvironmental conditions, how those environments were established and impacted by volcanism, and the tempo of volcanic activity, because they can provide information about the duration and relative timing of periods of quiescence. Here, we focus particularly on two interbeds of the Interbasaltic Formation revealed at Ross's Quarry and combine these findings with observations from other interbeds across the Antrim plateau (principally within the Interbasaltic Formation and adjacent strata, e.g. the Port na Spaniagh Member of the Lower Basalt Formation) (Simms, 2021; Figure 4.1). Within the NAIP, this wide range of lithotypes formed or deposited during an eruptive hiatus is seemingly a unique feature of the Antrim Lava Group. It also provides an opportunity to elucidate the range of environmental variation, the pace of environmental change and the wider impacts of this eruptive hiatus early in the formation of the NAIP.

4.2 Methods

4.2.1 Lithology

Interbed exposures and cored sections of the Interbasaltic Formation were selected for this study from sites across the extent of the Antrim Lava Group. For each exposure or borehole, the lithologies present were recorded in graphic logs, which provided the basis for further sampling. For field sampling of exposures, the surface of the interbeds was cleaned to remove the weathered, uneven outer face. For interbeds of sedimentary origin, a small steel trowel was then used to excavate samples from the main sedimentary subunits. Between samples, all equipment was washed clean using fresh mains tap water to remove soil and sediment and thereby minimise the risk of cross contamination.

Continuous cores from four boreholes penetrating the Interbasaltic Formation were logged for lithology and are included in this study (NIRE 02/08-0001, NIRE 03/08-0001, NIRE 09/08-0001 and NIRE 09/08-0002) (Figure 4.1). These are part of a total of nineteen boreholes comprising over 8.5 km of core, drilled by Lonmin (NI) Ltd. and deposited with the Geological Survey of Northern Ireland (GSNI). Along with the cores, datasets of portable X-ray fluorescence (pXRF) geochemistry and magnetic susceptibility data were also donated to the GSNI and made available to the authors.

4.2.2 Basalt weathering depth and interbed thickness / character

Lonmin NIRE borehole log records were investigated for detailed log information on the presence of vesicles and amygdales as well as noting the depth of weathering measured from flow tops. By examining and processing these data we were able to identify flow crusts and calculate depth of weathering through the flow tops and into the flow cores.

Petrological and palynological examination of interbeds within the NIRE borehole core samples and field exposures was carried out to determine their lithology, depositional environment and catchment ecology.

4.2.3 Palynology Laboratory processing

Samples from outcrop sections and core were selected based on lithology, sampling at 10 cm intervals at outcrop where possible. The lithologies of interest were identified between lava flows, appearing variously as sediments, lignitic material, volcaniclastic tuffs, palaeosols and other interbeds situated between lava flows. These lithologies were sampled before undertaking detailed identification in order to minimise the risk of sampling bias. Both exposure and borehole core samples were prepared using the standard techniques detailed below.

First, rock material was broken down into sub-4 mm size fragments and then demineralized by digestion in HF. Residues were boiled in 40% hydrochloric acid to remove calcium fluorite precipitate. Residues were sieved through a nylon 7 µm mesh and subsequently treated with dilute 40% nitric acid to remove pyrite. Where necessary, samples were subjected to heavy liquid separation using Sodium-Polytungstate ($3Na_2WO_4 \cdot 9WO_3$) at a specific gravity of 2.2 g/cc. The resultant residues were strewn mounted on glass microscope slides using a permanent epoxy mounting medium and analysed using an Olympus BX53 transmitted light microscope. Counts of > 200 palynomorphs per sample were taken where possible, all specimens within the strew mounts being recorded in depauperate samples.

Because of the complexity of some of the palynofloras recovered from the Interbasaltic Formation, specific taxa were targeted for more detailed analysis using a scanning electron microscope (SEM). Strew mounts were made of the selected residues, suspended in glycerine. Selected palynomorphs were picked out from the residue using an eyelash picking

tool and concentrated in a small blob of glycerine. Transmitted light photographs of these specimens were then taken as a record of their identity (Figure 4.9) and the specimens were transferred to SEM stubs following the methods of Halbritter et al. (2020). Scanning Electron Microscopy (SEM) was conducted in the Aberdeen Centre for Electron Microscopy, Analysis and Characterisation (ACEMAC) facility at the University of Aberdeen using a Carl Zeiss GeminiSEM 300 VP equipped with Deben Centaurus CL detector, an Oxford Instruments NanoAnalysis Xmax80 EDS detector and AZtec software suite. Prior to electron microscopy at ACEMAC the stubs were coated with Au-Pd 80/20 in a sputter coater. Imaging was conducted with low accelerating voltages with the secondary electron detector (SE2) and an InLens secondary electron detector for higher magnification images. The acceleration voltage used was 5 kv with a working distance of ~ 6 mm.

4.2.4 Statistical data analysis

Because of the complexity of the data set derived from the principal study sections, an initial statistical analysis was undertaken to determine the overall characteristics of the data. This was followed by a multivariate statistical analysis to identify the main trends in the data and simplify its presentation (Hill and Gauch, 1980). Following data normalisation and reduction to remove rare or singleton taxa, Detrended Correspondence Analysis (DCA) was undertaken (Hill, 1979; Hill and Gauch, 1980). DCA arranges data along two principal axes which represent variables, such as environmental factors. The eigenvalues associated with each axis reflect the extent to which each axis influences the data (Ramette, 2007).

4.2.5 pXRF Analysis

Existing pXRF analysis of all cores held by GSNI, and new analyses of lithologies of interest, were obtained using an Olympus Vanta M Series Delta Premium model with a rhodium anode tube. The pXRF data inherited by GSNI with the core samples were taken by Lonmin staff at set intervals, e.g. 1 m, 2 m, rather than by geological unit or feature. Lithologies of research interest were often missed by this method due to being relatively thin, hence the need to re-analyse certain specific horizons of NIRE borehole core samples by pXRF.

All new analyses were obtained by placing samples within an Olympus Vanta workstation for analysis. Individual readings were taken over a two minute count time. Beam 1 (<40 kV) ran for 60 seconds, then beam 2 (<10kV) ran for another 60 seconds.

Geochemical data generated using a handheld portable X-Ray Fluorescence tool (pXRF) were examined to identify geochemical trends among and between lava flow packages, as well as to help identify interbeds and weathered horizons when core samples could not be viewed in person. In case of the latter, pXRF data already held by GSNI was used.

In order to both calibrate and ascertain reliability, pXRF data values were compared with geochemical results generated by WD-XRF methods on identical samples. This process revealed that while the absolute values generated by pXRF tended to be unreliable (assuming WD-XRF values are more accurate and precise), the trends of element ratios used for identifying weathered horizons and interbeds (e.g. Ba/Sr) were consistently similar to those produced by WD-XRF data.

One key drawback of pXRF analysis for this application is that sodium cannot be detected, and that magnesium values above 3000 ppm are unreliable.

Additionally, pXRF data held by GSNI only had analyses for silicon, magnesium and aluminium in 2 of the 13 boreholes.

4.2.6 pXRF geochemical data usage

The barium (Ba) and strontium (Sr) ratio Ba/Sr is used as a proxy in this study. While soluble, barium has a tendency to adsorb onto clay minerals and so its resulting mobility is reduced in weathering and soil conditions. Strontium has a smaller ionic radius and is highly mobile in the weathering environment. In this regard, the ratio of Ba to Sr represents a proxy for weathering intensity (Price *et al*., 1991; Babechuk *et al*., 2014).

Values for lead and zirconium that were measured on borehole cores were also plotted alongside plant ecology group data as peaks in these datasets may indicate the presence of limited thickness acidic tephra in the core (see Results; Figures 3, 4 and 5).

4.2.7 Magnetic susceptibility data usage

Chen, An & Head (1998) compared Ba/Sr ratios with magnetic susceptibility values of interglacial loess profiles and found remarkable similarities in the plotted trends. In Figures 4 and 5 we have plotted magnetic susceptibility values alongside plant ecology group data and Ba/Sr ratios to provide another proxy for the climate and weathering while the lavas were subaerially exposed. Additionally, peaks in magnetic susceptibility, e.g. visible towards the top of section in Figure 4, may also point toward the presence of thin basaltic ash deposits in the core.

4.3 Materials

Analysis of the depositional history of the Interbasaltic Formation north of the Tow Valley Fault was based around three key sections: an operational quarry (Ross's Quarry) 4 km southwest from Ballycastle, and two cored boreholes NIRE 09/08-0001 and NIRE 09/08-0002 (Figure 4.1). Additional samples were incorporated from previously sampled exposures at Craigahulliar Quarry and the Giant's Causeway / Causeway Coast (Jolley, 1997), as well as

from cored boreholes NIRE 02/08-0001 and NIRE 03/08-0001 situated to the south of the fault (Figure 4.1, Table 4.1).

Table 4.1. List of key localities and Irish Grid references.

Locality	Easting	Northing
Giant's Causeway	292903	444476
Craigahulliar Quarry	287110	438954
Ross's Quarry	308097	438438
NIRE 09/08-0001	294362	434582
NIRE 09/08-0002	290853	434532
NIRE 02/08-0001	316129	412540
NIRE 03/08-0001	326391	406143
NIRE 01/08-0001	306212	417691

4.3.1 Ross's Quarry

Ross's Quarry was visited in October 2020, at which time two interbeds were exposed: interbed 1 and a younger interbed 2, with thicknesses of 1.5 m and 2.5 m, respectively. The base of the 2.4 m thick sedimentary interbed 2 is at 69 mAOD, comprising several horizons from top to bottom, presented here:

A6. Grey carbonaceous mudstone: 25 to 70 cm thick silver grey brittle, slightly hard clay with fine black carbonaceous material throughout. Rootlets throughout.

A5. Brown carbonaceous mudstone: 0 to 20 cm thick brown grey silty sandy clay with fine black carbonaceous material throughout. Sometimes absent, leaving A6 sitting on A4. Brittle, slightly hard clay. Darker brown horizon at top of unit. Thin but variable thickness carbonaceous horizon on top of unit.

A4. Cross-bedded silty sandstone: 1.3 m thick cream to pale tan cross-bedded silty very fine to medium sand with silt horizons. Bedding has well-developed fining-upwards cycles, sometimes with coarse sands at the base, with cross-cutting decreasing and beds become more horizontal up the unit. Clasts of organic material throughout in

cycles. Rootlets present, increasing to upper contact. Top 15 cm more brown in colour. Thin but variable thickness carbonaceous horizon on top of unit. A3. Mudstone/Sandstone with organic material: 0 to 15 cm thick cream clayey very fine to medium sand with black carbonaceous clasts up to 0.5 cm. In some outcrops this was seen as a well-lithified lignite up to 20 cm thick with no visible silt or sand content.

A3. Lignite / lignitic silty sandstone: Laterally variable subunit with end members of 0 to 20 cm thick horizon of well-compacted lignite in some places and silty sandstone with organic debris elsewhere.

A2. Mudstone: 10 cm thick green grey mudstone (weathered basalt?). Slightly friable, semi-competent.

A1. Weathered basalt: 10 cm thick silver grey green, conchoidal fracture weathered and altered basalt flow top. Relict basalt textures visible in hand specimen. Moderately competent.

The geology exposed at Ross's Quarry in the Craignagat townland consists of basalts and interbeds of the Antrim Lava Group (Figure 4.2, plate I), but identifying the specific formations and members present in the quarry is difficult. The lower two flows (f1, f2) are laterally extensive, massive, thick (9–10 m), aphyric and lacking significant internal structure aside from jointing. The three upper flows (f3, f4 & f5) are of varying thickness at outcrop, contain phenocrysts of olivine, and are physically quite different; the thickness of f3 varies significantly across the site, pinching out in places, and displays disordered structures, not clearly identified but reminiscent of pillow lavas. Lava flows f4 and f5 show reasonably well-developed columnar jointing and compared to f3 have a more consistent thickness. In Figure 4.2, plate C shows f3 and f4, plate E shows f4.

4.3.2 Craigahulliar Quarry

The Port na Spaniagh Member of the Lower Basalt Formation and the Causeway Tholeiite Member of the Interbasaltic Formation (Figure 4.1) crop out at this repurposed quarry (now a landfill site). Here, a deep red silty clay palaeosol with a carbonaceous/lignitic claystone horizon has been attributed to the Port na Spaniagh Member (the Lower Interbasaltic Bed of Patterson, 1955; Figure 4.1). It is overlain by columnar jointed flows mapped as the Causeway Tholeiite Member, with evidence of the lava ploughing into the underlying palaeosol interbed and filled topographic lows (Wilson, 1965). The oldest of these flows has a well-preserved pahoehoe flow top, itself being overlain by a lignitic sedimentary interbed of uncertain thickness (due to a cover of thick vegetation). This interbed is overlain by a second columnar jointed tholeiitic basalt flow which crops out at the top of the hill within the Craigahulliar landfill site.

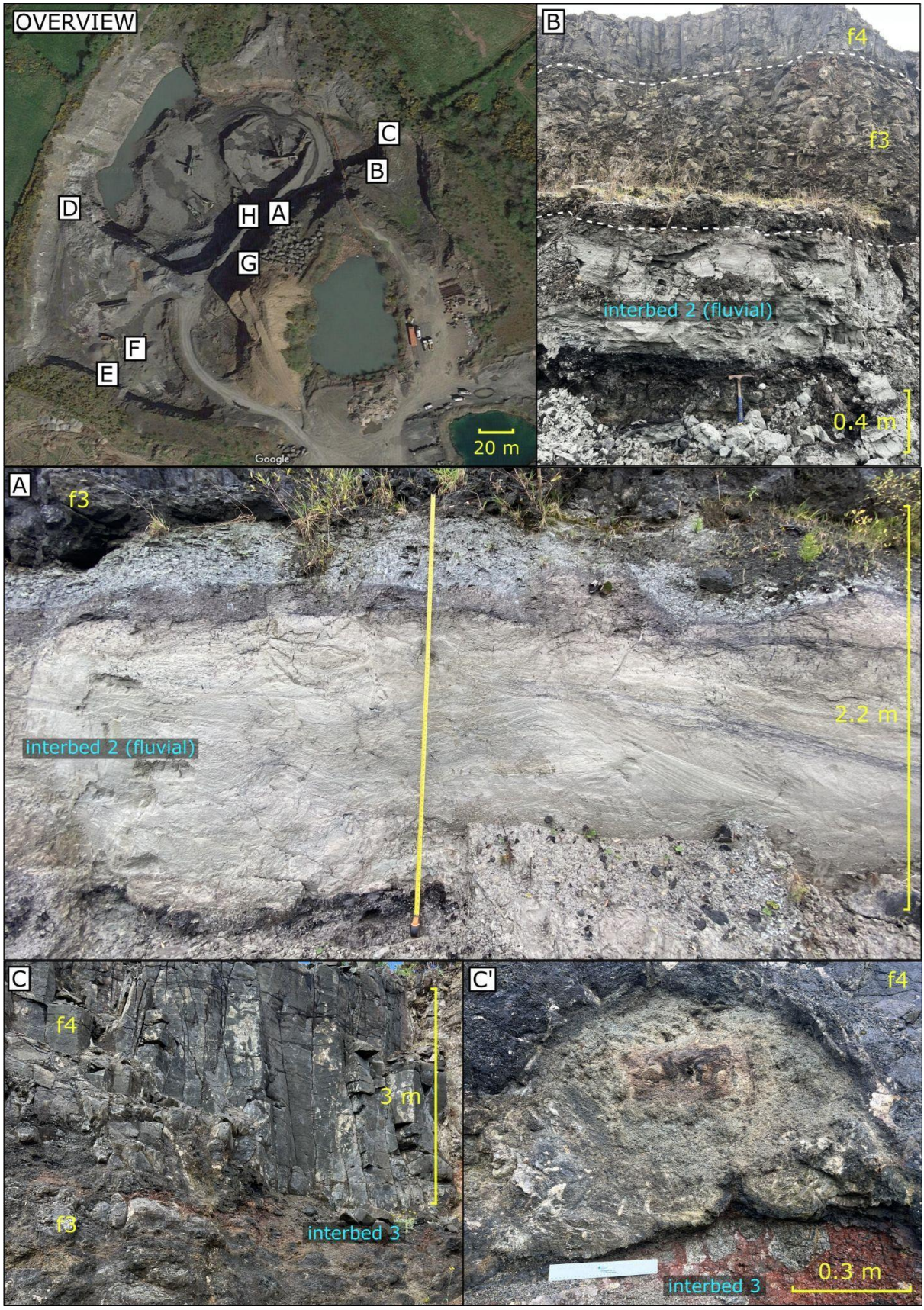

Figure 4.2. Field photos from Ross's Quarry. OVERVIEW. Aerial view of the quarry and locations of images. A. Interbed 2 detail. B. Interbed 2 setting below subsequent lava flows. C. Interbed 3 between lava flows f3 and f4

(showing weak columnar jointing). C'. Fossilised fallen tree trunk on interbed 3 surrounded by f4 lava flow. D. Fossilised root structures (within interbed 3) between f3 and f4 lava flows. E. Well-developed columnar jointing in flow f4. F. Example of the well-preserved fossilised wood found within interbed 2 (although not found in situ). G. Detail of interbed 1. H. Detail of hollow structure located within flow f4, possibly evidence of sediment ploughing or cavity infill where once a tree had been. I. Detail of interbed 1 between flows f1 and f2. J. Section of the northwest wall of the quarry detailing the stratigraphy.

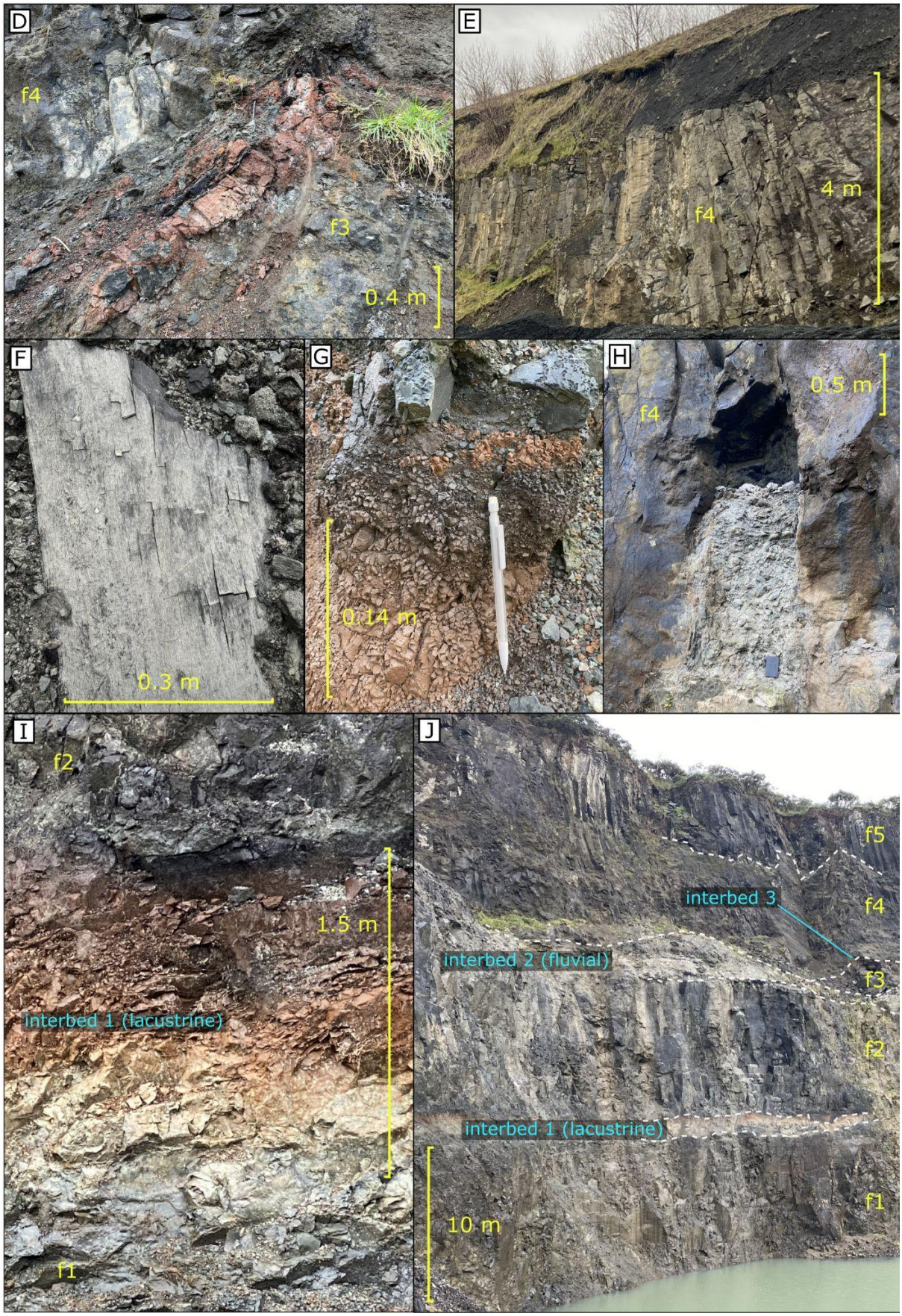

Causeway Coast

The lavas exposed along Causeway Head between Portnaboe and Port Noffler bays have recently been mapped at high resolution by Simms (2021). Starting at sea level, Simms identified five flows of the LBF, the uppermost of which weathered to form the sediments and lateritic palaeosol of the Port na Spaniagh Member prior to the eruption and emplacement of the Causeway Tholeiite Member flows. Two flows of the Causeway Tholeiite Member are exposed above this. The structural relationship between exposures on the foreshore and those in the cliffs of Causeway Head remains under debate.

4.3.3 Boreholes

Horizons interpreted as being of the Interbasaltic Formation are visible in core retrieved from the NIRE boreholes in this study. NIRE 09/08-0001 was also inspected, however, core from the lower section of this borehole was not available for inspection.

Composite logs were drafted using existing borehole logs provided by GSNI and supplemented by subsequent logging undertaken during fieldwork in October 2020 and October 2021. They are presented in part in Figures 4, 5, 6 and 7. Figure 4.8 presents selected core examples highlighting the nature of the lava flows as described within this study.

4.4 Results

4.4.1 Palynology

The results of the palynological analysis presented here by the PhD candidate were carried out by Professor David Jolley, University of Aberdeen. All images and text were compiled and edited by the PhD candidate.

Twenty eight samples from interbeds 1 and 2, exposed in the Ross's Quarry succession, were collected and analysed for their palynofloras (Figure 4.3).

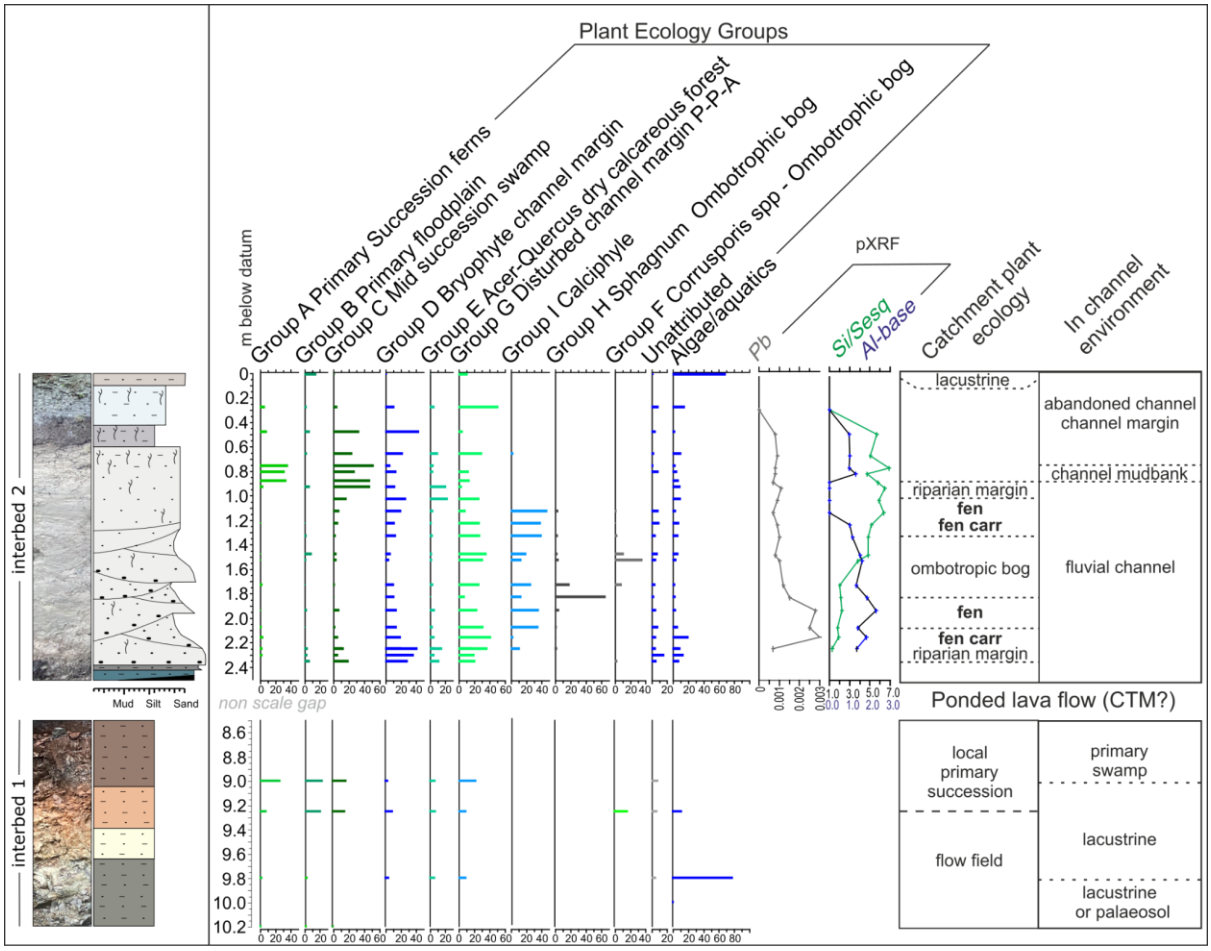

Figure 4.3 Ross's Quarry lithology and palynofloral communities.

This analysis yielded variably diverse palynofloras with a total of 115 taxa, mostly comprising pollen and spores. These floras were dominated by taxa derived from the families Sphagnaceae, Polypodiaceae, Cupressaceae, Pinaceae, Betulaceae, Juglandaceae and Hamamelidaceae in assemblages of varying composition (Supplementary data 2). Algal palynomorphs were distributed throughout the Ross's Quarry interbeds succession, occurring in all samples. Recovery of palynomorphs was moderate to high, with two intervals (samples 215–217 and 220–221; Figure 4.3) of lower recovery. The lower of these intervals sampled an erosively-based coarse sandstone unit, the higher depositional energy probably caused winnowing of palynomorphs (Figure 4.3).

Palynofloras recovered from 52 core pieces from borehole NIRE 09/08-0002 were diverse (105 taxa) and revealed stratigraphical variation. The palynofloral assemblages can be divided into three intervals; the oldest occurs within both the youngest interbed within the Lower Basalt Formation and the lowermost Interbasaltic Formation lithologies, separated from each other by a deeply weathered lava flow; the next youngest assemblage occurs in carbonaceous shales and coals of the middle Interbasaltic Formation, and finally; the third assemblage occurs within mudstones separated by deeply weathered lavas near the top of the Interbasaltic Formation (Figure 4.4).

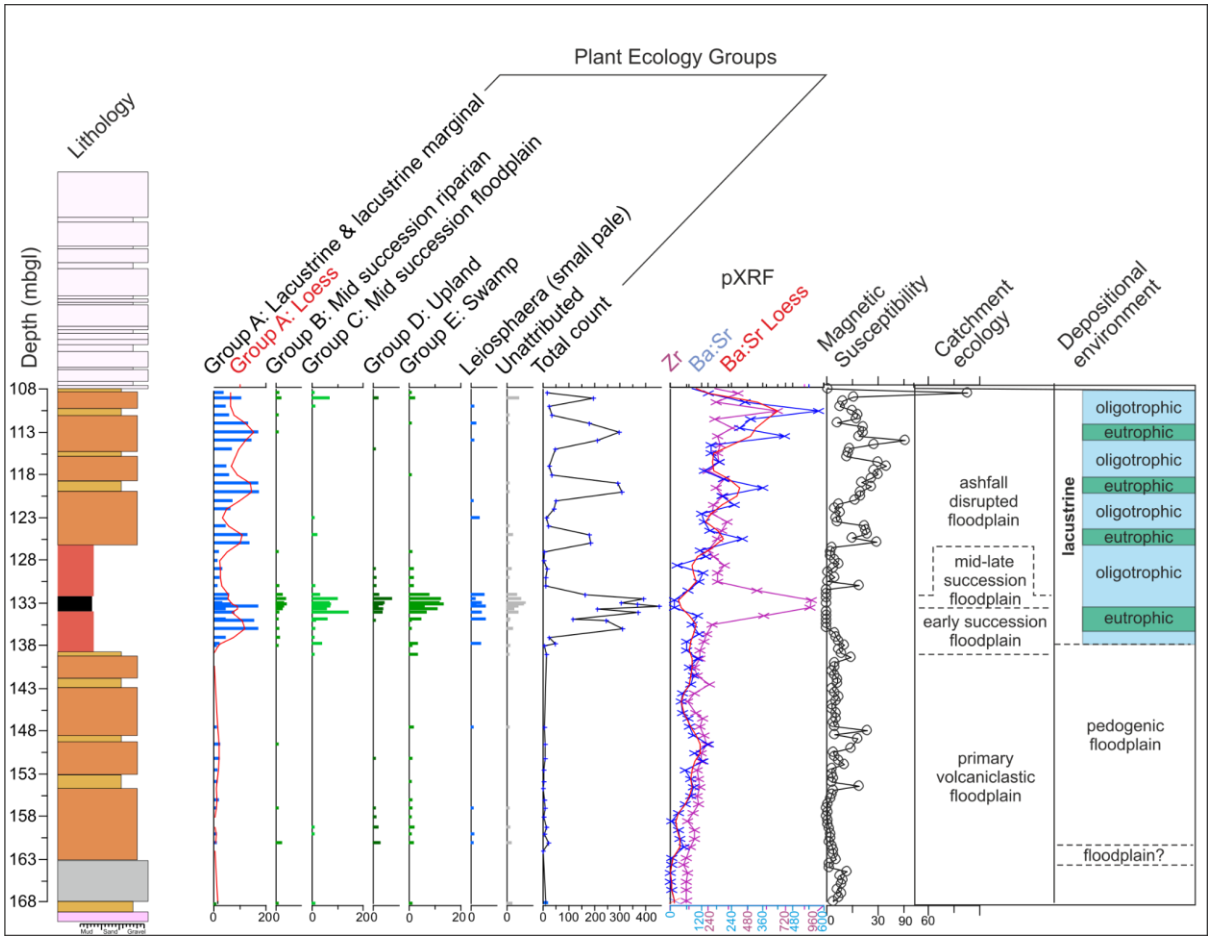

Figure 4.4 Borehole NIRE 09/08-0002 lithology and palynofloral communities.

The oldest floras are of low diversity and frequency, containing pine (*Pityosporites* spp) and swamp cypress (Taxodiaceae; *Inaperturopollenites hiatus*) pollen. These taxa are associated with a low frequency, moderately diverse angiosperm pollen flora, bryophyte spores and

freshwater algae (Figure 4, Supplementary data 1). Carbonaceous sediments in the middle part of the Interbasaltic Formation yielded a palynoflora with sub-dominant *Cupuliferoidaepollenties, Cupuliferoipollenties* and *Tricolpites* species (Fagaceae). These are associated with common occurrences of other angiosperm pollen including *Nyssapollenites* species (Nyssaceae)*, Retitricolpites* species (Platanaceae), Myricaceae type pollen (*Triporopollenties coryloides*), bryophyte spores and variably abundant freshwater algae. The upper part of the Interbasaltic Formation in borehole NIRE 09/08-0002 is characterised by a palynoflora totally dominated by abundant *Botryococcus braunii* (green algae, Chlorophyceae). Only in the uppermost bed of this unit is a moderately diverse higher plant palynoflora recovered, dominated by *Tricolpites* cf. *hians* (Fagaceae), fern spores (*Laevigatosporites haardtii*) and alder type pollen (*Alnipollenties verus*).

Recovery of palynomorphs from borehole NIRE 09/08-0001 is limited, no cores being available below the uppermost few metres of the Interbasaltic Formation (Figure 4.5). Samples from this interval yielded palynofloras dominated by fern spores, in particular *Deltoidospora adriennis* and green algae (*Botryococcus braunii*). They also had a low diversity and frequency of angiosperm pollen. A more impoverished palynoflora was also recovered from an interbed within the Upper Basalt Formation, which was dominated by fungal hyphae (Supplementary data 1).

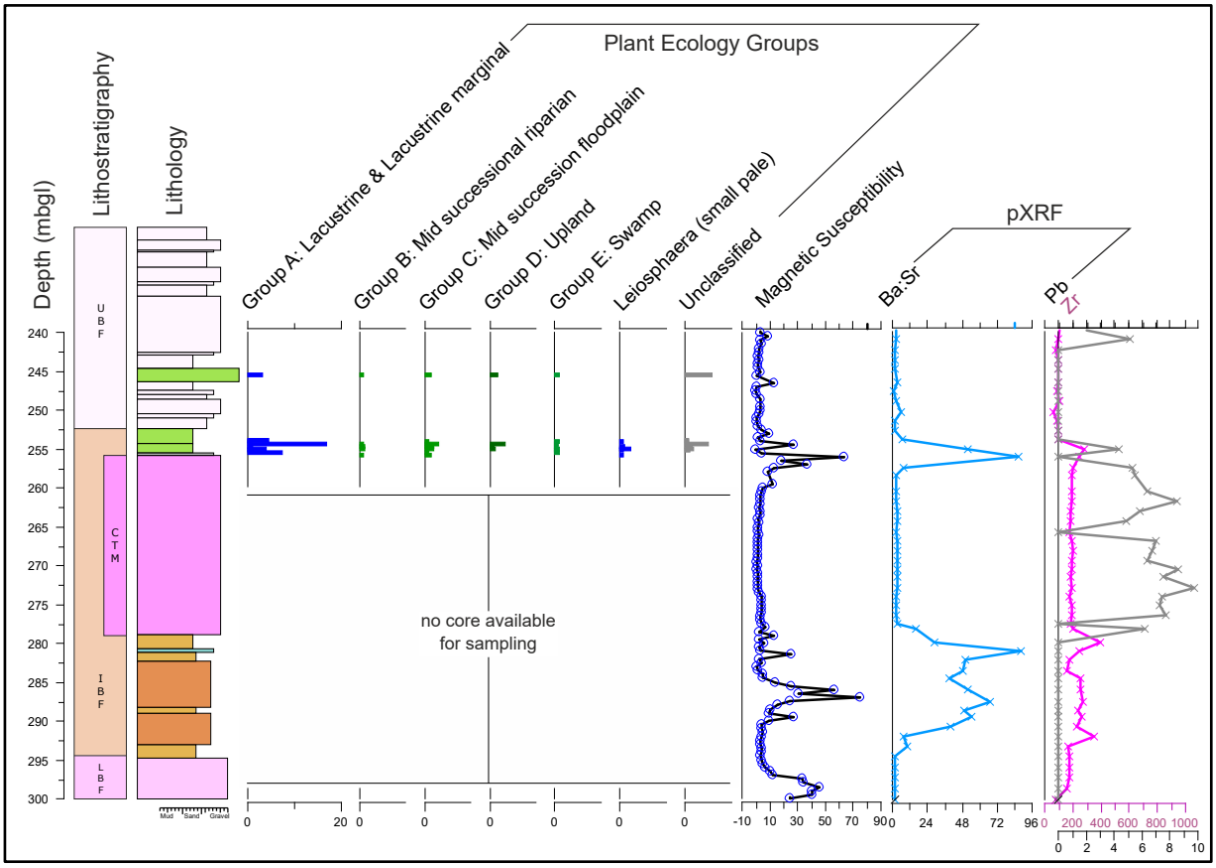

Figure 4.5. Borehole NIRE 09/08-0001 lithology and palynofloral communities.

Samples taken from the deeply weathered basalt lavas of the Interbasaltic Formation in boreholes NIRE 02/08-0001 and NIRE 03/08-0001 yielded similar palynofloras, wholly dominated by green algae (Figures 6,7). A few scattered occurrences of pollen and spores were noted, an influx of *Retitricolpites retiformis* (Platanaceae) and *Tricolpites* cf. *hians* (Fagaceae) recovered from the lowermost bed of NIRE 02/08-0001.

A more diverse palynoflora was recovered from two thin beds of carbonaceous shales above the oldest lava flow of the Upper Basalt Formation in borehole NIRE 02/08-0001. These palynofloras are dominated by swamp cypress pollen (*Inaperturopollenites hiatus*), sub-dominant bryophyte and pteridophyte spores (*Stereisporites (Stereisporites) stereioides* and *Deltoidospora adriennis*) and common *Momipites tenuipolus* (Juglandaceae, hickory types). A similar, *M. tenuipolus* rich palynoflora of this type was also recovered from lignites

cropping out between the two columnar jointed flows mapped as the Causeway Tholeiite Member at Craigahulliar Quarry (Figure 4.1; Supplementary data 1).

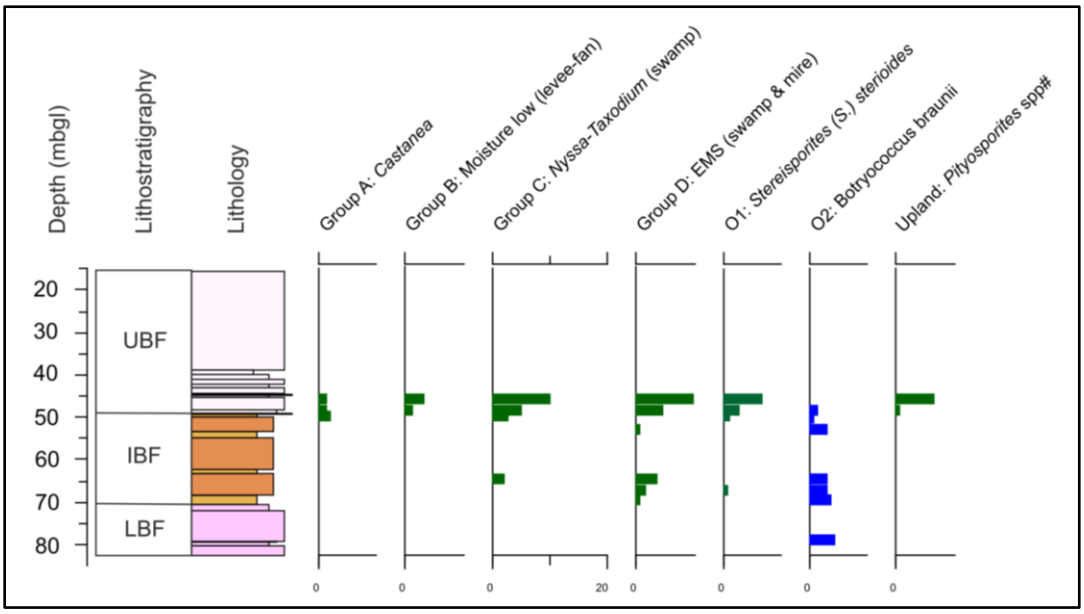

Figure 4.6. Borehole NIRE 02/08-0001 lithology and palynofloral communities.

Additional samples from sedimentary interbeds within the Lower Basalt Formation exposed at Port Noffler to the east of the Giant's Causeway yielded palynofloras dominated by swamp cypress pollen (*Inaperturopollenties hiatus*). These were associated with sub-dominant fern spores (*Laevigatosporites haardtii*) and the angiosperm pollen *Retitricolpites retiformis* (Platanaceae) and *Cupuliferoipollenties* species (Fagaceae).

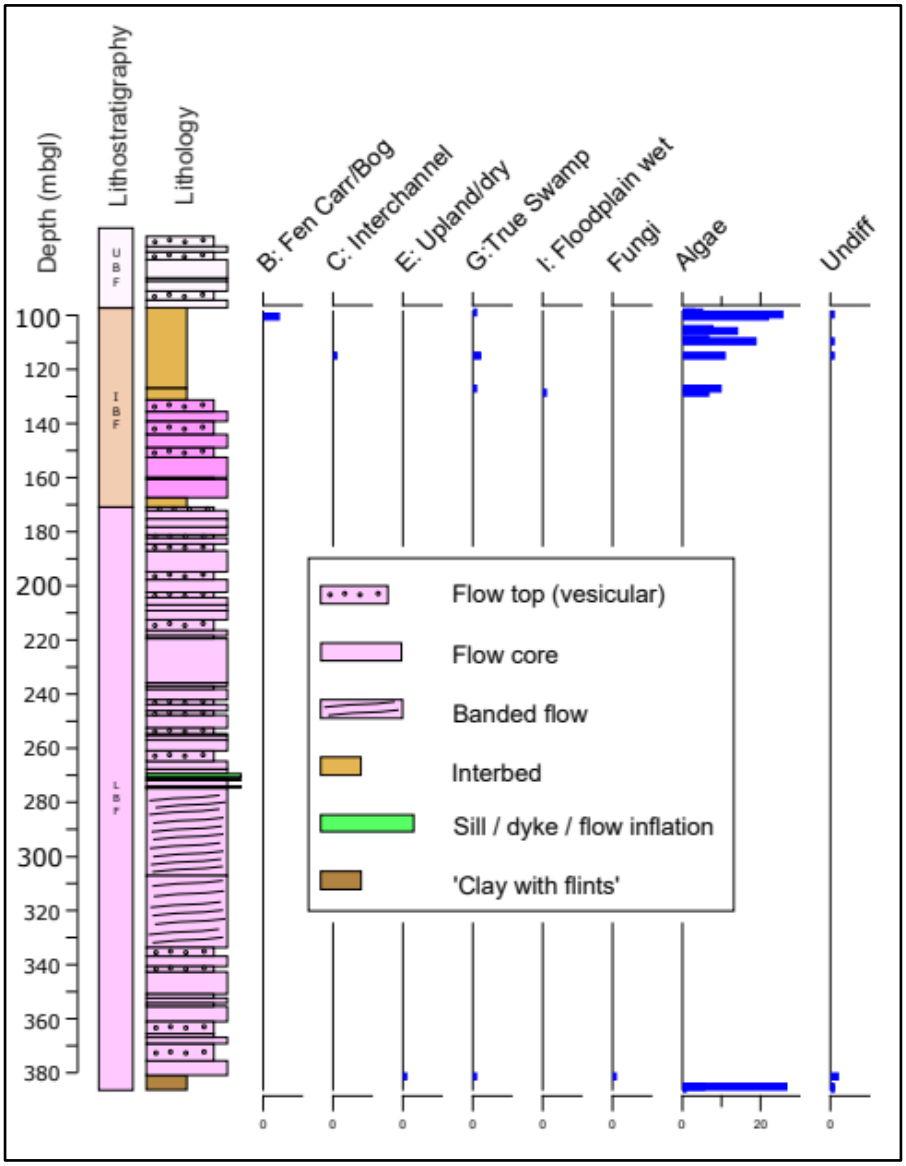

Figure 4.7. Borehole NIRE 03/08-0001 lithology and palynofloral communities.

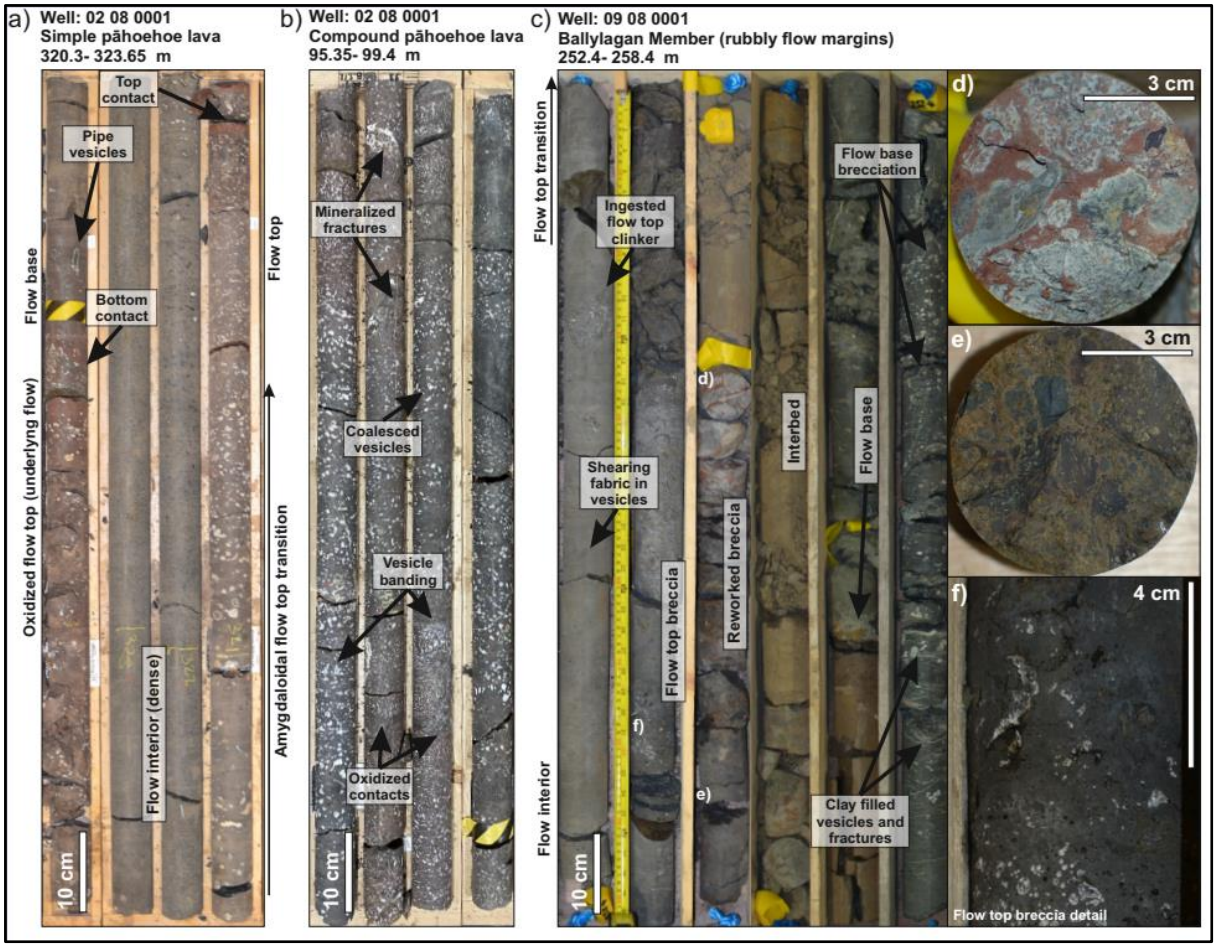

*Figure 4.8: Figure compiled by Dr John Millett for this study highlighting typical features of the Antrim lava pile as seen in NIRE borehole core. (**a**) Example of a simple pāhoehoe lava flow from within Lower Basalt Formation of the 02 08 0001 borehole showing typical asymmetrical vesicle distribution and oxidation towards the flow top. (**b**) Example of a compound pāhoehoe lava flow from within the Lower Basalt Formation of the 02 08 0001. (**c**) Details from the Ballylagan Member of the Inter-basaltic Formation highlighting the presence of rubbly flow margins associated with flow margin autobrecciation. (**d**) Reworked and leached scoriaceous breccia clasts in oxidized matrix. (**e**) Reworked and deeply altered volcaniclastic breccia with scoriaceous clasts likely reworked from underlying rubbly flow top. (**f**) Detail of flow top breccia.*

4.4.2 Age of the Palynofloras

Occurrences of the Normapolles taxon *Complexipollis sp* (Figure 4.9) are recorded in the lowermost samples from the Interbasaltic Formation in both the lowermost

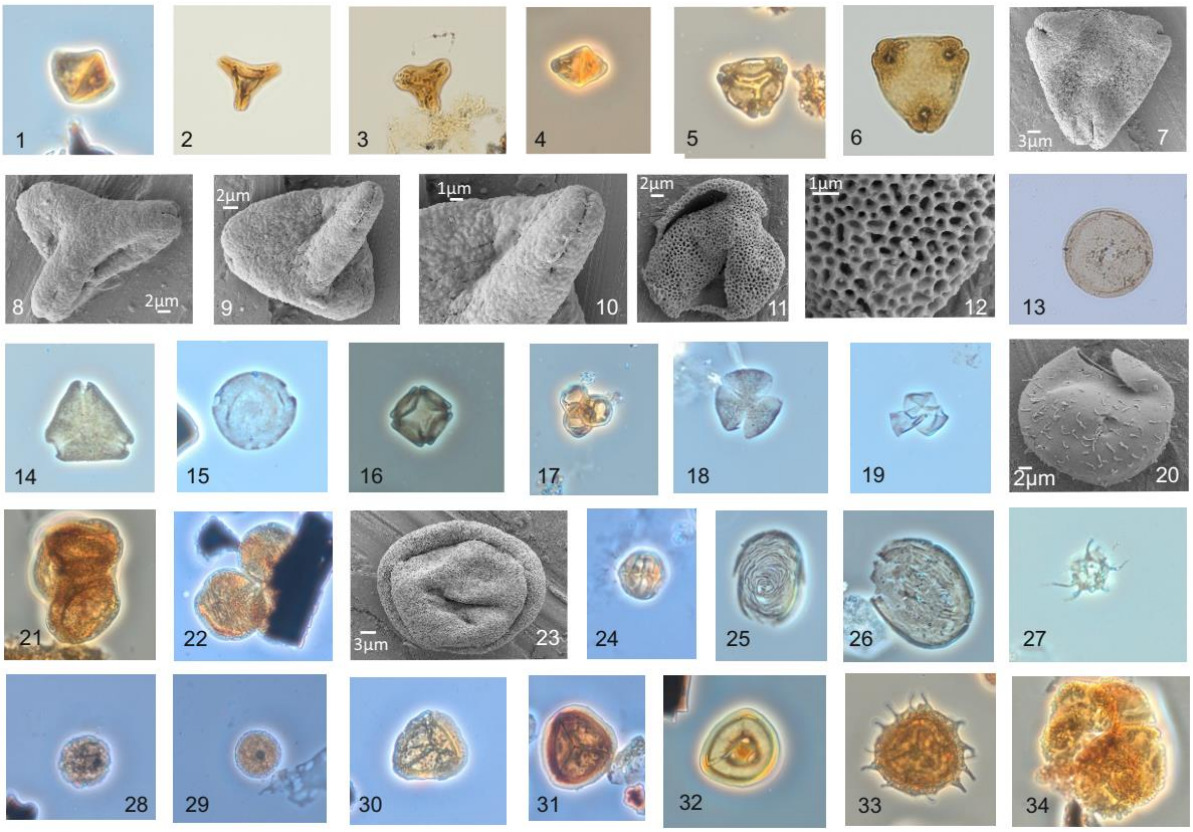

Figure 4.9: Palynomorphs from the Antrim Lava Group taken by Prof David Jolley, compiled and presented by the PhD candidate. Complexipollis sp. 1) sample LAT005, Clinty Quarry, K39/1; 2) 09/08-0002 161m U41/2; 3) 09/08-0002, 167.85m Q41; 4) Ross's 207, M35; 5) Nudopollis terminalis 09/08-02, 132.5m, T34/2. Trudopollis hammenii, 6) 09/08-0002 109m, C39/4, 7)SEM photograph, Ross's. Complexipollis sp. 8-10) Ross's, 10 showing high magnification of the colpate aperture in 9. 10, 11) Tricolpites cf hians, 09/08-0002, 131m, 11, showing high magnification view of Platanaceae type reticulum. Arcella sp. testate amoeba from Ross's 222, X42/2. 12) Cupaneidites sp (Loranthaceae), 09/08-0001, 254.25m, R48/1. Caryapollenites circulus, 09/08-0002 109m, Q27. 13) Alnipollenites verus, Ross's 205, U21. 14) Ericipites ericius 09/08-0002, 112m, Q31/1. 14)Tricolpites hians, 09/08-0002 109m, L33/1. 15) Cupuliferoidaepollenites liblarensis 09/08-0002, 109m, V43/4. 15) Acanthomorph acritarch, SEM photograph, 09/08-0002, 133m. 16) Classopollis spp., characteristic cluster, Ross's 206, G31/1, 17) Classopollis spp., Ross's 208, J41/3. 18) Classopollis spp., SEM photograph showing single sulcus. Note the thick, ornamented wall, Ross's. Pentacolporites sp Ross's 212, L39/3. 25) Concentricystes sp. 09/08-0002, 109m, N46. 26) Concentricystes sp., 09/08-0002, 110m, R32/3. 27)Micrhystridium stellatum, Ross's 206, W46/4. 28, 29) Corrusporis sp. Ross's 209, G43/4. Ballycastle 208, F31/1. 30) Stereisporites (Dicyclosporis) sp. Ross's 208, M23/4. 31) Stereisporites (Dicyclosporis) sp. Ross's 210, N18. 32) Stereisporites (Distannulisporis) sp. Ross's 0.15, N17. 33) Echinosporis cycloides Ross's 207, L23. 34) Botryococcus braunii, Ross's 206, M47/4.

carbonaceous bed of interbed 2 in Ross's Quarry (Figures 2, 3) and within interbeds in the lowermost Interbasaltic Formation and Lower Basalt Formation of borehole NIRE 09/08-0002. This taxon is widely recorded from the Late Cretaceous (e.g., Tschudy, 1980). The scarcity of drilled subsurface, or exposed Danian strata, limits the record of this taxon in NW Europe, (see Krutzsch, 1966). Recent investigation of palynofloras from offshore Norway (Ormen Lange well 6305/8-2; Vieira et al., 2018) by one of the authors has consistently recorded *Complexipollis* sp. in Danian strata. Correlation with dinoflagellate cyst stratigraphy for this well (Vieira et al., 2018), indicates that this taxon occurs within an age range from 64.5 Ma to 63 Ma. This age is in agreement with the Ar-Ar age (63.24+/-0.61 MSWD) derived from Lower Basalt Formation lavas (Ganerød et al., 2009; Wilkinson et al., 2017).

The common to abundant occurrences of *Cupuliferoidaepollenites* and *Cupuliferoipollenites* in the middle beds of the Interbasaltic Formation in NIRE 09/02-0002 (Figures 4,8), and in the upper interbeds of the Lower Basalt Formation at Port Noffler (Supplementary data 1) probably reflect the widespread regional distribution of these taxa. Raised frequencies of these taxa have been recorded in strata of the Vaila and Lamba formations, deposited 61.3 Ma to 59.6 Ma in the Faroe-Shetland and Rockall basins (Jolley et al., 2021).

The lignites exposed between the lower two flows of the Causeway Tholeiite Member at Craigahulliar Quarry (Figure 4.1) yielded common *Momipites tenuipolus* (Figure 4.9). An influx of *M. tenuipolus* was also recorded in carbonaceous interbeds between the oldest flows of the Upper Basalt Formation in borehole NIRE 02/08-0001. Similar common occurrences of *Momipites* species and *M. anellus* in particular, have been recorded across the Selandian–Thanetian boundary in the North Sea Basin (Jolley & Morton, 1992) and the Faroe Shetland Basin (Jolley et. al., 2021). A correlative flora with common to abundant

Momipites species, including *M. tenuipolus* has also been recorded from the Thanet Sands Formation of Kent, southern England (Jolley, 1998). In the NAIP, common occurrences of *M. tenuipolus* have been recorded within the upper Vaila to early Lamba formations of the Faroe Shetland Basin to the northeast and occurs in the Thanet Sands Formation of south eastern England and is therefore indicative of an age of approximately 59.5 Ma to 59.0 Ma (Jolley et al., 2021) for the oldest units of the Upper Basalt Formation in borehole NIRE 02/08-0001.

4.4.3 Depositional Environments of Interbed 1 (Ross's Quarry)

Exposed between two flows of the Causeway Tholeiite Member, the lower part of this < 2 m thick unit is barren of palynoflora. This may indicate that these oldest sedimentary rocks were derived relatively rapidly from eroded basaltic lava flows or reworked basaltic tephra. However, 20 cm above the base of the unit, lacustrine palynofloras dominated by green algae are recorded. Frequencies of lacustrine palynomorphs decline up-section, reflecting a decline of lacustrine influence (Figure 4.3). The youngest palynoflora is dominated by bryophyte spores and early to mid-succession angiosperm pollen. The absence, or sparse occurrences of such pollen in the lower 0.5 m of this bed suggests that the sedimentary source may have been reworked tephra (Ebinghaus et al., 2017). The increase of pollen and spore frequency up-section is mirrored in kerogen sorting. Very well-sorted vitrinite characterises the oldest samples. Sorting decreased up-section, reflecting encroachment of vegetation in the lacustrine catchment. Although this is predominantly a reddened interbed of the kind often described as a laterite, the abundance and preservation of structured organic material negates formation by weathering. Instead, the red colour of the bed is probably derived from the source material of which it is composed. Red sandstone and claystone units of this character are common in the NAIP (e.g., Passey & Jolley, 2009), and

while some are formed from pedogenic degradation of basaltic lavas (e.g., Williamson *et al*., 1996), many are derived from transported and degraded basaltic volcaniclastic material (e.g. Jolley *et al*., 2022).

4.4.4 Depositional Environments of Interbed 2 (Ross's Quarry)

The lowest subunit of interbed 2 is a carbonaceous siltstone passing laterally into lignite deposits including fossilised wood and bark fragments (Figure 4.2 plate F and F'). Palynofloras from this interval include common algae, spores derived from a bryophyte-dominated wetland community and riparian associations, indicating deposition in a lacustrine palaeoenvironment. Cross stratification of the overlying 1.7 m of interbed 2 indicates that it was laid down by a shallow fluvial channel system (Figure 4.3). The occurrence of acritarchs, chlorophycean algae, copepod eggs and testate amoebae (*Arcella* spp.) support an interpretation that it was deposited in a fresh- to weakly-brackish water environment. Occurrences of the acritarchs *Micrhystridium* and *Leiofusa* spp. are concordant with deposition in a very low salinity fluvial system with a link to the marine environment. Assemblages of this type have been recorded in tidally influenced fluvial channels in the lava fields of the Faroe Islands Basalt Group (Jolley et al., 2022). Overlying this tidally influenced fluvial channel is a unit of darker silty clays with abundant rhizomatous root structures (Figure 4.3). These originate within and at the top of the silty clay bed, but penetrate down > 30 cm into the underlying cross bedded sandstones. Abundant occurrences of the pteridophyte fern spores *Deltoidospora maxoides* and *D. adriennis* in high dominance, low diversity samples (samples 216–219, Figure 4.3) from the silty clays indicate that the rhizome structures belong to ferns which likely colonised intra-channel mudbanks.

The 55 cm claystone bed between the top of the silty clays and the overlying basalt lava flow was also penetrated by more infrequent rootlet structures (Figure 4.3). The palynoflora from this interval is of lower diversity, but the spore/pollen assemblages are again dominated by *D*. *adriennis* and *D*. *maxoides* suggesting that the root structures originated from ferns colonising the emergent surface of the claystone unit. Occurrences of *Arcella* spp. (testate amoebae), *Botryococcus braunii (*green algae)*,* Copepod eggs and *Concentricystes* sp. within this claystone unit indicate that it was deposited in a quiescent freshwater environment. Taken together with only minimal indications of lava – surface water (or wet sediment) interaction at the base of the overlying basalt flow, these data indicate that a low energy channel margin was likely abandoned and colonised by ferns. The fall in base level that this resulted from ensured that the overlying lava flow was able to completely fill and overstep the accommodation space previously occupied by the fluvial system.

Catchment vegetation ecology

Because interbed 2 was deposited within a fluvial channel system, pollen and spores derived from the catchment area are well-preserved. These complex assemblages reflect changes in the plant ecology of the catchment. Because of this complexity, the pollen and spore data was subjected to DCA to express the variability in the data set on two principal axes. This analysis identified nine groups, of which three were based on single outlying taxa (Supplementary data 2). Multi species groups were named according to the known botanical affinities and environmental tolerances of the taxa included in them (Gruas Cavagnetto, 1978; Jolley et al., 2009). The stratigraphical distribution of these DCA groups was plotted against the graphic lithology logs to highlight correspondence between bed units and changes in catchment palaeoecology.

The lowermost sedimentary rocks of interbed 2 (0.2–0.5m, Figure 4.3) were co-dominated by pollen from the True Swamp (Group D) and Fluvial/Fen Carr (Group F) communities. Dominated by *Inaperturopollenites hiatus* and *Pityosporites* spp. respectively, this co-dominance of True Swamp and Fluvial/Fen Carr groupings is characteristic of fluvial channel facies. Both groups are dominated by pollen from known pollen overproducers (Pinaceae, Cupressaceae), these taxa occurring abundantly in fluvial to shallow marine Paleogene sediments of the NAIP (Simpson., 1961, Jolley, 1997; Jolley et al., 2021). Evidence of increased influence from a Fen Carr association along the riparian margin is presented by increased frequencies of the betulaceous pollen *Alnipollenites verus.* Occurring commonly at the base of the cross-bedded sandstone unit (Figure 4.3), this Fen Carr association declines in frequency up-section. This decline is correlated to a change in assemblage character from 0.5 m to 0.65 m, where palynofloras are dominated by *Classopollis* sp pollen (Group I). The parent plants of these pollen are included in the family Cheirolepidaceae, plants held to become extinct at the Cretaceous-Paleogene boundary. While there is no conclusive evidence that these pollen were reworked from Upper Cretaceous strata in the catchment area, a reworked Ulster White Limestone source within the catchment area appears likely. It is notable that the common occurrences of *Classopollis* pollen do not correspond to lithofacies changes in the exposure (Figures 4.2, 4.3), suggesting a catchment control on their occurrence.

Overlying these transported fen carr and fen assemblages, is an abrupt shift at 1.725 m (Figure 4.3), to spores derived from a Sphagnaceae ombrotrophic bog, dominated by *Stereisporites (Dicyclosporis)* spp. The total dominance of this taxon is indicative of the development of a raised, ombrotrophic bog. Further development of the bog is marked by the replacement of Sphagnaceae spores by abundant bryophyte spores (*Corrusporis* spp.).

These spores wholly dominated the transported in-channel assemblage sampled at 1.05 m, marking the upper limit of a base level fall trend within the catchment (Figure 4.3). Overlying the ombotrophic bog associations, an abrupt assemblage change was recorded at 1.425 m (Figure 4.3), reverting to dominance by Fluvial/Fen Carr community (groups F, G). There is no apparent major corresponding change in the sedimentary structures of interbed 2 at this level, but this assemblage change signifies a shift in the catchment from ombrotrophic bog to riparian fen carr. This is associated with an influx of Copepod eggs, occurring with *Micrhystridium fragile*, *M*. *stellatum* and a dinocyst fragment indicating a weak brackish water penetration into the fluvially dominated channel system.

At 1.025 m (Figure 4.3) the fen community is abruptly terminated, reflecting the incision of a separate cross-bedded channel (Figure 4.2). Palynofloras derived from these coarser channel sandstones are of lower diversity and abundance. The palynoflora was initially dominated by an in-channel taphonomic grouping of transported taxa (groups D and E), which is rapidly replaced by mid-successional community taxa (Group C). This largely pteridophyte spore dominated group includes *Deltoiospora adriennis*, a taxon associated with crevasse splay and inter-channel sand bank colonisation.

Occurrences of abundant *D. adriennis* continued to dominate the mid-successional community (Group C) recovered from the overlying rhizomatous silty clays (1.77–1.83 m). Within this unit, assemblage diversity fell and abundant *Deltoidospora maxoides* was recorded. The dual dominance of polypodiaceous and schizaceous ferns in this silty clay unit indicates deposition as an inter-channel emergent sandbank. This emergent sandbank deposit is overlain by claystones with poor palynofloras which are essentially similar to those recovered from the silty clays below. Taken together with the fine grain size and

laminar bedding, this unit can be interpreted as being deposited in a low energy channel marginal area, or abandoned channel.

The uppermost 1 cm unit of interbed 2 is significantly different, being marked by an influx of fresh water palynomorphs at 2.3 m, including testate amoebae and *Concentricystes* sp. (Zygnemataceae; Grenfell, 1995). Pollen and spores occur in a low diversity and high dominance assemblage with high frequencies of transported *Pityosporites* spp. (Pinaceae, Group G: Riparian/Channel. Transported Pinaceae pollen and the common occurrence of mixed freshwater-brackish algae indicate deposition of this interval in a fluvially dominated channel. Although rootlets penetrate this bed, there is no evidence for a horizon with rootlets at the top of interbed 2. The non-invasive lower surface of the overlying basalt lava flow indicates that the underlying sediments were probably a dry surface and may have been partly lithified or consolidated. It could be expected that the flooding event at 2.3 m would be overlain by sedimentary rocks deposited during a falling base level, like those seen in the two preceding cycles (Figure 4.3). The absence of such deposits at the top of interbed 2 could potentially either reflect (a) thermal uplift and landscape rejuvenation associated with eruption of the overlying Upper Basalt Formation lava flows, (b) the lowering of hydrological and hydrogeological water levels due to fracture propagation and expansion associated with thermal uplift, (c) some other mechanism or a combination of all of these.

4.4.5 Depositional Environment, Borehole NIRE 09/08-0002

The majority of the palynofloras recovered from the Interbasaltic Formation of borehole NIRE 09/08-0002 contained algae, indicating that the deposits originated in a succession of freshwater lacustrine environments. The lower unit of the Interbasaltic Formation contained a sparse palynoflora, but with no evidence of degradation of the organic debris. Frequent occurrences of *Pityosporites* spp from 161 to 157 mbgl are associated with a low frequency

flora, including early mid successional angiosperm pollen and bryophyte spores. Influxes of *Pityosporites* spp in lacustrine deposits are normally a reflection of wind transport or fluvial input, the pollen being readily transported from an upland or topographically raised source area. The low frequency of other pollen and the numbers of *Stereisporites* species (bryophyte) indicate that the catchment area was only poorly vegetated or barren. Ba/Sr ratio trends derived from pXRF data indicate that the rocks comprising the lower interval of the Interbasaltic Formation in this borehole were moderately weathered. Ratios for interbeds and lavas from both the Lower Basalt Formation and the overlying Upper Basalt Formation flows are typically <3. From the base of the lower interval of the Interbasaltic Formation, Ba/Sr increases to 146.5 (149.5m), remaining at comparable levels until within the oldest part of the upper Interbasaltic Formation unit (Figure 4.4). This includes the middle section of the Interbasaltic Formation where palynofloras are diverse and abundant. While the increase in Ba/Sr within the upper part of the Interbasaltic Formation probably reflects increased weathering of the sediment, it does not demonstrate that this weathering happened in-situ. The presence of freshwater algae in this interval suggests deposition in ephemeral lakes or floodplains with little surrounding vegetation. Other examples from the Faroe Islands Basalt Group (Passey & Jolley, 2009; Jolley et al., 2022) are interpreted as accumulations of redeposited volcanic ash and erosion products from adjacent flow fields. In addition, two prominent increases in magnetic susceptibility (Figure 4.4) could potentially reflect the presence of airfall ash layers (Rosenthal et al., 2018). The most probable interpretation is that this interval represents a complex period of slow vegetation recovery after cessation of Lower Basalt Formation eruptions, and a disturbed floodplain environment in which ashfall may have reset the vegetation communities within the area (Ebinghaus et al. 2015).

4.4.6 Depositional Environment, Borehole NIRE 09/08-0001

There is limited data from this borehole, samples only being available from an interbed above the Causeway Tholeiite Member lavas. In this interbed, abundant *Deltoidospora adriennis*, a taxon associated with crevasse splays and channel margins, dominated an early succession flora. Abundant lacustrine and lacustrine marginal palynomorphs indicate that these spores were deposited in ephemeral lakes (Figure 4.5). In contrast to the extensively weathered lavas and late successional swamp communities identified in the nearby borehole NIRE 09/08-0002, the flora recovered in NIRE 09/08-0001 indicates only a short term eruption hiatus.

4.4.7 Depositional environment, boreholes NIRE 02/08-0001 and NIRE 03/08-0001

The Interbasaltic Formation penetrated by these two cored boreholes is composed of deeply weathered basalts. Short intervals where green algae are recorded commonly indicates that these weathered flow fields periodically hosted lakes. The low frequency of higher plant pollen is probably partly attributable to extensive oxidation of organic matter during this long period of slow sedimentation and weathering. This does not explain the low frequencies of pollen and spores in samples with common algal preservation. This can be attributed to volcanic disturbance of the catchment vegetation similar to that observed in the Columbia River Large Igneous Province (Ebinghaus et al., 2017), or alternatively that the interbed sediments were deposited rapidly in ephemeral lakes.

The flora recovered from interbeds in the lowermost Upper Basalt Formation of borehole NIRE 02/08-0001 were sourced from a well-established, transitional swamp, mid successional floral community. This is closely comparable to the *Momipites tenuipolus* dominated palynoflora from the interbed within the Causeway Tholeiite Member at Craigahulliar Quarry, which was deposited in a similar, transitional swamp environment.

4.5 Discussion

4.5.1 Exceptional Ecosystem

There are numerous palynofloral records from acid swamps within the NAIP, with communities ranging from lacustrine and riparian to transitional and true swamp (e.g. Jolley, 1997; Schofield & Jolley., 2013). These are characterised by abundant pteridophyte fern spores, often *Laevigatosporites haardtii or Deltoidospora* species derived from primary coloniser ferns (e.g., Figures 3, 5; Jolley et al., 2009). In early to mid seral successional states, swamp palynofloras include juglandacaeous angiosperm pollen (e.g., *Caryapollenties* species, *Momipites* species, *Platycaryapollenites* species), alongside *Cupuliferoipollenites* species (derived from Fagaceae) and Normapolles pollen, probably from herbaceous plants (e.g., Figures 5, 6; Daly & Jolley, 2012). Recorded diversities are high with mid succession communities being well-developed in floodplain swamp community mosaics. Plant macrofossil assemblages of similar composition, dominated by *Glyptostrobus (*pollen taxon *Inaperturopollenites)* and *Cupuliferites* (related to several *Favitricolporites, Tricolpites* and *Cupuliferoipollenties* species) have been recorded from Glenarm Quarry (grid ref: D304156, Figure 4.1) in 19th Century fossil collections (Boulter & Kvacek., 1989).

Climax or late seral succession vegetation is mostly preserved as Cupressaceae dominated lowland swamp, often partly as a coastal ecosystem (e.g., Jolley et al., 2009). An alternative to lowland swamp cypress (Cupressaceae, *Taxodium* or *Metasequoia*) late succession communities have been recorded more rarely as upland fern-conifer forest within the basalt lava fields of the Skye Main Lava Series (Jolley, 1997). Macrofloras of comparable composition have been recorded from Ballypalady and Glenarm Quarries (Figure 4.1) by Gardner (1883-1886), the flora being interpreted as being derived from a mixed mesophytic forest by Boulter & Kvacek (1989) in their review of museum specimens.

In the majority of the records of swamp vegetation communities both within and immediately preceding a period of active volcanism, water draining into the catchment may have been dominantly acidic. Macronutrient availability would have been highly variable in these settings (Jolley et al., 2008), and only sites proximal to contemporary volcanism would have experienced significant eutrophication. While this is true of interbasaltic sedimentary depositional systems, the more limited record of plant ecosystems deposited in environments immediately prior to the onset of volcanism also follows this pattern. Examples from sub-basaltic strata in the NAIP (Mull Lava Field, Jolley et al., 2008; Faroe Islands Basalt Group, Passey & Jolley, 2009, Faroe Shetland Basin, Schofield & Jolley, 2013; Jolley et al., 2021) show limitation of seral succession by the onset of volcanism but are essentially all swamp-dominated ecosystems.

An exception to these acidic swamp ecosystems was identified from the palynofloras of interbed 2, which point to a significant influence on the pH of groundwater chemistry within the catchment area (Wheeler & Proctor, 2000). The palynoflora of interbed 2 represents the only known published record of a fen ecosystem in the Paleocene of the Northeast Atlantic margin.

The common occurrence of *Alnipollenites verus* in sample 205 (at 2.155 m below datum, Figure 4.3) marks the establishment of an Alder fen carr community within the catchment. In addition to confirming a falling base level during deposition of the lower 1 m of interbed 2, the transition from channel to fen carr and succeeding fen communities identifies the necessity for a higher pH groundwater (Godwin et al., 1974; Wheeler & Proctor, 2000). Although the current land surface of the Ballycastle region is covered by extensive basaltic lavas, the fen ecosystem indicates that this area drained a landscape which was at least in

part formed by the Late Cretaceous Ulster White Limestone Group (Figure 4.1), of which the remaining extent is now almost entirely covered by the Antrim Lava Group.

The subsequent gradation of the oldest identified fen community into sphagnum bog and subsequently a bryophyte dominated raised ombrotrophic bog formed the late successional vegetation during this first period of base level fall. A subsequent rise in base level at the start of the second depositional sequence raised the groundwater table and reset the vegetation ecology. This second depositional cycle occurred during a second period of base level fall and resulted in a second influx of transported upland pollen and dominance by the riparian *Alnipollenties* (Alder) fen carr.

4.5.2 Interbeds, laterites and lithomarges

Our palynological investigations have revealed that all but a few of the red interbeds examined in this study have a significant component of lacustrine influence, showing a floral assemblage of a landscape experiencing a temperate climate not dissimilar to our modern climate. Of the few red interbeds without lacustrine signals in the palynological data, most were barren.

The floral assemblage of Paleocene Antrim varied spatially and temporally for several reasons, with explosive volcanic activity represented by the rocks of the Interbasaltic Formation being of particular importance. Deepening our understanding of interbed palynology will be critical in building up a story of the timing of Antrim Lava Group volcanic activity.

The palynofloral evidence recovered in this study is that all of the palynofloras were derived from mesic vegetation communities. Previous studies including evidence from macrofloras and palynology have attributed the macrofossil record of the Antrim Lava Group to a mixed mesophytic forest (Boulter & Kvacek, 1989) which was stated to be subtropical. Palynofloral

assemblages recovered for this study concur that the vegetation was derived from mesic vegetation, including communities which could be attributed to a mixed mesophytic forest. However, other authors (Wang, 1961, Wolfe, 1979, Bondarenko et al., 2020) describe floras of this character as warm temperate.

4.5.3 Palaeoclimate context

Because of the long period of time spanned by Antrim Lava Group activity, the Antrim area was undoubtedly subject to climatic variation during the Paleocene. The Lower Basalt Formation postdates the early Danian Dan-C2 hyperthermal (65.2 Ma, Quellevere et al., 2008), being erupted during a period of relatively stable $\delta^{18}O$ and $\delta^{13}C$ values (Westerhold et al., 2020). Although the time interval spanned by the Antrim record includes the Late Danian Event (62.2 Ma, Westerhold et al., 2011; Bornemann et al., 2021) and the Early Latest Paleocene Event (Bralower et al., 2002), these are short duration potential warming events which would not induce long duration tropical weathering. Our data supports extensive weathering of basaltic lava flows, principally during the period of the Interbasaltic Formation. Evidence that this period of low tempo eruptions and volcanic quiescence experienced two or more phases of long term lava flow weathering is clear in the lithological and biostratigraphical data (Figure 4.10). Alteration and weathering of lava flows continued during the Interbasaltic Formation and appears to have been contemporary with eruptions (e.g. weathering of the upper Interbasaltic Formation in 09/08-0002 potentially co-occurred with eruption of the Causeway Tholeiite Member, e.g. NIRE 03/08-0001).

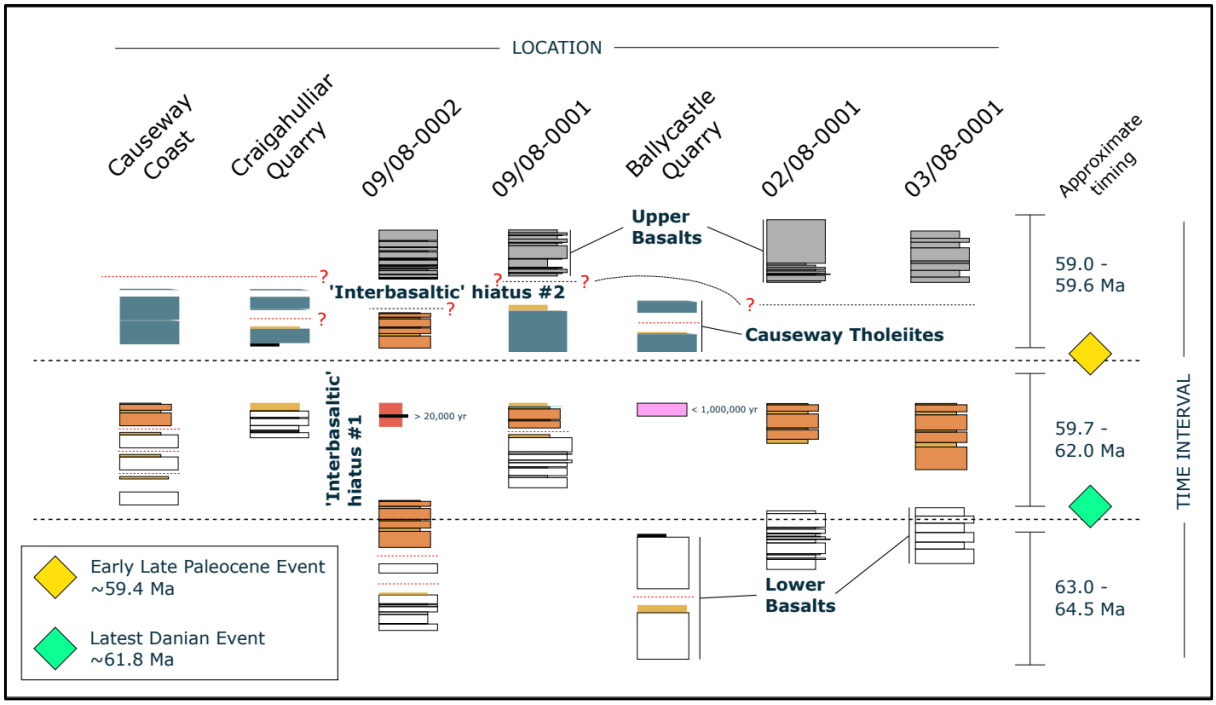

Figure 4.10. Antrim stratigraphic table showing interpretations from palynological and geochemical findings.

There is currently no convincing evidence that Antrim Lava Group volcanic activity was linked to either the Latest Danian Event (Sprong et al., 2013) or the Early Late Paleocene Event (Petrizzo, 2005), both of which occurred within the period of Interbasaltic Formation deposition (Figure 4.10). Volcanic activity during the Interbasaltic Formation period is broadly coincidental with eruptions in the Inner Hebrides (Figure 4.10). Eruption of the Upper Basalt Formation has limited absolute age control (Wilkinson et al., 2017), but could be contemporaneous with eruptions of the Skye Main Lava Series. Constrained by isotopic dates for the Isle of Rum western granophyre and the Skye Cuillins Complex pegmatite dyke (Wilkinson et al., 2017; Jolley et al., 2021), the Skye Main Lava Series erupted during volcanic Phase 1 of the British and Irish Paleogene Igneous Province (BIPIP). This late stage Phase 1 effusive volcanism could be linked to the negative carbon excursion of the Early Late Paleocene Event, although a more precise chronostratigraphy is desirable.

4.5.4 Antrim Lava Group thickness and volume

Examination of 19 borehole records with detailed log notes gave a range of lava flow counts per borehole from 5 to 104, with one of these being excluded as only tuffaceous rhyolite was encountered (NIRE 01/08-0001). The remaining borehole records from 18 Lonmin boreholes showed flow counts from 5 to 84 individual lava flows, with an average lava flow thickness of 4.82 m based on 581 discrete flows, the thickest of which was 32.77 m. The distribution of flow thicknesses is presented in Figure 4.11.

Using a combination of open source satellite data and GSNI geological maps in QGIS we estimate the areal extent of the Antrim Lava Group to be 4,093 km^2. Using geological data from 55 boreholes across the Antrim plateau we found the following average thickness values for the Antrim Lava Group sub-units and as a whole:

Upper Basalt Formation *158.90 m*

Interbasaltic Formation *37.01 m*

Lower Basalt Formation *132.48 m*

Antrim Lava Group ***328.40 m***

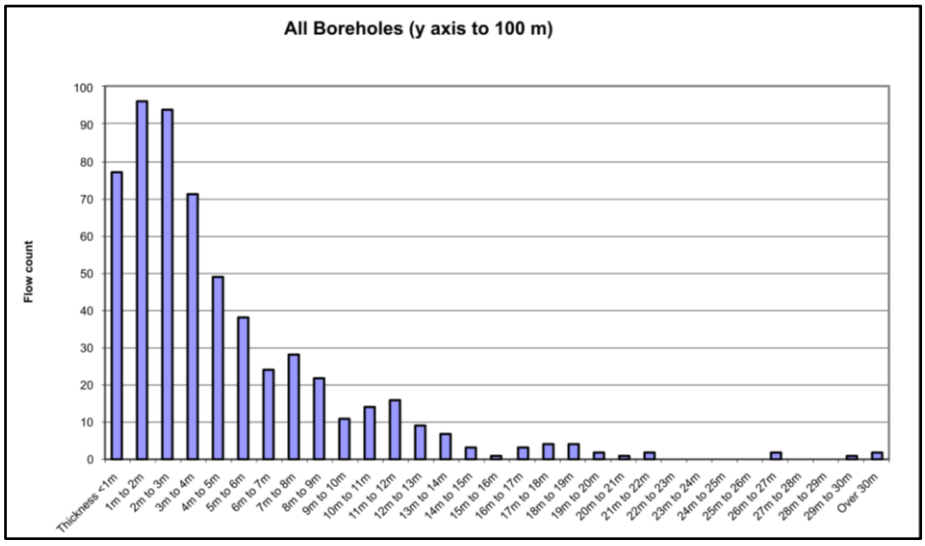

Figure 4.11. Antrim Lava Group flow thickness histogram summarising the distribution of lava flow thicknesses encountered in all NIRE boreholes.

The thickness of the Antrim Lava Group varies significantly over the plateau but from the 55 borehole records we have calculated an average thickness of 328.40 m, and note the maximum recorded thickness of 771 m in the Ballymacilroy borehole (Thompson, 1979). If this maximum thickness were taken as being the originally emplaced thickness across the entire lava field, we get an estimated emplaced lava volume of 3,156 km^3. If we instead take the average measured thickness, we would arrive at an emplaced lava volume of 1,344 km^3. Clearly significant erosion has taken place during and subsequent to effusive volcanism, whilst the component of the province that would originally have extended beyond the modern day coastline is unconstrained and would imply estimates based on preserved thickness are likely conservative.

4.5.5 Rates of lava emplacement

Approximating the rates of effusion, eruption or emplacement for a sub-province of the Paleogene NAIP is not straightforward. However, recently active volcanic systems might give us the closest analogous data for rates of effusion of the Antrim Lava Group flood basalts, as well as the wider NAIP and potentially other basaltic LIPs. In the last 1100 years there have been two large basaltic eruption events in Iceland; Eldgjá in 934 and Laki in 1783. These events have been studied and their rates of effusion have been calculated (Eldgjá; Thordarson & Self, 2001) or gleaned from anecdotal evidence (Laki; Thordarson & Self, 2003). These basaltic effusions on Iceland provide relevant examples for interpreting the ALG due to their geographic location within the NAIP and possible connection with the tectonic and mantle processes that gave rise to the lavas of Antrim.

Thordarson & Self (2001) stated that the Eldgjá basaltic flood lava eruption is the largest on Earth in the last millennium. These fissures produced 19.6 km^3 of basalt in 8 distinct phases of activity that spanned 3 to 8 years (in the period 933 to 941 AD). Conversely, Thordarson &

Self (2003) calculated that the Laki fissure eruption had effused around 90% of the total volume of basaltic lava within just 5 months (14 km^3), reaching 100% in just 8 months (14.7 km^3). To give context to these events, the 6 month eruption at Holuhraun, Iceland (2014-15) produced just 1.44 km^3.

If we take their calculated rates of magma effusion for these volcanic events (Table 4.2) and apply it to the possible total volumes for the Antrim Lava Group estimated above, we find that volcanic events on the scale of Eldgjá and Laki would be capable of emplacing the entire Antrim Lava Group within 40 to 1288 years (Table 4.3).

Table 4.2 Rates of effusion for Icelandic flood basalt eruptions at Laki (1783 AD) and Eldgjá (952 AD) based on measured volumes and duration from anecdotal evidence. Superscripts a and b refer to the associated 'Rate of effusion' and 'Time taken' columns in Table 3

	Volume erupted	Time taken	Time taken	Rate of effusion
	measured km^3	*Months*	*Years*	*calculated km^3/year*
Laki (90% volume)[a]	14.0	5	0.42	33.60
Laki (100% volume)[b]	14.7	8	0.67	22.05
Eldgjá (short duration)[a]	19.6	36	3	6.53
Eldgjá (long duration)[b]	19.6	96	8	2.45

Table 4.3 Emplacement duration for the Antrim Lava Group based on hypothetically continuous eruptions at rates of effusion calculated in Table 2, showing that the extant ALG lavas could have been emplaced in under 1,300 years if emplacement had been uninterrupted. Superscripts a and b cross-reference to Table 2.

	Areal extent	Thickness	Volume	Rate of effusion[a]	Rate of effusion[b]	Time taken[a]	Time taken[b]
	measured km^2	*estimated m*	*estimated km^3*	*est. km^3/year*	*est. km^3/year*	*Years (est.)*	*Years (est.)*
Antrim Lava Group	4093.05	328.40	1344	33.60	22.05	**40**	61
***cf.* Laki**		771.00	3156			94	143
Antrim Lava Group	4093.05	328.40	1344	6.53	2.45	206	549
***cf.* Eldgjá**		771.00	3156			483	**1288**

We know, from a variety of existing research as well as our own findings, that the emplacement of the Antrim Lava Group spanned several million years, perhaps as long as 4.5 million years. Combining this information with the evidence of abundant weathered tops, palaeosols and other well-developed interbeds between flows of the Antrim Lava Group (Hill et al., 2000), even our most conservative estimates of effusion rate imply that

>99.9% of the geological time locked away in the ~800 m thickness of basalt resides within these palaeosols, boles and interbeds.

4.5.6 Interbeds of the Antrim Lava Group

To date, mostly due to the geochemical and petrological similarities between the lavas of the Lower and Upper Basalt Formations, differentiating these lava formations has mostly focussed upon identifying the presence and relative position of the well-developed 'Interbasaltic Formation' interbeds that signify a break between these two distinct episodes of flood basalt volcanism. Where the interbed is absent or not seen, field identification of the Lower or Upper Basalt Formation is almost impossible.

We have focused primarily on the boles and interbeds of the Interbasaltic Formation, but numerous interbeds are found at various horizons among the basalt flows of the Lower and Upper Basalt Formations (Figure 4.12), signifying indeterminate periods of subaerial or subaqueous exposure and weathering throughout the emplacement of the Antrim Lava Group. The regular occurrence of these interbeds among the lava flows of the Antrim Lava Group suggests that relatively long periods of quiescence were common throughout the emplacement of this sub-province.

Figure 4.12. Antrim Lava Group boles and interbeds. A. Craig's Quarry. B. Blackmountain Quarry. C. Clinty Quarry. D. Clinty Quarry E. Corky Quarry. F. Roveran Valley Head, Causeway Coast. G. Croaghan Quarry. H. Cam Quarry. I. Craighall Quarry. J. Craighall Quarry. K. Knocklaughrim Quarry. L. Interbed 1 at Ross's Quarry, Ballycastle.

In this work we have linked the formation of these interbeds to a wet and fertile landscape of swamps, mesic vegetation, rivers and lakes; all of which require time and the absence of significant local volcanism in order to develop. Our results suggest that a chronology based on hiatus duration and weathering horizons holds strong potential to constrain eruptive tempo. At this stage, we provide an initial qualitative analysis; a full quantitative

investigation would require additional methodological development and dating that falls outside the scope of our current research.

Focusing on these interbeds is key to unlocking the emplacement timing of the Antrim Lava Group, and this likely applies to different sub-provinces of the NAIP as well as other basaltic LIPs around the globe. Plotting the depth of basalt weathering against flow group thickness (Figure 4.13) provides a glimpse of the eruptive tempo analysis that may be possible, but quantifying rates of basalt weathering, particularly given uncertainties over contemporary climatic and hydrological/hydrogeological conditions, remains highly challenging. The thickness of weathered horizons among a lava pile is not a robust indicator of time between flows since numerous factors are at work, such as flow composition, flow crust thickness and type, run-off and climate.

The process behind the generation of Figure 4.13 is discussed in more detail in Chapter 5, but appears here as it was relevant to the publication from which this chapter is derived (Beresford-Browne *et al.*, 2023).

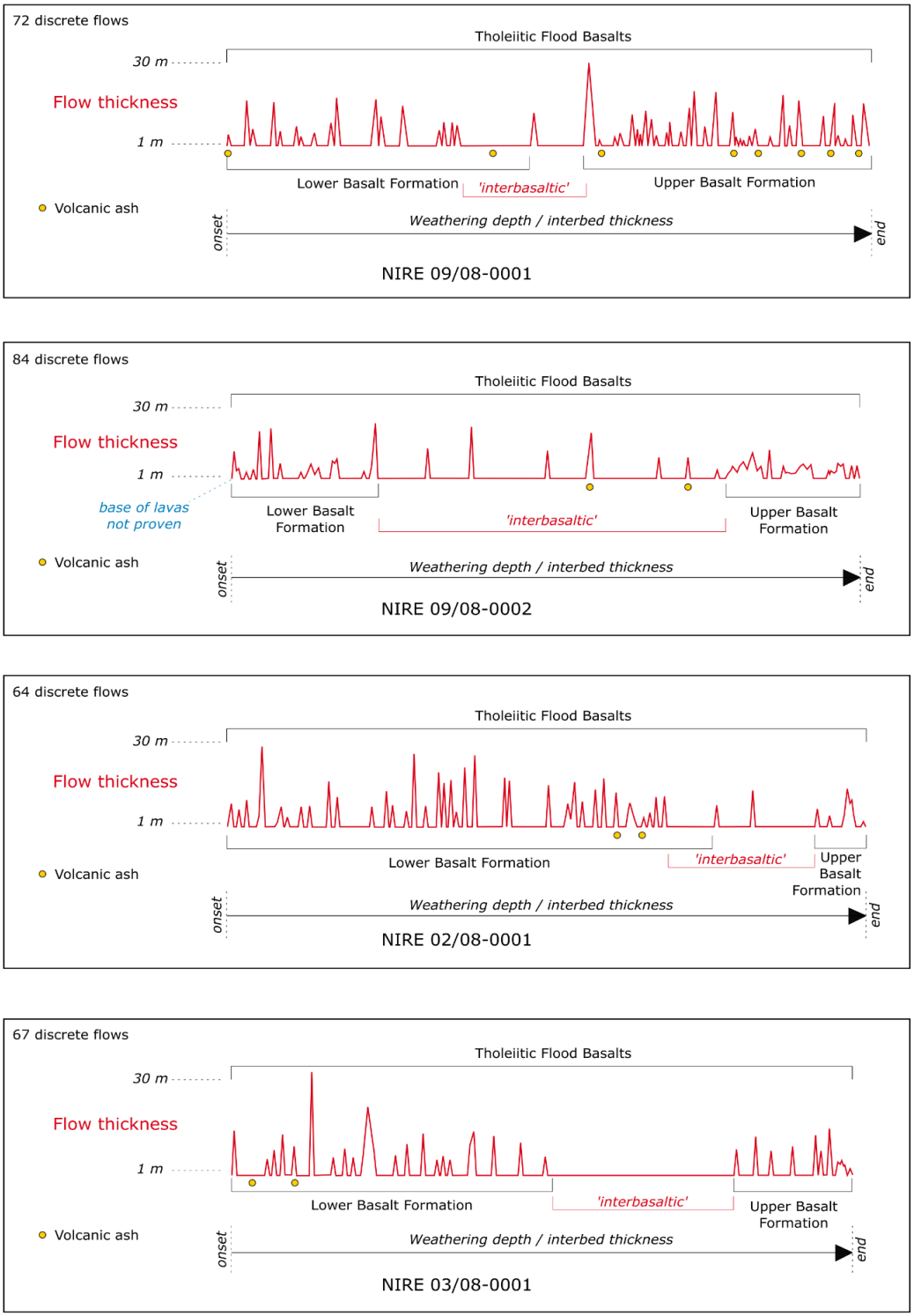

Figure 4.13. Cartoon of Antrim Lava Group eruptive tempo estimate based on weathering depth and interbed characteristics. Horizontal scale is an approximate time estimate based on weathering depths, interbed and palaeosol development and lava superposition, with flat areas of the plot indicating periods of quiescence between lava flows. The width of lava flow 'spikes' are equal and for graphical purposes only. Vertical scale represents lava flow thickness. Interbasaltic is in quotes due to the evident presence of basalt lava flows during this time period.

That said, the plots in Figure 4.13 give some early indication of the non-linear distribution of effusive episodes and intervening time hidden in these thin horizons pointing towards the need for more detailed future investigations.

The emplacement timing, or volcanic tempo, must also take account of the spatial variability of eruptions, i.e. the presence of the Causeway Tholeiite Member appears to be restricted only to the north of the Tow Valley Fault and suggests that not every episode of volcanicity would have contributed to emplacement across the entire Antrim Plateau, an observation that is also well documented in other parts of the province such as on the Faroe Islands and in the Faroe Shetland Basin (Millett et al., 2017; 2021).

Investigation of NIRE borehole cores has identified certain geochemical flow groups that are absent at other locations. Indeed, analysis of the earliest basalt flows in some NIRE boreholes suggests that first flows at those locations were of the Upper Basalt Formation, likely millions of years after the initial onset of Lower Basalt Formation volcanism elsewhere in the ALG. Combined with the knowledge that calciphile ecologies were providing pollen and spores at the time that sands and silts of the sedimentary interbed at Ross's Quarry were being deposited (interbed 2), it is inferred that some limestone uplands must have persisted after the cessation of Lower Basalt Formation lava emplacement. The present day configuration of the Antrim Lava Group almost entirely covering the limestones of the Ulster White Limestone Formation therefore reflects burial that must have been completed during emplacement of the Interbasaltic and the Upper Basalt Formations.

Increasing our understanding of the basaltic lava fields of the BIPIP and the interbeds contained within has implications beyond academic research. Important hydrocarbon reserves are held within siliciclastic interbeds within the Faroe-Shetland Basin north of the UK with fields such as Cambo and Rosebank looking like they will move towards

development (Hardman et al. 2018; Duncan et al. 2020). Recent studies focused on the sub-surface characterisation of the volcanic sequences in the Rosebank Field have highlighted the potential for integrating sub-surface borehole data to better understand the volcanic facies, their distribution, correlation, and implications for associated sediment reservoirs (Millett et al. 2021). Similar approaches to the sub-surface characterization of the Antrim borehole data for facies analyses may be applied going forward and will help to improve future appraisal of energy resources within the province. In the same way, the potential for Carbon Capture and Storage (CCS) projects within the province (e.g. Andrews, 2023) will benefit from an improved appreciation of how these lava fields develop over time in terms of emplacement, volcanic facies, volcanic tempo and associated alteration which can significantly impact reservoir properties (e.g. Liu et al., 2012; Rosenqvist et al., 2023; Millett et al., 2023) and the presence of potential inter-lava sediments.

Integration of focused and detailed palynological studies with high resolution petrological and laboratory geochemical analysis of NIRE borehole core samples and field exposures holds further potential to advance the understanding of flood basalt emplacement mechanisms and timing, the ecology of the local environment and climatic impacts of these eruptions.

4.6 Summary

The Antrim Lava Group of northeast Ireland comprises a volcanic sequence dominated by basaltic lava flows. Including subsidiary sedimentary interlayers and some evolved lavas and intrusions, the overall sequence reaches a cumulative thickness of ~800 m. The tempo of the eruption of the Antrim Lava Group is poorly constrained but can be evaluated via weathering patterns and environmental reconstructions derived from lava-flow interbeds. In

this contribution we present palynology from a newly-identified and well-developed 2 - 2.5 m thick sedimentary sequence (interbed) at Ross's Quarry, Ballycastle, Co. Antrim, that helps elucidate the contemporary development of environments in a setting subject to periodic basaltic volcanism. The interbed is subdivided into geologically distinct subunits of cross-bedded and parallel-bedded sandstones and sandy siltstones, all rich in visible organic remains such as rootlets and fragments of wood and bark. A total of 19 samples were collected from the sequence and subsequently analysed for palynological content. The palynomorph data point toward a diversity of inputs ranging from estuaries, chalky soils, dry soils, swamps, lakes, floodplains, sand bars, wet soils, established bogs and fenlands. In contrast to current understanding, the palynological data and their inferred environments collectively reveal the presence of flora that favour a temperate climate rather than the subtropical climate that has previously been inferred from the lateritic interbeds of the Antrim Lava Group. By combining the Ross's Quarry observations with palynological data from other quarry sites and boreholes in Antrim, we provide new insights into the climate, weathering systems and eruptive history of the Antrim Lava Group.

4.7 Conclusions

Within this study, a detailed appraisal of interbeds among the lavas of the Antrim Lava Group, focussing on the Interbasaltic Formation, was carried out using a combination of geochemical and palynological analyses. From this study we can draw the following conclusions:

1. New palynological evidence suggests:
    i. A warm temperate climate, not subtropical,

ii. An established fen carr was in the catchment area of sediments deposited during the emplacement period of the Causeway Tholeiite Member, and that

iii. Areas of Ulster White Limestone Group persisted coevally with the emplacement of the Causeway Tholeiite Member.

2. Re-evaluation of NIRE borehole core and field outcrop revealed:

i. The presence of a 2.5 m thick sedimentary unit among flows of the Causeway Tholeiite Member at Ross's Quarry, near Ballycastle,

ii. Much of the Interbasaltic Formation is, or was, basaltic lava, and that

iii. In places the Antrim Lava Group has at least 84 discrete lava flows (NIRE 09/08-0002).

3. The presence and distribution of weathering horizons among the Antrim Lava Group is not evenly distributed and suggests that the locations of effusion and eruption moved around over the period of emplacement and that the eruptions were often significantly spaced out over time.

4. Improved knowledge of the internal structure and composition of BIPIP lava fields can aid with understanding energy resources and associated reservoirs in the province, e.g. Rosebank, Cambo as well as the assessment of potential reservoir rocks for CCS.

5. This study highlights the need for high resolution, focussed palynological and geochemical investigation of all Antrim Lava Group boles, laterites and interbeds in order to more fully constrain the volcanic tempo, ecological diversity, local environment and the wider environmental impacts of the basaltic, intermediate and acidic volcanism of the Antrim Lava Group.

CHAPTER 5 – BASALT FLOW WEATHERING, AGE AND VOLUME BEARING ON VOLCANIC TEMPO

5.1 Volcanic activity from examination of weathered flow tops

5.1.1 Overview

The first part of this chapter more fully presents a potential tool for estimating the duration of inter-volcanic quiescence by measuring the weathering depth of individual lava flows, or indeed the absence of such layers. This method, introduced in Chapter 4 (showcased in Figure 13 of that chapter), was devised for this research by the author and applied to the borehole logs generated by Lonmin staff. Knowing the precise weathering rate to apply on a flow-by-flow basis is essentially impossible so instead we took the approach to apply a constant rate of weathering to every weathered horizon. This method would overestimate some intervals and underestimate others, but even in doing so would still serve the valuable purpose of providing us with a tool by which to graphically represent volcanic tempo.

5.1.2 Limitations and decisions

The absolute weathering rate was not considered to be relevant to this analytical method, since the purpose is simply to explore the relative tempo of activity and evidence for episodic behaviour. In applying a weathering rate, I sought to provide an indicative timescale that is consistent with known ages of the ALG. Although this may be incorrect in terms of absolute timing, any error introduced will be systematic. The major assumption is that the weathering rate was constant through time (this cannot be evaluated).

Basalt weathering rates reported by Navarre-Sitchler & Brantley (2007) for Deccan, Hawaii, Columbia Plateau, Reunion Island and Iceland were also used to generate an estimate for the time required to completely change 1 m thickness of basalt to weathered products but as these values ranged from 81,000 to 252,000 years we had little confidence in applying them to our research.

When these values were put into my calculations, the ensuing age range for the whole of the ALG spanned a time period way longer than any currently accepted range. Following on from this, the work of Gislason et al. (1996) was discovered and this value of 25,000 years per metre depth of basalt weathering was applied, based on their Icelandic basalt weathering studies.

This process has produced the first estimate of Antrim Lava Group volcanic activity on a flow-by-flow basis and should be considered as a first step in defining this process as a useful tool for broader application.

5.1.3 A note on hydrology and hydrogeology

The conditions of formation for laterites and bauxites do not necessarily require a subtropical climate so much as the appropriate ratio of mechanical to chemical rates of denudation (Gislason et al., 1996; Nesbitt & Wilson, 1992; Taylor et al., 1992). Recent palynological investigations on interbeds throughout the Antrim Lava Group have shown the palaeoclimate of Antrim to be temperate to warm temperate (Beresford-Browne et al., 2023, Chapter 4 of this thesis) so we must consider this when estimating the rate of basalt weathering and soil formation. It has also been shown that a significant number of the sampled interbeds have a strong lacustrine signal (Beresford-Browne et al., 2023), so the process of interbed ('laterite') formation must also take this into account.

Hydrogeological and hydrological systems would have been operating at elevated temperatures due to the presence of erupting or cooling lavas at and near the surface, and a generally elevated geothermal gradient due to magmatic activity near the surface (Lyle & Preston, 1993). Circulating groundwater is likely to have been significantly higher than the 10–12°C, which would be normal for a warm temperate climate. Elevated groundwater temperatures would lead to accelerated water-rock interactions, which would likely have an as-yet undetermined impact on attempts to estimate basalt weathering times with any accuracy.

Work on the Ulster White Limestone Group in Northern Ireland has already established the presence of thermally-driven meteoric, marine and/or mixed marine-meteoric fluids during diagenetic processes (Scholle, 1975; Maliva & Dickson, 1997). These fluids were present during the main episode of recrystallisation but no evidence was found to associate observed hydrothermal alteration with overlying basalts (Maliva & Dickson, 1997). By constraining groundwater temperatures during the time of ALG emplacement, and searching for hydrothermal and/or geothermal activity at or near surface, future workers may be able to shed more light on this potentially critical aspect of interbed laterite formation within the ALG.

The model proposed here suggests that elevated groundwater temperatures, as opposed to a warmer climate, played a critical role in the formation of laterites within the ALG. The palaeoecological evidence of a warm temperate climate means that a subsurface heat source is the next likely factor responsible for accelerated rates of weathering (cf. rates of basalt weathering calculated for Java (Navarre-Sitchler & Brantley, 2007) are ~19,700 years per 1 m). To constrain this, future workers could focus on finding evidence for hydrothermal activity at or near the palaeosurfaces recorded as red interbeds, lithomarges, laterites, etc. within the lava pile.

Alternatively, future research could focus on developing a sampling strategy that could support the generation of meaningful geochemical proxies for Mean Annual Rainfall and Mean Annual Temperature.

5.1.4 Methodology

Geological information and details of basalt freshness/weathering were extracted from the Lonmin (NI) Plc borehole core logs provided by GSNI. The borehole logs contained detailed information on the amygdaloidal nature of the flow tops of the basalts, as well as notes on the depth of weathering and alteration for each flow.

CHAPTER 5 – BASALT FLOW WEATHERING, AGE AND VOLUME BEARING ON VOLCANIC TEMPO

The primary minerals in basalts (olivine, pyroxenes, plagioclase, K-feldspar, groundmass glass) tend to chemically weather to poorly crystallised iron oxides and hydroxides (Douglas, 1987), a variety of smectite clays, leaving some primary opaque minerals in the weathered matrix (Gislason et al., 1996). Compared with minimum values of ~1,670,000 years per vertical metre weathered (0.6 mm per thousand years) estimated by palaeomagnetic studies from the Monaro Region of New South Wales (Taylor *et al.*, 1992), the rates of basalt weathering in southwest Iceland are reported to be 120 tonnes/km^2/year (Gislason et al., 1996), which equates to 25,000 years per vertical metre weathered (Table 5.1).

Table 5.1. Approximate, estimated rate of vertical, in situ basalt weathering based on Gislason et al. (1996). 3 tonnes/m^3 for basalt density.

tonnes/km^2/year	tonnes/m2/year	m3/m2/year	years/m
120	0.00012	0.00004	25,000

This approximate rate will vary due to several factors, including but not limited to:

- topographic controls
    - slope
    - basins
- climate
    - air temperature
    - surface water temperature
    - rainfall
- lava flow architecture
    - presence and distribution of fractures
    - glass/crystalline ratio
- geothermal activity
    - rock temperature
    - groundwater temperature
- vegetation cover

- time since the last eruption (re: development of soils, etc.)

More refined models attempting this method will need to account for these variables, and possibly more, including the additional facts:

1. the dissolution rate of silicates increases by an order of magnitude between temperatures of 0° to 25°C (Lasaga et al., 1994) and
2. the glassy tops and bases of basalt flows will weather faster than the crystalline flow core by a factor of 10 (Gislason & Eugster, 1987).

5.1.5 Results

Applying the weathering rate of 25,000 years per metre (Gislason et al., 1996) to the depth of weathering recorded in the Lonmin (NI) Plc boreholes is summarised in Table 5.2. The full data set is supplied in Appendix H.

Dividing the estimated weathering time by the number of flows counted in each borehole allows us to estimate the eruptive cyclicity at each location (Table 5.2). By doing this we can see that over the whole of the ALG the eruptive cyclicity ranged from approximately 11,000 to 41,000 years, with an average of 24,000 years between significant eruptions.

The estimated data in Table 5.2 suggest that the maximum recorded length of weathering throughout the ALG at the location of NIRE 03/08-0001 was 2,750,000 million years (My). If we sum the longest estimated times for each formation we get a suggested maximum of 3,880,250 years for the emplacement of the remnant Antrim Lava Group. The Antrim Plateau has been uplifted and denuded since its emplacement (Simms, 2000), which is further evidenced by the coexistence of late Paleocene to early Eocene granitic bodies (e.g. Mourne, Carlingford, Slieve Gullion) alongside Paleocene dolerite dikes (basalt feeder dykes) at current ground levels (Figures 6.7 and 6.8, Chapter 6), so all attempts to estimate the length of emplacement timing might be considered as minima under these circumstances.

*Table 5.2. Estimated and average time spans and eruptional cycles represented by weathered horizon geometries from borehole data. (*excluding intrusive, e.g. dolerite sills)*

Borehole ID	Total estimated weathering time (years)	Lower Basalt Formation	Interbasaltic Formation	Upper Basalt Formation	Flow count	Eruption cycle (yr-1)
NIRE 01 08 0002	881,000				37	23,811
NIRE 01 08 0003	150,500				6	25,083
NIRE 01 08 0005	839,250				34	24,684
NIRE 01 08 0006	503,500				36	13,986
NIRE 01 08 0009	158,250				5	31,650
NIRE 02 08 0001	2,239,250	1,540,750	537,000	161,500	64	34,988
NIRE 03 08 0001	2,752,500	972,000	1,656,500	156,000	67	41,082
NIRE 03 08 0002	562,250				29	19,388
NIRE 03 08 0003	554,500				49	11,316
NIRE 03 08 0004	351,000				25	14,040
NIRE 04 08 0001	727,000				20	36,350
NIRE 04 08 0002	134,000				6	22,333
NIRE 05 08 0002	502,750				17	29,574
NIRE 08 08 0001	494,750				25	19,790
NIRE 08 08 0002	237,250				13	18,250
NIRE 09 08 0001	1,752,000	631,500	437,500	683,000	79	22,177
NIRE 09 08 0002	2,667,500	596,750	1,519,500	551,250	84	31,756
NIRE 11 08 0001	691,000				51	13,549
				Minimum	*5*	*11,316*
				Average	**36**	**24,100**
				Maximum	*84*	*41,082*

Patterson & Mitchell (1955) presented an account of the Causeway Tholeiite Member lava flows, including notes on the "Characteristics of upper surface" which presented an approximate account of the depth of weathering for each of the seven flows listed. This information is summarised in Table 5.3 along with the application of our time estimation process on flow tops based on their weathering depths. It is interesting to consider that the emplacement of the Causeway Tholeiite Member lavas may have taken almost 400,000 years!

We can visualise this volcanic tempo by plotting the volcanic eruptions by their measured thickness (y-axis) at a given location and putting the time estimated by weathering depth on the x-axis. It is important to reiterate that the onset of volcanism was not coeval across the BIPIP or the Antrim region, nor is it possible to regionally correlate flows based on their thickness due to pre-volcanic

topographic variation. Based on the assumed weathering constant, we find the plotted data representative of volcanic tempo. We note that the assumed weathering rate would impact the exact times shown on the X-axis.

Table 5.3. Summary of Table 1 data (Patterson & Mitchell, 1955)

Flow	Thickness (ft)	Depth of weathering (ft)	Weathering %	Estimated weathering time (years)
7	50	25	50%	190,500
6	50	10	20%	76,200
5	80	1.5	2%	11,430
4	80	1.5	2%	11,430
3	60	10	17%	76,200
2	75	0	0%	0
1	100	2	2%	15,240
Total	**495**	**50**	**10%**	**381,000**

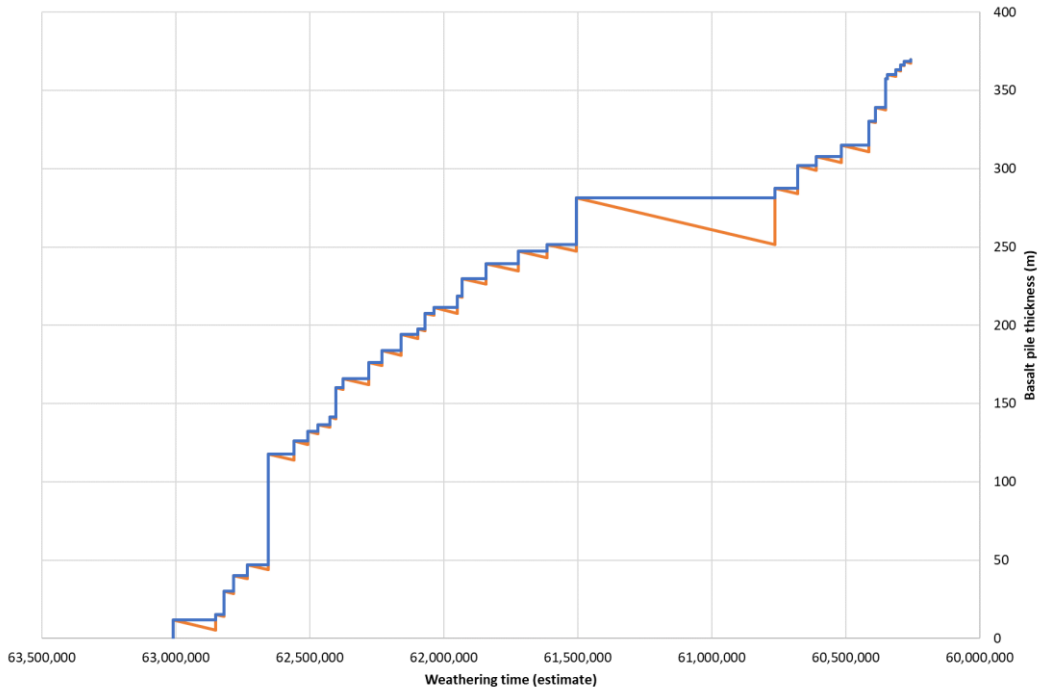

*Figure 5.1. Data from borehole **NIRE 02/08-0001** showing basalt accumulation (blue) and associated depth of weathering used to estimate the time taken (orange).*

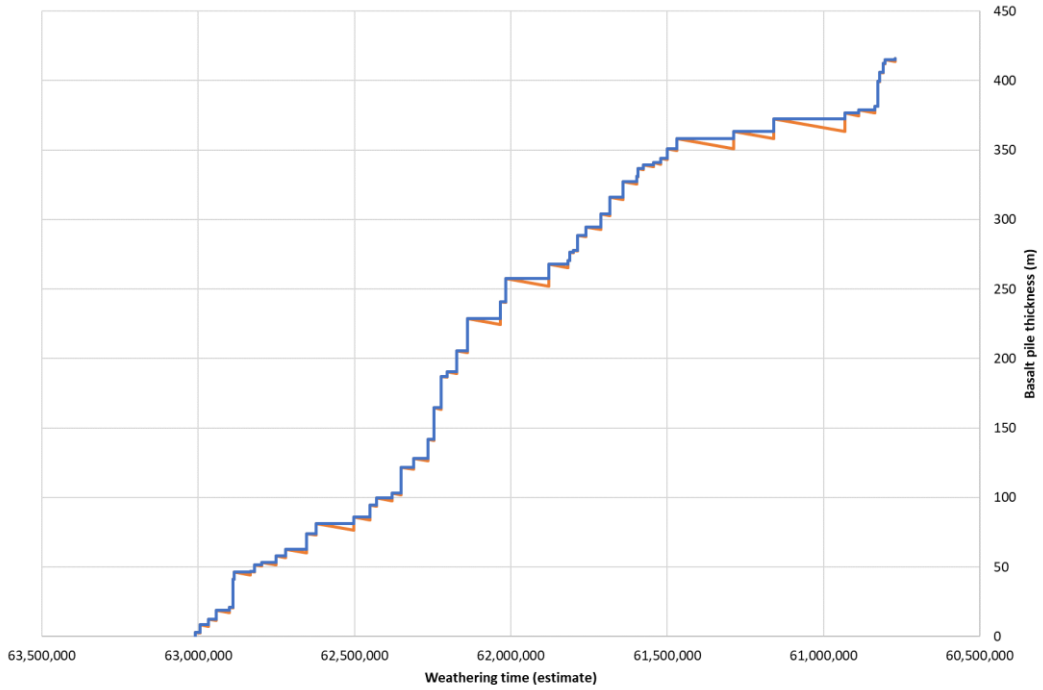

*Figure 5.2. Data from borehole **NIRE 03/08-0001** showing basalt accumulation (blue) and associated depth of weathering used to estimate the time taken (orange).*

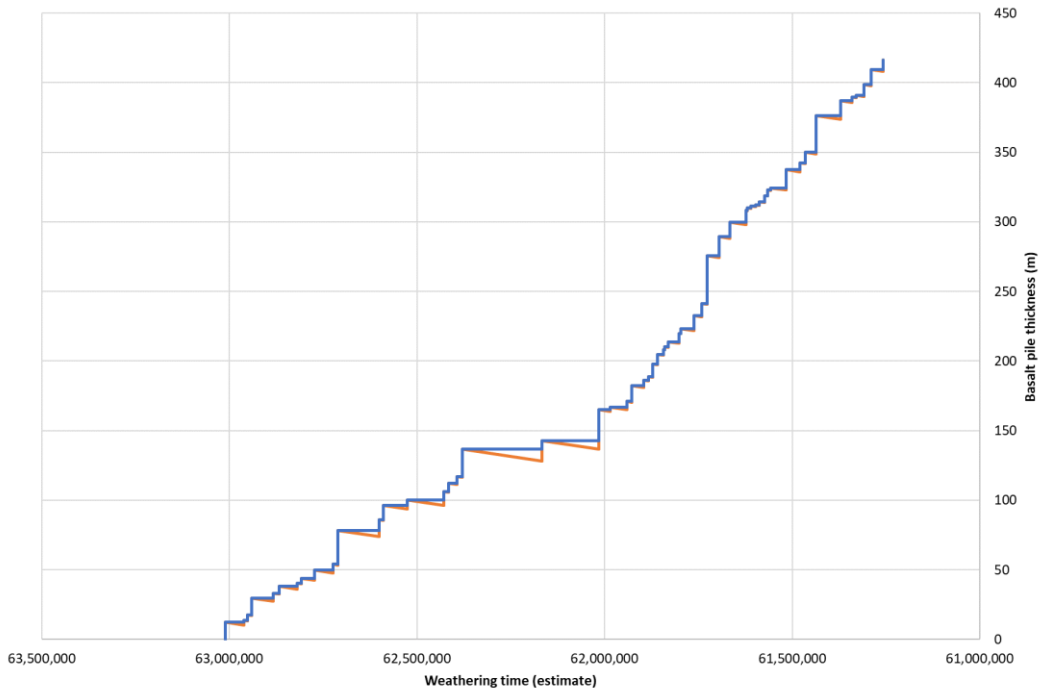

*Figure 5.3. Data from borehole **NIRE 09/08-0001** showing basalt accumulation (blue) and associated depth of weathering used to estimate the time taken (orange).*

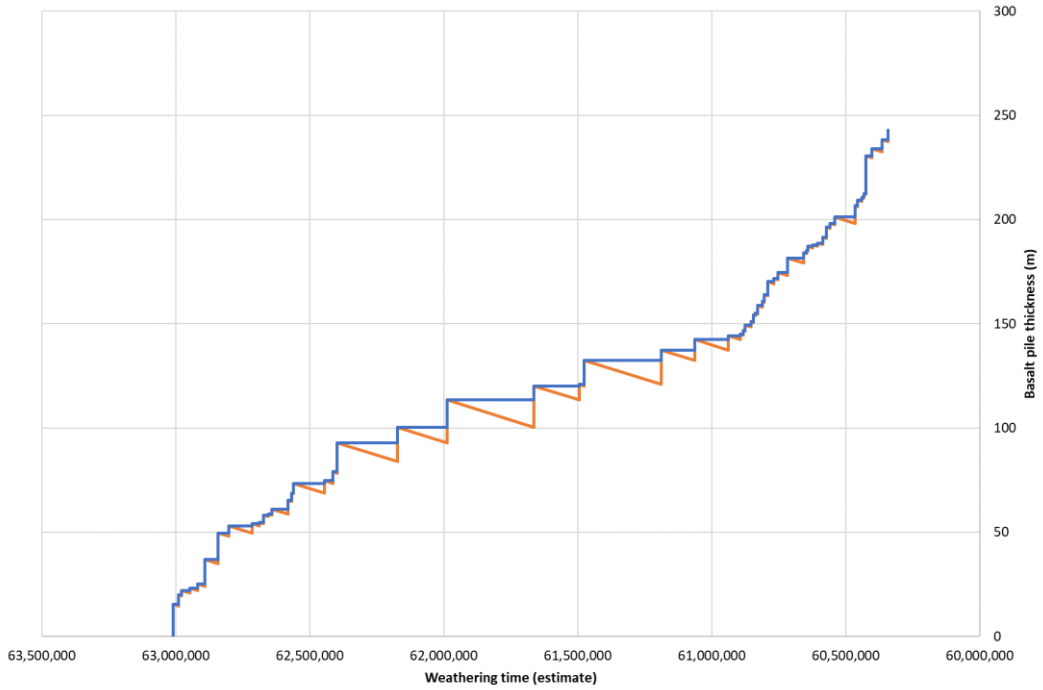

*Figure 5.4. Data from borehole **NIRE 09/08-0002** showing basalt accumulation (blue) and associated depth of weathering used to estimate the time taken (orange).*

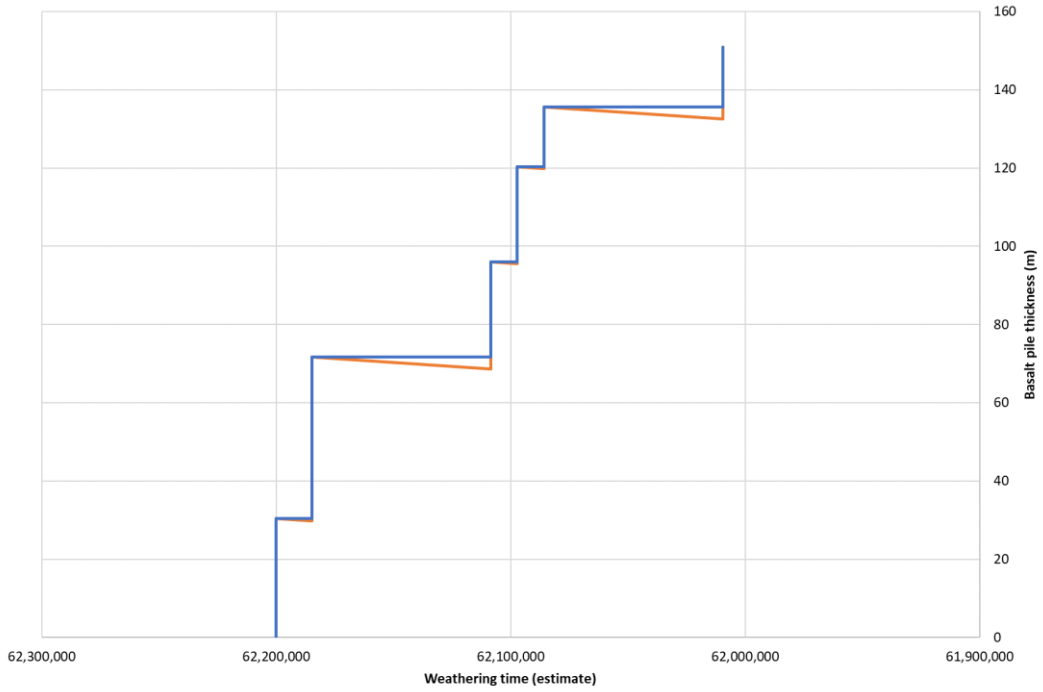

Figure 5.5. Data of the Causeway Tholeiite Member from Patterson & Mitchell (1955) showing basalt accumulation (blue) and associated depth of weathering used to estimate the time taken (orange).

5.1.6 Discussion

Our preliminary findings suggest that this novel approach toward studying the tempo of volcanism could be refined into a useful tool for determining the volcanic tempo of ancient systems. For example, the sketched timeline in Figures 5.1 to 5.4 could be calibrated by known age data to provide reasonably reliable anchors upon which to calibrate the plots.

More detailed sampling and analysis of basalt flows and interbeds would yield higher resolution data for calculating estimates of annual rainfall and temperature by geochemistry, indicators of ecological stability and rates of change by palynology, etc.

5.1.7 Conclusions

In this section we have discussed, and reinforced, the hypothesis that the geological time recorded in the lithologies of the ALG is almost exclusively locked away among the interbeds and weathered basalt flow tops, rather than in the lava flows themselves. It would be reasonable to extend this to the BIPIP, the wider NAIP as well as other continental LIPs of basaltic composition since the essential mechanisms at work are likely to be similar.

5.2 Review of published volcanic timing of the ALG, BIPIP and NAIP

5.2.1 Overview

The first part of this chapter discussed the role of inter-volcanic quiescence as a tool by which we can estimate the emplacement timing and volcanic tempo of flood basalts of the ALG and perhaps the wider BIPIP and NAIP. This chapter focuses on the published age data for igneous rocks of the ALG, BIPIP and NAIP, and their role in providing another data stream to aid with clarifying the volcanic tempo and volcanotectonic setting of the Antrim lavas.

5.2.2 Methodology

As part of the NAG-TEC project (Northeast Atlantic Geoscience - Tectonics), Wilkinson et al. (2017) compiled, evaluated and corrected a significant body of age data for NAIP rocks. By so doing, they have revealed that subject to any sampling bias present in pre-existing work there was a near-constant sequence of volcanic activity across the NAIP between 65 – 40 Ma (Figure 5.6).

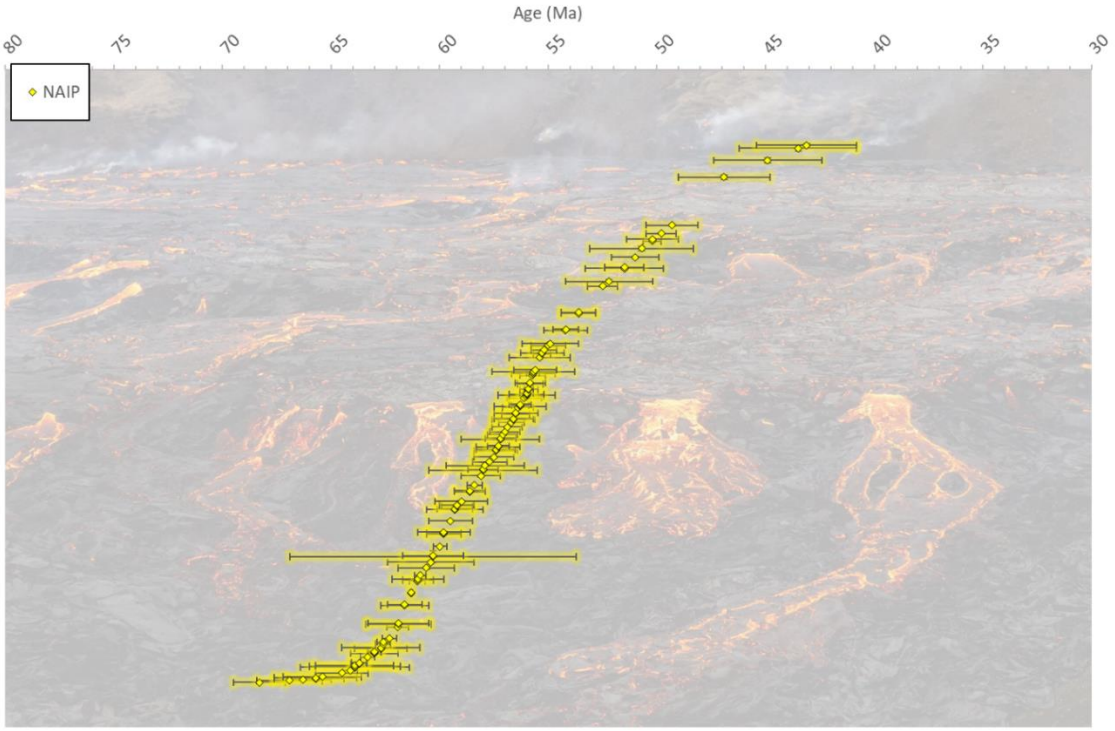

Figure 5.6. Replotted NAIP age data from Wilkinson et al., 2017 (yellow diamonds ± 1σ error bars) with a background image of basalt flows in Iceland. The age data are ordered sequentially from oldest to youngest, and this numbering is applied to the y-axis to separate data points visually. NB. This potentially creates a bias in the sample distribution, as discussed below.

SAMPLE BIAS IN NAIP AGE DATA: A side note is required here concerning the limited sampling distribution and inherent sample bias in the NAG-TEC dataset: due to the apparent access limitations to most rocks of the NAIP, the distribution map behind Figures 5.6 to 5.9 is only partially representative of the volcanic activity from 65 to 50 Ma (a narrower range than the plotted data from 80 to 30 Ma). The curved pattern of the plotted age data is simply a function of the order in which the data points self-organise when put in age order from oldest to youngest. The geometry of the curve is indicative of the intensity and location of sampling by workers and not a geological function. More samples within a certain timeframe will increase the slope, fewer samples will cause a concomitant decrease.

To check for undercoverage bias in the dataset we can compare the distribution of characteristics between the sample set and the target population; marked differences are likely to indicate undercoverage bias. Due to accepted geological time constraints for the NAIP we would expect the age range for NAIP rocks to mainly fall between early Danian and middle Ypresian ages (~65 and ~50 Ma). As presented in Table 5.4, approximately 72% of the sample dataset ages fall within this range, thereby suggesting negligible bias in the dataset.

NAG-TEC sample count (65 to 50 Ma)	NAG-TEC total count (Greenland/Faroe/BIPIP)	Population count as %
468	654	72%

Table 5.4. NAG-TEC data population (Wilkinson et al., 2017)

If correct, the long-held model of binary volcanic activity in the formation of the ALG would be visibly supported by these age data. However, replotting Figure 5.6 with only data points from the BIPIP (Figure 5.7), and again with only data points from the island of Ireland (Figure 5.8), reveals a different story; one of apparent continued volcanic activity that shifted around the subprovince and subprovince regions (Figure 5.7 includes Scottish volcanics, Figure 5.8 presents only Irish volcanic samples), particularly from ~65 to ~55 Ma (mentioned as this is the range within which we should expect to find the 'Interbasaltic' hiatus).

It is only once the age data reported from the Mourne Mountain basaltic dykes are removed (Figure 5.9) that we see what appears to be a less continuous system after ~57 Ma but we must consider whether this is due to an actual gap in basaltic volcanism from ~57 to 53 Ma, or simply whether basaltic rocks of that age have not been analysed due to access limitations, incomplete study or because the effused lavas have been eroded in the time since deposition (e.g. denuded flood basalts to the south of the Laggan Valley).

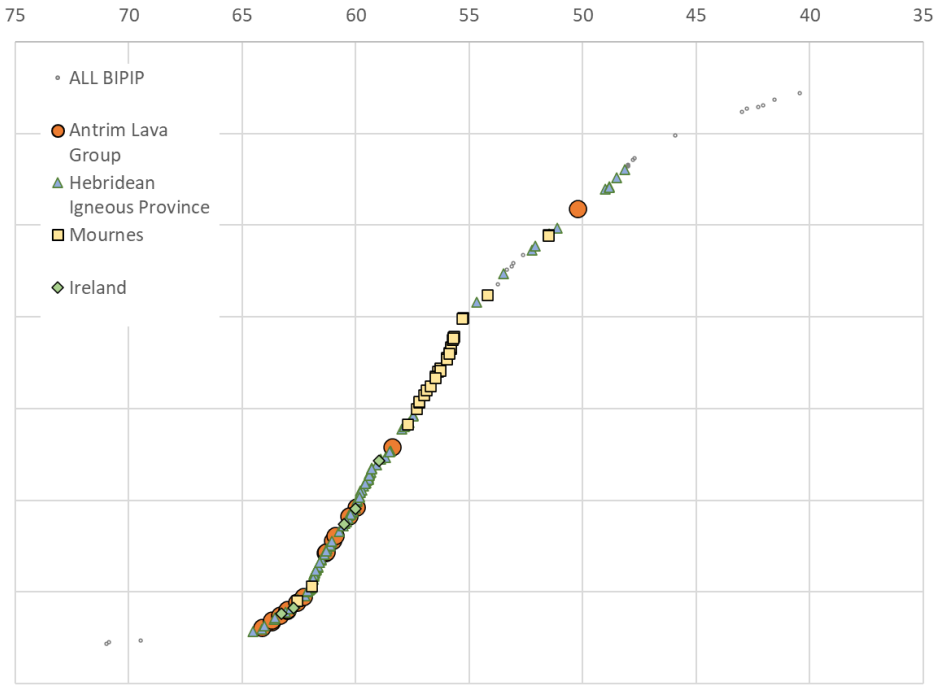

Figure 5.7. BIPIP age data from Wilkinson et al., 2017. Data points and errors as Figure 5.6.

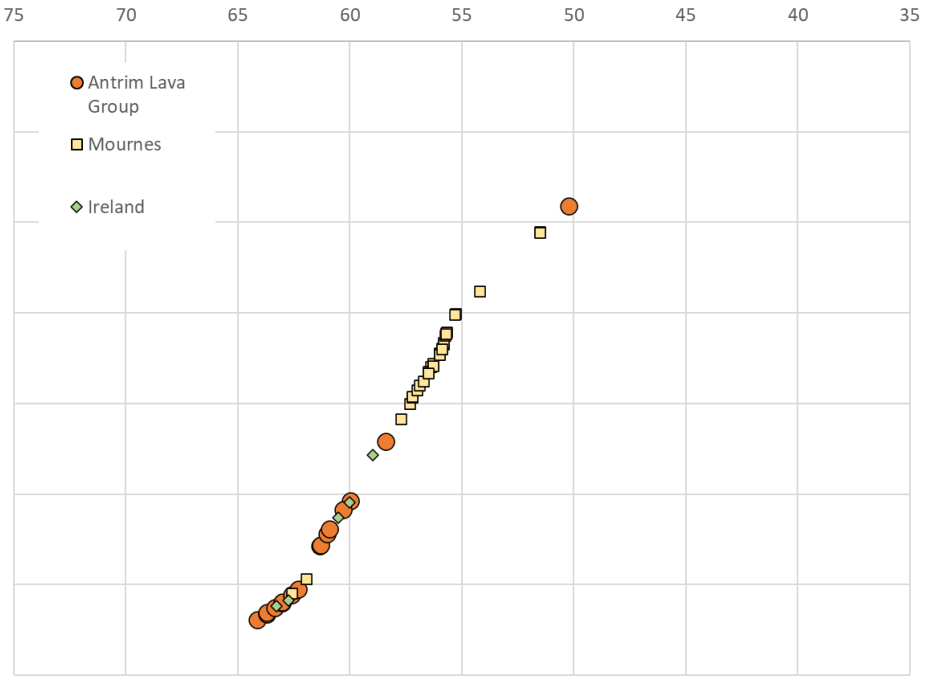

Figure 5.8. Irish-only age data from Wilkinson et al., 2017 including basaltic dyke data from the Mourne Mountains. Data points and errors as Figure 5.6.

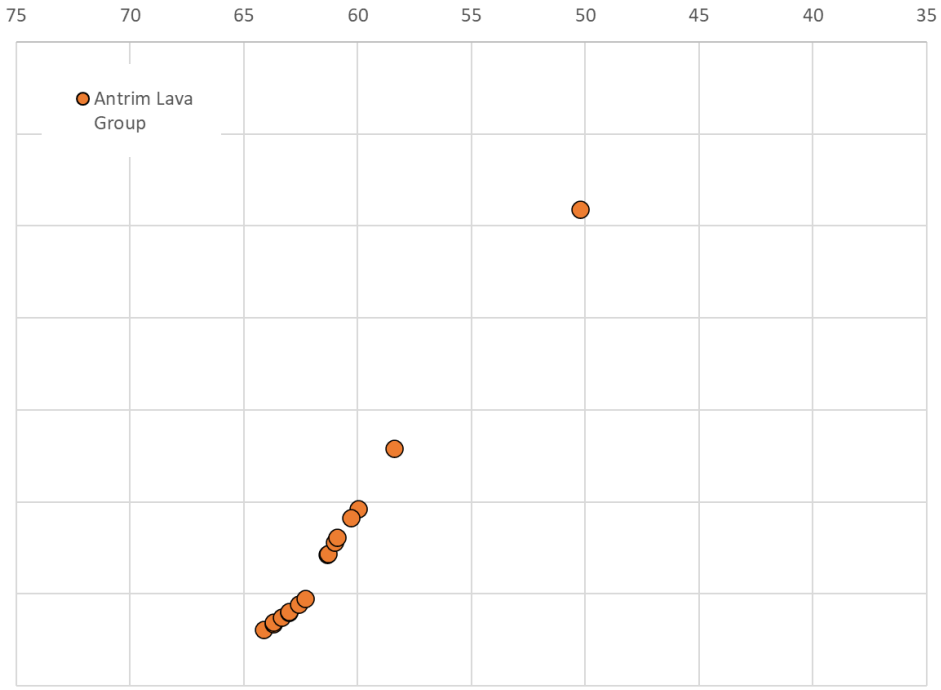

Figure 5.9. ALG age data from Wilkinson et al., 2017 without the basaltic dyke data from the Mourne Mountains. Data points and errors as Figure 5.6.

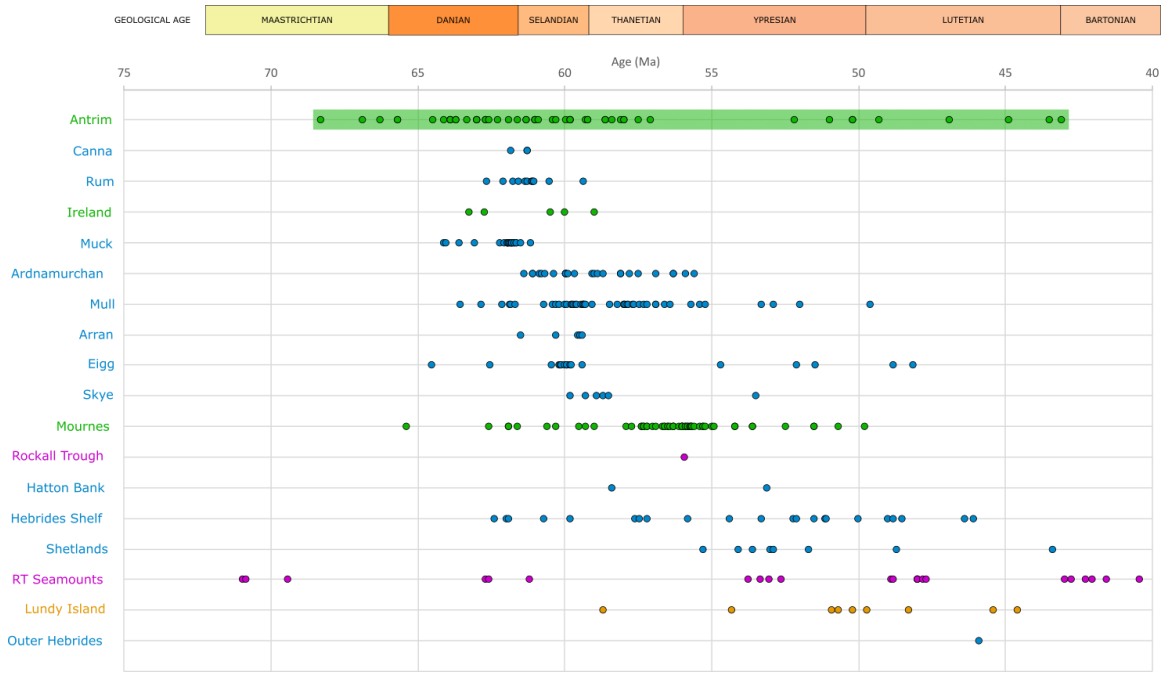

Figure 5.10. Age data from the BIPIP (Wilkinson et al., 2017) showing dated volcanic activity separated by minor regions of the subprovince.

5.2.3 Discussion

Although samples of Antrim basalt yield ages as old as 68.3 million years ago (Ma), there are very few data across the plateau to support that as an agreed time for the onset of flood basalt volcanism (Figures 5.9 and 5.10). Instead, we can look to when age data begin to cluster, and thereby give a more rigorous and defensible age for the onset of flood basalt activity. By 64.11 ±0.34 Ma we are seeing an increase in Antrim basalt samples with an approximate age of 64 Ma (Wilkinson et al., 2017), with 9 samples all yielding ages in the range from 65.71 ±1.3 Ma to 63.01 ±1.1 Ma (maximum 67.61 Ma, minimum 61.41 Ma, average 64.06 Ma). While we accept an age of ~64.1 Ma for the onset of flood basalt volcanism in Antrim we should again note that not all areas of Antrim received lava flows this early on, either due to topographic controls or simply due to unfavourable fissure/dyke swarm locations.

Next, we applied the same process to the waning phase of flood basalt volcanism across the data for Ireland (Wilkinson et al., 2017), i.e. when the volcanic activity becomes far less frequent (albeit based on the limited population of available age samples). This shows a decrease at ~55.7 Ma, with 15 samples all yielding ages in the range from 55.90 ±0.4 Ma to 54.91 ±1.3 Ma (maximum 57.58 Ma, minimum 53.61 Ma, average 55.53 Ma).

So here we present an updated timespan of 64.1 to 55.7 Ma for volcanic activity in the Antrim subprovince. Previous work, including the work that presented the age data, has tended to suggest that dates that fall outside what is expected to fit the pre-existing model are spurious or incorrect. Here we propose that the ages of NAIP basaltic rocks of the ALG (and indeed the BIPIP and NAIP) span much more time than previously considered and that the bimodal model of volcanics and tectonics (Phase 1: 62 - 58 Ma, Phase 2: 56 - 53 Ma) requires revision in light of the plethora of published age data and the interpretations and discussion presented in this work. Figure 5.11 presents histograms of the volcanic and plutonic events that have been dated, presented in peer-

reviewed publications and re-reviewed in 2017 (Wilkinson et al.) as part of the NAG-TEC project. Looking at Figure 5.11(a), it is easy to see that background volcanic activity in the NAIP that had been rumbling away from c.80 Ma gained momentum c.64 Ma. This activity increased, reaching its peak between 61.5 and 55.7 Ma before entering a more calm phase between 55.7 and 46 Ma. This apparent calm may be due to sampling bias associated with the bulk of volcanic activity happening within the rifting North Atlantic basin that is currently dated at c.56-54 Ma (Saunders et al., 1997; Ellis & Stoker, 2014) . If the majority of volcanism was indeed occurring in submarine conditions, e.g. emplacement of seaward dipping reflectors (SDRs), there would be far fewer observable rocks for geologists to sample and thereby a reasonable basis for a certain degree of sampling bias. However, the Wilkinson et al. (2017) age data set used here has ~48 samples taken from 7 offshore sites of investigation across the NAIP so it is fair to state that the oceanic phase of NAIP volcanism is represented to an acceptable level for this application.

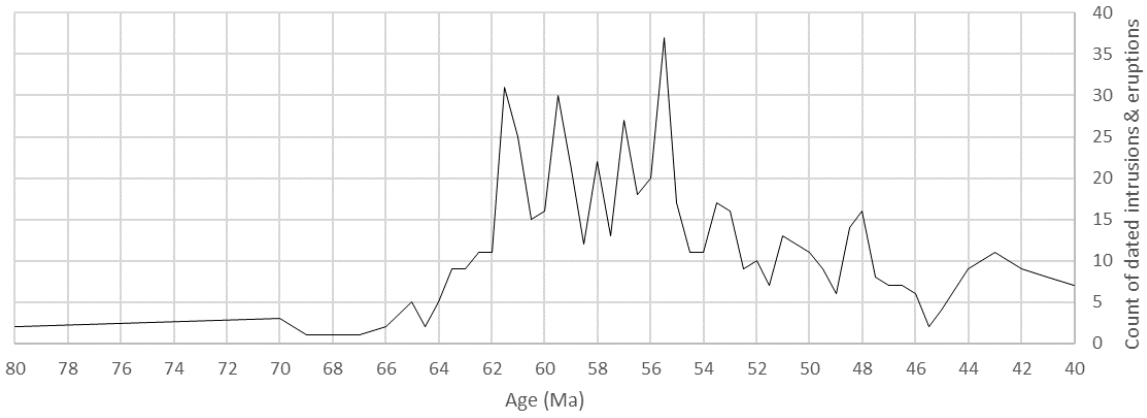

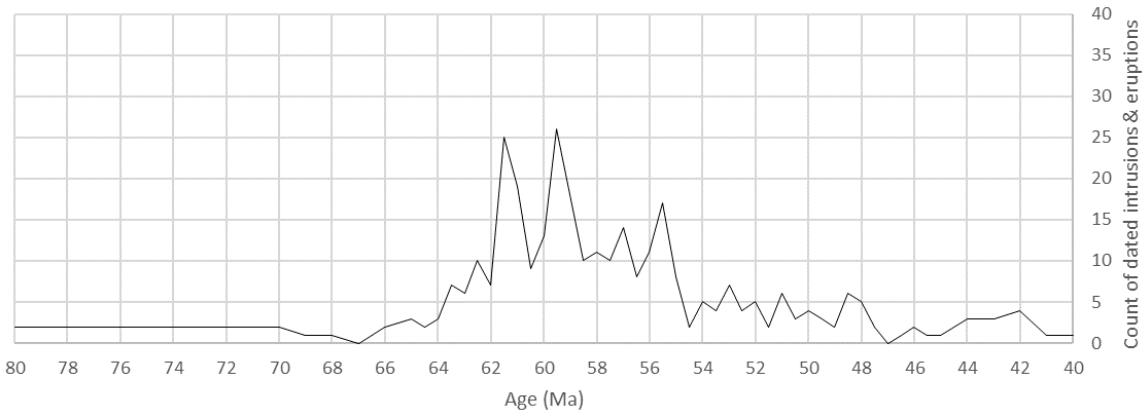

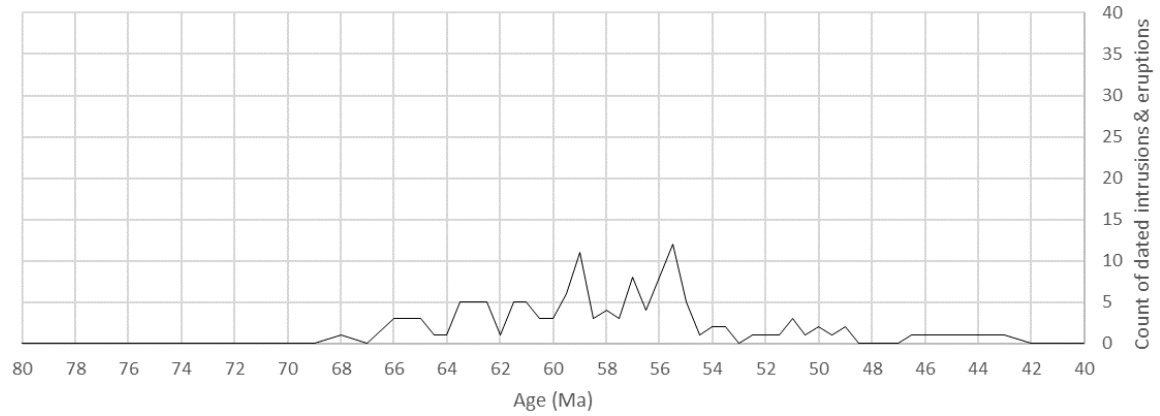

Figure 5.11. Histograms of dated samples presented in Wilkinson et al., 2017. (a) All NAIP activity. (b) Only BIPIP activity. (c) Only Irish/ALG activity. Data tables for these plots are presented in Appendix J.

The same pattern is evident in the BIPIP and ALG (Figures 5.11(b) and (c)), suppressed due to the lower event counts expected of subprovince and regional volcanism. BIPIP activity peaked between 61.5 and 55.7 Ma, notably more between 61.5 and 59.5 Ma. To date, it appears that this peak activity has been identified as the 'correct' timing for the emplacement of the ALG.

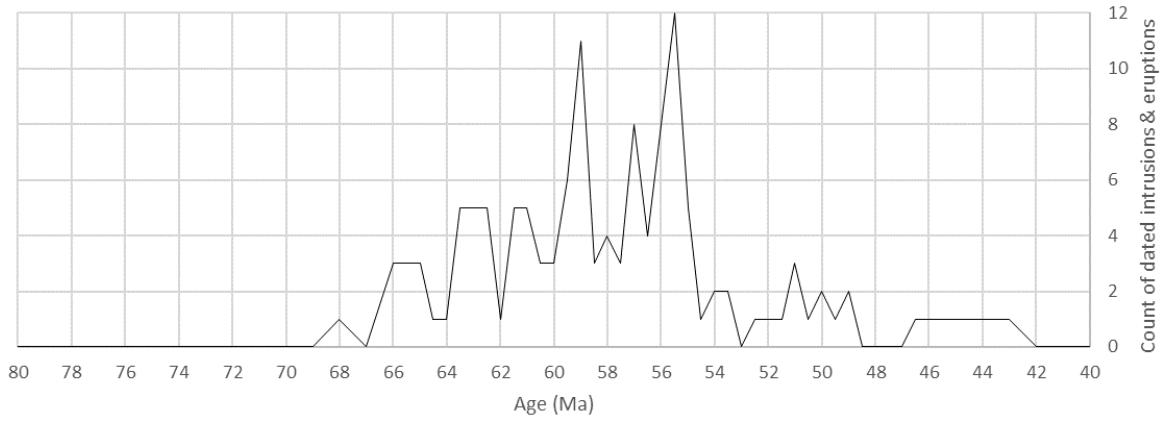

Figure 5.12. Histogram of dated Irish/ALG volcanic and plutonic activity. Data table for this plot is presented in Appendix J.

Replotting Figure 5.11(c) with a more data-sensitive y-axis shows that unlike in the rest of the BIPIP, the peak activity in Ireland appears to be concentrated a little later, in the 59 to 55.5 Ma range (Figure 5.12).

By visually grouping volcanic activity into tentative phases for the NAIP, we might reasonably arrive at Figure 5.13. The naming of these phases is indicative only, as it is quite possible that the lack of

dated samples in the 'Waning phase' is simply because they are all now submarine and not readily exposed for sampling.

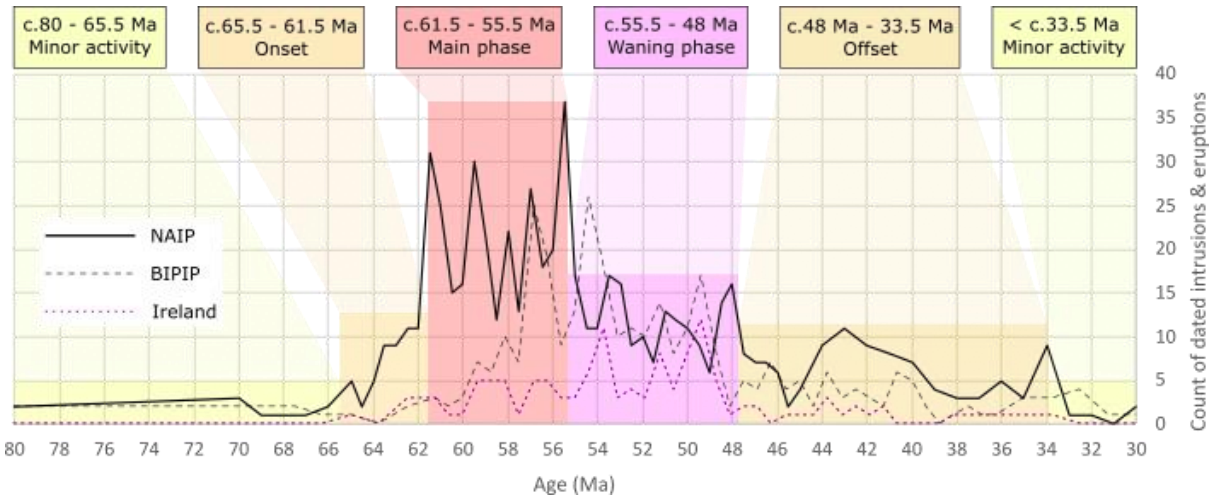

Figure 5.13. Histogram of NAIP volcanic activity counts annotated with tentative phases for NAIP volcanism. These phases are solely based on published ages for igneous rock samples and do not attempt to include or correlate with North Atlantic oceanic extension data. Data credit: Wilkinson et al., 2017. (n = 658)

While this part of the plot could give a false indication of activity (because volcanic activity may have continued apace but we simply don't have the samples to fill our dataset) it may also hint at the point at which NAIP volcanic activity moved from predominantly continental to predominantly oceanic and thereby offer agreement for the timing of the opening of the North Atlantic Ocean. If this were shown to be the case, the two central phases might accordingly be renamed as the "Continental Phase" and the "Oceanic Phase".

Figure 5.14 was compiled by combining the age histogram plots with the timeline of previously investigated and published events already discussed in the thesis. In addition, tentative annotations have been made that lead the reader towards the need for further research.

The histograms presented in Figures 5.11 and 5.12, and summarised in Figure 5.13, are incorporated in Figure 5.14 to provide a visual sense of the volcanic tempo across the whole of the NAIP, with individual subprovince tempo histograms revealing their roles in the overall level of activity.

CHAPTER 5 – BASALT FLOW WEATHERING, AGE AND VOLUME BEARING ON VOLCANIC TEMPO

The youngest (Maastrichtian) components of the Ulster White Limestone Group are shown here to be approximately coeval with thermal uplift, volcanic activity and the formation of facies 1 (Cooper et al., 2018) of the 'Clay with Flints' unit. The various geological remnants and deposits from this complex period require further investigation to clarify the role of the budding LIP on the chemistry and temperature of the North Atlantic ocean, and to develop a clearer picture of the location and nature of the early onset, explosive volcanic activity on and near the Irish landmass(es) of the time.

The notion that flood basalt activity did not entirely cease during the time that the weathered rocks and other deposits of the Interbasaltic Formation were being formed leads us to question not only the erroneous name of that formation but also suggests that the stratigraphic column of the Antrim Lava Group requires a rethink and rebuilding from the ground up. The existing understanding is founded on certain principles being broadly applied across the extant plateau, but it appears that the geological truth may be quite different, e.g. a thorough investigation into the age and geochemistry of the basaltic dikes in and around the Mourne Mountains, and generally those found to the south and southeast of the Laggan Valley, is likely to reveal a more complete history of volcanic activity in the subprovince.

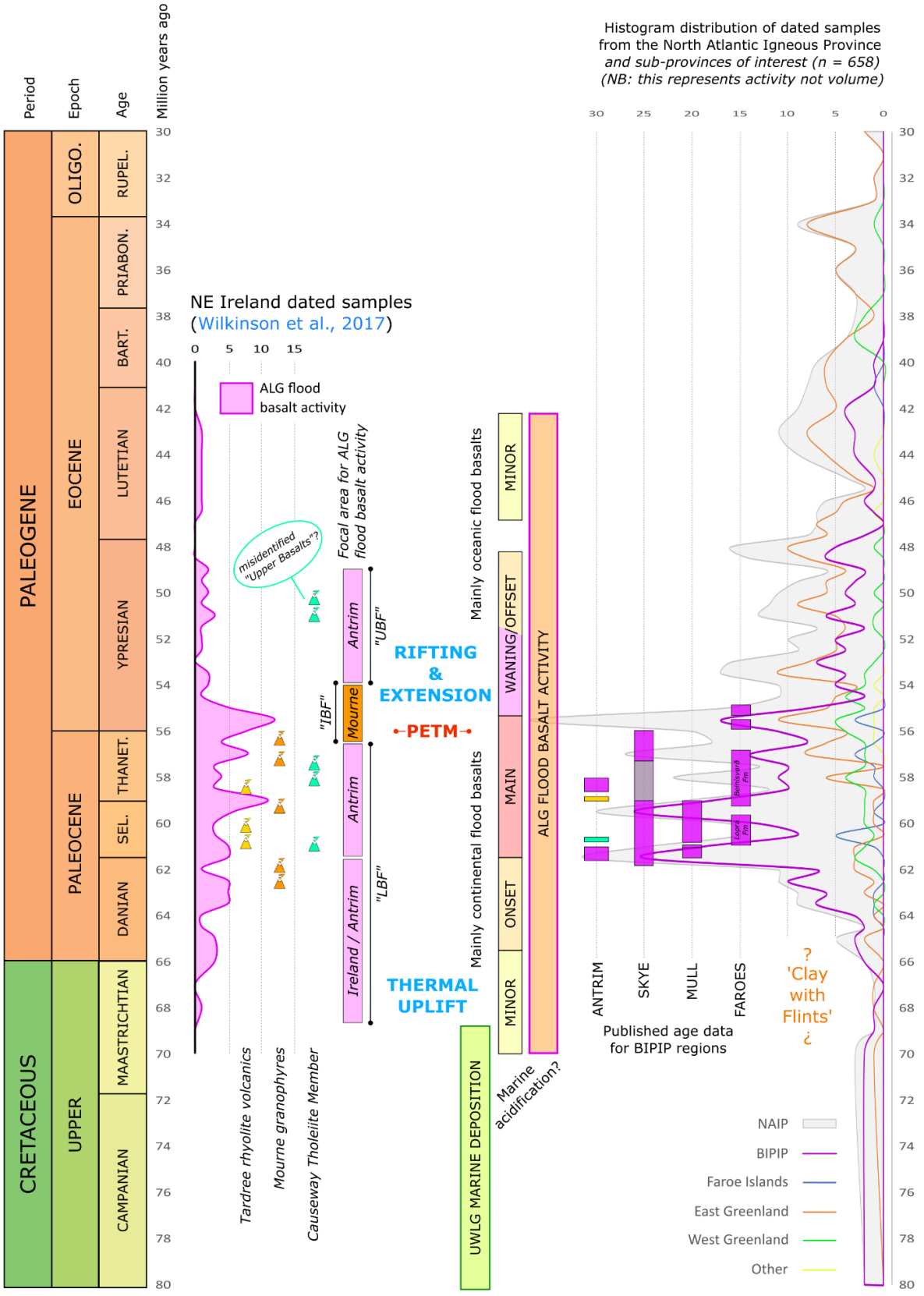

Figure 5.14 Chronostratigraphic timescale from 80 to 30 Mybp, with details from the NAIP, BIPIP and ALG

5.3 Flow volumes as an indicator of activity and tempo

5.3.1 Overview

The first two parts of this chapter presented potential methods for investigating the tempo of NAIP volcanic activity based on weathered horizons within the ALG basalts and published age data for the NAIP. This section embraces the findings of the two previous sections to build on published work to estimate the mean eruption rate of the NAIP (e.g. Eldholm & Grue, 1994). We start by considering a model of the NAIP as a whole, before turning our attention to the Antrim Lava Group.

5.3.2 Methodology

The NAIP has been shown to have been consistently (if periodically) active for approximately 32 million years, from c. 65.5 to c. 33.5 Ma (Figure 5.6, data from Wilkinson et al., 2017), therefore calculations to estimate rates of volcanic activity should be based on the currently estimated time span, rather than the understandably outdated concept of 3 million years applied by Eldholm & Grue in 1994 (Eldholm et al., 1989).

5.3.3 Calculations

The area covered by the NAIP is ~1,300,000 km^2, with a volume of ~1,800,000 km^3 (Table 3, Eldholm & Grue, 1994). Given a defendable, calculated volume of 1.8 x 10^6 km^3 for the NAIP, and a revised emplacement period of 32 million years, this gives us a mean eruption rate of 0.06 km^3/yr. If the volume of the new North Atlantic oceanic plate (total NAIP crustal volume) is added into the equation we arrive at a mean eruption rate of 0.21 km^3/yr.

On the east flank of the Antrim Lava Group, between the Inver River waterfall and Garron Point, there is a single, mappable basalt lava flow that is ~9.7 km long, 3.5 km at its widest point and

between 18 and 24 m thick (Walker, 1959). Allowing for tapering at the ends, this yields an approximate volume of 0.5 km^3 for this single lava flow.

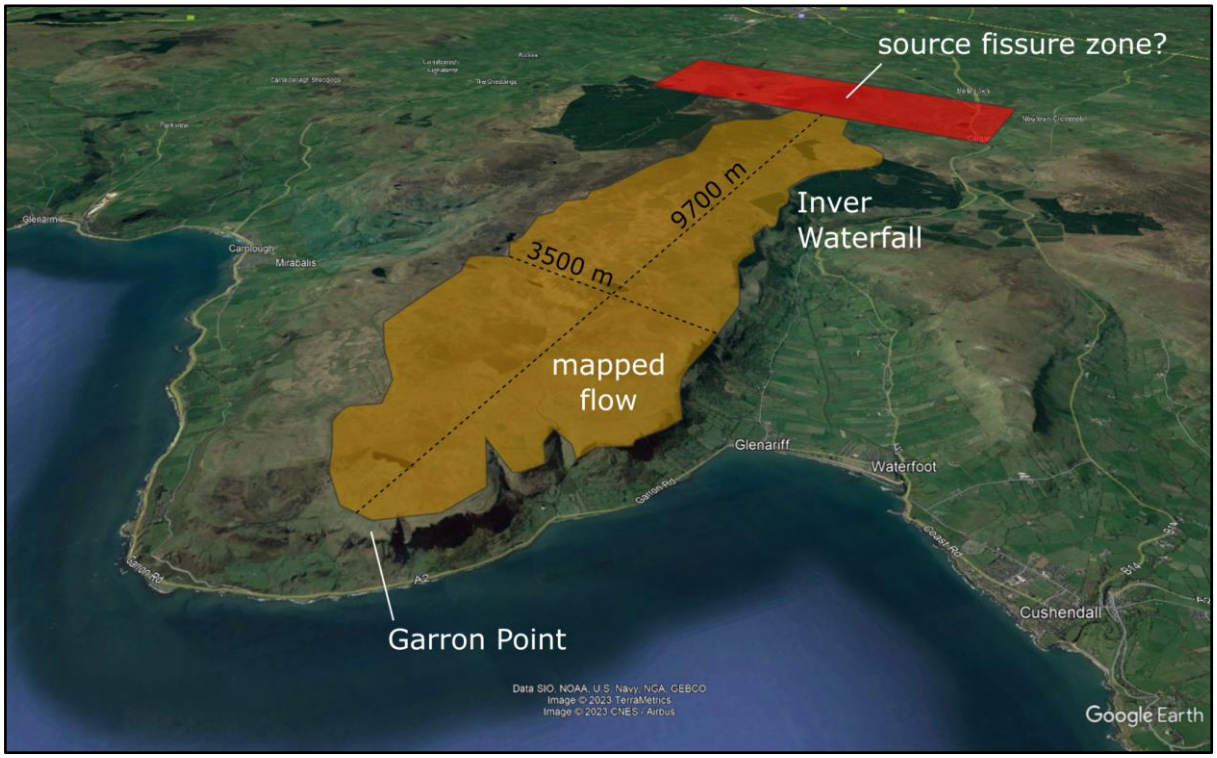

Figure 5.15. View from 5 km altitude looking southwest of an ALG lava flow mapped by Walker (1959) between Inver Waterfall and Garron Point. Base image ©Google Earth.

This one flow is at least twice the volume of the calculated average extruded volume, so averaging the eruption rate over the entire 32 million year span of the LIP probably gives a spurious indication of the annual rate of eruptive volumes.

5.3.4 Discussion

Here we propose that the mean eruption rate of 0.6 km^3/yr estimated by Eldholm & Grue (1994) was an order of magnitude higher than the recalculated rate of 0.06 km^3/yr.

From the available subset of sampled igneous rocks, the revised age data for NAIP has clearly shown a near-continuous sequence of activity from ~65.5 to ~33.5 Ma. While the plotted data (Figure 5.6) does offer visual bias due to the availability of analysed samples, the pattern density offers a very clear indication of how volcanic activity was temporally spread over much more than 3 million years.

However, simply quoting the mean rates of effusion will not give a reasonable indication of the actual tempo of the tectonovolcanic system responsible for ALG volcanism. As we have shown in this work, the history of the NAIP is full of breaks in volcanic activity, periods of time during which basalts weathered and eroded, ecologies established and flourished, fens and boglands thrived, all in landscapes dotted with lakes and rivers. This is also widely evidenced by work done on several regions of the BIPIP and subprovinces of the NAIP, e.g. North Sea (Jolley & Morton, 1992), Skye (Jolley, 1997), Mull (Jolley et al., 2009), Faroe Islands & Rockall (Jolley et al., 2021), Greenland, Arctic & Norway (Hovikoski et al., 2021), Faroe Islands (Jolley et al., 2022), Antrim (Beresford-Browne et al., 2023).

When volcanism occurred, it tended to occur in significant volume but only in certain areas at any given time (even if coevally occurring in separate subprovinces). In this work, the nexus of volcanic activity has been shown to have moved around the NAIP as dictated by the tectonic and magmatic stresses and strains on the lithosphere. Leaving aside the potential variability of melt input presented by mantle plume pulsing (Jones et al., 2019), volcanic activity would also jump around locally between fissure/dyke swarms in response to more local stresses and strains in the crust. This can be seen in the distribution and variability of fissure/dyke swarms and volcanic activity in modern-day Iceland and is hinted at by the distribution of fissures, dykes, flood basalts and volcanic centres in the ALG and BIPIP.

To illustrate this we might consider a phase of rapid periodicity fissure volcanic activity occurring across Antrim for a period spanning tens to thousands of years, while essentially no activity is taking place in the Hebrides. Then the volcanic activity in Antrim wanes or stops completely and instead, we see fissure volcanics occurring in Skye or Mull.

Next, we might consider scaling this up and broadly applying it to the NAIP. Sporadic bursts of volcanic activity across the BIPIP might be diminishing while flood basalts are beginning to erupt onto the landscape of coastal Greenland or a rhyolitic volcano is erupting in the Faroe Islands.

The model that we have arrived at here tells us that within any given period of 10,000 years, it was likely that somewhere in the NAIP there was some kind of volcanic activity happening between 65 and 40 Ma.

5.4 Summary

Section 5.1 highlighted that the bulk of time represented by the ALG is within the manifold hiatuses rather than the physical act of volcanic emplacement. Section 5.2 establishes the timespan for emplacement for the NAIP from onset around 65.5 Ma to completion of the waning phase around 33.5 Ma, making the total duration to be 32 Ma. Section 5.3 ties together the findings of sections 5.1 and 5.2 and applies them to the ALG, demonstrating that flow volume calculations based on the observations above are consistent with the model of low tempo volcanic activity.

CHAPTER 6 – CONTEMPORARY ICELANDIC VOLCANISM AS A COROLLARY FOR THE ANTRIM LAVA GROUP

6.1 Introduction to Iceland

Iceland, situated on the Mid-Atlantic Ridge in the North Atlantic between Europe and Greenland, is a geologically dynamic island known for its unique and dramatic landscapes shaped by volcanic and tectonic activity. The island's geology is primarily characterised by extensive basaltic volcanism resulting both from its location atop a divergent tectonic plate boundary and the presence of a mantle plume, often referred to as the Icelandic hotspot.

Iceland's basaltic formations result from numerous volcanic eruptions over millions of years, essentially building Iceland up from the ocean floor of the North Atlantic. These basaltic lava flows form some of Iceland's most iconic landscapes, including the rugged highlands and the picturesque basalt columns at sites like Reynisfjara beach and the Svartifoss waterfall (at internet: https://guidetoiceland.is). Basaltic dikes are also prevalent in Iceland, being critical in the island's volcanic system, serving as conduits for magma to reach the surface.

Although Iceland often experiences Plinean, Vulcanian and Strombolian explosive volcanism (Thordarson & Larsen, 2007), some of which have profound impacts on the upper atmosphere and air travel, it is volcanic fissure eruptions that are a hallmark of Icelandic volcanism. These eruptions occur along elongated cracks or fissures in the crust, often stretching for several kilometers. The Laki eruption of 1783-1784 already introduced in Chapter 4 is one of the most notable examples, where a massive fissure

eruption produced significant lava flows and had profound climatic and environmental impacts.

6.2 Reasoning for considering Iceland

Throughout this research, the volcanic activity, structure and geological history of Iceland has cropped up time and again, to the point that we were led to investigate the possibility that the Antrim Lava Group basalts were emplaced in a manner not too dissimilar to the historic flood basalt eruptions/effusions on Iceland. The specifics of the two comparable eruptions (10th century, Eldgja and 18th century, Laki) have already been introduced earlier in this thesis and examined in more detail in Chapter 4. Carrying on from this, we will compare the general form and distribution of Icelandic fissures and dikes to those of the Antrim Lava Group.

The scene is well set from the point of view of the Antrim Lava Group, so we will now add the findings of recent research into the geochemistry of the 2021 Icelandic basalt eruption at Fagradalsfjall (Section 2). Section 3 of this chapter considers the ramifications of the findings of Marshall et al. (2021) on how we approached the sampling and analysis of ALG lava flows.

Section 4 below considers the similarities in spatial surface geometry of fissures and dikes responsible for conducting magma from source to surface in both Iceland and Antrim.

6.3 Geochemical findings from 2021 eruption at Fagradalsfjall

On 19th March 2021 a fissure eruption began in the Fagradalsfjall complex within the Western Volcanic Zone of Iceland (Figure 6.1).

Figure 6.1. Fagradalsfjall volcanic activity (Photo credit: Bessi Eydal Egilsson, 2021. Reproduced under Wikipedia creative commons licence)

Samples of the effused lava were taken for geochemical analysis regularly throughout the Fagradalsfjall volcanic episode of 2021 (Marshall et al., 2021; Sigmarsson et al., 2022; Marshall et al., 2022). This showed that during that eruptive cycle:

- **Early/onset** lavas have a depleted composition, being sourced from crustal storage (Figure 6.2);
- Highly fluid, olivine tholeiite, **main phase** lavas arrive after only a few months, rapidly ascending through existing plumbing systems from LAB source to erupt

at the surface with little discernable interaction with crustal magma or wall rock (Figure 6.3); and

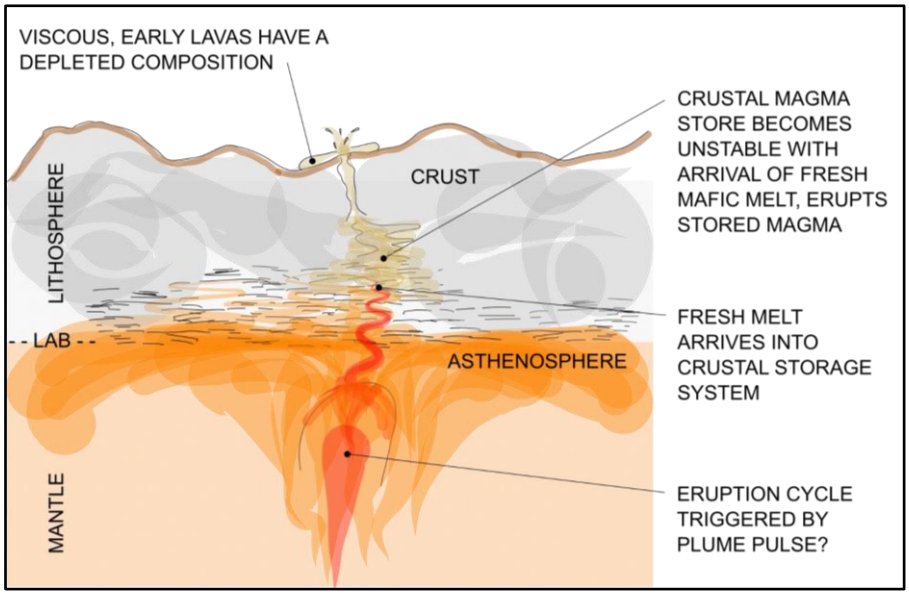

*Figure 6.2. Cartoon model developed by this author (not to scale) of **early/onset** conditions of an Icelandic fissure basalt eruption (mainly after Marshall et al., 2022. Plume pulse trigger after Jones et al., 2019). LAB = lithosphere-asthenosphere boundary.*

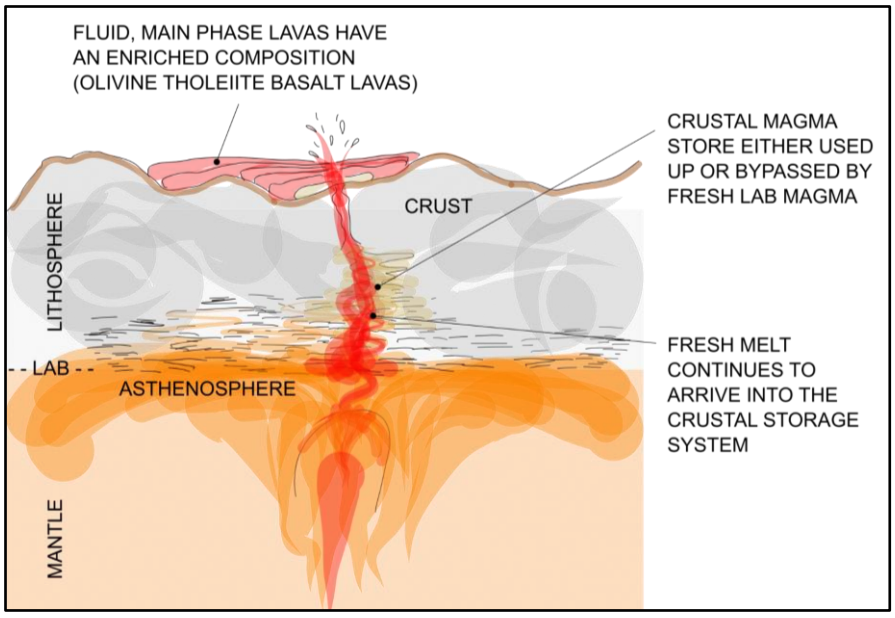

*Figure 6.3. Cartoon model developed by this author (not to scale) of **main phase** conditions of an Icelandic fissure basalt eruption (mainly after Marshall et al., 2022. Plume pulse trigger after Jones et al., 2019). LAB = lithosphere-asthenosphere boundary.*

- **Waning/late-stage** lavas slowly trend to a more depleted composition as CMB source productivity declines (Figure 6.4).

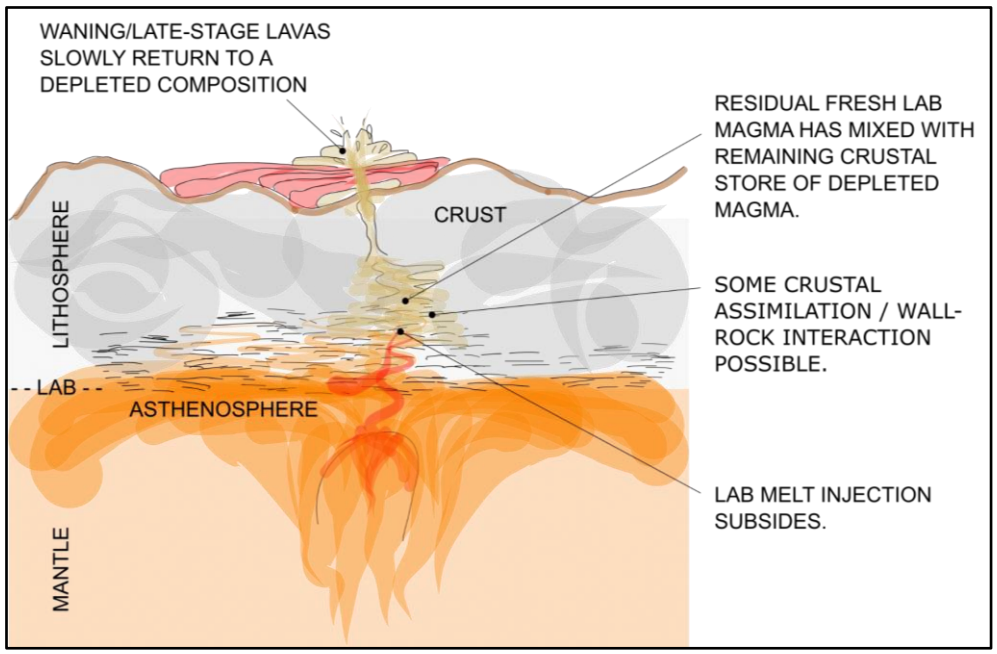

*Figure 6.4. Cartoon model developed by this author (not to scale) of **waning/late-stage** conditions of an Icelandic fissure basalt eruption (mainly after Marshall et al., 2022. Plume pulse trigger after Jones et al., 2019). LAB = lithosphere-asthenosphere boundary.*

One of the key takeaways from this research was the detection of olivine tholeiite basalts being effused during the main phase of the eruption, and the possible similarity in the magmatic mechanisms of melt, storage and transit between modern-day Iceland and ancient Antrim.

Based on the findings from Fagradsfjall (Marshall et al., 2021; Sigmarsson et al., 2022; Marshall et al., 2022), Figure 6.15 presents a cartoon sketch of the possible magma-wall rock interactions that may be responsible for much of the geochemical data scatter seen in the ALG basalts when compared to those of other subprovinces.

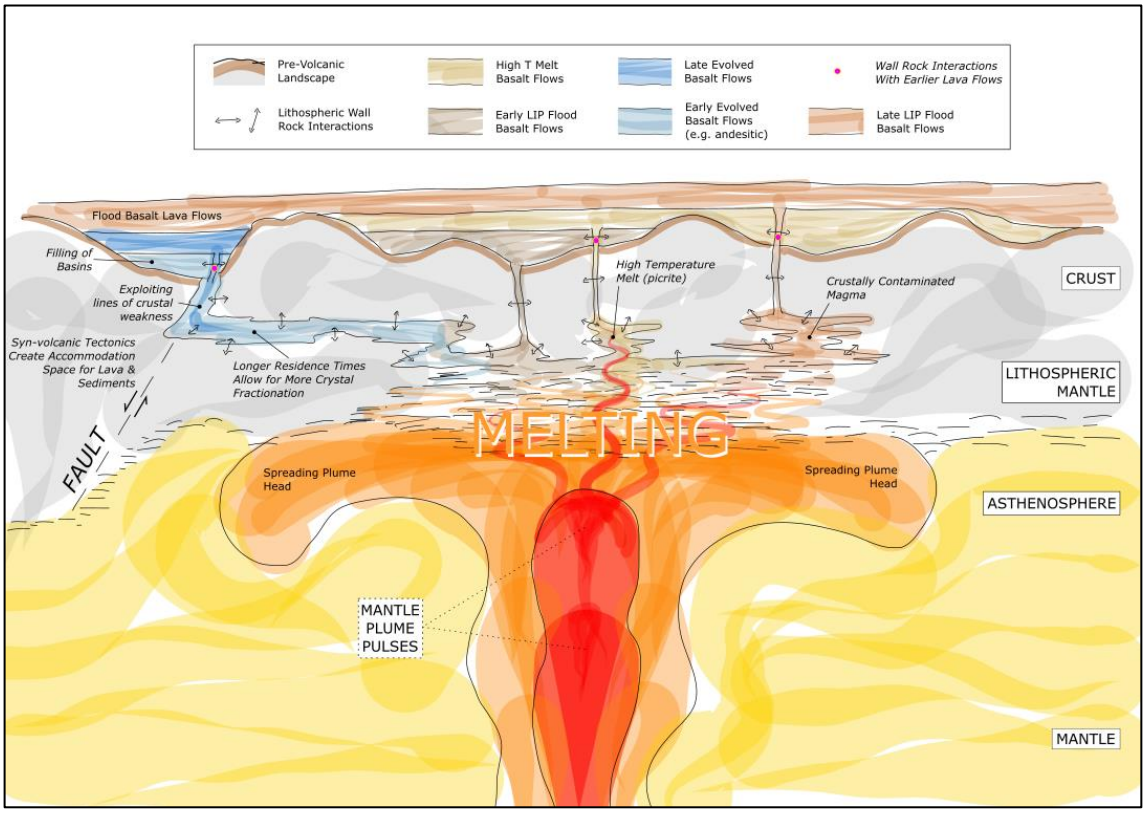

Figure 6.5. Cartoon model (not to scale) of mantle-crust volcanic interactions connected with a flood basalt province (developed by this author) showing possible genesis scenarios for various basaltic lava flows within the ALG.

Unlike the relatively young and unchanged lava flows of the Columbia River, which have been mapped over considerable distance either by tracing outcrops or measuring their distinctive geochemistry (Hooper, 1982; Tolan et al., 1989; Camp & Ross, 2004), the remnant flood basalts of Antrim researched here have a restricted extent which means it has not been possible to map them over any significant distance. The lack of distinctive geochemical signatures of individual flows or flow groups already discussed in this work (Chapter 3) means that chemostratigraphic correlation of lava flows across the plateau has not been possible to the required degree of confidence.

6.4 Side note regarding sampling of ALG basalt flows

At the time of sampling we believed that fresh-looking samples from the core of lava flows (i.e. between the base and the crust of the lava flow) would yield the most indicative and informative geochemical results for our analysis. Following the findings of recent work carried out on the lavas of Fagradalsfjall (Marshall et al., 2021; Sigmarsson et al., 2022; Marshall et al., 2022) it has been found that lavas effused during a single volcanic fissure event evolve significantly over a very short period of time (i.e. < 1 year). Initial lavas were depleted, being sourced from crustal storage, but over ~2 months the flows began to display a more enriched composition as rapidly ascending magmas from the lithosphere-asthenosphere boundary (LAB) created a pathway from source to surface. Interestingly, these basalts were found to be rich in olivine phenocrysts sourced from the LAB, thus emplacing olivine tholeiite lavas akin to those of the Lower and Upper Basalt Formations. Over time, as the arrival/injection of LAB-sourced magma into the system began to decline, the lava composition slowly shifted towards being depleted once more. Any future investigations involving the sampling of basalt cores held at GSNI, or indeed field sampling of basalt outcrops, should take account of this volcanic mechanism to more fully understand the process and timing of effusive volcanics of the ALG, BIPIP and NAIP.

6.5 Icelandic fissure and dike geometry compared to those of the British and Irish Paleogene Igneous Province

Understanding the apparent volcanic tempo of the ALG (and possibly the wider NAIP) requires visualisation of the spatial and temporal activity. Recent basaltic fissure eruptions in Iceland (< 1,100 years old) provide some comparative data for the volcanic mechanisms involved.

Iceland's Krafla volcanic vent system is present as a swarm of tension fractures, normal faults and volcanic fissures around 80 km in length and 10 km wide (Opheim & Gudmundsson, 1989). Individual fractures range in length from 350 m to 3.5 km, occasionally terminating in large chambers that accommodate intrusions. The larger Western Volcanic Zone is approximately 120 km in length and 40 km wide. Individual fissures are subparallel to one another, trending spatially along lines of crustal weakness and tectonic stress fields. These fissure swarms are located where the lithospheric plates are diverging. Later eruptions will generally happen at new fractures that are parallel and thousands of meters from the previous ones (at internet: Fissure Vent Volcano - Basic Planet). The Laki system of fissures actually produced the largest eruption in historical times on the planet when a flood basalt event occurred in 934 during the eruption of Eldgja. The Laki fissure system also produced a significant volume of flood basalts during the eruptions of 1783-84.

The pattern and extent of volcanic fissure swarms in Iceland (Figure 6.6) bear a striking resemblance to those of the BIPIP (Figure 6.7); particularly the dyke swarms and

volcanic centres of the west coast of Scotland (Emeleus & Bell, 2005). Figure 6.8 presents landscape scenes from Antrim and Iceland.

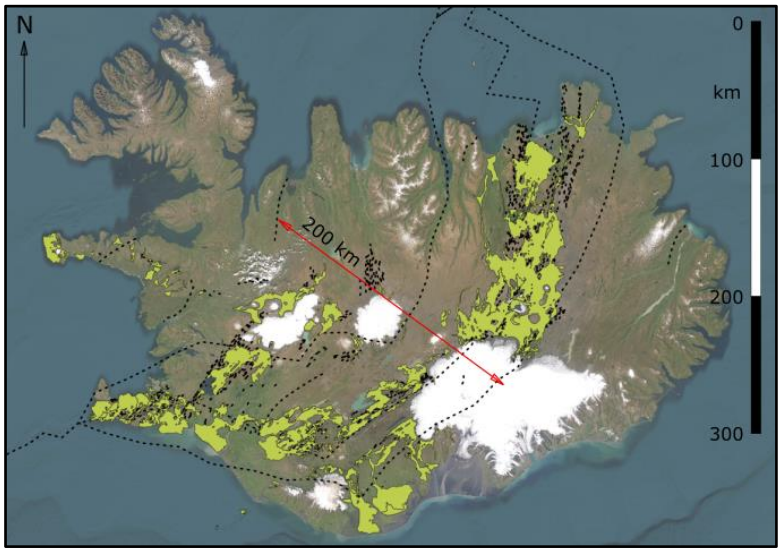

Figure 6.6 Map of Iceland showing the geometry of volcanic fissure swarms (black dash) and lava fields (light green). GIS data courtesy of the Natural History Institute of Iceland. Satellite imagery courtesy of ESRI (ArcGIS online), showing glaciated regions in white. Scale 1:1,850,000.

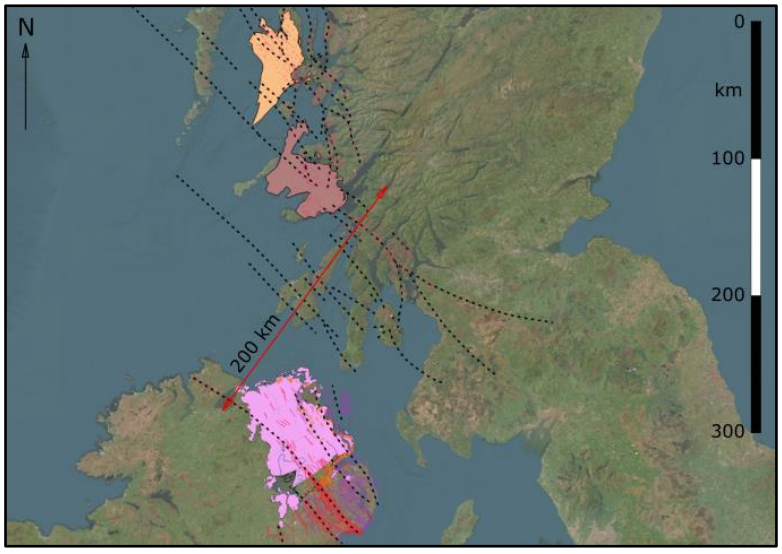

Figure 6.7. The current location of Antrim (purple), Mull (brown) and Skye (orange) lava fields, with Palaeogene fissure swarms (black dash, red and purple lines). Satellite imagery courtesy of ESRI (ArcGIS online). Scale 1:1,850,000.

Figure 6.8. (a) an escarpment of Antrim Lava Group rocks in Northern Ireland. (b) Icelandic landscape (Credit: Örvar Þorgeirsson and Kanya Hanklang, 2010)

In the absence of firm evidence to suggest the location(s) and geometry of the mantle plume head(s) c. 62 - 58 Ma (e.g. Hughes et al., 2015), one could posit that the similarity of the fault and fissure swarm density and overall geometry in Iceland and the BIPIP might suggest that a plume head should have been directly underneath the BIPIP at the time of volcanic activity. However, as this model is not supported by published research (which either discount mantle plume interaction or position the mantle plume arrival under Greenland) alternative models must be considered. A thorough examination of the melt mechanism(s) responsible for the ALG/BIPIP flood basalts in a scenario with the proto-Icelandic mantle plume arriving under Greenland lies outside the scope of this research.

One of the main differences between the spatial properties of the Paleogene dyke swarms of the BIPIP compared with those of Iceland is their orientation; UK and Ireland dykes trend NW to SE, whereas those of Iceland are trending N to S/SW.

The approximate extent of the BIPIP dyke system, measured by current representations, is 400 x 150 km. The current extent of Icelandic dykes and faulting is 390 x 145 km, which is notably similar.

The area to the south and southeast of the Laggan Valley (Antrim) is largely devoid of surface basalts but Paleogene basaltic dykes are mapped across that region, hinting that any basalts that were present at the surface have since been removed by weathering, erosion, glaciation or a combination of these forces. Although the age data were generated using the K-Ar method on whole rock samples, the Mourne Mountain basalt dykes offer a range of ages from 65.41 to 49.80 Ma (Wilkinson et al., 2017, Figure 6.9).

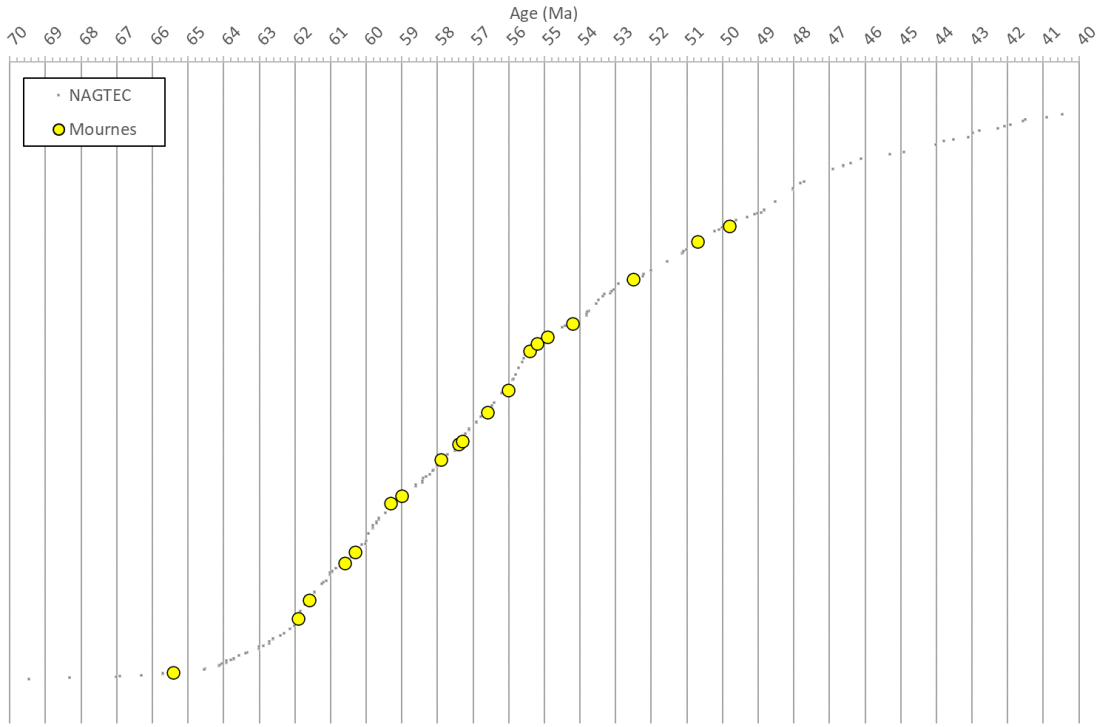

Figure 6.9 Basaltic dyke ages from the Mourne region, Northern Ireland. Data from Wilkinson et al., 2017

The dyke swarm associated with lavas of the Lower Basalt Formation, the St. John's Point - Lisburn dykes, are positioned along the central-southwest margin of the subprovince. The dyke swarm associated with lavas of the Upper Basalt Formation, the Ardglass - Ballycastle dykes, are positioned along the central-northeast margin of the subprovince (Figure 6.10).

This binary system of fissures and dykes across Northern Ireland could be named as the Southwest Antrim Volcanic Zone (St. John's Point - Lisburn) and the Northeast Antrim Volcanic Zone (Ardglass - Ballycastle) of the Antrim Lava Group region

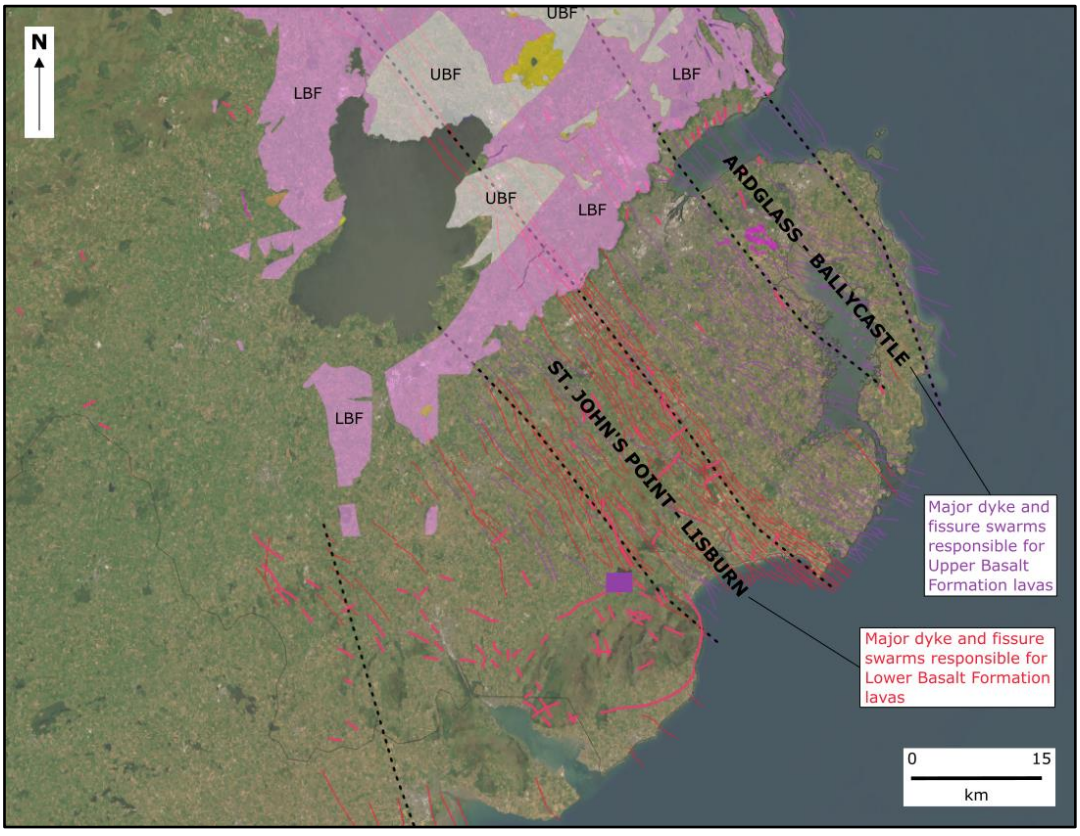

Figure 6.10. The Paleogene dyke swarms of Northern Ireland are well-exposed in County Down due to uplift and erosion.

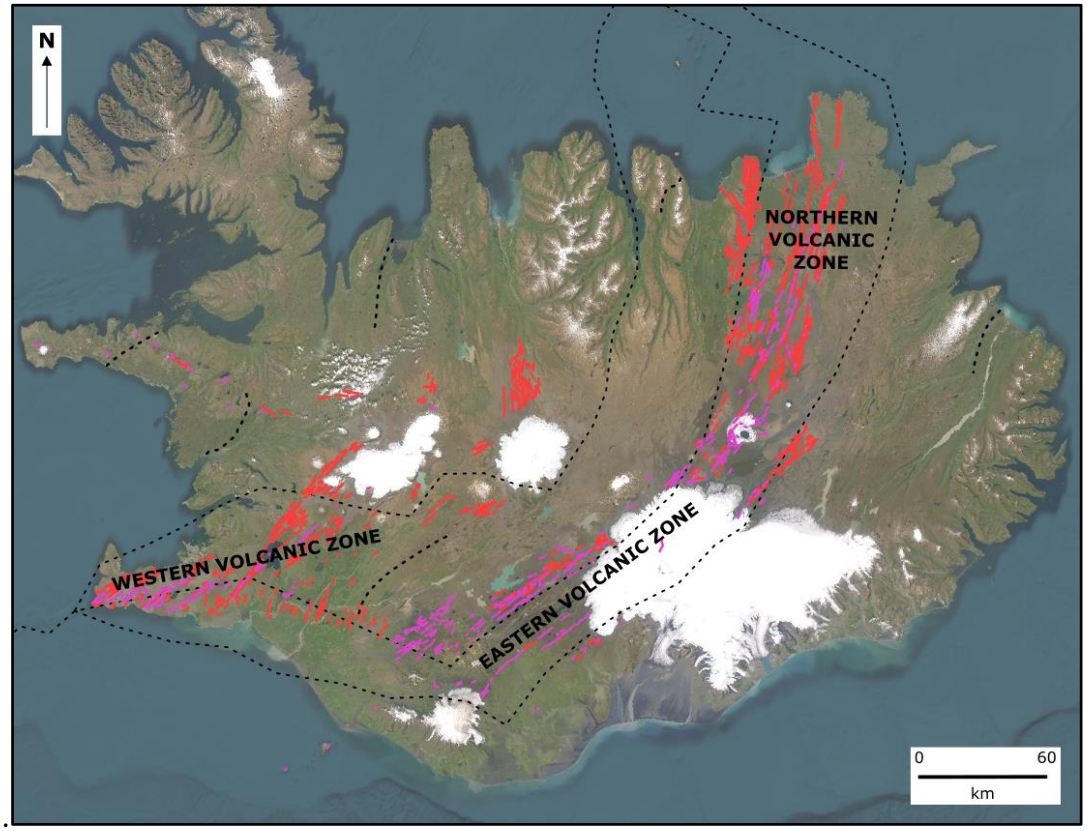

Figure 6.11. The location and distribution of fissure and dyke swarms of Iceland.

Indeed, the similarity in the spatial distribution and overall geometries of the fissure and dyke swarms in Northern Ireland and those of modern-day Iceland are hard to ignore (Figures 6.10, 6.11). Future research may wish to consider the various zones of the BIPIP in much the same way as the fissure/dyke fields of Iceland (Figure 6.12).

To further understand the emplacement processes of the Antrim Lava Group we examined the nature and distribution of Paleogene dykes in the Antrim subprovince. The dykes of Antrim and surrounding counties in Northern Ireland have been measured and digitised into a publicly available GIS, curated by BGS/GSNI, mapped and presented in Figure 6.13.

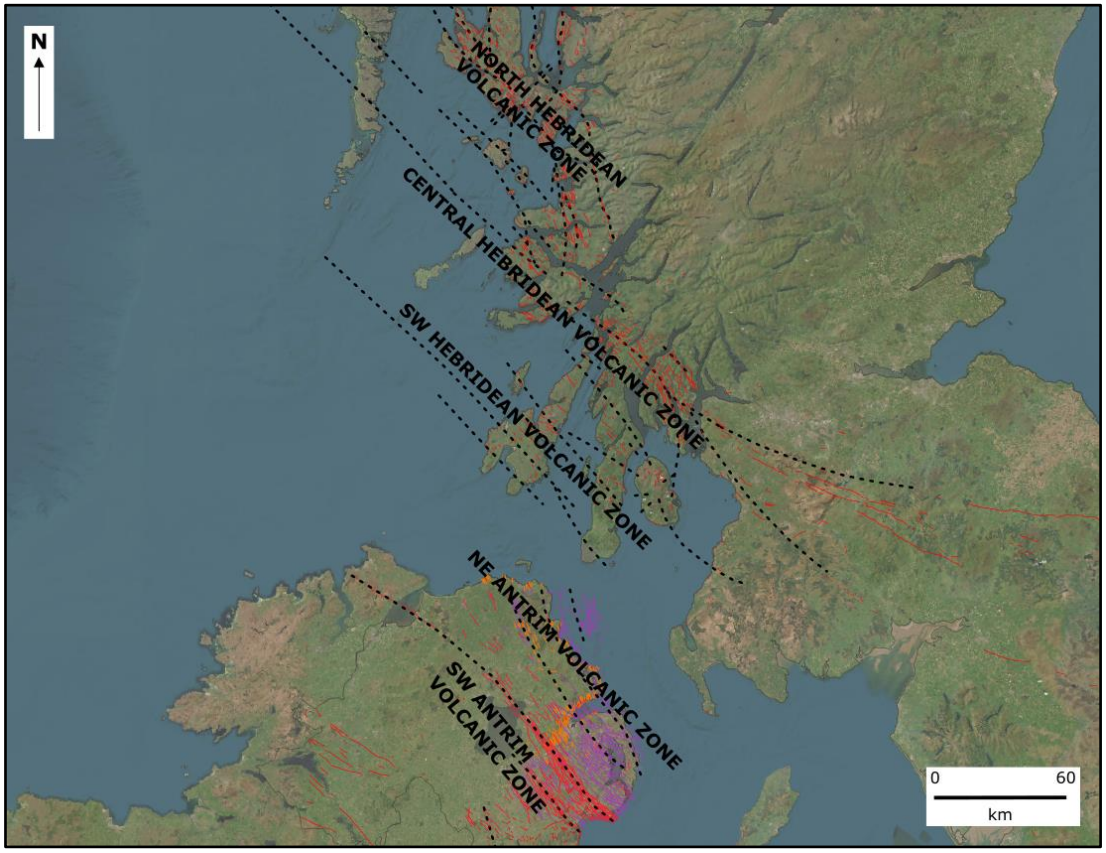

Figure 6.12. BIPIP regions as discrete volcanic zones within the overall volcanic setting. The author labelled volcanic zones.

Overlain on the image are two polygons that estimate the original extent of the fissure/dyke swarms, now either covered by basalts, soils or the Irish Sea. In drawing the polygons, attention was paid to the form of similar fissure/dyke swarms in modern-day Iceland in an attempt to create a geologically likely scenario.

Dyke geometry data were extracted from the GIS, and are presented in Table 6.1.

Table 6.1. Paleogene dyke geometry data from Northern Ireland (BGS/GSNI)

Dyke swarm	n	Min Length (m)	Ave Length (m)	Max Length (m)	Sum Length (m)
Ardglass - Ballycastle	403	170	3,817	33,246	1,538,230
St Johns Point - Lisburn	278	317	4,376	25,252	1,216,409
Combined	*681*	-	*4,096*	-	*2,754,639*

Because the Antrim Plateau still covers the Paleocene landscape, it is likely that many more, unmapped dykes exist beneath and among the extant basalts of the Antrim Plateau. To give a more realistic estimate of the total number of dykes associated with the Antrim Lava Group we examined the density of dykes in the southeast corner of Northern Ireland where any ALG basalts that may have been present have long since been removed by agencies of climatic, oceanic or glacial erosion.

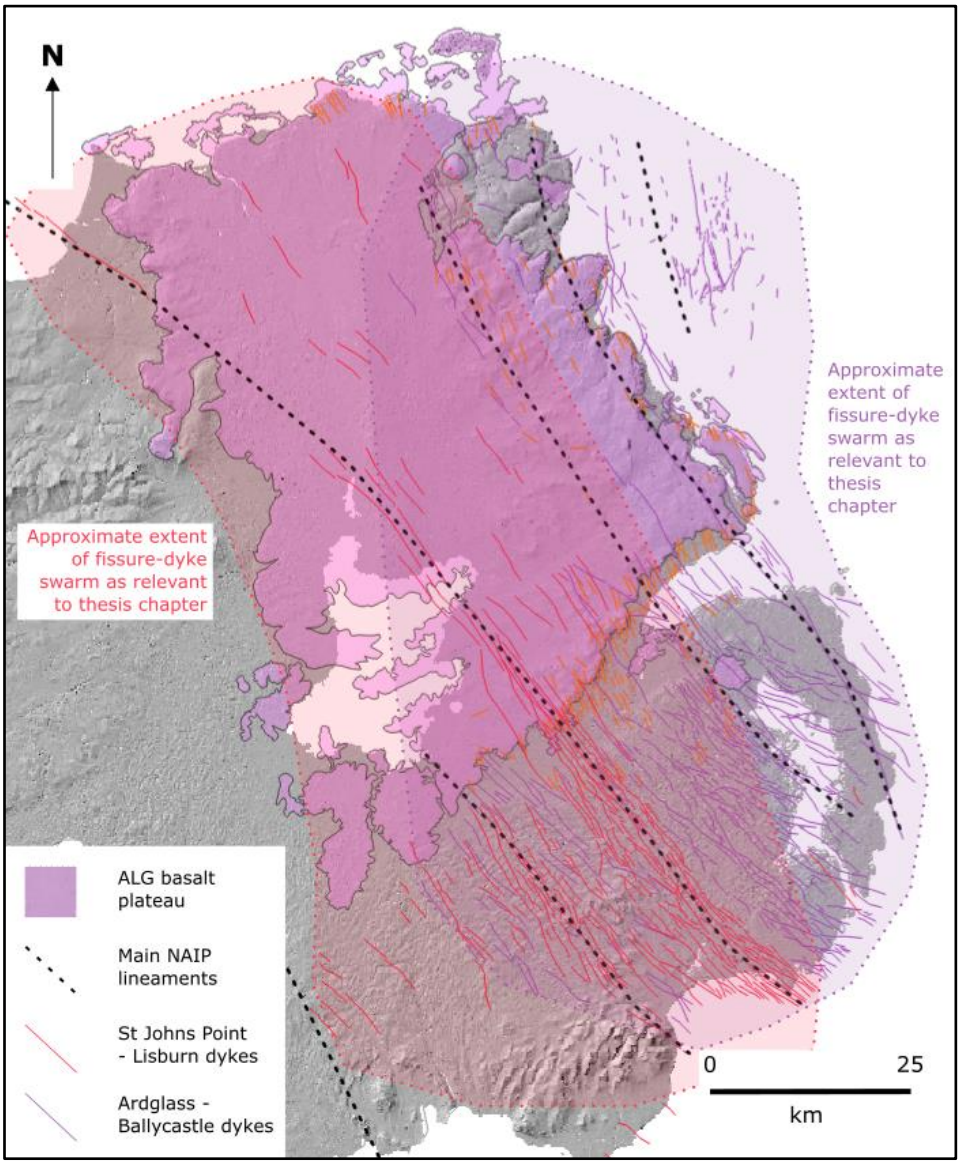

Figure 6.13. Shaded relief map of Northern Ireland detailing the main lineaments of the NAIP and outcrops of the two main dyke swarms believed to be connected to the effusion of the Antrim Lava Group (BGS/GSNI data). The pale purple polygon outlines the approximate extent of the Ardglass-Ballycastle fissure/dyke swarm (~5,400 km2). The pale red polygon outlines the approximate extent of the St John's Point-Lisburn fissure/dyke swarm (~5,690 km2). These extents are very approximate and only related to the discussion at hand, i.e. extrapolated and logical effusion points for ALG basalts.

Figures 6.13(a) and (b) present the sample polygons that we drew to define the area used for extrapolation of dyke presence under the Antrim Plateau.

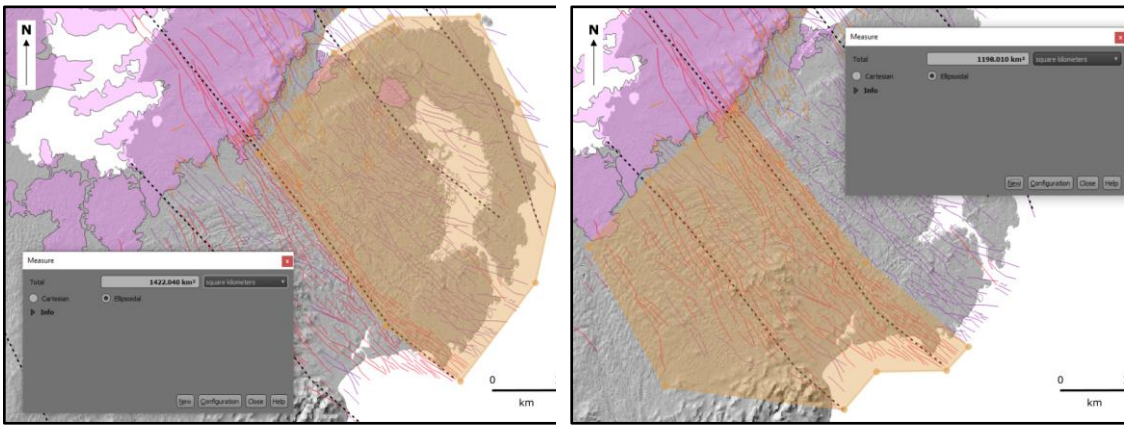

Figure 6.14. Shaded relief maps of Northern Ireland. (a) Sample area for Ardglass - Ballycastle dykes. (b) Sample area for St John's Point - Lisburn dykes.

The geometry data for the subset of dykes that fell within each sample polygon were processed in the same way as for the total dataset (presented in Table 6.1). The extrapolated data are presented in Table 6.2.

Table 6.2. Extrapolated Paleogene dyke data for Northern Ireland (original data from BGS/GSNI)

Dyke swarm	Estimated n	Estimated sum length (m)
Ardglass - Ballycastle	976	3,580,918
St Johns Point - Lisburn	1,076	4,550,020

If we compare the values presented in Table 6.2 with the geometric data of two of the fissure/dyke swarms in modern-day Iceland we find that the data are reasonably comparable (Table 6.3). While this is not intended to strengthen any hypothesis regarding the similarity of volcanic activity between Iceland and the BIPIP, it does lend some tentative confidence to the extrapolated data for Antrim.

Table 6.3. Fissure swarm/dyke data from Iceland (data from Icelandic Institute of Natural History)

Dyke swarm	n	Min Length (m)	Ave Length (m)	Max Length (m)	Sum Length (m)
Gosspr Li	588	407	1,403	8,023	824,713
Brotolina	760	518	3,379	23,598	2,567,907
Combined	*1348*	*407*	*2,391*	*23,598*	*3,392,620*

Now we have some indication, and estimation, of the Paleocene geometry and position of the fissures and dykes under Antrim, we can look at some examples of large basalt flows that have been mapped over distance. The three flows identified by Walker (1959) are still among the best examples, namely:

- Inver River waterfall to Garron Point (9.7 km long, 3.5 km wide, 18 - 24 m thick)
- Hannahstown to Whiterock, Black Mountain (3.5 km long)
- White Mountain to Collin Glen (4 km long)

The extant flow at Garron Point has an estimated volume of at least 0.5 km^3, (presented in Chapter 5), and is likely to have effused from the distinctive dyke swarm to the southwest of the flow (Figure 6.15).

As we have no measurement of the original dimensions of the lava flow, nor how much has been eroded by glaciation, ocean or weathering, the calculated estimate of 0.5 km^3 should be considered a likely minimum for the original volume emplaced.

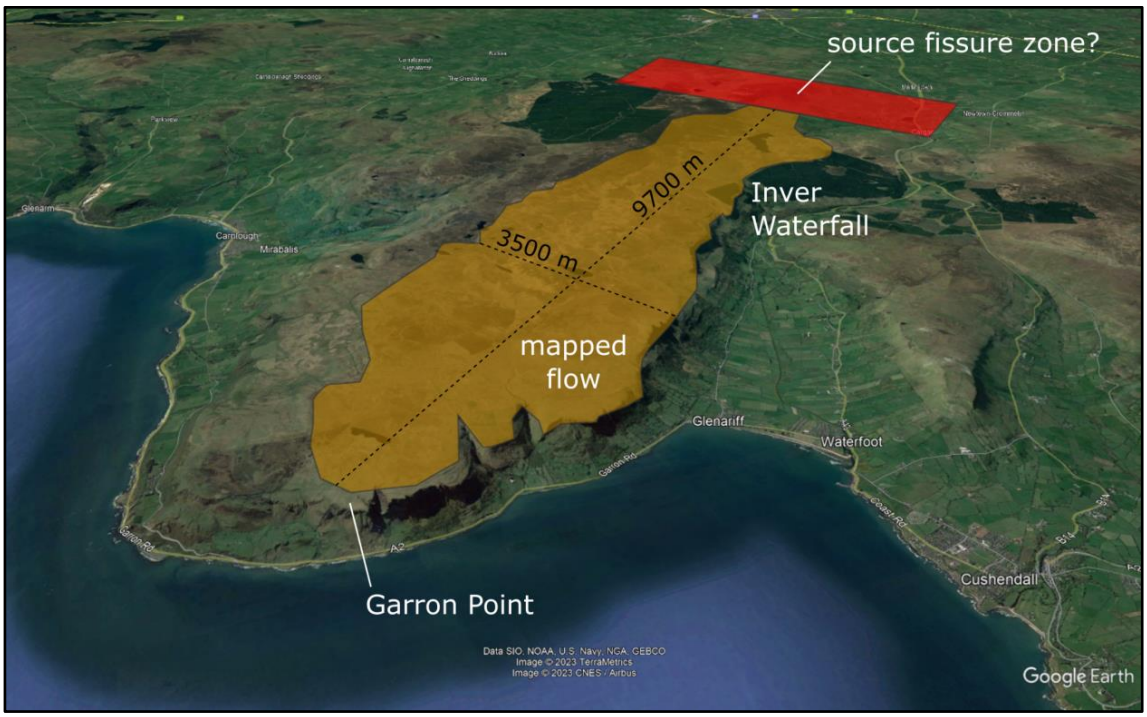

Figure 6.15. Annotated view from 5 km altitude looking southwest of an ALG lava flow mapped by Walker (1959) between Inver Waterfall and Garron Point. Base image ©Google Earth.

6.6 Location and volume of volcanic activity

Iceland's volcanic activity is fundamentally different from that of the ALG because it is built on thickened oceanic crust, rather than the thinning continental crust onto which much of the early NAIP lavas were extruded. However, the Icelandic system has been shown to have assimilated continental crust at a deep level (Torsvik *et al.*, 2015) and also had to accommodate tectonic extension at a spreading ridge, and it shown to do so by cracking at various places wherever it is easiest for crustal fracturing to

propagate; i.e. volcanic activity in Iceland has jumped between the West, East and North Volcanic Zones, the Westman Islands, the Snaefellsnes Zone and the Orarfajokull Belt (Thordarson & Larsen, 2007). The geometry of Iceland and the GIF Ridge shows how the focus of volcanic activity shifts from one fissure system to another over time, a mechanism that is seen to have operated during the emplacement of the ALG, BIPIP and wider NAIP based on age dating (Wilkinson *et al*., 2017).

6.7 Questions relating to intermediate and acidic volcanism in ALG

In this thesis, we have used the volcanic systems of Iceland as a modern approximation for methods of emplacement and volcanic tempo, which raises interesting questions about magma differentiation and the presence of various types of erupted lavas. Addressing these questions falls beyond the scope of this work, but here we might consider the following.

- Studies of the Icelandic volcanic systems have revealed a ratio of 91.5% basic to 6% intermediate to 2.5% silicic material (Thordarson & Hoskuldsson, 2008). The same ratio has been found in the records of eruption events.
- Can this ratio be applied to the Antrim Lava Group rocks? Given the estimated basalt volume of 1,344 km^3 the ratios suggest approximately 84 km^3 of andesite and 4 km^3 of rhyolite/dacite could be present. No work to date has attempted to quantify these volumes, so this would be interesting to try and quantify in future work.

- Lonmin borehole 01/08-0001 (306212E, 417691N) encountered tuffaceous/porphyritic rhyolite and rhyolitic pumice throughout the 162.3 m of penetration. Nearby boreholes did not encounter rhyolite, which implies the low viscosity event was localised.

As they are 20 times more prolific than rhyolites, we should be seeing some andesitic lavas in the ALG rocks. If we are, what can we learn from their distribution? If we're not, why not? (cf. Lyle & Thompson, 1983).

6.8 Summary

Two hypotheses fall out of this discussion:

a. that the distribution and geometry of fissures and dykes in the BIPIP were directly connected to lithospheric extension, and
b. that there was a significant plume presence below the BIPIP region.

The first hypothesis, that lithospheric extension was at work, is at odds with the generally held model that rifting and extension in the North Atlantic began with the start of the second phase of NAIP activity and the associated Paleocene-Eocene Thermal Maximum, c. 56 Ma. We have already discussed the need for a fresh look at the age and distribution of NAIP volcanism, and as part of this research we have seen evidence for lithospheric extension between Greenland and UK/Scandinavia as early as 72 Ma, possibly even earlier. Seafloor spreading along parts of the northeast Atlantic rift zone (~3000 km in length) may have been active from as early as 83 Ma (Gaina *et*

al., 2017), so questions about the precise shift or increase (?) in spreading associated widely with the PETM around 56 Ma remains unanswered here.

The second hypothesis, that there was a significant mantle plume presence directly below the BIPIP, has already been tabled by Ganerød (2010) and could be explained by bifurcation (at least?) or partial redirection of the rising mantle plume due to the presence of the trapped Iapetus oceanic plate slab under the NAIP area (Foulger et al., 2003). The precise lithospheric/asthenospheric mechanics responsible for the essentially coeval onset of flood basalt volcanism in the UK and Ireland with the onset of flood basalt volcanism on the east and west coasts of Greenland lies beyond the scope of this research. However, the fact that these two geographic regions were separated by hundreds of kilometres of thinned crust under extensional forces makes it difficult to visualise how there was no significant volcanic activity in the area between them unless the crustal region that would become the Greenland-Iceland-Faroes Ridge had developed lines of weakness or channels that were being exploited by the generated melt.

CHAPTER 7 – DISCUSSION & CONCLUSIONS

In this final chapter, all discussion threads from chapters 3 to 6 will be brought together to provide clear and concise conclusions.

7.1 Geochemistry of the ALG

For the first time in the history of researching the chemical stratigraphy of the Antrim Lava Group, thanks to pXRF and WD-XRF analysis on the continuous core recovered from NIRE 02/08-0001 and NIRE 09/08-0001 boreholes, we have been able to examine sequential lava flows of the ALG without the need for potentially unreliable correlation.

The lavas of the Lower and Upper Basalt Formations plot as sub-alkaline basalts in Figure 3.2, which also highlights the similarity between these two flood basalt formations. The two samples of Causeway Tholeiite Member, sampled at Ross's Quarry (Ballycastle), plot as basaltic andesite on a standard TAS plot (Figure 3.2).

It is interesting to note that sample CRQ14 (a basaltic dyke sampled at Craig's Quarry) plots within the Hawaiite field. To our knowledge, this is the first recorded measurement of such a composition within the Antrim Lava Group.

The relationship of the elements K, Ti and Zr through the extant plateau lavas, currently assigned the names Lower Basalt Formation and Upper Basalt Formation, show a distinct trend between these two formations that may prove useful in the correlation of isolated basalt outcrops.

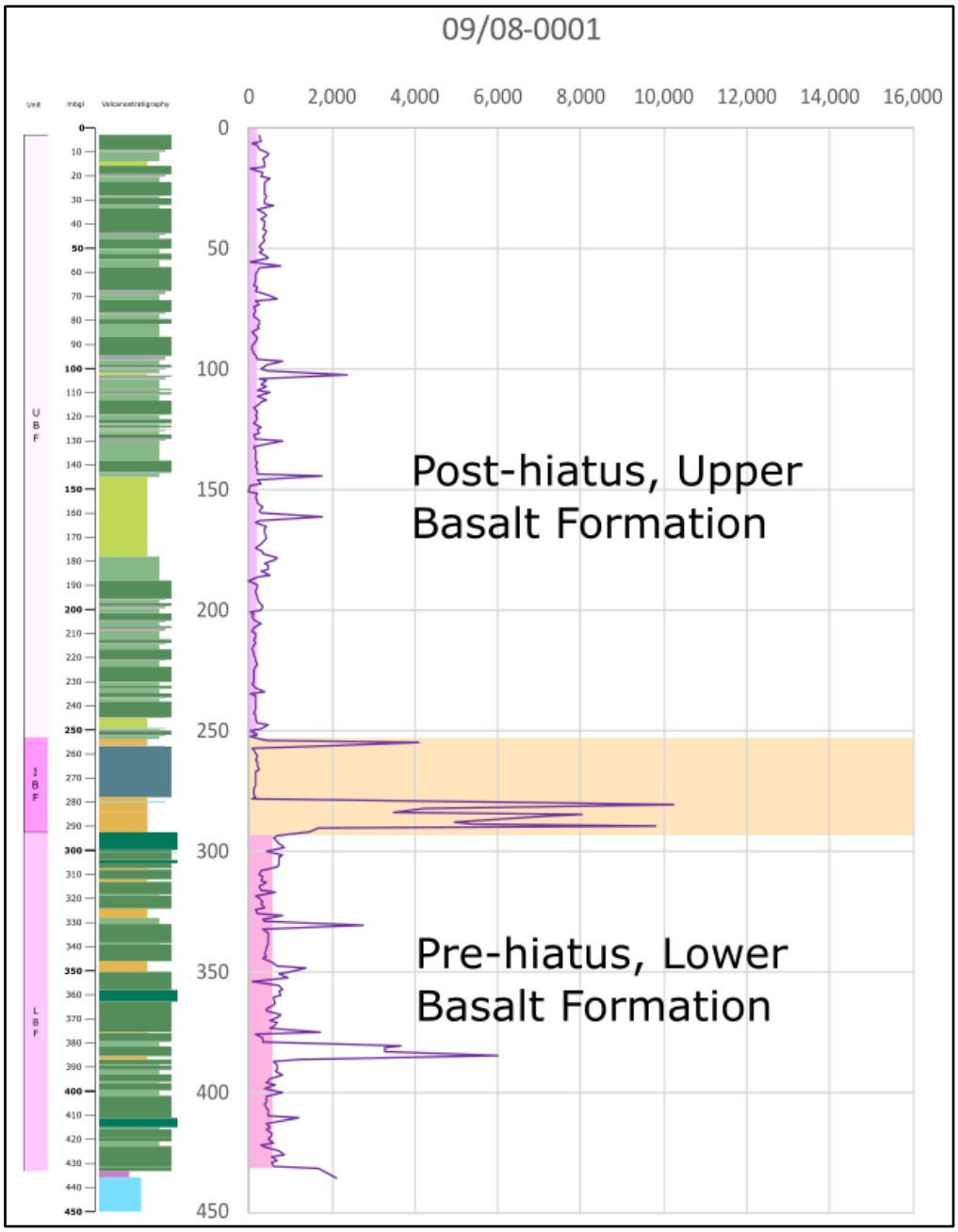

Figure 7.1 Volcanostratigraphy and (K/Ti)/Zr plot (pXRF data) for borehole NIRE 09/08-0001 showing the distinctive and sustained difference in (K/Ti)/Zr values before and after the IBF

Lavas that erupted before the most notable hiatus of the Antrim Lava Group, i.e. the Interbasaltic Formation (IBF), have consistently higher average values of (K/Ti)/Zr than post-IBF hiatus lavas (Figure 7.1).

Interestingly, the (K/Ti)/Zr data for borehole NIRE 09/08-0001 also show a change in values at 180 mbgl which was not seen in any other pXRF data. Had this trend been noted in another location we may have surmised that there could be cause to propose the existence of an as-yet undefined, third 'Basalt Formation' of the Antrim Lava Group. Further research might also include the dikes exposed at the surface to the south/southeast of the Laggan Valley, as these would likely have been feeding surface basalt flows now lost to erosion. Data revised and presented in Wilkinson et al. (2017) suggests that these may well have been active during the so-called Interbasaltic.

The consistency and distinctiveness of the chemical shift between the LBF and UBF, while not fully explored here in terms of magma generating processes, implies a systematic difference between these two periods. Given that they are separated by a major hiatus, where our analysis of timescales suggests a substantial gap in time, it is reasonable to posit that the focus of the NAIP volcanism migrated away to another zone during that period.

If we assume that the same plume source is persistently feeding this volcanism and given that the trends are static within both the LBF and UBF rather than showing linear trends in time, it doesn't seem likely that the shift relates to mantle source depletion. Similarly, given the consistency of the trend, it needs to be clarified that crustal contamination would explain this, or why such a consistent shift would occur from crustal input alone.

The trend might be explained by a systematic shift in the extent of partial melting, driven by either pressure or temperature. This could plausibly be associated either with a change in the relative position of Paleogene Antrim to the proto-Icelandic plume head or changes in the strength (i.e. temperature structure) of the plume through time. The geochemical shift could also be due to changes in the mantle source, but perhaps it is less clear why this

would occur. In either case, it would be a relative change in the plume configuration between the two major episodes of Antrim volcanism. It may prove informative to expand this analytical method to other parts of the NAIP to more fully understand the relative plume behaviour and positioning through time (and indeed to explore this relative to the Icelandic model explored throughout this work).

To explore the extent of melting and how this might explain the signatures, significantly more trace element data is required than we can obtain from pXRF equipment. At this point, where we have insufficient data to say whether the melting temperature had a bearing on the geochemistry, it seems wiser to simply refer to these basalts as high-Ti type and low-Ti type.

7.2 Palaeoenvironment of northeast Ireland

Palynological investigations of sedimentary interbeds of the ALG have revealed an ecological assemblage suggestive of a temperate to warm temperate climate.

Analysis of the sedimentary interbeds revealed the presence of shallow lakes and suggests that shallow lake environments are playing a key role in the formation of the 'so-called' laterite interbeds, quite possibly at water temperatures that have been artificially elevated by cooling lavas, or near-surface magma, through the presence of geothermally warmed groundwater, or some combination of these (and other as yet unconsidered) factors.

The excellent preservation and minimal thermal alteration of palynological samples retrieved from fluvial interbed (2) from Ross's Quarry had a spore colour index of 1 or 2, which suggests that this sedimentary unit has not been buried more than ~200 m nor exposed to temperatures over 90°C.

We propose the name 'Craignagat Member' for the 2.4 m thick fluvial interbed at Ross's Quarry since the type locality (i.e. Ross's Quarry) is situated in the local townland of Craignagat. Even if the unit is proven to be contemporaneous with the Ballylagan Member, as is hinted at by its stratigraphic position, it has a significantly different composition and mode of formation and therefore requires individual naming.

7.3 Rates of ALG eruption/effusion

Building on palynological investigations, combining examination of the weathered horizons and other interbeds formed or deposited in the lengthy hiatuses between basalt lava flows, with the rates of effusion revealed from Icelandic flood basalt events, suggests that practically all of the time represented by the lava pile is locked away in these interbeds. This conclusion is supported by palynological evidence of significant ecological and environmental stability, revealing that not only was volcanic quiescence required at the local scale, but that there also must have been regional environmental stability given the variety of environments recorded and the estimated timeframe required for established, complex ecologies to develop.

Geochemical flow groups hint at volcanic tempo and activity but as this is rife with caveats and complications it is the least robust method compared to palynology or interbed weathering. However, it has shown that (K/Ti)/Zr values can effectively differentiate between early and late lava flows of the Lower and Upper Basalt Formations respectively, representing a major and persistent geochemical shift between the basalts of the LBF and UBF. This seemingly abrupt geochemical shift in basalts of the LBF and UBF also suggests that this hiatus was of a different order to those found scattered elsewhere throughout the ALG (evidenced by the well-developed interbeds already presented in this work). The

significantly more silicic lavas of the Causeway Tholeiite Member (once termed the Middle Basalts) point towards either crustal contamination due to longer residence time at shallow depths or greater crustal contamination at melt generation depths. Other workers have already assessed this and hypothesised that the CTM magma had a measurably shallower magma chamber than the other basalts of the ALG (Lyle, 1981). Perhaps this occurred as NAIP volcanic activity moved to another zone, leaving a significant volume of magma in the shallow crust to fractionate and interact with country rock. We might boldly predict that the eruption of the CTM was essentially awaiting the return of volcanic activity to the Antrim area, with fresh melt arriving in the shallow chamber leading to a geochemical chain reaction that destabilised the magma chamber.

7.4 Timing and tempo of the NAIP

When the geochronological data for the entire NAIP are presented together, as in Figure 2 of Wilkinson et al. (2017) presented unedited here for convenience (Figure 7.2), it becomes abundantly clear that even though a significant hiatus is recorded in the rocks of Antrim, there was no great hiatus in NAIP volcanism as might have been inferred by looking at the Lower and Upper Basalt Formations of Antrim alone. Instead, the data gathered by other workers plot as an essentially continuous curve of dates (see Wilkinson et al., 2017 for further information).

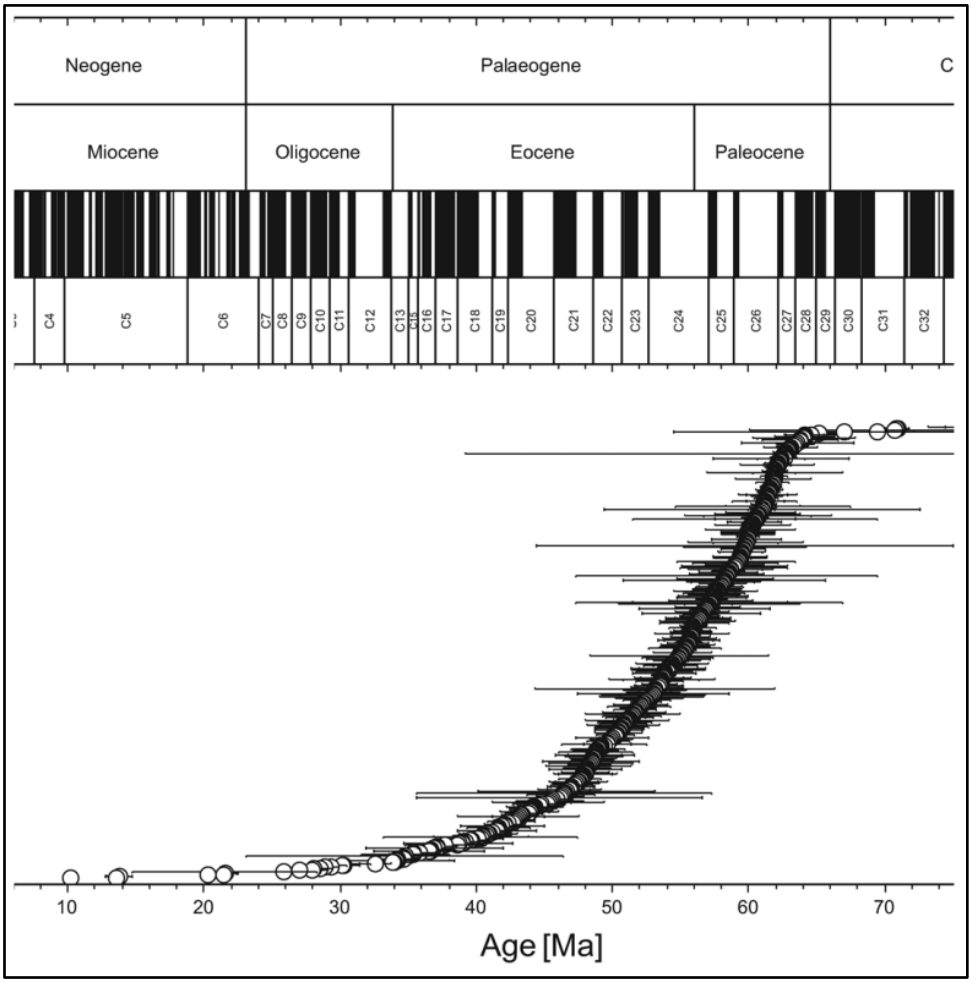

Figure 7.2. Direct reproduction of Figure 2 from Wilkinson et al., 2017, showing the same data adapted for Figure 5.6 of this thesis. NB. Potentially spurious K-Ar dates have not been removed from this original image. No authorship or participation in that work is intended or implied.

Examining each subprovince in detail has brought significant advances in our understanding of those volcanic terranes, but it is only when the larger picture is considered that we can achieve a broader comprehension of the activity in the system being investigated. Rather than representing geologically separate terranes that developed during evolution of the NAIP, the dates suggest contemporaneous activities across several subprovinces or a picture of volcanic activity switching between zones that may have been more or less active at different times. We surmise that the UBF and LBF may simply fit into this broader pattern of migrating volcanic foci.

The data in Table 7.1, sourced from Wilkinson *et al.* (2017), presents robust evidence for the timings of the earliest volcanic activity in each of the four main subprovinces of the NAIP, ordered left to right by the maximum recorded age analysed. It is immediately clear that the oldest igneous rocks of the BIPIP are older than those of West Greenland and significantly older than those of East Greenland or the Faroe Islands.

Table 7.1. Summary NAIP subprovince age data table from Wilkinson et al., 2017

	BIPIP			West Greenland			East Greenland			Faroes		
	-error	*value*	*+error*	*-error*	*value*	*+error*	*-error*	*value*	*+error*	*-error*	*value*	*+error*
Min	49.52	50.22	50.92	34.05	34.75	35.45	12.86	13.56	14.26	54.87	55.57	56.27
Average	59.93	60.63	61.33	54.67	55.37	56.07	52.12	52.82	53.52	57.82	58.52	59.22
Max	63.42	**64.12**	64.82	62.88	**63.58**	64.28	61.45	**62.15**	62.85	60.13	**60.83**	61.53
n	*37*			*40*			*40*			*6*		

It is interesting to note that the dating work behind Table 7.1 (Wilkinson et al., 2017) also suggests a far more persistent and continuous period of volcanic activity than previously forwarded by those whose work focused on improving the understanding of specific subprovinces.

The volcanostratigraphy of the Antrim Lava Group has strong evidence of a long hiatus, which has been subject to investigation and discussion for over two centuries; namely the lateritic horizon(s) of the Interbasaltic Formation. Yet the evidence that we have gathered has pointed towards the notion that volcanic quiescence in one area of the Antrim subprovince does not imply quiescence across the entire subprovince. Volcanic activity in one area of Antrim could be quite extensive, yet just a few tens of miles away there may be little or no record of volcanic activity that was discernible by the type and resolution of analyses available for this research. Indeed, the removal of significant volumes of basalts, etc. from the ALG due to erosion, etc. only serves to further confuscate the truth. As we have already seen from the age data presented by Wilkinson *et al.* (2017), volcanic activity

hopped around the region, from subprovince to subprovince, much in the way that it has done during the formation of Iceland, albeit on a much smaller scale.

To further strengthen this hypothesis we can replot the data from Wilkinson *et al.* (2017), filtered for basic volcanic products only (basalts (tholeiite, Hawaiite), lamprophyre, dolerite, gabbro) and separate the four key subprovinces (Figure 7.3 a and b). We can see that early volcanism was predominantly within the BIPIP, followed by a period of activity in West Greenland, then the Faroe Islands, then BIPIP again, and so on.

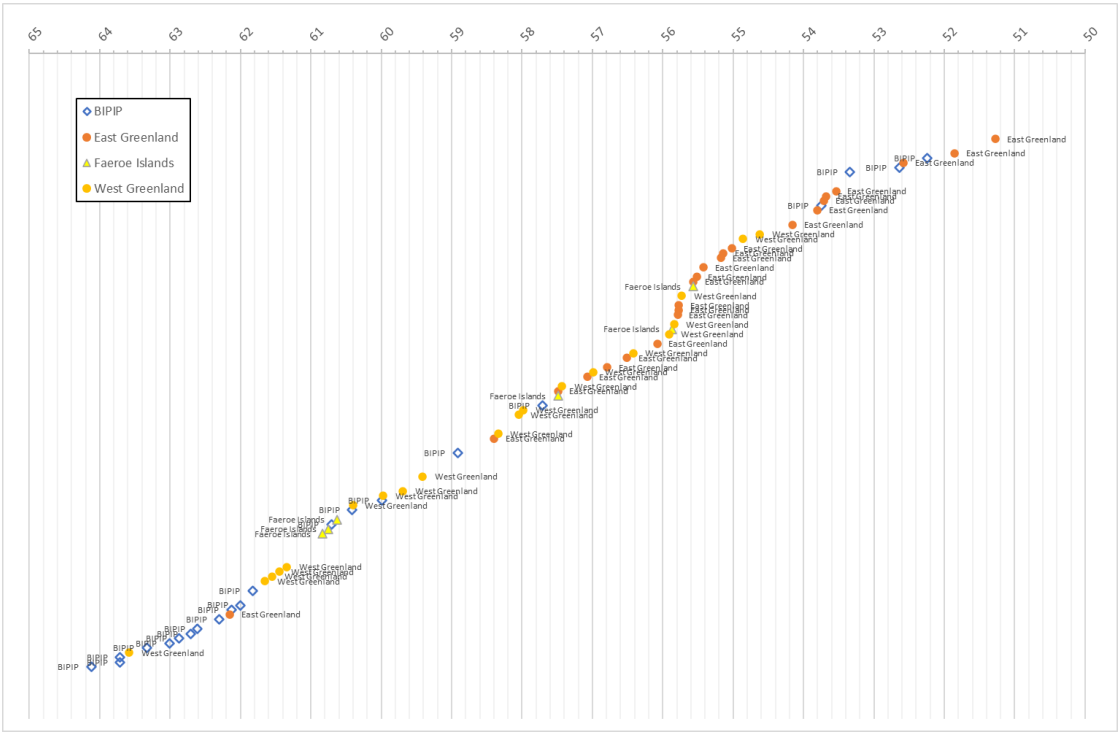

Figure 7.3. (a) Data from Wilkinson et al., 2017 replotted to illustrate the near-continuous nature of volcanic activity throughout the emplacement of the NAIP. No authorship or participation in that work is intended or implied.

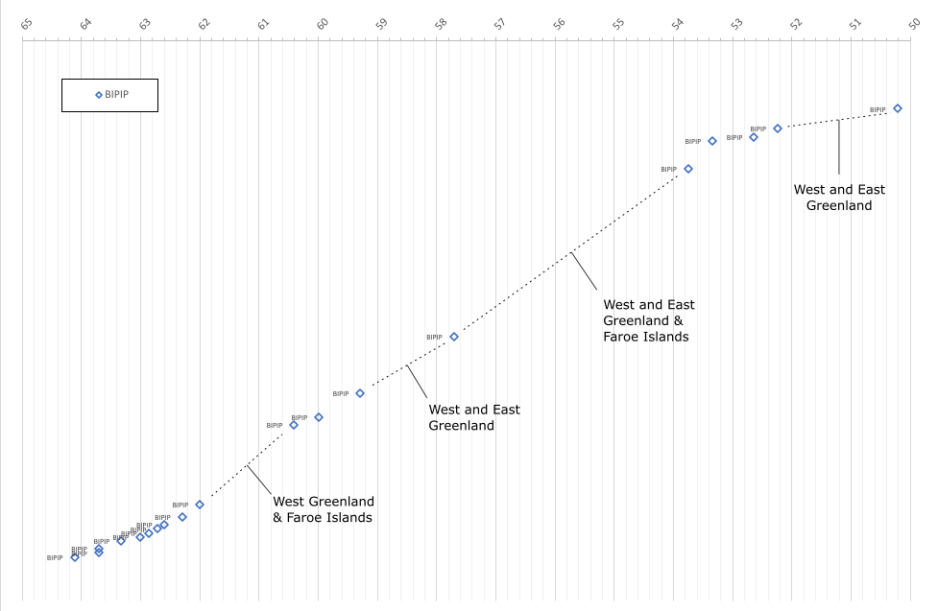

Figure 7.3. (b) Data from Wilkinson et al., 2017 replotted to highlight BIPIP mafic volcanism through time. Mafic volcanic activity elsewhere in the NAIP is indicated by text. No authorship or participation in that work is intended or implied.

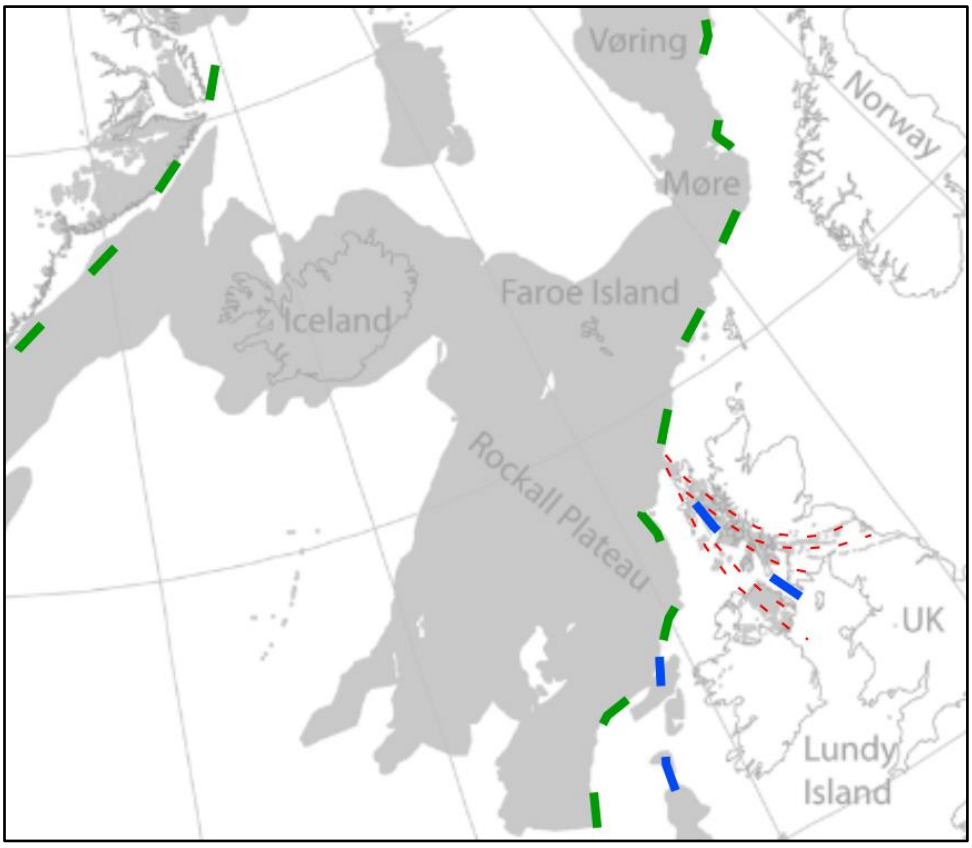

Figure 7.4. The modern extent of the NAIP area showing the approximate margins of the North Atlantic oceanic crust (green dash), the failed rifting spines (blue dash) and the associated dyke swarm geometry in the BIPIP (thin red dash). Modified by the author after Horni et al, 2017.

7.5 Synthesis

If we merge the previous discussions we find ourselves reasonably asking the question: was spreading already happening during the emplacement of the Antrim Lava Group and wider BIPIP? If so, should we be reconsidering the two-fold nature of phased ALG igneous activity that has persisted from one investigation to the next? To recap:

1. The geometry of the fissure swarms mapped in the BIPIP bears a striking resemblance to those that are or have recently been active in Iceland.
2. A review of age dating data suggests periodic, sustained relocation of volcanic activity around the NAIP.
3. Our findings also suggest that volcanic activity relocated locally within the Antrim Lava Group, leaving some areas to develop soils and associated ecological diversity while other areas were being buried by flood basalt lava flows.

7.6 Future work

a. Publications arising from this research

   i. Relationship between Clay with Flints and the basalts of the Antrim Lava Group

   ii. Statistical analysis of the geochemistry of the Antrim Lava Group

   iii. The case for revising the stratigraphy of the Antrim Lava Group

b. Questions arising from this research

   i. Is a flood basalt formation missing from the 'Interbasaltic Formation' period, evidenced by dated basic dykes across the area south of the Laggan Valley?

   ii. Can the timing of emplacement of the Upper Basalt Formation be constrained?

iii. Can the impact position(s) of the mantle plume(s) under the BIPIP be more clearly understood in relation to the onset of the NAIP?

c. Ideas for future research

i. A detailed/high sample resolution rock magnetic study of NIRE borehole core and natural/quarried field outcrops (paleomagnetism for timing and AMS for emplacement)

ii. High sample resolution geochemical (pXRF? WD-XRF?) palynological study of the Causeway Coast interbeds/'laterites'

iii. A detailed investigation into the potential presence of hydrogeothermal activity markers within the interbeds of the Antrim Lava Group

iv. Testing the geochemical discriminant (namely (K/Ti)/Zr)) on basalts found in the other subprovinces of the NAIP

d. Review of new collaborations arising during this research

i. Dr Elliot Carter (Trinity College, Dublin)

ii. Prof David Jolley (University of Aberdeen)

iii. Dr John Millett (VBER, Norway and University of Aberdeen)

iv. Dr Timo Korth (ALG, Switzerland)

7.7 Conclusions

The key findings of this research are:

1. Lavas of the Upper and Lower Basalt Formation can be distinguished geochemically using (K/Ti)/Zr. Higher values (300 - 1000+) signify Lower Basalts, and lower values (<400) signify Upper Basalts.
2. Detailed basalt flow geochemistry of the Antrim Lava Group varies significantly throughout the entire column of material, not necessarily only between formally recognised members and formations.
3. Palynological evidence from sedimentary interbeds throughout the Antrim Lava Group points towards a temperate to warm temperate climate.
4. The tempo of volcanic activity varied significantly throughout the emplacement of the Antrim Lava Group.
5. The vast majority of time spanned by the Antrim Lava Group passed without significant volcanic activity, as evidenced by interbeds.
6. Volcanic activity consistently has moved around the NAIP region between ~64 and 50 Ma, with minor activity up to as recently as 28 Ma.
7. The recent flood basalt volcanic activity of Iceland is a reasonable corollary for the emplacement of Antrim flood basalts.

REFERENCES

á Horni, J., Hopper, J.R., Blischke, A., Geisler, W.H., Stewart, M., McDermott, K., Judge, M., Erlendsson, Ö. and Árting, U., 2017. Regional distribution of volcanism within the North Atlantic Igneous Province. Geological Society, London, Special Publications, 447(1), pp.105-125.

Anderson, F.W. and Dunham, K.C., 1966. The geology of northern Skye. HM Stationery Office.

Andrews, G., 2022. Geological Carbon Storage in Northern Irish Basalts: Prospectivity and Potential. Available at SSRN 4157443.

Babechuk, M.G., Widdowson, M. and Kamber, B.S., 2014. Quantifying chemical weathering intensity and trace element release from two contrasting basalt profiles, Deccan Traps, India. Chemical Geology, 363, pp.56-75.

Bailey, E.B., Clough, C.T., Wright, W.B., Richey, J.E., Wilson, G.V., 1924. Tertiary and Post-Tertiary Geology of Mull, Loch Aline and Oban. Memoir of the Geological Survey of Great Britain, HMSO, Edinburgh

Bas, M.L., Maitre, R.L., Streckeisen, A., Zanettin, B. and IUGS Subcommission on the Systematics of Igneous Rocks, 1986. A chemical classification of volcanic rocks based on the total alkali-silica diagram. Journal of petrology, 27(3), pp.745-750.

Bell. B.R., Williamson, I.T., Head, F.E. & Jolley, D.W. 1996. On the origin of a reddened interflow bed within the Paleocene lava field of north Skye. Scottish Journal of Geology 32. (2). 117-26.

Beresford-Browne, A.N.W.; Jolley, D.; Millett, J.; Stevenson, C.; Watt, S.; Raine, R.; Carter, E., 2023. Depositional system and plant ecosystem responses to long-term low-tempo volcanism, the Interbasaltic Formation, Antrim Lava Group. Geological Society of London. Collection. https://doi.org/10.6084/m9.figshare.c.6949132.v2

Berger, H. and Vincent, E., 1981. Chemostratigraphy and biostratigraphic correlation: exercises in systematic stratigraphy. Oceanologica Acta, Special issue.

Bondarenko, O.V., Blokhina, N.I., Mosbrugger, V. and Utescher, T., 2020. Paleogene climate dynamics in the Primorye Region, Far East of Russia, based on a Coexistence Approach analysis of palaeobotanical data. Palaeobiodiversity and Palaeoenvironments, 100, pp.5-31.

Bornemann, A., Jehle, S., Lägel, F., Deprez, A., Petrizzo, M.R. and Speijer, R.P., 2021. Planktic foraminiferal response to an early Paleocene transient warming event and biostratigraphic implications. International Journal of Earth Sciences, 110, pp.583-594.

Bralower, T., Premoli Silva, I. and Malone, M., 2002. Leg 198. Proceedings of the Ocean Drilling Program: Initial Reports, College Station, TX (Ocean Drilling Program), https://doi. org/10.2973/odp. proc. ir, 198.

Brooks, C.L., 2016. The Stratigraphy of the Lower Basalt Formation, Antrim Lava Group, Northern Ireland. MSc Thesis (unpublished). School of Geography, Earth & Environmental Sciences, University of Birmingham.

Bryan, S.E. and Ferrari, L., 2013. Large igneous provinces and silicic large igneous provinces: Progress in our understanding over the last 25 years. GSA Bulletin, 125(7-8), pp.1053-1078.

Camp, V.E. and Ross, M.E., 2004. Mantle dynamics and genesis of mafic magmatism in the intermontane Pacific Northwest. Journal of Geophysical Research: Solid Earth, 109(B8).

Candra, I.N., Gerzabek, M.H., Ottner, F., Wriessnig, K., Tintner, J., Schmidt, G., Rampazzo, N. and Zehetner, F., 2023. Soil formation and mineralogical changes on basaltic lava vs scoria along a hydroclimatic gradient on Santa Cruz Island, Galápagos. CATENA, 220, p.106696.

Carter, R.W.G., 1982. Sea-level changes in Northern Ireland. Proceedings of the Geologists' Association, 93(1), pp.7-23.

CIPW Norm Calculations https://www.science.smith.edu/~jbrady/petrology/igrocks-tools/norm-calc.php

Coffin, M.F. and Eldholm, O., 1991. Large igneous provinces: JOI/USSAC workshop report.

Cole, G.A.J., Wilkinson, S.B., M'Henry, A.R., Kilroe, J.R., Seymour, H.J., Moss, C.E. & Haigh, W.D., 1912. The Interbasaltic Rocks (Iron Ores and Bauxites) of North-East Ireland. Memoirs of the Geological Survey of Ireland (Economic), 129.

Cooper, M.R., Troll, V.R. and Lemon, K., 2018. The 'Clay-with-Flints' deposit in Northern Ireland: reassessment of the evidence for an early Paleocene ignimbrite. Geological Magazine, 155(8 (13)), pp.1811-1820.

Das, A., Krishnaswami, S., Sarin, M.M. and Pande, K., 2005. Chemical weathering in the Krishna Basin and Western Ghats of the Deccan Traps, India: Rates of basalt weathering and their controls. Geochimica et Cosmochimica Acta, 69(8), pp.2067-2084.

Dessert, C., Dupré, B., François, L.M., Schott, J., Gaillardet, J., Chakrapani, G. and Bajpai, S., 2001. Erosion of Deccan Traps determined by river geochemistry: impact on the global climate and the 87Sr/86Sr ratio of seawater. Earth and Planetary Science Letters, 188(3-4), pp.459-474.

Douglas, G.R., 1987. Manganese-rich rock coatings from Iceland. Earth surface processes and landforms, 12(3), pp.301-310.

Duncan, L.J., Dennehy, C.J., Ablard, P.M. and Wallis, D.W., 2020. The Rosebank Field, Blocks 213/27a, 213/26b, 205/1a and 205/2a, UK Atlantic Margin. Geological Society, London, Memoirs, 52(1), pp.980-989.

Ebinghaus, A., Jolley, D.W. & Hartley, A. Extrinsic forcing of plant ecosystems in a large igneous province: The Columbia River flood basalt province, Washington State, USA. Geology, published online on 6 November 2015 as doi:10.1130/G37276.1

Eldholm, O. and Grue, K., 1994. North Atlantic volcanic margins: dimensions and production rates. Journal of Geophysical Research: Solid Earth, 99(B2), pp.2955-2968.

Eldholm, O., 1989. Evolution of the Vøring volcanic margin. In Proc. ODP, Sci. Results (Vol. 104, pp. 1033-1065).

Ellis, D. and Stoker, M.S., 2014. The Faroe–Shetland Basin: a regional perspective from the Paleocene to the present day and its relationship to the opening of the North Atlantic Ocean. Geological Society, London, Special Publications, 397(1), pp.11-31.

Ernst, R.E. and Youbi, N., 2017. How Large Igneous Provinces affect global climate, sometimes cause mass extinctions, and represent natural markers in the geological record. Palaeogeography, palaeoclimatology, palaeoecology, 478, pp.30-52.

Evans, A.L., Fitch, F.J. and Miller, J.A., 1973. Potassium-argon age determinations on some British Tertiary igneous rocks. Journal of the Geological Society, 129(4), pp.419-438.

Eyles, V.A. 1950. Note on the interbasaltic horizon in Northern Ireland. Quarterly Journal of the Geological Society, 106(1-4), 136-137. https://doi.org/10.1144/GSL.JGS.1950.106.01-04.10

Eyles, V.A., 1952. The composition and origin of the Antrim laterites and bauxites. Mem. Geol. Surv. N. Ireland.

Fissure vent volcano - basic planet

Fitch, F.J., Heard, G.L. and Miller, J.A., 1988. Basaltic magmatism of late Cretaceous and Palaeogene age recorded in wells NNE of the Shetlands. Geological Society, London, Special Publications, 39(1), pp.253-262.

Fitton, J.G., Saunders, A.D., Larsen, L.M., Hardarson, B.S. and Norry, M.J., 1998. 28. VOLCANIC ROCKS FROM THE SOUTHEAST GREENLAND MARGIN AT 63 N: COMPOSITION, PETROGENESIS, AND MANTLE SOURCES1.

Foulger, G.R., Natland, J.H. and Anderson, D.L., 2003. Iceland is fertile: The geochemistry of Icelandic lavas indicates extensive melting of subducted Iapetus crust in the Caledonian suture. J. Volc. Geotherm. Res.

Foulger, G.R., Pritchard, M.J., Julian, B.R., Evans, J.R., Allen, R.M., Nolet, G., Morgan, W.J., Bergsson, B.H., Erlendsson, P., Jakobsdottir, S. and Ragnarsson, S., 2001. Seismic tomography shows that upwelling beneath Iceland is confined to the upper mantle. Geophysical Journal International, 146(2), pp.504-530.

Gaillardet, J., Millot, R. and Dupré, B., 2003. Chemical denudation rates of the western Canadian orogenic belt: the Stikine terrane. Chemical Geology, 201(3-4), pp.257-279.

Ganerød, M., Chew, D.M., Smethurst, M.A., Troll, V.R., Corfu, F., Meade, F. & Prestvik, T. 2011. Geochronology of the Tardree rhyolite complex, Northern Ireland; implications for zircon fission-track studies, the North Atlantic igneous province and the age of the Fish Canyon sanidine standard. Chemical Geology, 286, 222–228, https://doi.org/10.1016/j. chemgeo.2011.05.007

Ganerød, M., Chew, D.M., Smethurst, M.A., Troll, V.R., Corfu, F., Meade, F. and Prestvik, T., 2010. Geochronology of the Tardree Rhyolite Complex, Northern Ireland: Implications for zircon fission track studies, the North Atlantic Igneous Province and the age of the Fish Canyon sanidine standard. Chemical Geology, 286(3-4), pp.222-228.

Ganerød, M., Smethurst, M.A. et al. 2010. The North Atlantic Igneous Province reconstructed and its relation to the Plume Generation Zone: the Antrim Lava Group revisited. Geophysical Journal International, 182, 183–202, https://doi.org/10.1111/j.1365-246X. 2010.04620.

Ganerød, M., Smethurst, M.A., Rousse, S., Torsvik, T.H. and Prestvik, T., 2008. Reassembling the Paleogene–Eocene North Atlantic igneous province: new paleomagnetic constraints from the Isle of Mull, Scotland. Earth and Planetary Science Letters, 272(1-2), pp.464-475.

Ganerød, M., Smethurst, M.A., Torsvik, T.H., Prestvik, T., Rousse, S., McKenna, C., Van Hinsbergen, D.J.J. and Hendriks, B.W.H., 2010. The North Atlantic Igneous Province reconstructed and its relation to the plume generation zone: the Antrim Lava Group revisited. Geophysical Journal International, 182(1), pp.183-202.

Geochemical Rock Database-Query (gwdg.de) - https://georoc.mpch-mainz.gwdg.de/georoc/ (last accessed 2023)

Ghosh, P., Sayeed, M.R.G., Islam, R. and Hundekari, S.M. 2006. Inter-basaltic clay (bole bed) horizons from Deccan traps of India: Implications for palaeo-weathering and palaeo-climate during Deccan volcanism. Palaeogeography, Palaeoclimatology, Palaeoecology, 242(1-2), 90-109. https://doi:10.1016/j.palaeo.2006.05.018

Gislason, S.R. and Eugster, H.P., 1987. Meteoric water-basalt interactions. II: A field study in NE Iceland. Geochimica et Cosmochimica Acta, 51(10), pp.2841-2855.

Gislason, S.R., Arnórsson, S. and Armannsson, H., 1996. Chemical weathering of basalt in Southwest Iceland; effects of runoff, age of rocks and vegetative/glacial cover. American Journal of Science, 296(8), pp.837-907.

Godwin, H., Clowes, D.R. & Huntley, B. 1974. Studies in the Ecology of Wicken Fen: V. Development of Fen Carr. Journal of Ecology 62, 197-214. https://www.jstor.org/stable/2258889

Gould, R.J., 2004. Antrim Lava Field: Flow patterns and provenance of interbasaltic zircons. PhD thesis (unpublished). Trinity College, University of Dublin.

Green, T., Renne, P.R. and Keller, C.B., 2022. Continental flood basalts drive Phanerozoic extinctions. Proceedings of the National Academy of Sciences, 119(38), p.e2120441119.

Halbritter, H, Ulrich, S., Grimson, F., Weber, M., Zetter, R., Hesse, M., Buchner, R., Svoltke, M & Frosch-Radivo, A. 2018. Illustrated pollen terminology. Springer, 483pp, https://doi.org/10.1007/978-3-319-71365-6.

Hamilton, W., 1786. Letters Concerning the North Coast of County Antrim.

Hardman, J., Schofield, N., Jolley, D., Hartley, A., Holford, S. and Watson, D., 2019. Controls on the distribution of volcanism and intra-basaltic sediments in the Cambo–Rosebank region, West of Shetland. Petroleum Geoscience, 25(1), pp.71-89. https://doi.org/10.1144/petgeo2017-061

Henehan, M.J. and Witts, J.D., 2023. Continental flood basalts do not drive later Phanerozoic extinctions. Proceedings of the National Academy of Sciences, 120(21), p.e2303700120.

Hill, I.G., Worden, R.H., Meighan, I.G., 2000. Geochemical evolution of a palaeolaterite: the Interbasaltic Formation, Northern Ireland. Chemical Geology 166, pp 65-84.

Hill, I.G., Worden, R.H., Meighan, I.G., 2001. Formation of interbasaltic laterite horizons in NE Ireland by early Tertiary weathering processes. Proceedings of the Geologists' Association 112, pp 339-348.

Hill, M.O. & Gauch, H.G., 1980. Detrended correspondence analysis: an improved ordination technique. In: Classification and ordination (pp. 47-58). Springer, Dordrecht.

Hill, M.O., 1979. DECORANA. A Fortran program for detrended correspondence analysis and reciprocal averaging. Ecological and Systematics Department.

Hooper, P.R., 1988. The Columbia river basalt. Continental flood basalts, pp.1-33.

Hopson, P., 2005. A stratigraphical framework for the Upper Cretaceous Chalk of England and Scotland with statements on the Chalk of Northern Ireland and the UK Offshore Sector. British Geological Survey.

Hovikoski, J., Fyhn, M.B., Nøhr-Hansen, H., Hopper, J.R., Andrews, S., Barham, M., Nielsen, L.H., Bjerager, M., Bojesen-Koefoed, J., Lode, S. and Sheldon, E., 2021. Paleocene-Eocene volcanic segmentation of the Norwegian-Greenland seaway reorganized high-latitude ocean circulation. Communications Earth & Environment, 2(1), p.172.

https://www.basicplanet.com/fissure-vent-volcano/

Hughes, H.S., McDonald, I. and Kerr, A.C., 2015. Platinum-group element signatures in the North Atlantic Igneous Province: Implications for mantle controls on metal budgets during continental breakup. Lithos, 233, pp.89-110.

Hull, E., 1874. IV.—The Volcanic History of Ireland: Being the Anniversary Address delivered to the Royal Geological Society of Ireland, February 11th, 1874. Geological Magazine, 1(5), pp.205-210.

Hull, E., 1878. The physical geology & geography of Ireland. E. Stanford.

Jolley, D.W. & Morton, A.C., 1992. Palynological and petrological characterisation of a North Sea volcaniclastic sequence. Proceedings of the Geologists' Association 103, 119-127.

Jolley, D.W. 1997. Palaeosurface palynofloras of the Skye lava field and the age of the British Tertiary Volcanic Province. In: Widdowson, M. (ed.) Palaeosurfaces: Recognition, Reconstruction and Palaeoenvironmental Interpretation. Geological Society, London, Special Publications 120, 67–94.

Jolley, D.W., 1998. Palynostratigraphy and depositional history of the Paleocene Ormesby/Thanet depositional sequence set in southeastern England and its correlation with continental West Europe and the Lista Formation, North Sea. Review of Palaeobotany and Palynology 99 (1998) 265 315

Jolley, D.W., Bell, B.R., Williamson, I.T. & Prince, I. 2009. Syn-eruption vegetation dynamics, palaeosurfaces and structural controls on lava field vegetation: An example from the Paleogene Staffa Formation, Mull Lava Field, Scotland. Review of Palaeobotany and Palynology, 153, 19-33.

Jolley, D.W., Millett, J.M., Schofield, N., Broadley, L. & Hole, M.J., 2021. Stratigraphy of volcanic rock successions of the North Atlantic rifted margin: the offshore record of the Faroe–Shetland and Rockall basins. Earth and Environmental Science Transactions of the Royal Society of Edinburgh. Online First, DOI: https://doi.org/10.1017/S1755691021000037.

Jolley, D.W., Millett, J.M., Schofield, N., Broadley, L. & Hole, M.J., 2021. Stratigraphy of volcanic rock successions of the North Atlantic rifted margin: the offshore record of the Faroe–Shetland and Rockall basins. Earth and Environmental Science Transactions of the Royal Society of Edinburgh. Online First, DOI: https://doi.org/10.1017/S1755691021000037.

Jolley, D.W., Passey, S.R., Vosgerau, H & Sørensen, E.V. 2022. Volcanic landscape controls on pre-rift to syn-rift volcano sedimentary systems: the Prestfjall Formation eruptive hiatus, Faroe Islands Basalt Group, northeast Atlantic. Earth and Environmental Science Transactions of the Royal Society of Edinburgh, 1–24,

Jolley, D.W., Widdowson, M. & Self, S., 2008. Volcanogenic nutrient fluxes and plant ecosystems in large igneous provinces: an example from the Columbia River Basalt Group. Journal of the Geological Society, London 165, 955–966.

Jones, S.M., Hoggett, M., Greene, S.E. and Dunkley Jones, T., 2019. Large Igneous Province thermogenic greenhouse gas flux could have initiated Paleocene-Eocene Thermal Maximum climate change. Nature Communications, 10(1), p.5547.

Kerr, A.C., 1995. The melting processes and composition of the North Atlantic (Iceland) plume: geochemical evidence from the Early Tertiary basalts. Journal of the Geological Society, 152(6), pp.975-978.

Kovach, W.L. 1993. Multivariate techniques for biostratigraphical correlation. Journal of the Geological Society, London, 150, 697–705.

Lasaga, A.C., Soler, J.M., Ganor, J., Burch, T.E. and Nagy, K.L., 1994. Chemical weathering rate laws and global geochemical cycles. Geochimica et Cosmochimica Acta, 58(10), pp.2361-2386.

Le Bas, M., Maitre, R.L., Streckeisen, A., Zanettin, B. and IUGS Subcommission on the Systematics of Igneous Rocks, 1986. A chemical classification of volcanic rocks based on the total alkali-silica diagram. Journal of petrology, 27(3), pp.745-750.

Levlie, R., Gidskehaug, A. and Storetvedt, K.M., 1972. On the magnetization history of the Northern Irish basalts. Geophysical Journal International, 27(5), pp.487-498.

Lindgreen, H., Drits, V.A., Salyn, A.L., Jakobsen, F. and Springer, N., 2011. Formation of flint horizons in North Sea chalk through marine sedimentation of nano-quartz. Clay Minerals, 46(4), pp.525-537.

Liu, J., Wang, P., Zhang, Y., Bian, W., Huang, Y., Tang, H. and Chen, X., 2012. Volcanic rock-hosted natural hydrocarbon resources: a review. IntechOpen.

Louvat, P. and Allègre, C.J., 1997. Present denudation rates on the island of Reunion determined by river geochemistry: basalt weathering and mass budget between chemical and mechanical erosions. Geochimica et Cosmochimica Acta, 61(17), pp.3645-3669.

Lyle, P. & Preston, J., 1993. Geochemistry and volcanology of the Tertiary basalts of the Giant's Causeway area, Northern Ireland. Journal of the Geological Society, London. Vol 150, pp 109-120.

Lyle, P. and Patton, D.J., 1989. The petrography and geochemistry of the Upper Basalt Formation of the Antrim Lava Group in northeast Ireland. Irish Journal of Earth Sciences, pp.33-41.

Lyle, P. and Preston, J., 1993. Geochemistry and volcanology of the Tertiary basalts of the Giant's Causeway area, Northern Ireland. Journal of the Geological Society, 150(1), pp.109-120.

Lyle, P. and Thompson, S.J., 1983. The classification and chemistry of the Tertiary intermediate lavas of Northeast Ireland. Scottish Journal of Geology, 19(1), pp.17-27.

Lyle, P., 1979. A petrological and geochemical study of the Tertiary basaltic rocks of northeast Ireland. Journal of Earth Sciences, pp.137-152.

Lyle, P., 1985. The geochemistry and petrology of Tertiary basalts from the Binevenagh area, County Londonderry. Irish Journal of Earth Sciences, pp.59-64.

Lyle, P., 1985. The petrogenesis of the Tertiary basaltic and intermediate lavas of northeast Ireland. Scottish Journal of Geology, 21(1), pp.71-84.

Lyle, P., 1988. The geochemistry, petrology and volcanology of the Tertiary lava succession of the Binevenagh-Benbraddagh area of County Londonderry. Irish journal of earth sciences, pp.141-151.

Lyle, P., 2000. The eruption environment of multi-tiered columnar basalt lava flows. Journal of the Geological Society, 157(4),715-722.

Lyle, P., 2001. Phase relationships within the Causeway Tholeiite Member of the Tertiary Antrim Lava Group. Irish Journal of Earth Sciences, pp.37-41.

Macintyre, R.M., McMenamin, T. and Preston, J., 1975. K–Ar results from Western Ireland and their bearing on the timing and siting of Thulean magmatism. Scottish Journal of Geology, 11(3), pp.227-249.

Maliva, R.G. and Dickson, J.A.D., 1997. Ulster White Limestone Formation (Upper Cretaceous) of Northern Ireland: effects of basalt loading on chalk diagenesis. Sedimentology, 44(1), pp.105-112.

Mallet, F.R., 1881. On the Ferruginous Beds Associated with the Basaltic Rocks of Northeastern Ulster, in Relation to Indian Laterite. Rec. Geol. Surv. India, vol.xiv, p13

Marshall, E., Bar Rasmussen, M., Halldorsson, S., Matthews, S., Ranta, E., Sigmarsson, O., Gunnarsson Robin, J., Bali, E., Caracciolo, A., Gudfinnsson, G. and Mibei, G., 2021, December. Rapid geochemical evolution of the mantle-sourced Fagradalsfjall eruption, Iceland. In AGU Fall Meeting Abstracts (Vol. 2021, pp. V14B-06).

Marshall, E., Rasmussen, M., Halldorsson, S., Matthews, S., Ranta, E., Sigmarsson, O., Robin, J., Barnes, J., Bali, E., Caracciolo, A. and Guðfinnsson, G., 2022, May. An overview of the geochemistry and petrology of the mantle-sourced Fagradalsfjall eruption, Iceland. In EGU General Assembly Conference Abstracts (pp. EGU22-8304).

Martin, B.S., Tolan, T.L., Reidel, S.P., Camp, V.E., Ross, M.E., Wolff, J.A. and Wells, R.E., 2013. Revisions to the stratigraphy and distribution of the Frenchman Springs Member, Wanapum Basalt. Geological Society of America Special Papers, 497, pp.155-179.

Mégnin, C. and Romanowicz, B., 2000. The three-dimensional shear velocity structure of the mantle from the inversion of body, surface and higher-mode waveforms. Geophysical Journal International, 143(3), pp.709-728.

Middlemost, E.A., 1994. Naming materials in the magma/igneous rock system. Earth-science reviews, 37(3-4), pp.215-224.

Millet, J.M., Rossetti, L., Bischoff, A., Rossetti, M., Rosenqvist, M. P., Avseth, P., Hole, M.J., Pierdominici, S., Healy, D., Jerram, D.A., Planke, S., this volume. Lava flow hosted reservoirs: A review. In: Kilhams, B., Holford, S., Gardiner, D., Gozzard, S., Layfield, L., McLean, C., Thackrey, S. & Watson, D. (eds.). The Impact of Igneous systems on

sedimentary basins and their energy resources. Geological Society, London, Special Publications.

Millett, J.M., Hole, M.J., Jolley, D.W. and Passey, S.R., 2017. Geochemical stratigraphy and correlation within large igneous provinces: The final preserved stages of the Faroe Islands Basalt Group. Lithos, 286, pp.1-15.

Millett, J.M., Jerram, D.A., Manton, B., Planke, S., Ablard, P., Wallis, D., Hole, M.J., Brandsen, H., Jolley, D.W. and Dennehy, C., 2021. The Rosebank Field, NE Atlantic: Volcanic characterisation of an inter-lava hydrocarbon discovery. Basin Research, 33(6), pp.2883-2913.

Mitchell, W., Anderson, T.B., Johnstone, T.P., Cooper, M.R., Bazley, R.A.B., Reay, D.M., Arthurs, J.W., and Earls, G., 2004. The geology of Northern Ireland: our natural foundation. Geological Survey of Northern Ireland.

Muff, H.B., 1908. Report relating to the geology of the East Africa Protectorate. Colonial reports, miscellaneous, No. 45. p52.

Navarre-Sitchler, A. and Brantley, S., 2007. Basalt weathering across scales. Earth and Planetary Science Letters, 261(1-2), pp.321-334.

Nesbitt, H.W. and Wilson, R.E., 1992. Recent chemical weathering of basalts. American Journal of Science, 292(10), pp.740-777.

Nielsen, S.B., Stephenson, R. and Thomsen, E., 2007. Dynamics of Mid-Palaeocene North Atlantic rifting linked with European intra-plate deformations. Nature, 450(7172), pp.1071-1074.

Nielsen, T.K., Larsen, H.C. and Hopper, J.R., 2002. Contrasting rifted margin styles south of Greenland: implications for mantle plume dynamics. Earth and Planetary Science Letters, 200(3-4), pp.271-286.

O'Connor, J.M., Stoffers, P., Wijbrans, J.R., Shannon, P.M. and Morrissey, T., 2000. Evidence from episodic seamount volcanism for pulsing of the Iceland plume in the past 70 Myr. Nature, 408(6815), pp.954-958.

Old, R.A., 1975. The age and field relationships of the Tardree Tertiary Rhyolite Complex County Antrim Northern Ireland. Bull. Geol. Surv. G.B.; 1975, Num. 0051, P. 21 A 39

Old, R.A., 1975. The age and field relationships of the Tardree Tertiary rhyolite complex, County Antrim, Northern Ireland. Bulletin of the Geological Survey of Great Britain, No 51. HM Stationery Office.

Opheim, J.A. and Gudmundsson, A., 1989. Formation and geometry of fractures, and related volcanism, of the Krafla fissure swarm, northeast Iceland. Geological Society of America Bulletin, 101(12), pp.1608-1622.

Pálmason, G., Arnórsson, S., Fridleifsson, I.B., Kristmannsdóttir, H., Saemundsson, K., Stefánsson, V., Steingrímsson, B., Tómasson, J. and Kristjánsson, L., 1979. The Iceland

crust: Evidence from drillhole data on structure and processes. Deep drilling results in the Atlantic Ocean: Ocean crust, 2, pp.43-65.

Passey, S.R. & Jolley, D.W., 2009. A revised lithostratigraphic nomenclature for the Paleogene Faroe Islands Basalt Group, NE Atlantic Ocean. Earth and Environmental Science Transactions of the Royal Society of Edinburgh 99, 127-158.

Patterson, E.M. & Mitchell, W.A., 1955. The Tertiary lava succession in the northern part of the Antrim Plateau. Proceedings of the Royal Irish Academy. Section B: Biological, Geological, and Chemical Science , 1954 - 1956, Vol. 57 (1954 - 1956), pp. 79-122

Patterson, E.M. and Mitchell, W.A., 1955, February. The Tertiary lava succession in the northern part of the Antrim plateau. In Proceedings of the Royal Irish Academy. Section B: Biological, Geological, and Chemical Science (Vol. 57, pp. 79-122). Royal Irish Academy.

Patterson, E.M. and Swaine, D.J., 1955. A petrochemical study of Tertiary tholeiitic basalts: The middle lavas of the Antrim Plateau. Geochimica et Cosmochimica Acta, 8(4), pp.173-181.

Patterson, E.M., 1950. Preliminary note on the Tertiary lava succession in North Antrim. Quarterly Journal of the Geological Society, 106(1-4), pp.134-135.

Petrizzo, M.R., 2005. An early late Paleocene event on Shatsky Rise, northwest Pacific Ocean (ODP Leg 198): Evidence from planktonic foraminiferal assemblages. In Proceedings of the Ocean Drilling Program. Scientific Results (Vol. 198). Ocean Drilling Program.

Portlock, J.E., 1843. Report on the geology of the county of Londonderry, and parts of Tyrone and Fermanagh. HM Stationery Office.

Price, R.C., Gray, C.M., Wilson, R.E., Frey, F.A. and Taylor, S.R., 1991. The effects of weathering on rare-earth element, Y and Ba abundances in Tertiary basalts from southeastern Australia. Chemical Geology, 93(3-4), pp.245-265.

Ramette, A. 2007. Multivariate analyses in microbial ecology. FEMS Microbiology Ecology 62(2), pp. 142-160.

Ramkumar, M., 2015. Chemostratigraphy: Concepts, techniques, and applications. Elsevier.

Raza, A., Glatz, G., Gholami, R., Mahmoud, M. and Alafnan, S., 2022. Carbon mineralization and geological storage of CO2 in basalt: Mechanisms and technical challenges. Earth-Science Reviews, 229, p.104036.

Roddick, J.C. and Srivastava, S.P., 1989. K–Ar dating of basalts from Site 647, ODP Leg 105. In Proceedings of the Ocean Drilling Program, Scientific Results (Vol. 105, pp. 885-887). College Station, Texas: Texas A&M University.

Rohrman, M., 2022. Methodology for evaluating the North Atlantic Igneous Province reveals multiple hotspots at breakup. Geochemistry, Geophysics, Geosystems, 23(4), p.e2021GC010110.

Rosenqvist, M.P., Meakins, M.W., Planke, S., Millett, J.M., Kjøll, H.J., Voigt, M.J. and Jamtveit, B., 2023. Reservoir properties and reactivity of the Faroe Islands Basalt Group: Investigating the potential for CO2 storage in the North Atlantic Igneous Province. International journal of greenhouse gas control, 123, p.103838.

Rosenqvist, M.P., Millett, J.M., Planke, S., Johannesen, R.M., Passey, S.R., Sørensen, E.V., Vosgerau, H. & Jamtveit, B. this volume. The architecture of basalt reservoirs in the North Atlantic Igneous province with implications for basalt carbon sequestration. In: Kilhams, B., Holford, S., Gardiner, D., Gozzard, S., Layfield, L., McLean, C., Thackrey, S. & Watson, D. (eds.). The Impact of Igneous systems on sedimentary basins and their energy resources. Geological Society, London, Special Publications.

Rosenthal, Y., Holbourn, A.E., Kulhanek, D.K., Aiello, I.W., Babila, T.L., Bayon, G., Beaufort, L., Bova, S.C., Chun, J.-H., Dang, H., Drury, A.J., Dunkley Jones, T., Eichler, P.P.B., Fernando, A.G.S., Gibson, K., Hatfield, R.G., Johnson, D.L., Kumagai, Y., Li, T., Linsley, B.K., Meinicke, N., Mountain, G.S., Opdyke, B.N., Pearson, P.N., Poole, C.R., Ravelo, A.C., Sagawa, T., Schmitt, A., Wurtzel, J.B., Xu, J., Yamamoto, M., and Zhang, Y.G., 2018. Site U1487. In Rosenthal, Y., Holbourn, A.E., Kulhanek, D.K.,. Proceedings of the International Ocean Discovery Program, 363: College Station, TX (International Ocean Discovery Program). https://doi.org/10.14379/iodp.proc.363.108.2018

Saunders, A.D., Fitton, J.G., Kerr, A.C., Norry, M.J., Kent, R.W., Mahoney, J.J. and Coffin, M.F., 1997. The North Atlantic igneous province. Geophysical Monograph-American Geophysical Union, 100, pp.45-94.

Schofield, N & Jolley, D.W., 2013. Development of intra-basaltic lava-field drainage systems within the Faroe-Shetland Basin. Petroleum Geoscience, 19; p. 273-288; doi: 10.1144/petgeo2012-061.

Scholle, P.A., 1975. Diagenesis of Upper Cretaceous chalks from England, Northern Ireland and the North Sea. Pelagic Sediments: on Land and under the Sea, pp.177-210.

Scrivenor, J.B., 1937. A Note on “Buchanan's Laterite” 2. Geological Magazine, 74(6), pp.257-262.

Sigmarsson, O., Marshall, E.W., Bosq, C., Auclair, D., Rasmussen, M.B., Kleine, B.I., Ranta, E.J., Matthews, S., Halldórsson, S.A., Jackson, M.G. and Gudfinnsson, G.H., 2022, May. Basalt production controlled by mantle source fertility at Fagradalsfjall, Iceland. In EGU General Assembly Conference Abstracts (pp. EGU22-8479).

Sigmundsson, F., 2021. Recent basaltic eruptions in Iceland and the dynamics of co-eruptive subsurface magma flow. In Forecasting and Planning for Volcanic Hazards, Risks, and Disasters (pp. 413-438). Elsevier.

Simms, M.J., 2000. The sub-basaltic surface in northeast Ireland and its significance for interpreting the Tertiary history of the region. Proceedings of the Geologists' Association, 111(4), pp.321-336.

Simms, M.J., 2021. Subsidence, not erosion: Revisiting the emplacement environment of the Giant's Causeway, Northern Ireland. Proceedings of the Geologists' Association, 132(5), pp.537-548.

Simpson, J.B., 1961. The Tertiary pollen-flora of Mull and Ardnamurchan. Transactions of the Royal Society of Edinburgh 114, 421-468.

Sprong, J., Kouwenhoven, T.J., Bornemann, A., Dupuis, C., Speijer, R.P., Stassen, P. and Steurbaut, E., 2013. In search of the Latest Danian Event in a paleobathymetric transect off Kasserine Island, north-central Tunisia. Palaeogeography, Palaeoclimatology, Palaeoecology, 379, pp.1-16.

Steinberger, B., Bredow, E., Lebedev, S., Schaeffer, A. and Torsvik, T.H., 2019. Widespread volcanism in the Greenland–North Atlantic region explained by the Iceland plume. Nature Geoscience, 12(1), pp.61-68.

Stoker, M.S., Holford, S.P. and Hillis, R.R., 2018. A rift-to-drift record of vertical crustal motions in the Faroe–Shetland Basin, NW European margin: establishing constraints on NE Atlantic evolution. Journal of the Geological Society, 175(2), pp.263-274.

Storey, M., Duncan, R.A. and Tegner, C., 2007. Timing and duration of volcanism in the North Atlantic Igneous Province: Implications for geodynamics and links to the Iceland hotspot. Chemical Geology, 241(3-4), pp.264-281.

Storey, M., Pedersen, A.K., Stecher, O., Bernstein, S., Larsen, H.C., Larsen, L.M., Baker, J.A. and Duncan, R.A., 2004. Long-lived postbreakup magmatism along the East Greenland margin: Evidence for shallow-mantle metasomatism by the Iceland plume. Geology, 32(2), pp.173-176.

Tate, R. & Holden, J.S., 1870. On the iron-ores associated with the basalts of the north-east of Ireland. Quarterly Journal of the Geological Society of London. Vol xxvi, p 151.

Taylor, G., Eggleton, R.A., Holzhauer, C.C., Maconachie, L.A., Gordon, M., Brown, M.C. and McQueen, K.G., 1992. Cool climate lateritic and bauxitic weathering. The Journal of Geology, 100(6), pp.669-677.

Taylor, S.R. and McLennan, S.M., 2005. The evolution of continental crust. Scientific American, 15, pp.44-49.

Ter Braak, C.J.F. 1986. Canonical correspondence analysis: a new eigenvector technique for multivariate direct gradient analysis. Ecology, 67, 1167–1179.

Thompson, S.J., 1979. Preliminary report on the Ballymacilroy No 1 borehole, Ahoghill, Co Antrim. Geological Survey of Northern Ireland, Open File Report No 63.

Thordarson, T. and Larsen, G., 2007. Volcanism in Iceland in historical time: Volcano types, eruption styles and eruptive history. Journal of Geodynamics, 43(1), pp.118-152.

Thordarson, T. and Self, S., 2003. Atmospheric and environmental effects of the 1783–1784 Laki eruption: A review and reassessment. Journal of Geophysical Research: Atmospheres, 108(D1), pp.AAC-7.

Thordarson, T., Miller, D.J., Larsen, G., Self, S. and Sigurdsson, H., 2001. New estimates of sulfur degassing and atmospheric mass-loading by the 934 AD Eldgjá eruption, Iceland. Journal of Volcanology and Geothermal Research, 108(1-4), pp.33-54.

Tolan, T. L., Reidel, S. P., Beeson, M. H., Anderson, J. L., Fecht, K. R., & Swanson, D. A. (1989). Revisions to the estimates of the areal extent and volume of the Columbia River Basalt Group. In Reidel, S.P., and Hooper, P.R., (eds.), Volcanism and Tectonism in the Columbia River Flood-Basalt Province, Geological Society of America Special Paper 239, pp. 1-20.

Tomkeieff, S.I., 1940. The dolerite plugs of Tieveragh and Tievebulliagh near Cushendall, Co. Antrim, with a note on buchite. Geological Magazine, 77(1), pp.54-64.

Torsvik, T.H., Amundsen, H.E., Trønnes, R.G., Doubrovine, P.V., Gaina, C., Kusznir, N.J., Steinberger, B., Corfu, F., Ashwal, L.D., Griffin, W.L. and Werner, S.C., 2015. Continental crust beneath southeast Iceland. Proceedings of the National Academy of Sciences, 112(15), pp.E1818-E1827.

Tschudy, R.H. 1973. Complexipollis pollen lineage in Mississippi Embayment rocks. US Geological Survey Professional Paper 743-C, 40pp.

Walker, G.P.L., 1959. Some observations on the Antrim Basalts and associated dolerite intrusions. Proc. Geol. Assoc. Vol 70, pt 2.

Westerhold, T., Marwan, N., Drury, A.J., Liebrand, D., Agnini, C., Anagnostou, E., Barnet, J.S., Bohaty, S.M., De Vleeschouwer, D., Florindo, F. and Frederichs, T., 2020. An astronomically dated record of Earth's climate and its predictability over the last 66 million years. Science, 369(6509), pp.1383-1387.

Westerhold, T., Röhl, U., Donner, B., McCarren, H.K. and Zachos, J.C., 2011. A complete high-resolution Paleocene benthic stable isotope record for the central Pacific (ODP Site 1209). Paleoceanography, 26(2). Wheeler, B. & Proctor, M.C.F. 2000. Ecological Gradients, Subdivisions and Terminology of North-West European Mires. Journal of Ecology, pp. 187. https://www.jstor.org/stable/264852.

Wignall, P.B., 2001. Large igneous provinces and mass extinctions. Earth-science reviews, 53(1-2), pp.1-33.

Wilkinson, C. M., Ganerød, M., Hendricks, B. W. H. & Eide, E. A. 2017. Compilation and appraisal of geochronological data from the North Atlantic Igneous Province (NAIP). In: Peron-Pinvidic, G., Hopper, J. R., Stoker, M.S., Gaina, C., Doornanbal, J. C., Funck, T. & Arting, U. E. (eds); The NE Atlantic region: reappraisal of crustal structure, tectonostratigraphy and magmatic evolution, Geological Society of London, Special Publication 447, 69–103.

Wilkinson, C.M., Ganerød, M., Hendriks, B.W. and Eide, E.A., 2017. Compilation and appraisal of geochronological data from the North Atlantic Igneous Province (NAIP). Geological Society, London, Special Publications, 447(1), pp.69-103.

Wilson, H.E., 1965. Lava ploughing in the Tertiary basalts of County Antrim. Geological Magazine, 102(6), pp.538-540.

Wolfe, J., 1979. Temperature Parameters of Humid to Mesic Forests of Eastern Asia and Relation to Forests of Other Regions of the Northern Hemisphere and Australasia. Geological Survey Professional Paper 1106, 37pp.

Xia, L. and Li, X., 2019. Basalt geochemistry as a diagnostic indicator of tectonic setting. Gondwana Research, 65, pp.43-67.

Xia, L.Q., 2014. The geochemical criteria to distinguish continental basalts from arc-related ones. Earth-Science Reviews, 139, pp.195-212.

Young, K.E., Evans, C.A., Hodges, K.V., Bleacher, J.E. and Graff, T.G., 2016. A review of the handheld X-ray fluorescence spectrometer as a tool for field geologic investigations on Earth and in planetary surface exploration. Applied Geochemistry, 72, pp.77-87.

Young, K.E., Hodges, K.V. and Evans, C.A., 2012, January. Evaluating handheld X-ray fluorescence (XRF) technology in planetary exploration: Demonstrating instrument stability and understanding analytical constraints and limits for basaltic rocks. In 43rd Lunar and Planetary Science Conference (No. JSC-CN-25664).

Ziegler, P.A. and Dèzes, P., 2006. Crustal evolution of Western and Central Europe. Geological Society, London, Memoirs, 32(1), pp.43-56.

APPENDICES

https://drive.google.com/drive/folders/1CNKN5QqzdcROjQmBVUIVMxSOaefWmMDd?usp=sharing

APPENDIX A

pXRF WellCAD plots

NIRE 01/08-0002

WellCAD

alt Advanced Logic Technology

Company: Lonmin PLC
Well Name: 01/08-0002
Field:
Country: Northern Ireland **State:** Antrim

Location
East / Long: 302489 **North / Lat:** 419822

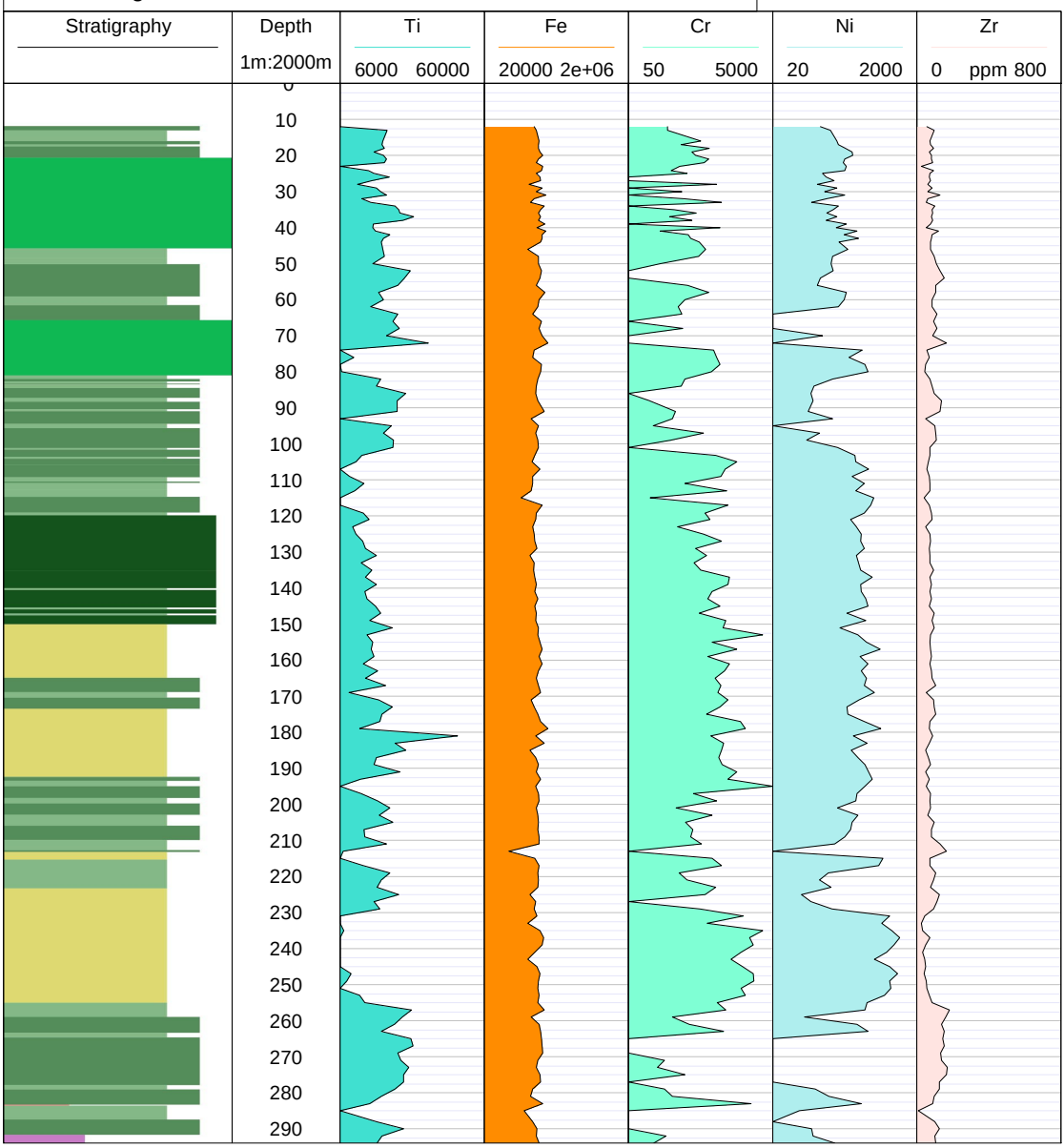

NIRE 02/08-0001

WellCAD

alt Advanced Logic Technology

Company: Lonmin PLC
Well Name: 02/08-0001
Field:
Country: Northern Ireland **State:** Antrim

Location
East / Long: 316129 **North / Lat:** 412540

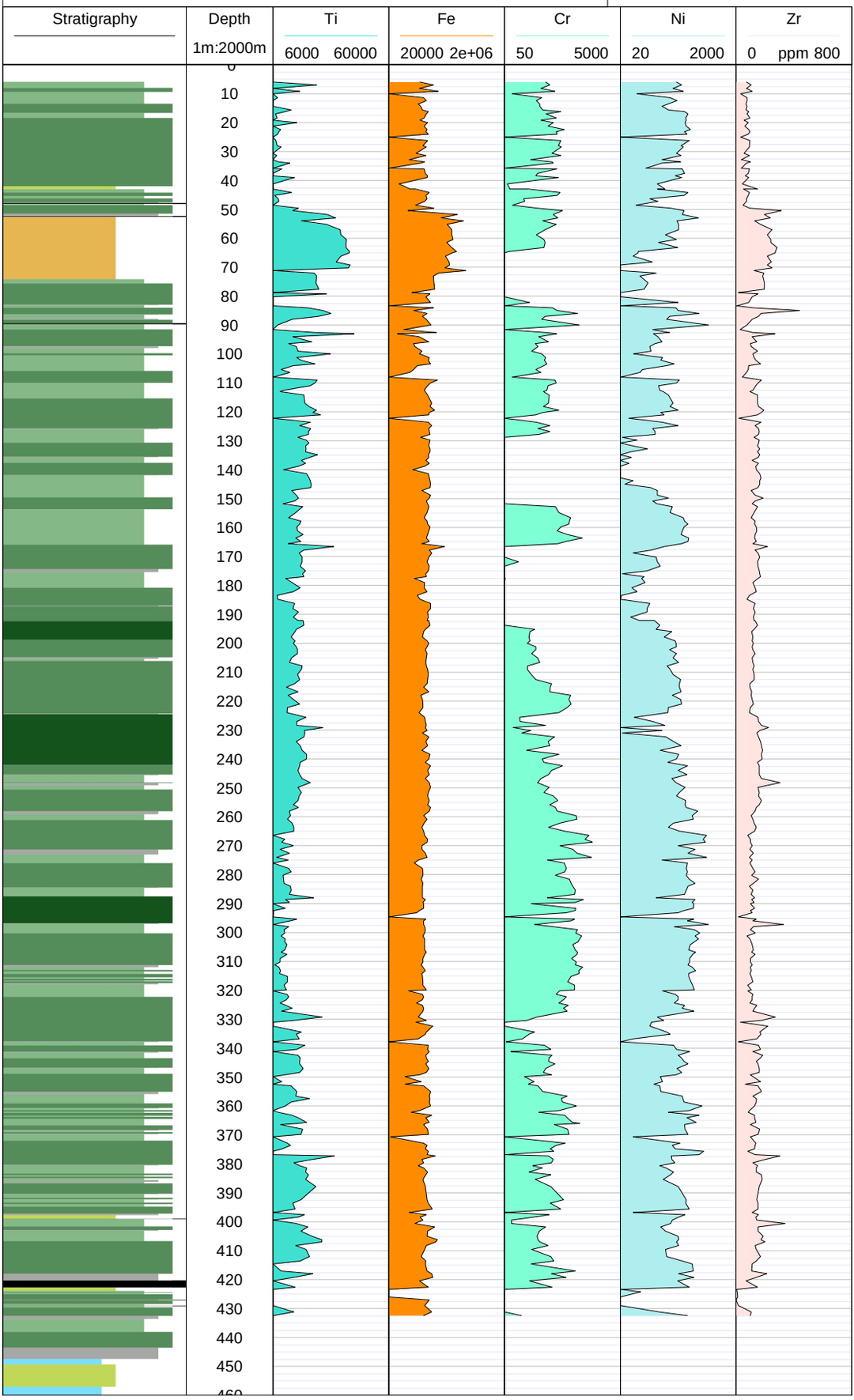

NIRE 03/08-0001

WellCAD
Advanced Logic Technology

Company: Lonmin PLC
Well Name: 03/08-0001
Field:
Country: Northern Ireland **State:** Antrim

Location
East / Long: 326391 **North / Lat:** 406143

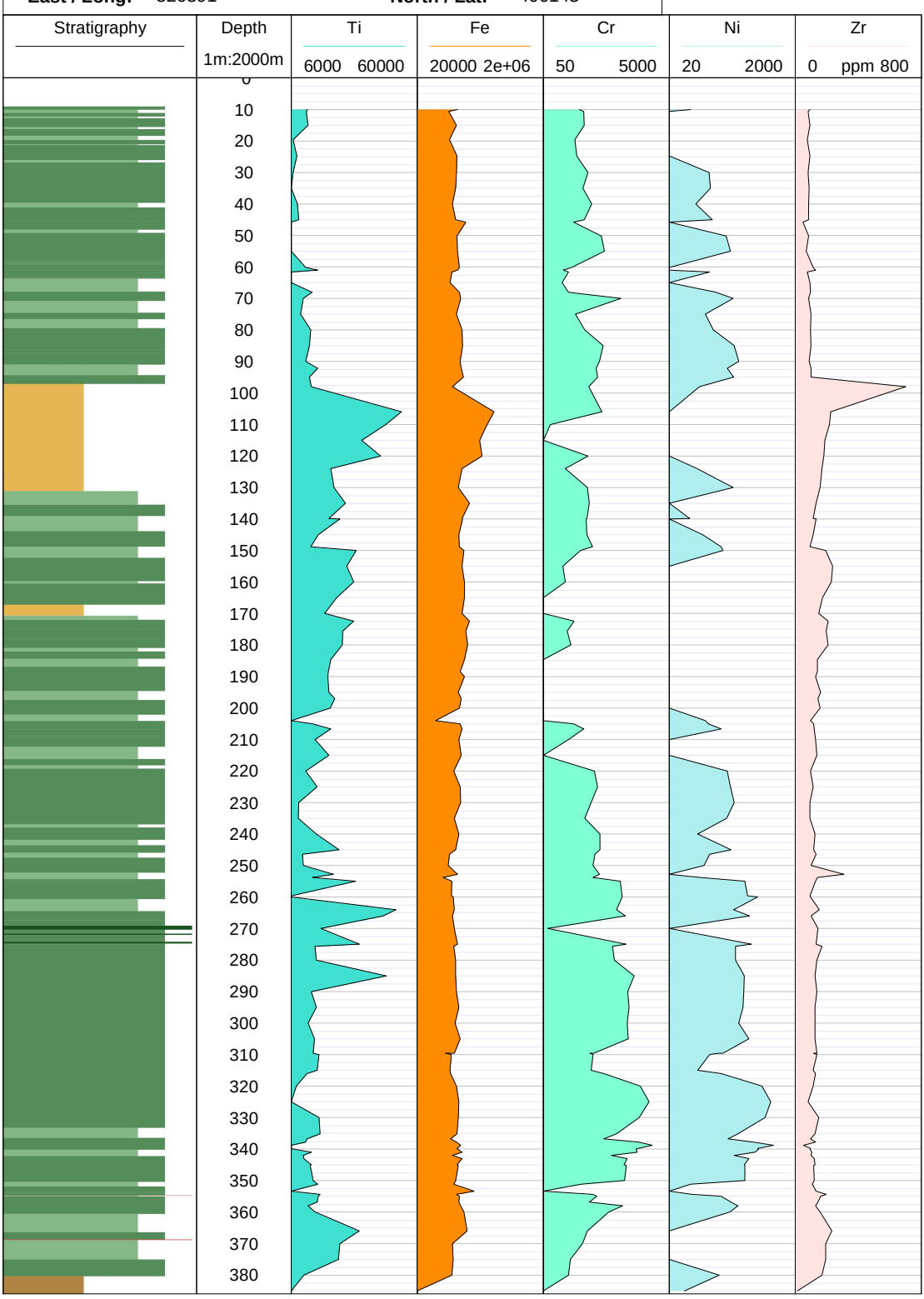

NIRE 04/08-0001

WellCAD

Advanced Logic Technology

Company: Lonmin PLC

Well Name: 04/08-0001

Field:

Country: Northern Ireland **State:** Antrim

Location

East / Long: 277233 **North / Lat:** 415430

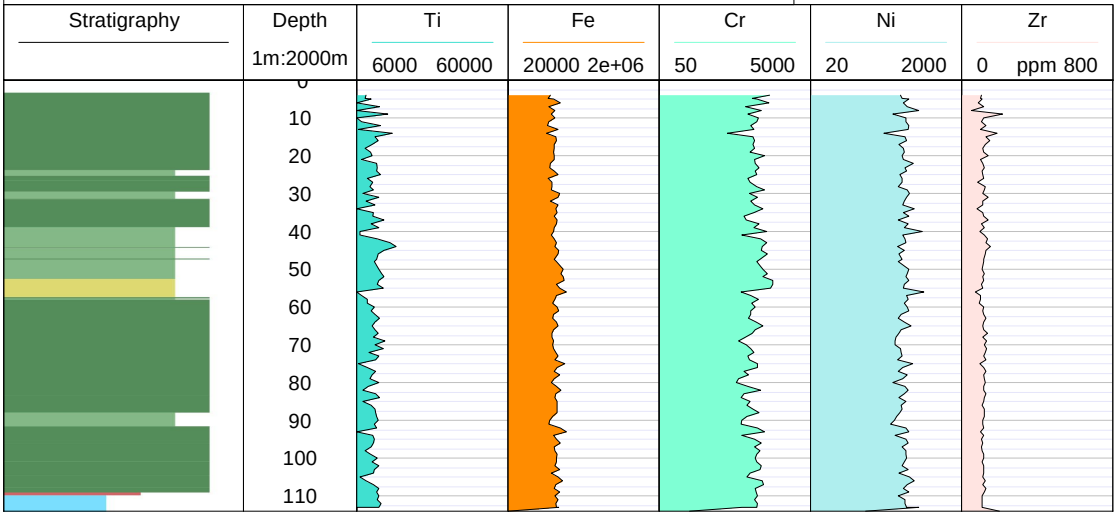

NIRE 09/08-0001

WellCAD
ALT Advanced Logic Technology

Company: Lonmin PLC
Well Name: 09/08-0001
Field:
Country: Northern Ireland **State:** Antrim

Location
East / Long: 294362 **North / Lat:** 434582

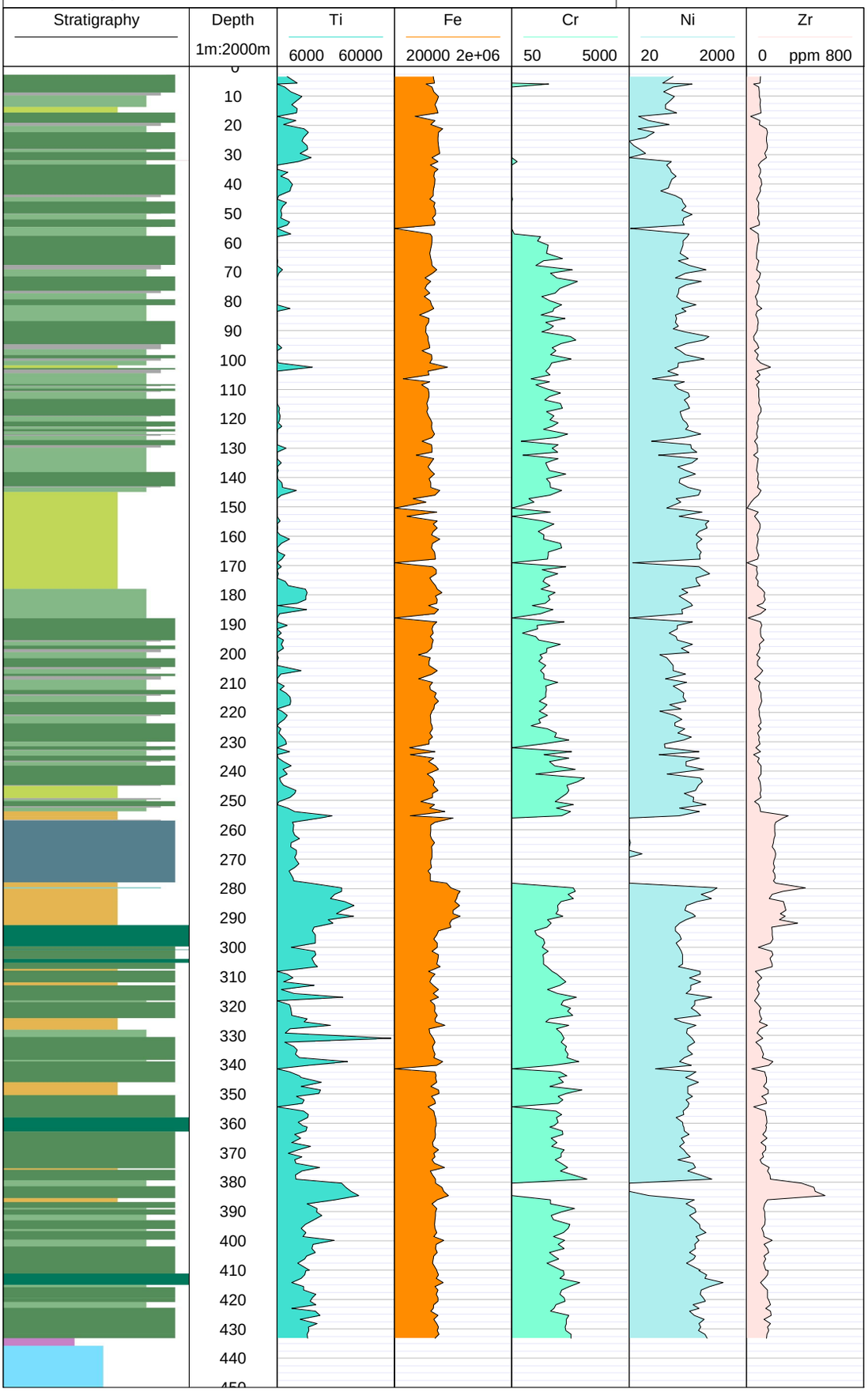

NIRE 09/08-0002

WellCAD
Advanced Logic Technology

Company: Lonmin PLC
Well Name: 09/08-0002
Field:
Country: Northern Ireland **State:** Antrim

Location
East / Long: 290853 **North / Lat:** 434532

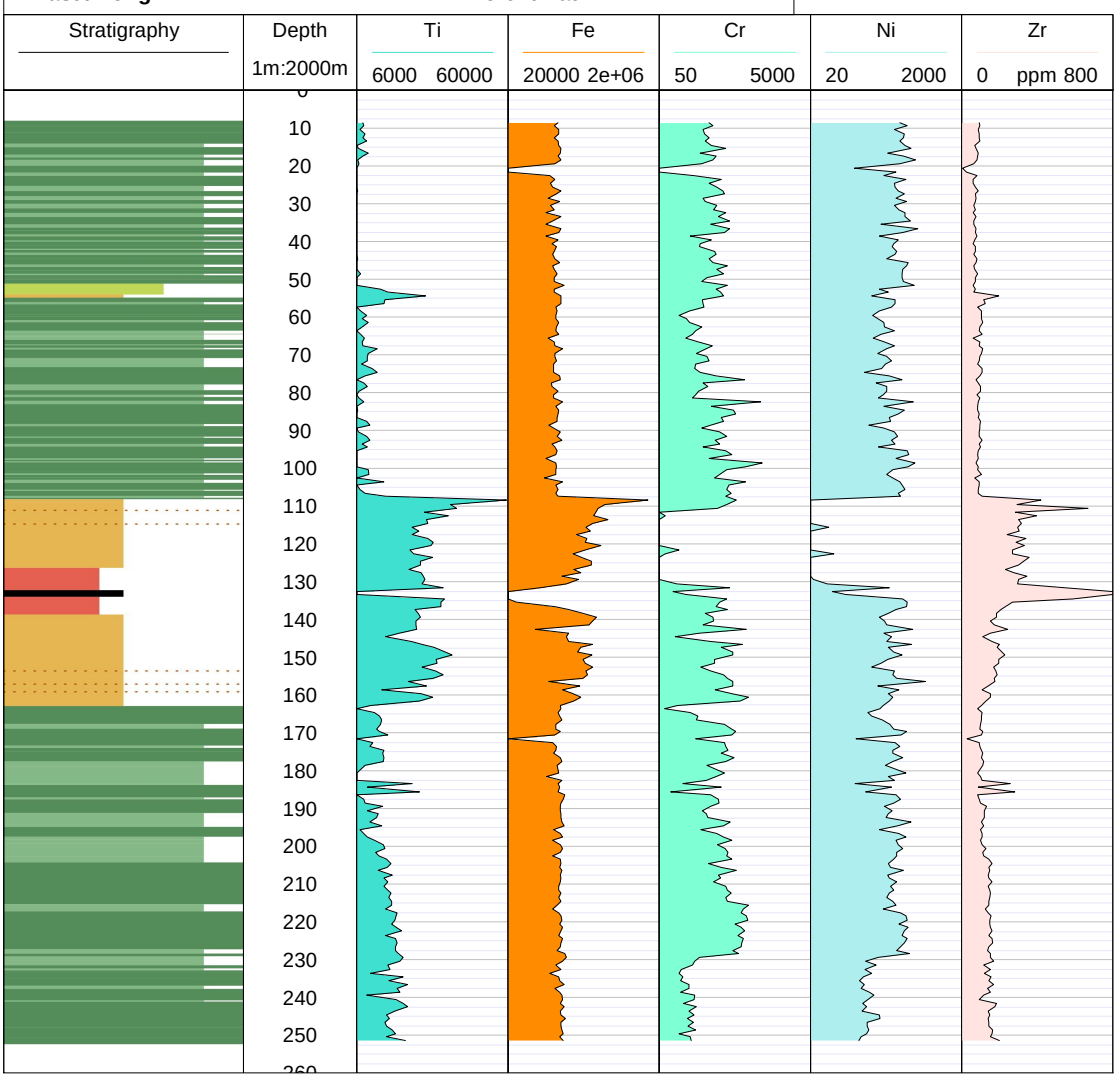

NIRE 11/08-0001

WellCAD
alt
Advanced Logic Technology

Company: Lonmin PLC
Well Name: 11/08-0001
Field:
Country: Northern Ireland **State:** Antrim

Location
East / Long: 287917 **North / Lat:** 413754

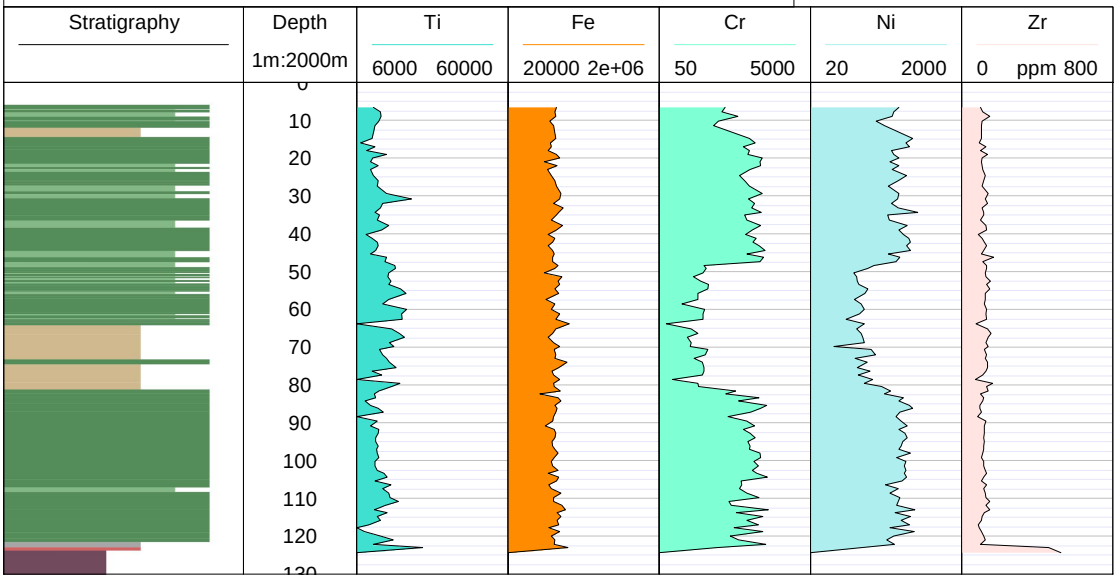

APPENDIX B

WD-XRF WellCAD plots

NIRE 02/08-0001

WellCAD
Advanced Logic Technology

Company: Lonmin PLC
Well Name: 02/08-0001
Field:
Country: Northern Ireland **State:** Antrim

Location
East / Long: 316129 **North / Lat:** 412540

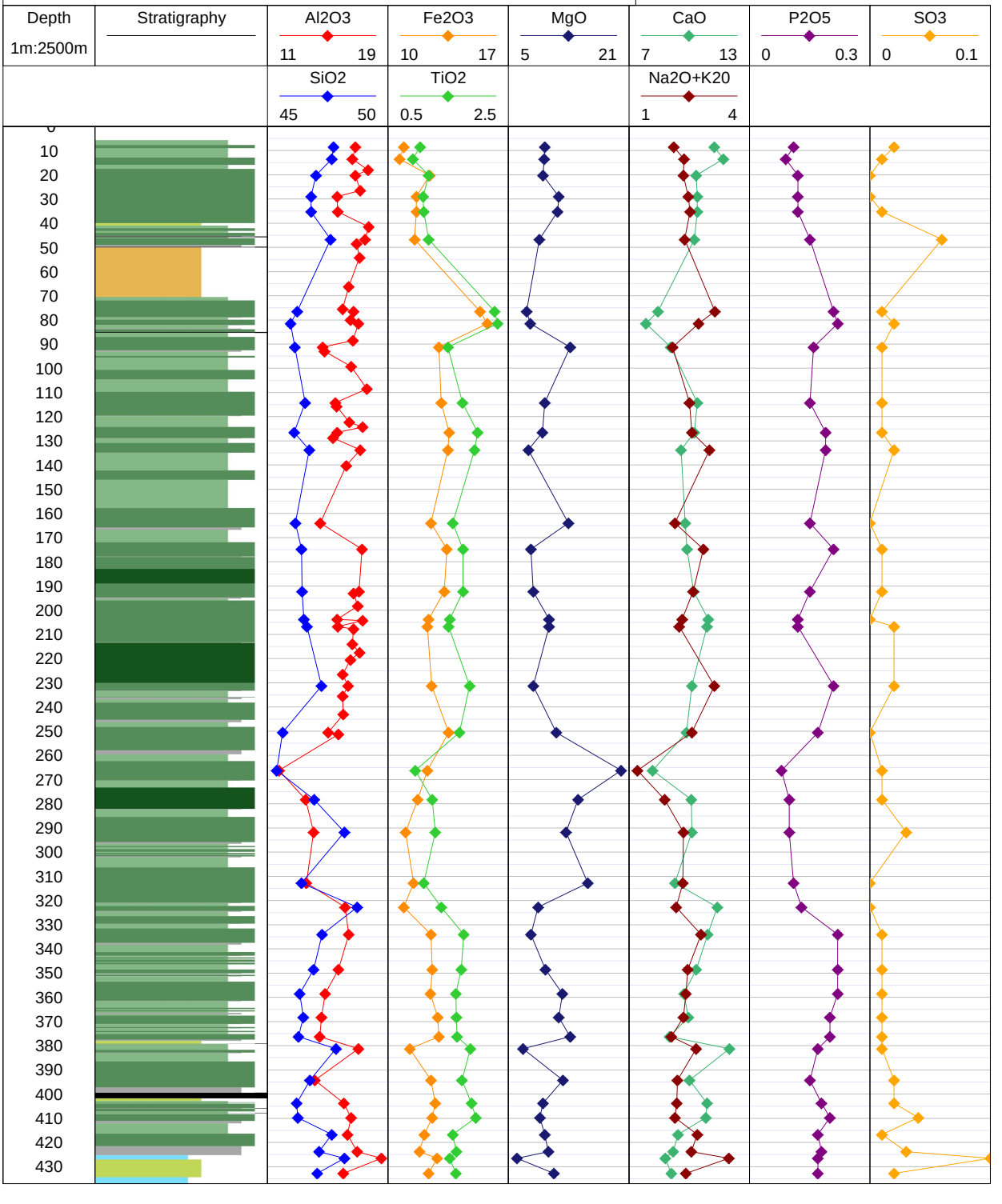

NIRE 09/08-0001

WellCAD
alt Advanced Logic Technology

Company: Lonmin PLC
Well Name: 09/08-0001
Field:
Country: Northern Ireland **State:** Antrim

Location
East / Long: 294362 **North / Lat:** 434582

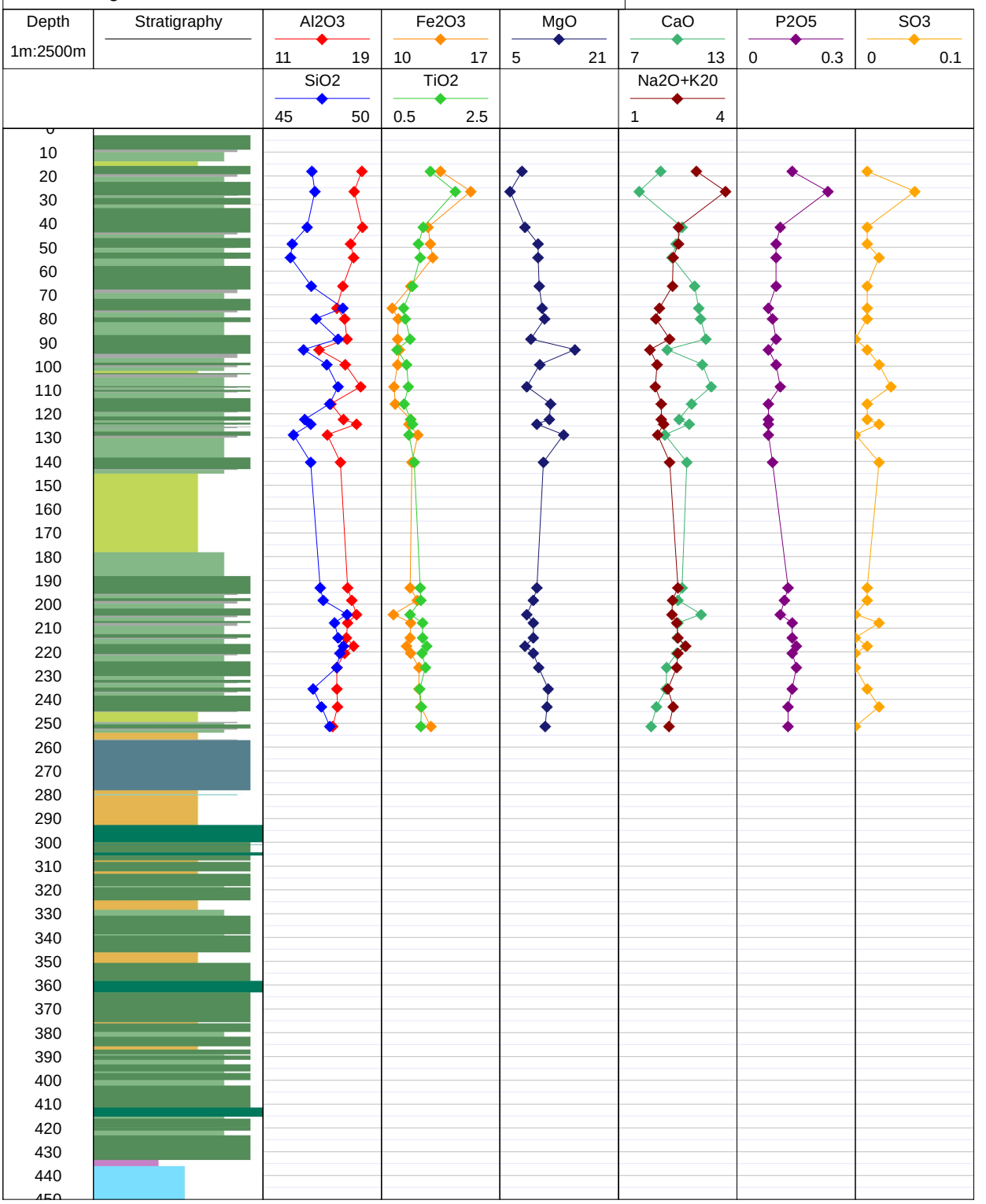

APPENDIX C

Quarry locations

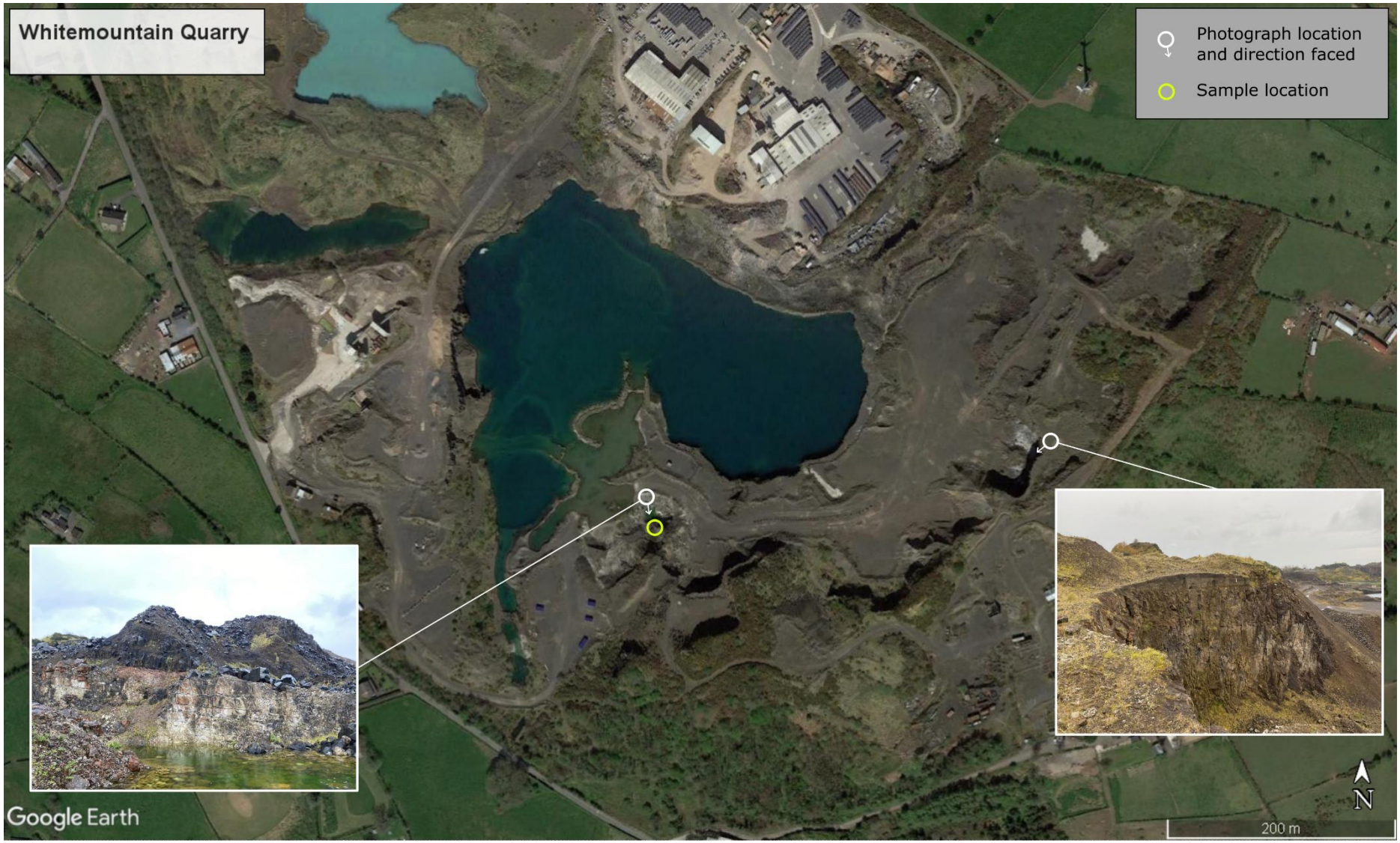

Whitemountain Quarry, 14 White Mountain Road, Lisburn, BT28 3QY.
Visited Monday 19th October, 2020

Blackmountain Quarry, Upper Springfield Road, Belfast, BT17 0LU.
Visited Monday 19th October, 2020

Craig's Quarry, 32 Glenhead Road, Ballymena, BT42 4RE.
Visited Tuesday 20th October, 2020

Clinty Quarry, 215 Doury Road, Ballymena, BT43 6SS.
Visited Wednesday 21st October, 2020

Corkey Quarry, 160 Corkey Road, Ballymena, BT44 9JQ.
Visited Thursday 22nd October, 2020

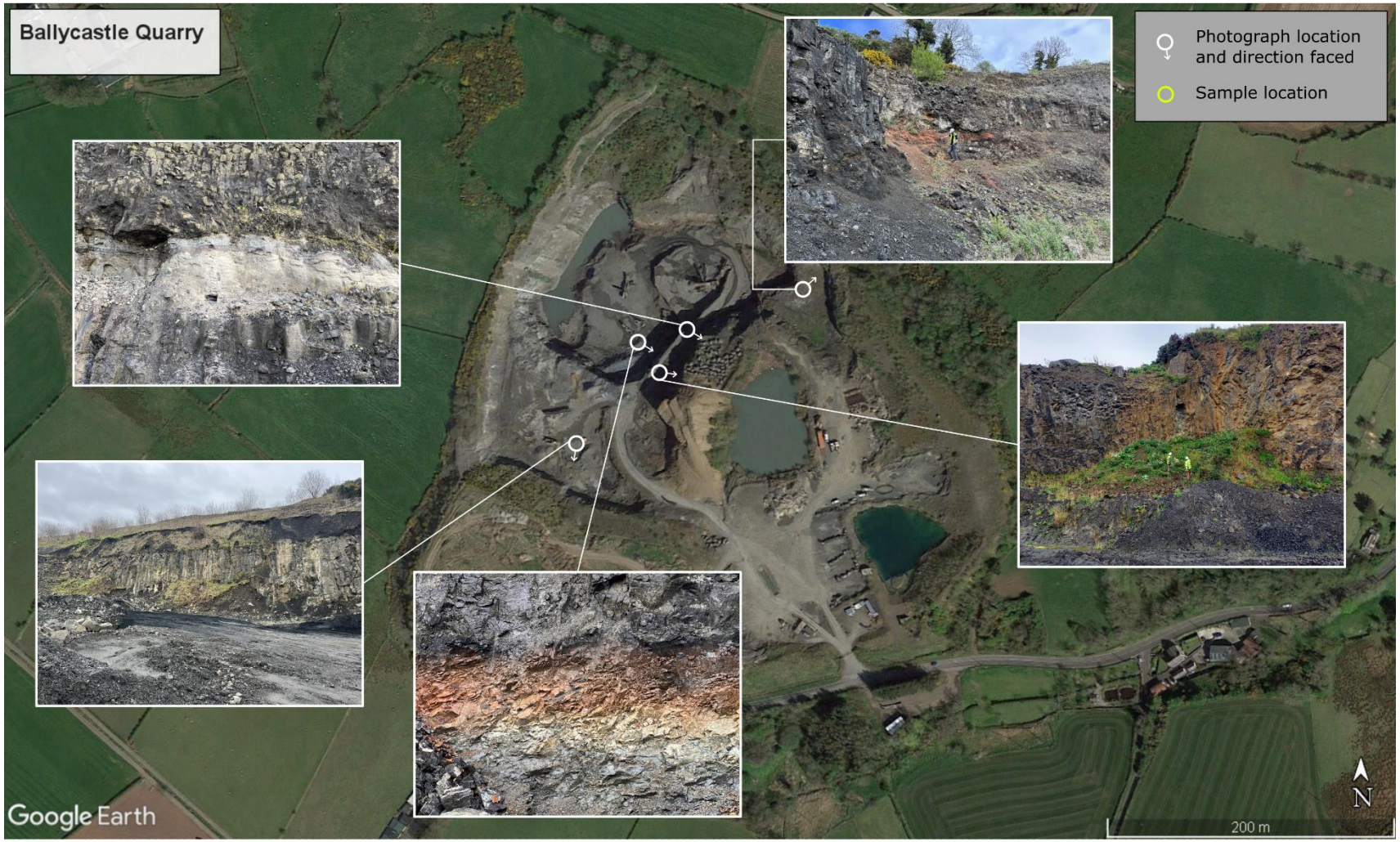

Ballycastle Quarry, 33 Magheramore Road, Ballycastle, BT54 6JE.
Visited Friday 23rd October, 2020


Giant's Causeway
Google Earth
Image © 2022 Maxar Technologies
500 m
N


Garron Point
Google Earth
500 m
N

Croaghan Quarry, Shinny Road, Coleraine, BT51 4PS.
Visited Monday 26th October, 2020


Binevenagh
Binevenagh
Google Earth
Image © 2022 Maxar Technologies
300 m
N

Cam Quarry, 39 Cam Road, Macosquin, Coleraine, BT51 4PX.
Visited Tuesday 27th October, 2020

Macosquin Quarry, 1 Letterloan Road, Macosquin, Coleraine, BT51 4PP.
Visited Tuesday 27th October, 2020

Craighall Quarry, 1 81 Drumsaragh Road, Kilrea, Coleraine, BT51 5XR.
Visited Wednesday 28th October, 2020

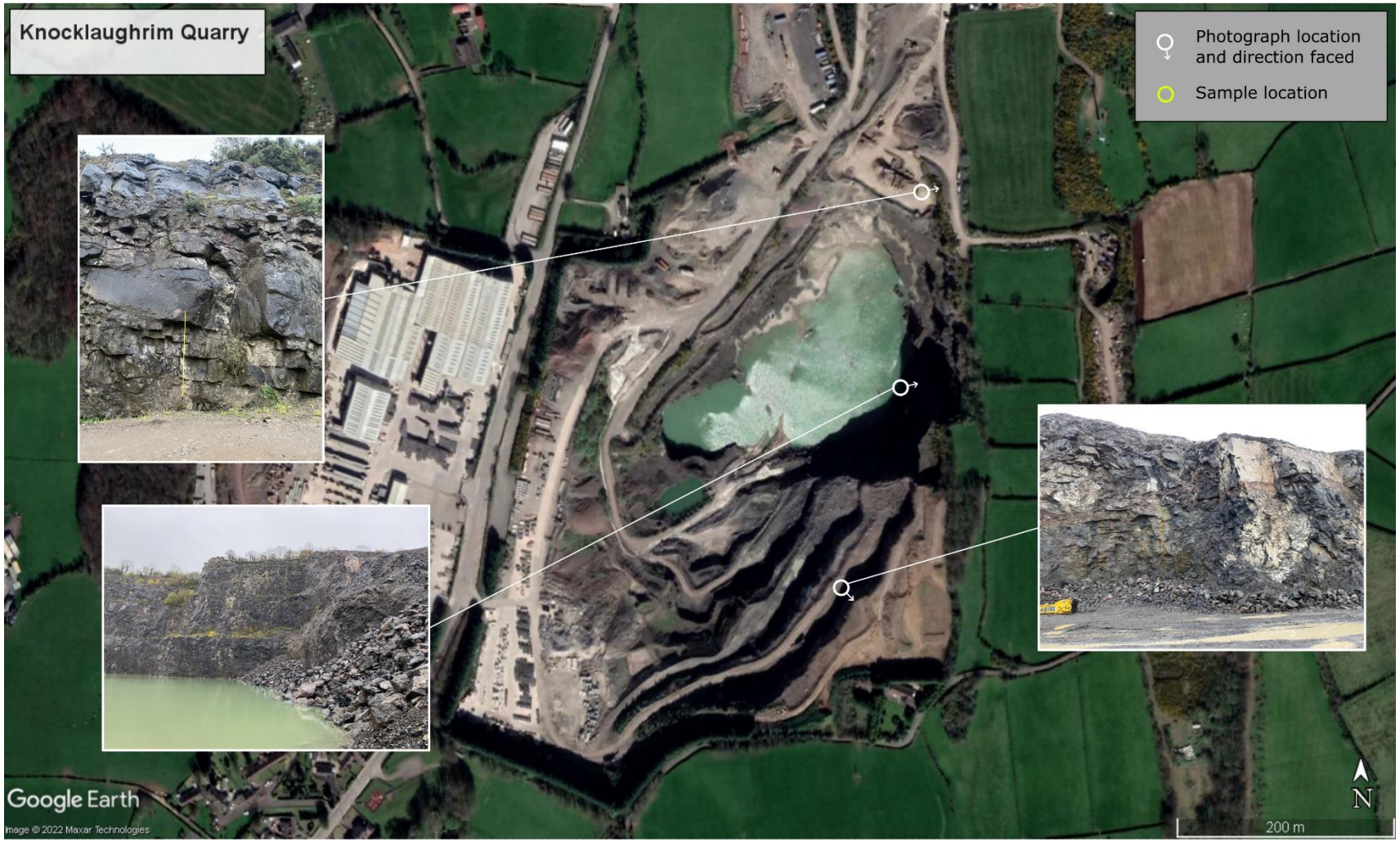

Knocklaughrim Quarry, 3 Drumard Road, Knocklaughrim, Magherafelt, BT45 8QA.
Visited Thursday 29th October, 2020

Ballymena Quarry, 54 Craigadoo Road, Moorfields, BT42 4RB.
Visited Friday 30th October, 2020

APPENDIX D

Field locations


Slemish
Slemish
Google Earth
Image © 2022 Maxar Technologies
N
300 m


Ballintoy Harbour
Ballintoy Point
Google Earth
200 m
N


Craigahulliar
Google Earth
Image © 2022 Maxar Technologies
100 m
N

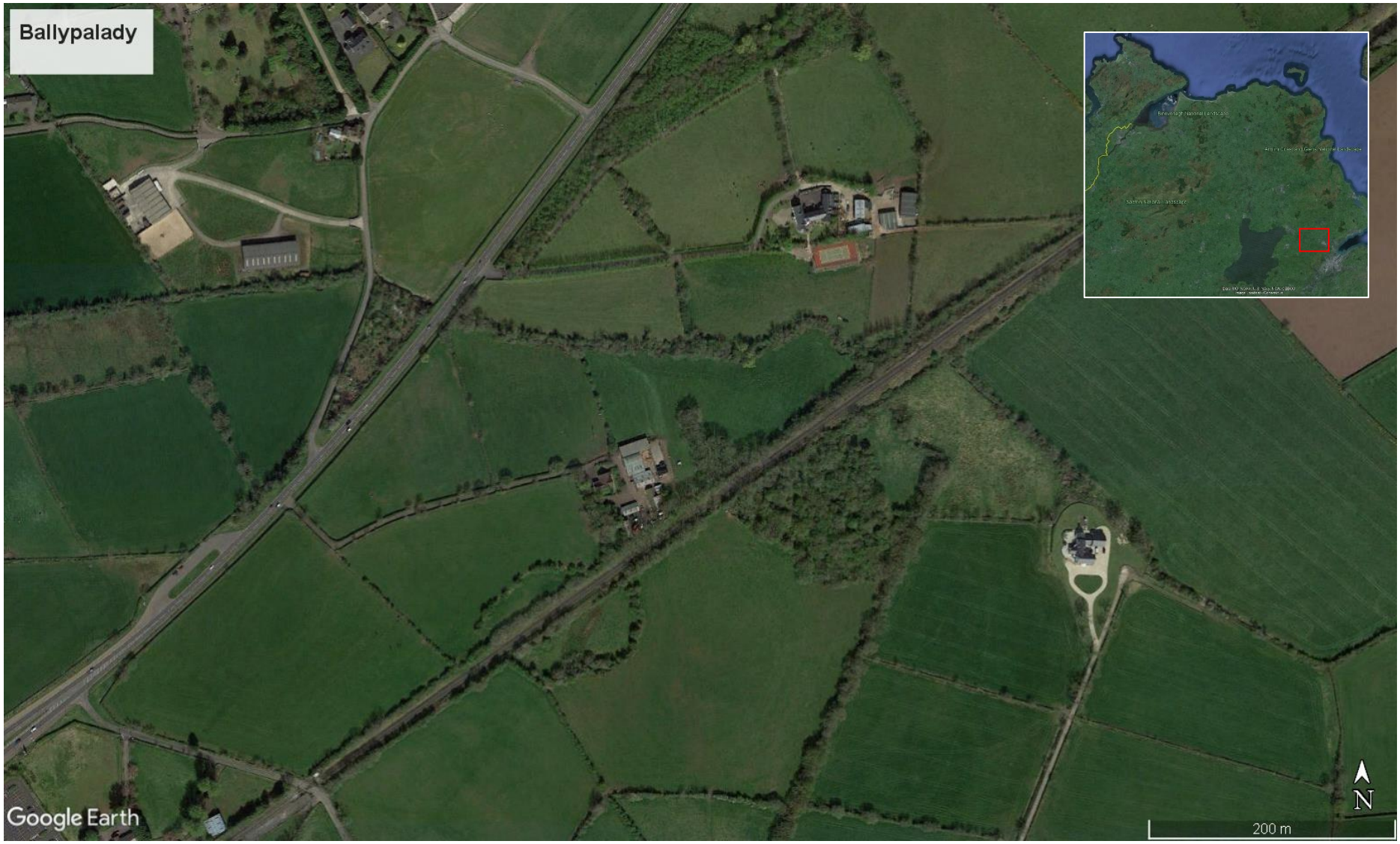
Ballypalady
Google Earth
N
200 m


Ballylagan
Google Earth
Image © 2022 Maxar Technologies
80 m
N

APPENDIX E

Quarry Field Slips

DRAWN WITH CARBONACEOUS CLASTS

ASH UNIT DETAIL

DATE	FRI/23/OCT	START DEPTH	+3	END DEPTH	0	BH ID	BALLYCASTLE

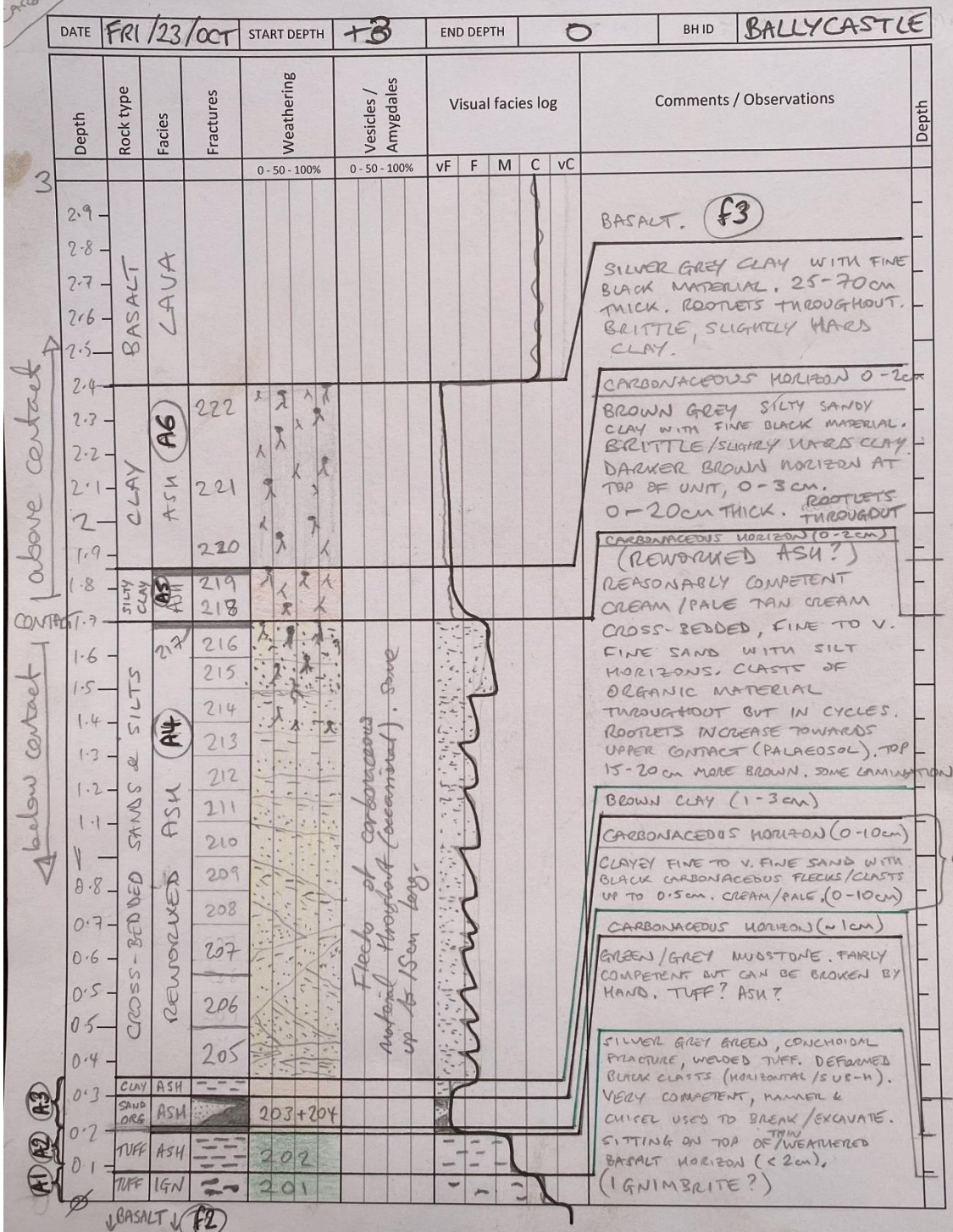

Adam Beresford-Browne 07979 962521 MAINS anb961@student.bham.ac.uk

SAMPLING TOOL WASHED BETWEEN SAMPLES USING TAP WATER FROM RESIDENCE AT BT57 8TL (east of Bushmills)

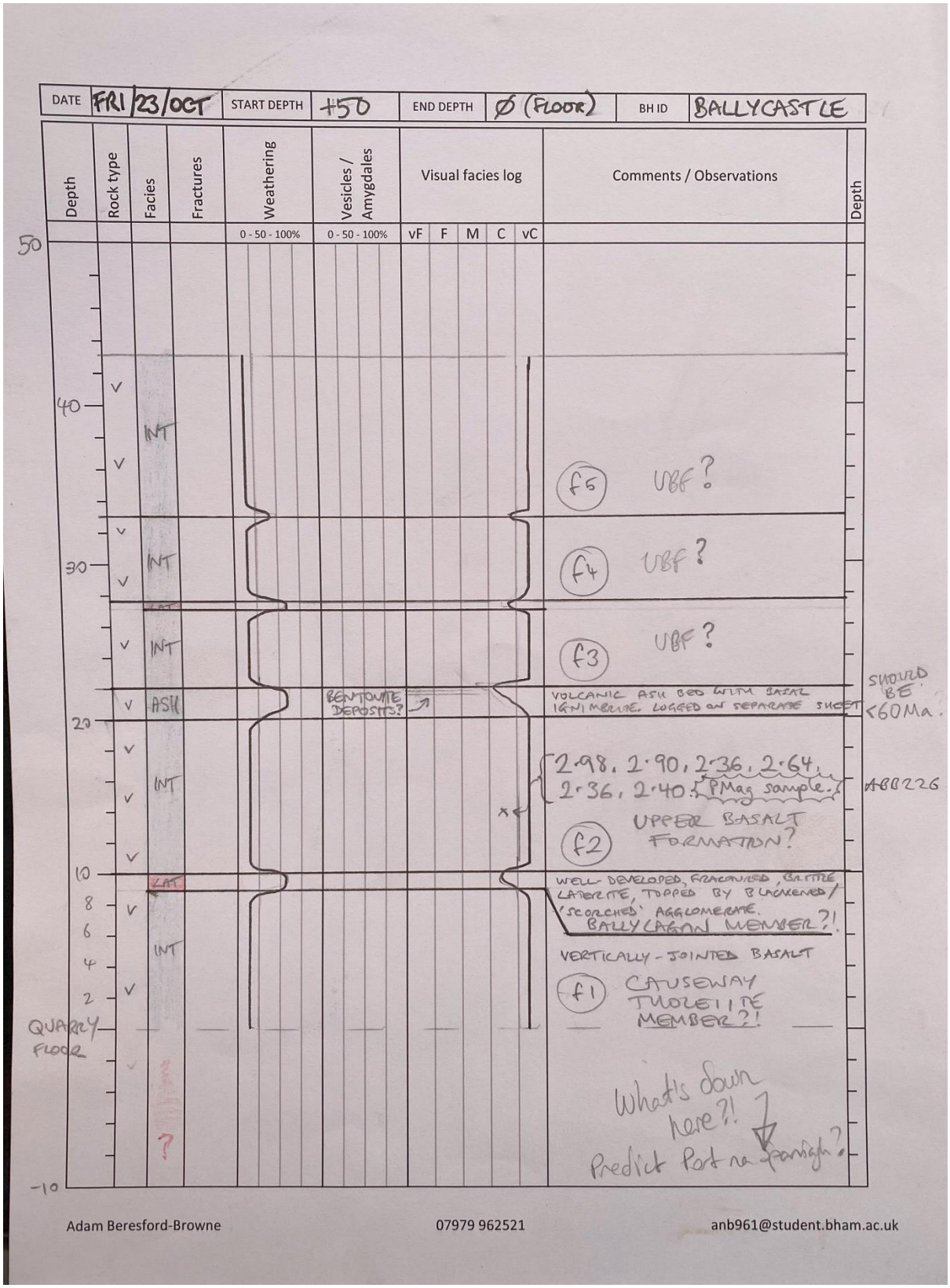

Adam Beresford-Browne 07979 962521 anb961@student.bham.ac.uk

DATE	TUE/27/OCT	START DEPTH		END DEPTH		BH ID	CAM QUARRY

Depth	Rock type	Facies	Fractures	Weathering (0 - 50 - 100%)	Vesicles / Amygdales (0 - 50 - 100%)	Visual facies log (vF F M C vC)	Comments / Observations	Depth
0	V V	INT					MASSIVE, BLOCKY / FRACTURED BASALT (f4)	
		LAT					BRIGHT RED/BROWN LATERITE.	
10		LAT/BAS					BROWN LATERITE / DEEPLY WEATHERED BASALT. VEINED.	
	V V	INTERIOR					pMag AB8303 (50/96°) HEAVILY FRACTURED ZONE. POSS. FLOW BOUNDARY BUT MORE LIKELY COMPOSITIONALLY DIFFERENT AS NOT TRACEABLE OVER DISTANCE.	
20	V						WHOLE UNIT GENERALLY MASSIVE & BLOCKY. (f2 actually part of f3) (f3)	
		LAT					LATERITE	
30							TOP OF FLOW SEEN BUT INACCESSIBLE. (f1) WEATHERED.	

Adam Beresford-Browne 07979 962521 anb961@student.bham.ac.uk

P1

DATE	WED/21/OCT	START DEPTH	0	END DEPTH	-30	BH ID	CLINTY QUARRY

Depth | Rock type | Facies | Fractures | Weathering (0 - 50 - 100%) | Vesicles / Amygdales (0 - 50 - 100%) | Visual facies log (vF F M C vC) | Comments / Observations | Depth

0 ct.

PMag sample (5196, 38.5°)
4.67, 4.35, 4.06,
4.27, 4.18, 4.79

{2.42, 2.41, 2.55,
2.40, 2.13, 2.36}

{8.95, 8.99, 8.92,
9.29, 9.50, 8.98}

(a) ? readings at bottom of sheet taken across flow (opposite side of hole)
1.64

{1.58, 1.78, 1.66,
1.64, 1.67, 1.71}

5
10
15
20
25
30

CR
INT
LI
INT
L2
L2

{2.53, 2.42, 2.43,
2.44, 2.59, 2.42}

Package 1

Laterite horizon (discontinuous) SAMPLED

PMag Sample (L1 3160.5, 71°)

{4.48, 3.77, 3.66,
4.89, 4.32, 4.44}

Discontinuous amygdale bands

{4.83, 5.04, 4.65
4.63, 4.56, 5.25}

(L2) Green clay developed on top of laterite, under basalt.

Adam Beresford-Browne 07979 962521 anb961@student.bham.ac.uk

(a) 25.9, 26.1, 25.5, 25.3, 24.1, 24.7

DATE	22/OCT/20	START DEPTH	-5	END DEPTH	25	BH ID	CORVEY QUARRY

Depth	Rock type	Facies	Fractures	Weathering (0 - 50 - 100%)	Vesicles / Amygdales (0 - 50 - 100%)	Visual facies log (vF F M C vC)	Comments / Observations	Depth
25								f9
	V							
	V							
	V							f8
	V							
20	V							
	V							f7
	V						3.78, 3.49, 3.47, 3.43, 4.07, 3.91. And pmag sample AB8105.	
15	V							
	V							f6
	V							
10	V							f5
	V							f4
	V							f3
	V							f2
	V							
5	V							f1
	V							
	CWF	BASALT DYKES Ba					Zoned cherty nodules of varying colour in a grey/white/pink/brown mudstone/claystone matrix. Rare basalt blocks/clasts.	
0	DAL						Dalradian metasediments. Schistose, dipping/deformed, with developed fractures. (Magsus ~4)	
-5								

Adam Beresford-Browne 07979 962521 anb961@student.bham.ac.uk

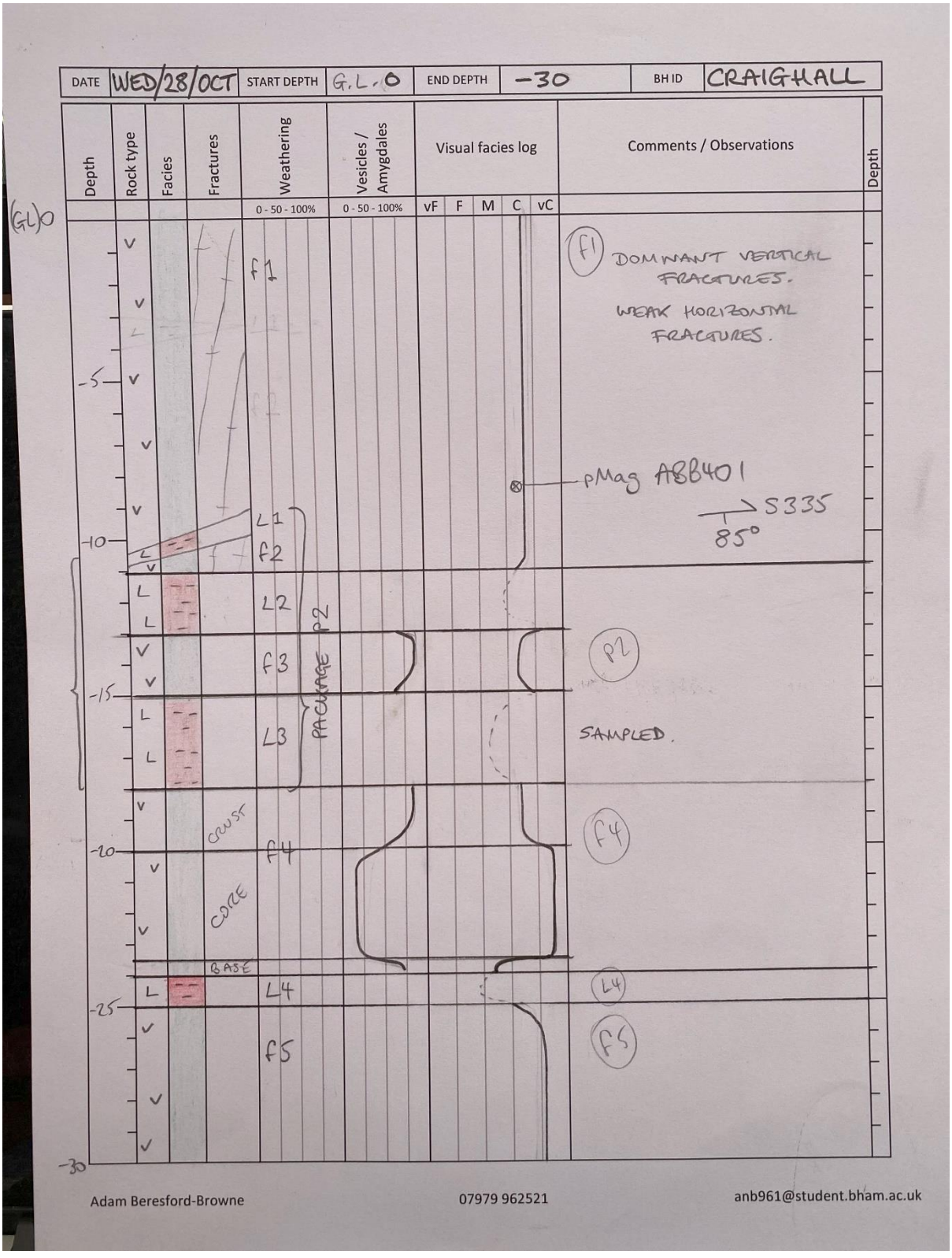

Adam Beresford-Browne 07979 962521 anb961@student.bham.ac.uk

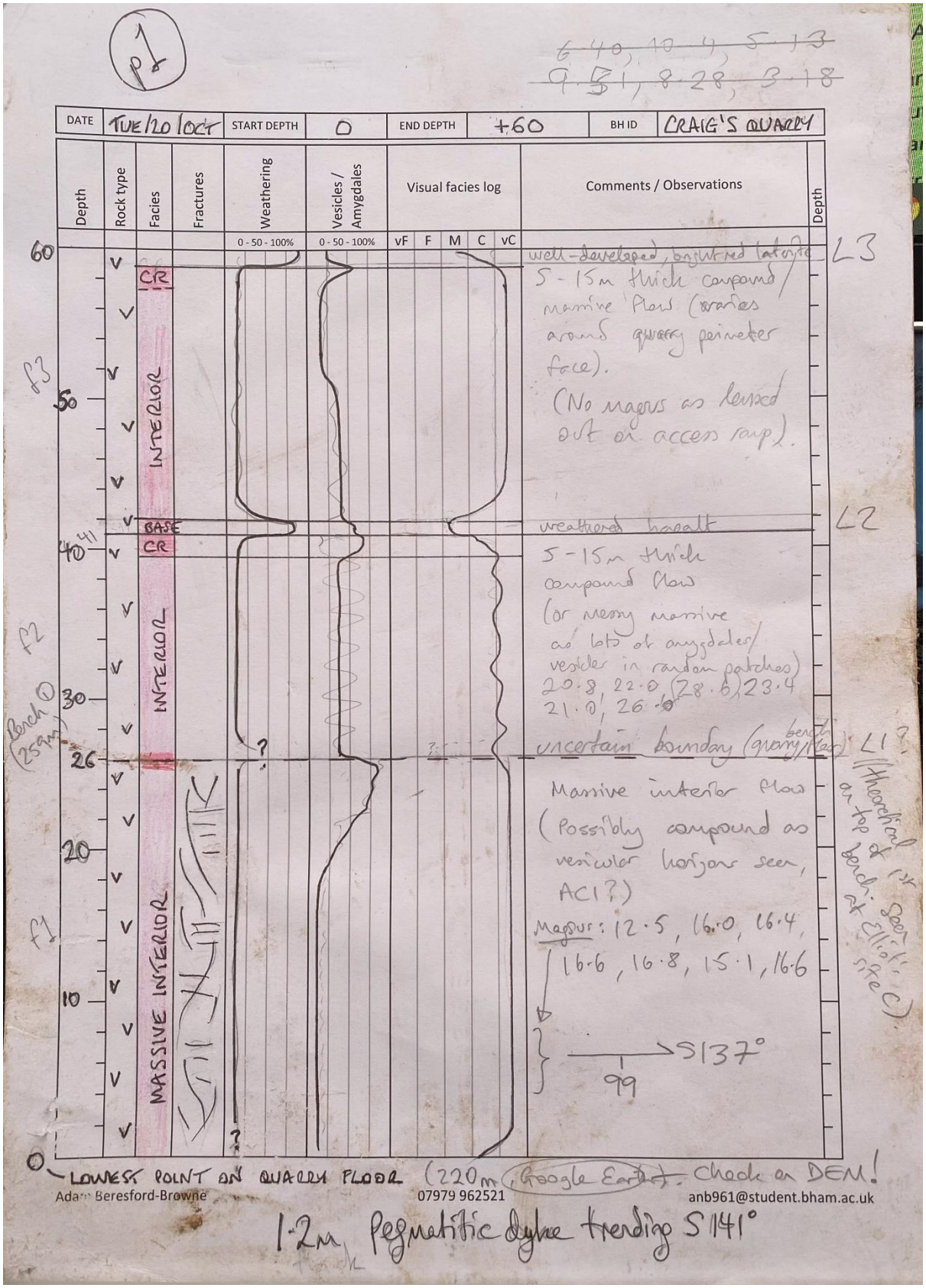
DATE
TUE 20 OCT
START DEPTH
0
END DEPTH
+60
BH ID
CRAIG'S QUARRY
Depth
Rock type
Facies
Fractures
Weathering
Vesicles / Amygdales
Visual facies log
Comments / Observations
0 - 50 - 100%
0 - 50 - 100%
vF F M C vC
CR
INTERIOR
BASE
CR
INTERIOR
MASSIVE INTERIOR
well-developed, brecciated lateritic
5-15m thick compound/massive flows (varies around quarry perimeter face).
(No magnetics as levelled out on access ramp).
weathered basalt
5-15m thick compound flow (or messy massive as lots of amygdales/vesicles in random patches)
20.8, 22.0, (28.6), 23.4, 21.0, 26.6
uncertain boundary (grassy bench)
Massive interior flow (Possibly compound as vesicular horizons seen, AC1?)
Magnetics: 12.5, 16.0, 16.4, 16.6, 16.8, 15.1, 16.6
S137°
99
LOWEST POINT ON QUARRY FLOOR (220m Google Earth) Check on DEM!
Adam Beresford-Browne
07979 962521
anb961@student.bham.ac.uk
1.2m Pegmatitic dyke trending S141°

P2

DATE	TUE/25/OCT	START DEPTH	+60	END DEPTH	+120	BH ID	CRAIG'S QUARRY

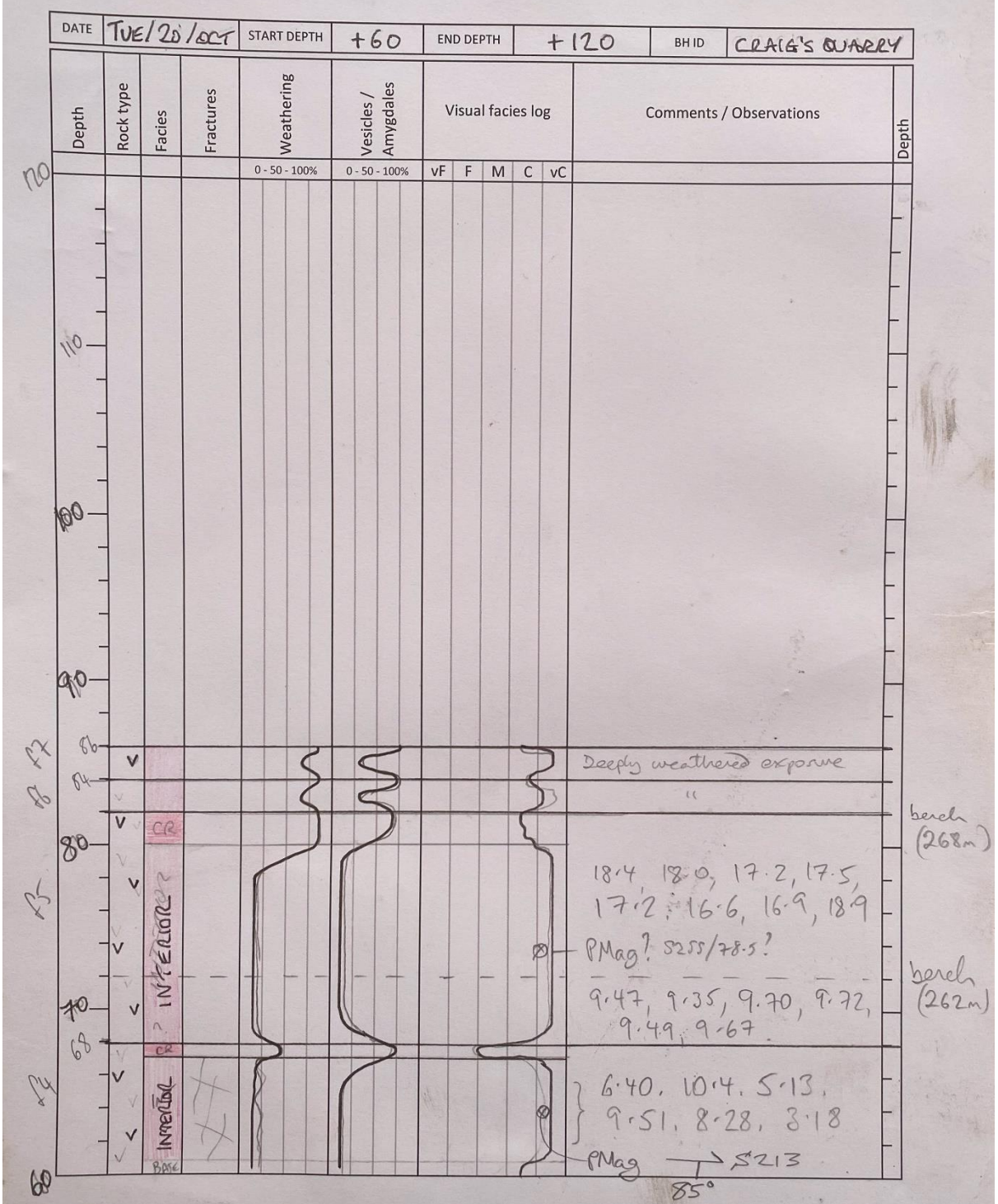

Adam Beresford-Browne 07979 962521 anb961@student.bham.ac.uk

DATE	MON/26/OCT	START DEPTH	0	END DEPTH	-6	BH ID	CROAGHAN QUARRY

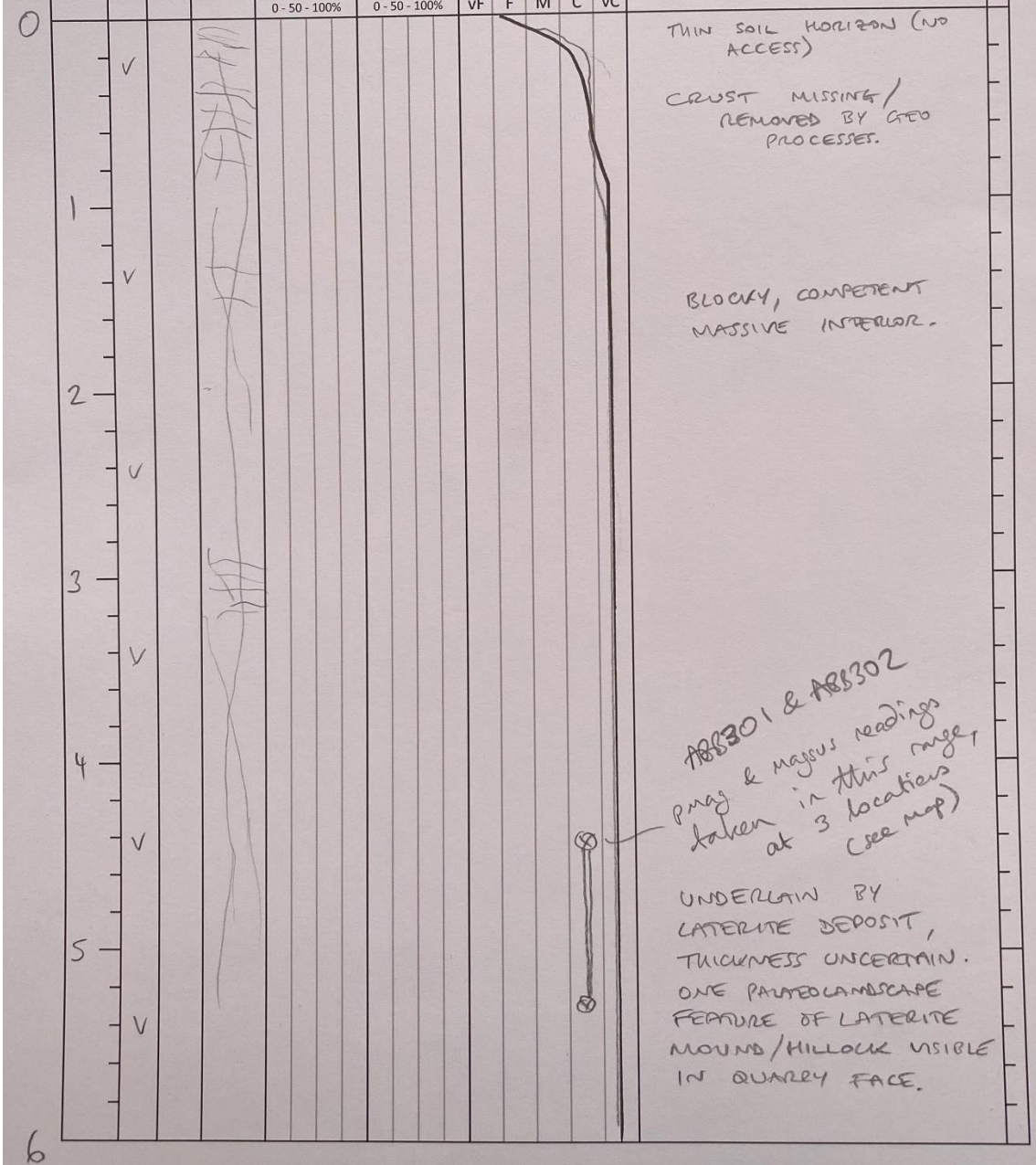

Adam Beresford-Browne 07979 962521 anb961@student.bham.ac.uk

DATE	TUE/27/OCT	START DEPTH		END DEPTH		BH ID	MACOSQUIN

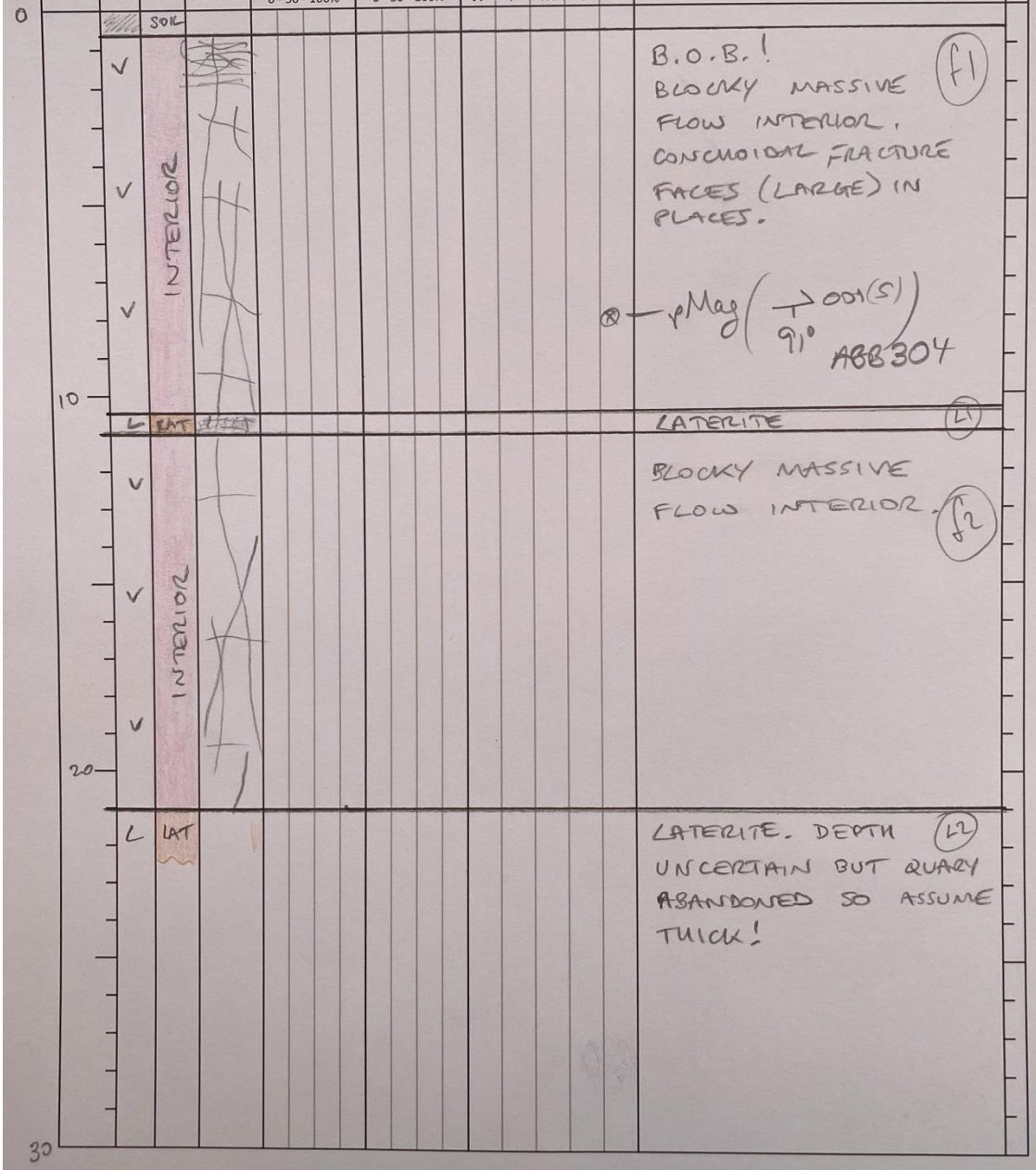

Adam Beresford-Browne 07979 962521 anb961@student.bham.ac.uk

APPENDIX F

Field Location Field Slips

DATE	MON/26/OCT	START DEPTH	0	END DEPTH	-42	BH ID	BINEVENAGH

Depth	Rock type	Facies	Fractures	Weathering (0 - 50 - 100%)	Vesicles / Amygdales (0 - 50 - 100%)	Visual facies log (vF F M C vC)	Comments / Observations	Depth	E-CODE
0									
							FLOW-BANDED, WEATHERED BASALT (CAR PARK).		A1
							FRACTURED, MASSIVE FLOW.		B0
							0.5m LATERITE TOP BLOCKY MASSIVE FLOW		B1
							BLOCKY MASSIVE FLOW		B2
10							LATERITIC TOP COMPOUND FLOWS, HEAVILY WEATHERED. 20-30cm FLOWS W/ LATERITISED/WEATHERED TOPS		B3
							MULTIPLE/COMPOUND FLOWS WITH 0.5m MASSIVE FLOW AT TOP.		B4
20							MASSIVE COMPETENT FLOW		B5
							MULTIPLE FLOWS (6?) WITH LATERITISED TOPS (SIMILAR TO B3)		B6
							MASSIVE FLOW		B7
							COMPOUND/MULTIPLE FLOWS WITH ORANGE/WEATHERED CORE.		B8
30							VERY VESICULAR MASSIVE FLOW.		B9
							FLOW BANDED, VESICULAR FLOW WITH FELSIC (?) BANDS		B10
40							VERY VESICULAR/AMYGDALOIDAL MASSIVE FLOW.		B11
							- NO EXPOSURE - (CLIFF BASE, COVERED BY SOIL)		
50									
60									

Adam Beresford-Browne 07979 962521 anb961@student.bham.ac.uk

APPENDIX G

pXRF and WD-XRF WellCAD plots

NIRE 02/08-0001

WellCAD

ALT Advanced Logic Technology

Company: Lonmin PLC
Well Name: 02/08-0001
Field:
Country: Northern Ireland **State:** Antrim

Location
East / Long: 316129 **North / Lat:** 412540

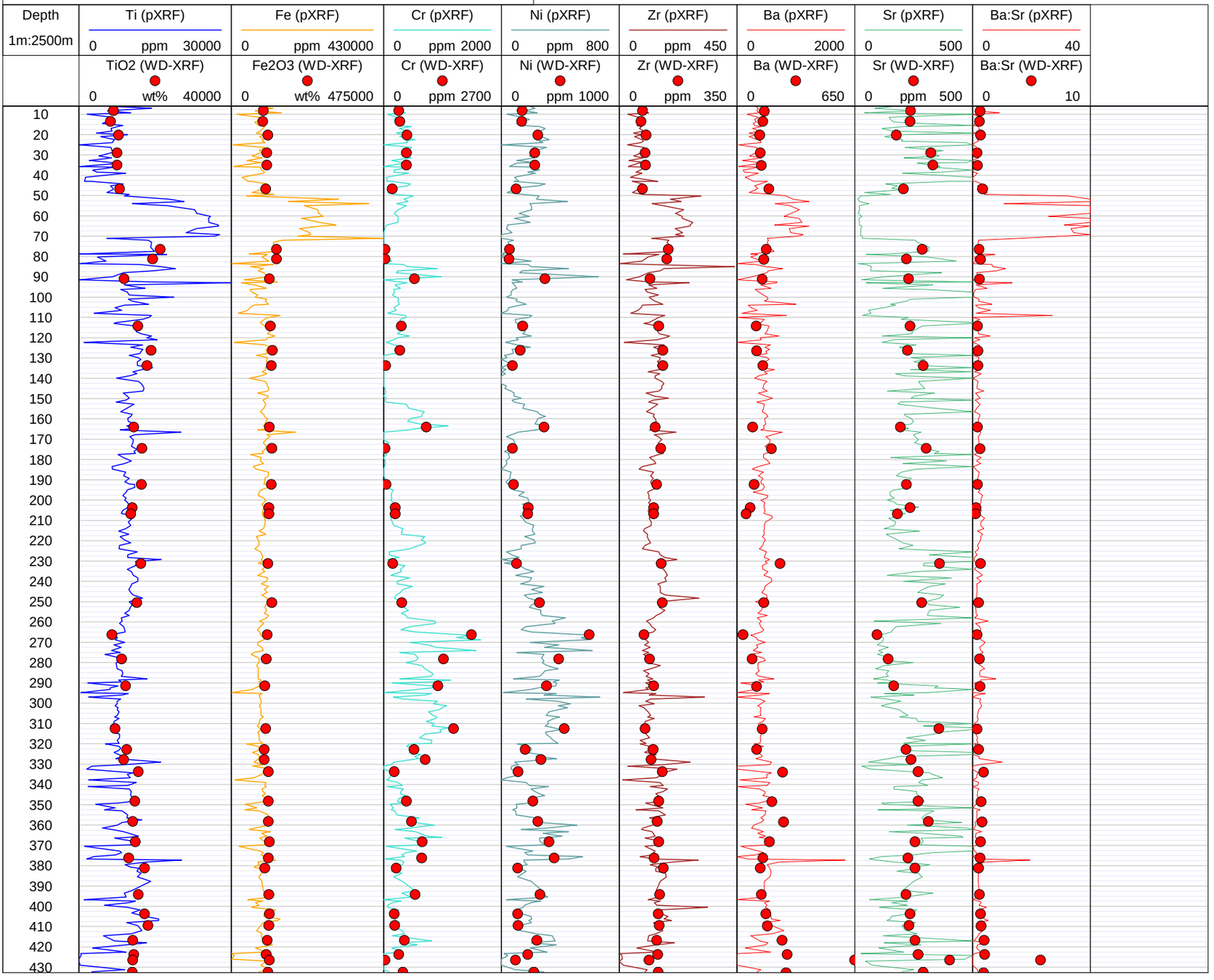

NIRE 09/08-0001

WellCAD

Advanced Logic Technology

Company: Lonmin PLC
Well Name: 09/08-0001
Field:
Country: Northern Ireland **State:** Antrim

Location
East / Long: 294362 **North / Lat:** 434582

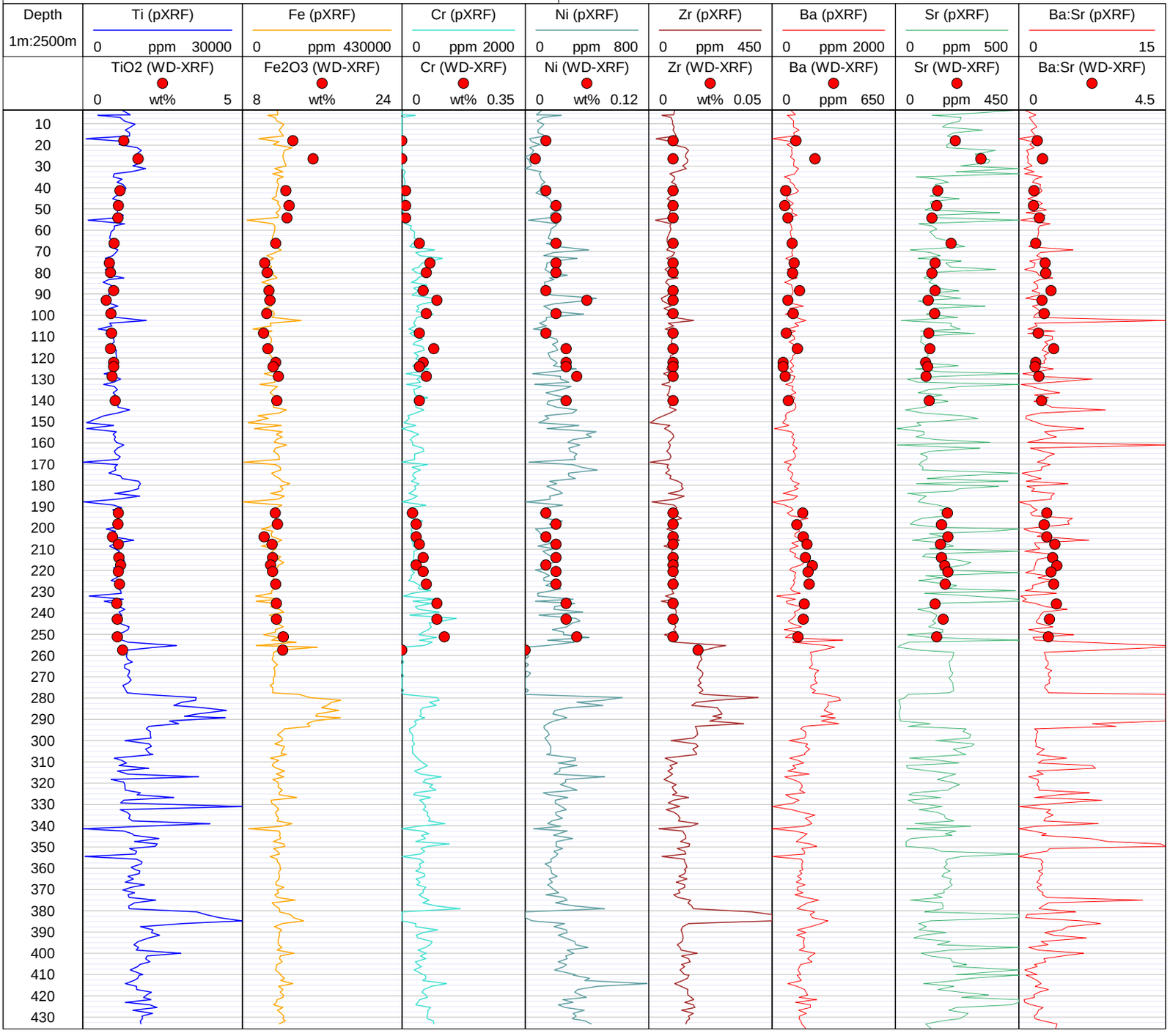

APPENDIX H

Sample list

List of all samples and analysis undertaken

Location	Depth	ID	Lithology	pXRF	WD-XRF	Palynology
01/08-0001	149.35	149.35	Rhyolitic tuff	Yes		
01/08-0001	149.40	149.4	Rhyolitic tuff	Yes		
01/08-0001	149.45	149.45	Rhyolitic tuff	Yes		
01/08-0003	44.30	44.3	Basalt (1st flow)	Yes		
01/08-0003	45.65	45.65	CWF	Yes		Yes
01/08-0005	211.33	211.33	Basalt (1st flow)	Yes		
01/08-0005	212.70	212.7	CWF	Yes		Yes
01/08-0005	213.75	213.75	CWF	Yes		Yes
01/08-0006	237.10	237.1	Basalt (1st flow)	Yes		
01/08-0006	237.75	237.75	CWF	Yes		Yes
01/08-0006	238.40	238.4	CWF	Yes		Yes
02/08-0001	50.37	50.37	Interbed	Yes		Yes
02/08-0001	52.92	52.92	Interbed	Yes		Yes
02/08-0001	64.60	64.6	Interbed	Yes		Yes
02/08-0001	67.52	67.52	Interbed	Yes		Yes
02/08-0001	69.67	69.67	Interbed	Yes		Yes

02/08-0001	79.13	79.13	Interbed	Yes		Yes
03/08-0001	97.48	97.48	Interbed	Yes		Yes
03/08-0001	99.83	99.83	Interbed	Yes		Yes
03/08-0001	100.00	100	Interbed	Yes		Yes
03/08-0001	100.30	100.3	Interbed	Yes		Yes
03/08-0001	100.94	100.94	Interbed	Yes		Yes
03/08-0001	105.91	105.91	Interbed	Yes		Yes
03/08-0001	106.66	106.66	Interbed	Yes		Yes
03/08-0001	109.48	109.48	Interbed	Yes		Yes
03/08-0001	110.47	110.47	Interbed	Yes		Yes
03/08-0001	115.67	115.67	Interbed	Yes		Yes
03/08-0001	127.63	127.63	Interbed	Yes		Yes
03/08-0001	129.80	129.8	Interbed	Yes		Yes
03/08-0001	377.40	377.4	Basalt (1st flow)	Yes		
03/08-0003	102.04	102.04	Basalt (1st flow)	Yes		
03/08-0003	103.65	103.65	CWF	Yes		Yes
03/08-0004	111.20	111.2	Basalt (1st flow)	Yes		
03/08-0004	113.60	113.6	CWF	Yes		Yes

03/08-0004	114.00	114	CWF	Yes		Yes
03/08-0004	114.25	114.25	CWF	Yes		Yes
03/08-0005	381.95	381.95	CWF	Yes		Yes
03/08-0005	385.65	385.65	CWF	Yes		Yes
03/08-0005	385.90	385.9	CWF	Yes		Yes
03/08-0005	386.65	386.65	CWF	Yes		Yes
04/08-0001	113.05	113.05	Basalt (1st flow)	Yes		
04/08-0001	114.35	114.35	CWF	Yes		Yes
04/08-0002	107.05	107.05	Basalt (1st flow)	Yes		
04/08-0002	109.10	109.1	CWF	Yes		Yes
05/08-0002	101.95	101.95	Basalt (1st flow)	Yes		
05/08-0002	102.40	102.4	CWF	Yes		Yes
05/08-0002	102.70	102.7	CWF	Yes		Yes
08/08-0001	155.95	155.95	Basalt (1st flow)	Yes		
08/08-0001	157.30	157.3	CWF	Yes		Yes
08/08-0001	157.40	157.4	CWF	Yes		Yes
08/08-0001	157.60	157.6	CWF	Yes		Yes
08/08-0002	82.10	82.1	Basalt (1st flow)	Yes		

08/08-0002	83.30	83.3	CWF	Yes		Yes
08/08-0002	83.50	83.5	CWF	Yes		Yes
09/08-0001	431.20	431.2	Basalt (1st flow)	Yes		
09/08-0001	433.45	433.45	CWF	Yes		Yes
09/08-0002	108.40	108.4	Interbed	Yes		Yes
09/08-0002	109.00	109	Interbed	Yes		Yes
09/08-0002	110.00	110	Interbed	Yes		Yes
09/08-0002	111.00	111	Interbed	Yes		Yes
09/08-0002	112.00	112	Interbed	Yes		Yes
09/08-0002	113.00	113	Interbed	Yes		Yes
09/08-0002	114.00	114	Interbed	Yes		Yes
09/08-0002	115.00	115	Interbed	Yes		Yes
09/08-0002	116.00	116	Interbed	Yes		Yes
09/08-0002	117.00	117	Interbed	Yes		Yes
09/08-0002	118.00	118	Interbed	Yes		Yes
09/08-0002	119.00	119	Interbed	Yes		Yes
09/08-0002	120.00	120	Interbed	Yes		Yes
09/08-0002	121.00	121	Interbed	Yes		Yes

09/08-0002	122.00	122	Interbed	Yes		Yes
09/08-0002	123.00	123	Interbed	Yes		Yes
09/08-0002	124.00	124	Interbed	Yes		Yes
09/08-0002	125.00	125	Interbed	Yes		Yes
09/08-0002	126.00	126	Interbed	Yes		Yes
09/08-0002	127.00	127	Interbed	Yes		Yes
09/08-0002	128.00	128	Interbed	Yes		Yes
09/08-0002	129.00	129	Interbed	Yes		Yes
09/08-0002	130.00	130	Interbed	Yes		Yes
09/08-0002	131.00	131	Interbed	Yes		Yes
09/08-0002	132.00	132	Interbed	Yes		Yes
09/08-0002	133.00	133	Interbed	Yes		Yes
09/08-0002	134.00	134	Interbed	Yes		Yes
09/08-0002	134.25	134.25	Ash/tuff	Yes		
09/08-0002	134.40	134.4	Ash/tuff	Yes		
09/08-0002	134.75	134.75	Ash/tuff	Yes		
09/08-0002	135.00	135	Interbed	Yes		Yes
09/08-0002	136.00	136	Interbed	Yes		Yes

09/08-0002	137.00	137	Interbed	Yes		Yes
09/08-0002	138.00	138	Interbed	Yes		Yes
09/08-0002	139.10	139.1	Interbed	Yes		Yes
09/08-0002	140.00	140	Interbed	Yes		Yes
09/08-0002	141.00	141	Interbed	Yes		Yes
09/08-0002	147.80	147.8	Interbed	Yes		Yes
09/08-0002	149.50	149.5	Interbed	Yes		Yes
09/08-0002	151.20	151.2	Interbed	Yes		Yes
09/08-0002	152.55	152.55	Interbed	Yes		Yes
09/08-0002	153.85	153.85	Interbed	Yes		Yes
09/08-0002	154.65	154.65	Interbed	Yes		Yes
09/08-0002	156.00	156	Interbed	Yes		Yes
09/08-0002	157.00	157	Interbed	Yes		Yes
09/08-0002	158.00	158	Interbed	Yes		Yes
09/08-0002	159.20	159.2	Interbed	Yes		Yes
09/08-0002	160.00	160	Interbed	Yes		Yes
09/08-0002	161.00	161	Interbed	Yes		Yes
09/08-0002	162.00	162	Interbed	Yes		Yes

09/08-0002	167.85	167.85	Interbed	Yes		Yes
09/08-0002	168.10	168.1	Interbed	Yes		Yes
Ballycastle Quarry	-	bc1a	Interbed			Yes
Ballycastle Quarry	-	bc1b	Interbed			Yes
Ballycastle Quarry	-	bc1c	Interbed			Yes
Ballycastle Quarry	-	bc1d	Interbed			Yes
Ballycastle Quarry	-	bc1e	Interbed			Yes
Ballycastle Quarry	-	bcc1a	Interbed			Yes
Ballycastle Quarry	-	bcc1b	Interbed			Yes
Ballycastle Quarry	-	bcc1c	Interbed			Yes
Ballycastle Quarry	-	bcc2	Interbed			Yes
Ballycastle Quarry	-	bcc3	Interbed			Yes
Ballycastle Quarry	-	bcc4	Interbed			Yes
Ballycastle Quarry	-	bcc4b	Interbed			Yes
Ballycastle Quarry	-	bcb1	Basalt			
Ballycastle Quarry	-	bcb2	Basalt			
Ballycastle Quarry	-	bcb3	Basalt			
Ballymena Quarry	-	LAT021	Interbed			Yes

Ballymena Quarry	-	LAT022	Interbed			
Ballypalady Plant Bed	-	bp1	Volcanoclastics			Yes
Ballypalady Plant Bed	-	bp2	Volcanoclastics			Yes
Ballypalady Plant Bed	-	bp2b	Volcanoclastics			Yes
Ballypalady Plant Bed	-	bp3	Volcanoclastics			Yes
Ballypalady Plant Bed	-	bp4	Volcanoclastics			Yes
Binevenagh	-	LAT012	Interbed			Yes
Binevenagh	-	LAT013	Interbed			Yes
Cam Quarry	-	LAT014	Interbed			Yes
Cam Quarry	-	LAT015	Interbed			Yes
Carnduff no.2	157.68	157.68	CWF	Yes		Yes
Carnduff no.2	158.26	158.26	CWF	Yes		Yes
Carnduff no.2	159.00	159	CWF	Yes		Yes
Clinty Quarry	-	LAT005	Interbed			Yes
Clinty Quarry	-	LAT006	Interbed			
Clinty Quarry	-	LAT007	Interbed			Yes
Corkey Quarry	-	LAT008	Interbed			Yes
Corkey Quarry	-	cq1	Dolerite			Yes

Corkey Quarry	-	cq2	CWF			Yes
Corkey Quarry	-	cq3	CWF			Yes
Corkey Quarry	-	cq4	CWF			Yes
Corkey Quarry	-	cq5	CWF			Yes
Corkey Quarry	-	cq6	CWF			Yes
Corkey Quarry	-	cq7	Basalt			Yes
Corkey Quarry	-	cq8	Interbed			Yes
Corkey Quarry	-	cq9	Interbed			Yes
Craig's Quarry	-	LAT002	Interbed			Yes
Craig's Quarry	-	LAT003	Interbed			Yes
Craig's Quarry	-	LAT004	Interbed			Yes
Craigall Quarry	-	LAT017	Interbed			
Craigall Quarry	-	LAT018	Interbed			Yes
Craigall Quarry	-	LAT019	Interbed			Yes
Croaghan Quarry	-	LAT011	Interbed			Yes
Knocklaughrim Quarry	-	LAT020	Interbed			Yes
Macosquin Quarry	-	LAT016	Interbed			Yes
NIRE 02/08-0001	8.42	ABB001	Basalt	Yes	Yes	

NIRE 02/08-0001	13.46	ABB002	Basalt	Yes	Yes	
NIRE 02/08-0001	20.33	ABB003	Basalt	Yes	Yes	
NIRE 02/08-0001	29.11	ABB004	Basalt	Yes	Yes	
NIRE 02/08-0001	35.20	ABB005	Basalt	Yes	Yes	
NIRE 02/08-0001	46.76	ABB006	Basalt	Yes	Yes	
NIRE 02/08-0001	48.50	ABL003	lignite			Yes
NIRE 02/08-0001	76.59	ABB007	Basalt	Yes	Yes	
NIRE 02/08-0001	81.42	ABB008	Basalt	Yes	Yes	
NIRE 02/08-0001	91.17	ABB009	Basalt	Yes	Yes	
NIRE 02/08-0001	114.22	ABB010	Basalt	Yes	Yes	
NIRE 02/08-0001	126.29	ABB011	Basalt	Yes	Yes	
NIRE 02/08-0001	133.80	ABB012	Basalt	Yes	Yes	
NIRE 02/08-0001	164.11	ABB013	Basalt	Yes	Yes	
NIRE 02/08-0001	174.65	ABB014	Basalt	Yes	Yes	
NIRE 02/08-0001	192.18	ABB015	Basalt	Yes	Yes	
NIRE 02/08-0001	203.82	ABB016	Basalt	Yes	Yes	
NIRE 02/08-0001	206.81	ABB017	Basalt	Yes	Yes	
NIRE 02/08-0001	231.25	ABB018	Basalt	Yes	Yes	

NIRE 02/08-0001	250.52	ABB019	Basalt	Yes	Yes	
NIRE 02/08-0001	266.36	ABB020	Basalt	Yes	Yes	
NIRE 02/08-0001	278.33	ABB021	Basalt	Yes	Yes	
NIRE 02/08-0001	291.64	ABB022	Basalt	Yes	Yes	
NIRE 02/08-0001	312.69	ABB023	Basalt	Yes	Yes	
NIRE 02/08-0001	322.79	ABB024	Basalt	Yes	Yes	
NIRE 02/08-0001	327.83	ABB025	Basalt	Yes	Yes	
NIRE 02/08-0001	333.88	ABB026	Basalt	Yes	Yes	
NIRE 02/08-0001	348.38	ABB027	Basalt	Yes	Yes	
NIRE 02/08-0001	358.40	ABB028	Basalt	Yes	Yes	
NIRE 02/08-0001	368.23	ABB029	Basalt	Yes	Yes	
NIRE 02/08-0001	376.23	ABB030	Basalt	Yes	Yes	
NIRE 02/08-0001	377.10	ABC002	clay/tuff?			Yes
NIRE 02/08-0001	377.28	ABC003	clay			Yes
NIRE 02/08-0001	381.27	ABB031	Basalt	Yes	Yes	
NIRE 02/08-0001	394.35	ABB032	Basalt	Yes	Yes	
NIRE 02/08-0001	399.50	ABC004	palaeosol?			Yes
NIRE 02/08-0001	403.83	ABB033	Basalt	Yes	Yes	

NIRE 02/08-0001	404.80	ABC005	carbonaceous material			Yes
NIRE 02/08-0001	409.64	ABB034	Basalt	Yes	Yes	
NIRE 02/08-0001	416.76	ABB035	Basalt	Yes	Yes	
NIRE 02/08-0001	423.81	ABB036	Basalt	Yes	Yes	
NIRE 02/08-0001	424.05	ABC006	carbonaceous material			Yes
NIRE 02/08-0001	426.59	ABB037	Basalt	Yes	Yes	
NIRE 02/08-0001	432.64	ABB038	Basalt	Yes	Yes	
NIRE 02/08-0001	328.78	ABC007	soil/clay?			Yes
NIRE 02/08-0001	45.60	ABL001	lignite			Yes
NIRE 02/08-0001	49.90	ABL002	lignite			Yes
NIRE 02/08-0001	85.05	ABC001	clay/tuff?			Yes
NIRE 09/08-0001	18.05	ABB901	Basalt	Yes	Yes	
NIRE 09/08-0001	26.55	ABB902	Basalt	Yes	Yes	
NIRE 09/08-0001	41.55	ABB903	Basalt	Yes	Yes	
NIRE 09/08-0001	48.55	ABB904	Basalt	Yes	Yes	
NIRE 09/08-0001	54.15	ABB905	Basalt	Yes	Yes	
NIRE 09/08-0001	66.15	ABB906	Basalt	Yes	Yes	
NIRE 09/08-0001	75.55	ABB907	Basalt	Yes	Yes	

NIRE 09/08-0001	80.05	ABB908	Basalt	Yes	Yes	
NIRE 09/08-0001	88.45	ABB909	Basalt	Yes	Yes	
NIRE 09/08-0001	93.05	ABB910	Basalt	Yes	Yes	
NIRE 09/08-0001	99.15	ABB911	Basalt	Yes	Yes	
NIRE 09/08-0001	108.55	ABB912	Basalt	Yes	Yes	
NIRE 09/08-0001	115.70	ABB913	Basalt	Yes	Yes	
NIRE 09/08-0001	122.25	ABB914	Basalt	Yes	Yes	
NIRE 09/08-0001	124.25	ABB915	Basalt	Yes	Yes	
NIRE 09/08-0001	128.80	ABB916	Basalt	Yes	Yes	
NIRE 09/08-0001	132.50	ABC023	lignite?			Yes
NIRE 09/08-0001	133.10	ABC024	sediment/lignite?			Yes
NIRE 09/08-0001	133.35	ABC025	clay			Yes
NIRE 09/08-0001	133.70	ABC026	lignite?			Yes
NIRE 09/08-0001	134.10	ABC027	clay			Yes
NIRE 09/08-0001	134.90	ABC028	clay			Yes
NIRE 09/08-0001	137.70	ABC029	red laterite			Yes
NIRE 09/08-0001	140.25	ABB917	Basalt	Yes	Yes	
NIRE 09/08-0001	192.90	ABB918	Basalt	Yes	Yes	

NIRE 09/08-0001	198.35	ABB919	Basalt	Yes	Yes	
NIRE 09/08-0001	204.25	ABB920	Basalt	Yes	Yes	
NIRE 09/08-0001	207.75	ABB921	Basalt	Yes	Yes	
NIRE 09/08-0001	213.95	ABB922	Basalt	Yes	Yes	
NIRE 09/08-0001	217.60	ABB923	Basalt	Yes	Yes	
NIRE 09/08-0001	220.60	ABB924	Basalt	Yes	Yes	
NIRE 09/08-0001	226.45	ABB925	Basalt	Yes	Yes	
NIRE 09/08-0001	235.55	ABB926	Basalt	Yes	Yes	
NIRE 09/08-0001	243.00	ABB927	Basalt	Yes	Yes	
NIRE 09/08-0001	245.00	ABC012	Interbed			Yes
NIRE 09/08-0001	251.15	ABB928	Basalt	Yes	Yes	
NIRE 09/08-0001	253.90	ABC013	clay/ash			Yes
NIRE 09/08-0001	254.10	ABC014	organic material			Yes
NIRE 09/08-0001	254.50	ABC016	laterite/palaeosol			Yes
NIRE 09/08-0001	254.75	ABC017	palaeosol?			Yes
NIRE 09/08-0001	255.00	ABC018	palaeosol?			Yes
NIRE 09/08-0001	255.20	ABC019	Interbed			Yes
NIRE 09/08-0001	255.50	ABC020	Interbed			Yes

NIRE 09/08-0001	255.90	ABC021	palaeosol/basalt?			Yes
NIRE 09/08-0001	257.25	ABC022	palaeosol/basalt?			Yes
NIRE 09/08-0001	257.45	ABB929	Basalt	Yes	Yes	
NIRE 09/08-0001	103.01	ABC010	clay vein			Yes
NIRE 09/08-0001	144.62	ABC011	clay horizon?			Yes
NIRE 09/08-0001	254.30	ABC015	laterite/palaeosol			Yes
NIRE 09/08-0001	9.83	ABC008	clay/tuff?			Yes
Ross's (Ballycastle) Quarry	-	LAT009	Interbed			Yes
Ross's (Ballycastle) Quarry	-	LAT010	Interbed			Yes
Upton Park No. 1	21.06	69' 1	Rhyolitic tuff	Yes		
Upton Park No. 1	21.08	69' 2	Rhyolitic tuff	Yes		
Whitemountain Quarry	-	LAT001	Interbed			Yes

APPENDIX I

Proxy weathering data

Borehole ID	Total estimated weathering time (years)	Time in Lower Basalt Formation	Time in Interbasaltic Formation	Time in Upper Basalt Formation	Flow count	Eruption cycle (yr-1)
NIRE 01 08 0002	881,000				37	23,811
NIRE 01 08 0003	150,500				6	25,083
NIRE 01 08 0005	839,250				34	24,684
NIRE 01 08 0006	503,500				36	13,986
NIRE 01 08 0009	158,250				5	31,650
NIRE 02 08 0001	2,239,250	1,540,750	537,000	161,500	64	34,988
NIRE 03 08 0001	2,752,500	972,000	1,656,500	156,000	67	41,082
NIRE 03 08 0002	562,250				29	19,388
NIRE 03 08 0003	554,500				49	11,316
NIRE 03 08 0004	351,000				25	14,040
NIRE 04 08 0001	727,000				20	36,350
NIRE 04 08 0002	134,000				6	22,333
NIRE 05 08 0002	502,750				17	29,574
NIRE 08 08 0001	494,750				25	19,790
NIRE 08 08 0002	237,250				13	18,250
NIRE 09 08 0001	1,752,000	631,500	437,500	683,000	79	22,177
NIRE 09 08 0002	2,667,500	596,750	1,519,500	551,250	84	31,756
NIRE 11 08 0001	691,000				51	13,549
				Minimum	*5*	*11,316*
	ALG maximum timespan	3,880,250		**Average**	**36**	**24,100**
				Maximum	*84*	*41,082*

APPENDIX J

Lonmin Borehole Summary Information

Borehole ID	Easting	Northing	Borehole elevation (mASL)	Drilling company	Lead Driller	Drilling Rig	Final depth (mbgl)	Depth to bedrock (mbgl)	Drilling Start	Drilling End	Logged by	Date Logged
01/08-0001	306212	417691	95.80	EM Drilling Ltd (UK)	Nathan Jones	Beretta T51- Track Mounted	162.30	17.00	09/12/2010	14/12/2010	Kieran Parker	22/03/2013
01/08-0002	302489	419822	90.70	Priority Drilling (Ireland)	Nebojsa Djokic	Atlas Copco CS14- Wheel Mounted	850.00	12.00	03/06/2011	20/07/2011	Tom Evans	31/03/2013
01/08-0003	309689	421897	?	Priority Drilling (Ireland)	?	Atlas Copco CS14- Wheel Mounted	769.62	8.95	?	?	Jonathan O'Callaghan	09/07/2013
01/08-0005	308528	416359	122.20	Priority Drilling (Ireland)	Nebojsa Djokic	Atlas Copco CS14- Wheel Mounted	752.00	3.16	14/11/2011	20/12/2011	Joan Darcy	26/09/2012
01/08-0006	309473	416438	182.80	Priority Drilling (Ireland)	Nebojsa Djokic	Atlas Copco CS14- Wheel Mounted	716.00	6.00	18/08/2011	27/09/2011	Jonathan O'Callaghan	31/03/2013
01/08-0009	309509	422616	?	Meehan Drilling	?	?	42.00	8.87	?	?	Kieran Parker	10/09/2013
02/08-0001	316129	412540	259.90	Priority Drilling (Ireland)	Nebojsa Djokic	Atlas Copco CS14- Wheel Mounted	437.00	5.80	04/05/2012	16/05/2012	Joan Darcy	23/11/2012
03/08-0001	326391	406143	218.30	Priority Drilling (Ireland)	Nebojsa Djokic	Atlas Copco CS14- Wheel Mounted	416.00	9.20	18/04/2012	01/05/2012	Joan Darcy	04/07/2012
03/08-0002	333053	414144	200.80	Priority Drilling (Ireland)	Nebojsa Djokic	Atlas Copco CS14- Wheel Mounted	96.15	6.00	19/07/2012	23/07/2012	Jonathan O'Callaghan	19/10/2012
03/08-0003	332828	414530	191.40	Priority Drilling (Ireland)	Nebojsa Djokic	Atlas Copco CS14- Wheel Mounted	117.10	6.20	25/07/2012	28/07/2012	Jonathan O'Callaghan	23/10/2012
03/08-0004	332255	414987	142.90	Priority Drilling (Ireland)	Nebojsa Djokic	Atlas Copco CS14- Wheel Mounted	126.40	6.20	01/08/2012	06/08/2012	Jonathan O'Callaghan	29/10/2012
04/08-0001	277233	415430	?	EM Drilling Ltd (UK)	Nathan Jones	Beretta T51- Track Mounted	201.00	3.50	?	?	Kieran Parker	07/02/2012
04/08-0002	277179	415701	?	Priority Drilling (Ireland)	Ondrej Krupicka	Atlas Copco CS14- Wheel Mounted	421.80	1.65	?	?	Kieran Parker	29/07/2013
05/08-0002	278240	430729	?	Priority Drilling (Ireland)	Ondrej Krupicka	Atlas Copco CS14	424.50	3.70	?	?	Jonathan O'Callaghan	22/05/2013
08/08-0001	296903	417587	116.00	Priority Drilling (Ireland)	Ondrej Krupicka	Atlas Copco CS14- Track Mounted	854.50	6.41	19/04/2013	04/06/2013	Kieran Parker	29/04/2013
08/08-0002	295284	417562	58.50	Priority Drilling (Ireland)	Ondrej Krupicka	Atlas Copco CS14- Track Mounted	528.15	14.94	07/06/2013	11/07/2013	Jonathan O'Callaghan	30/09/2013
09/08-0001	294362	434582	47.70	EM Drilling Ltd (UK)	Nathan Jones	Beretta T51- Track Mounted	698.00	3.10	05/08/2010	21/08/2010	Jonathan O'Callaghan	10/12/2012
09/08-0002	290853	434532	78.20	EM Drilling Ltd (UK)	Nathan Jones	Beretta T51- Track Mounted	252.00	8.12	31/08/2010	23/09/2010	Kieran Parker	19/02/2013
11/08-0001	287917	413754	79.00	Priority Drilling (Ireland)	Nebojsa Djokic	Atlas Copco CS14- Wheel Mounted	520.00	6.00	21/03/2012	13/04/2012	Jonathan O'Callaghan	14/11/2012

APPENDIX K

Wilkinson age data tables

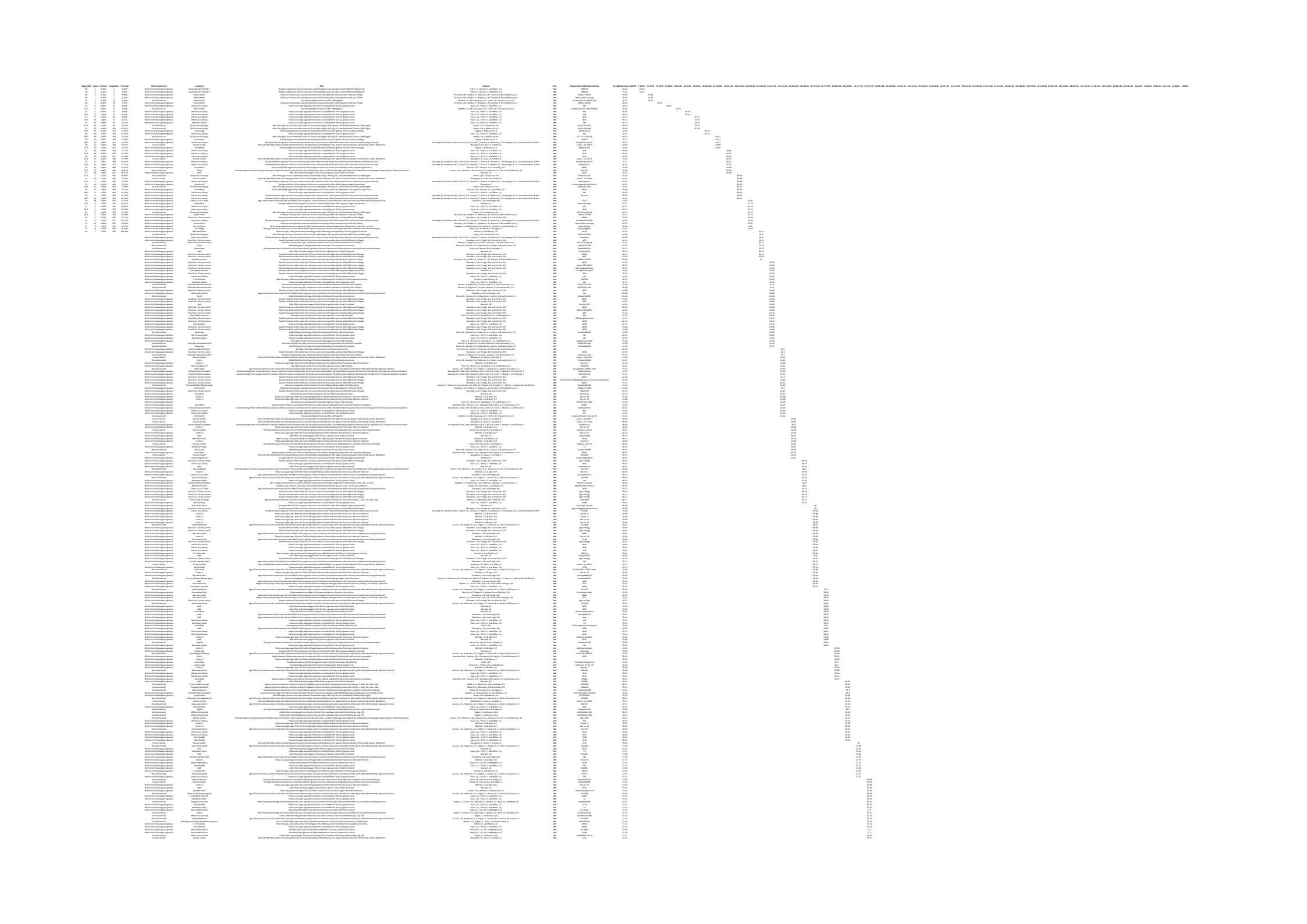

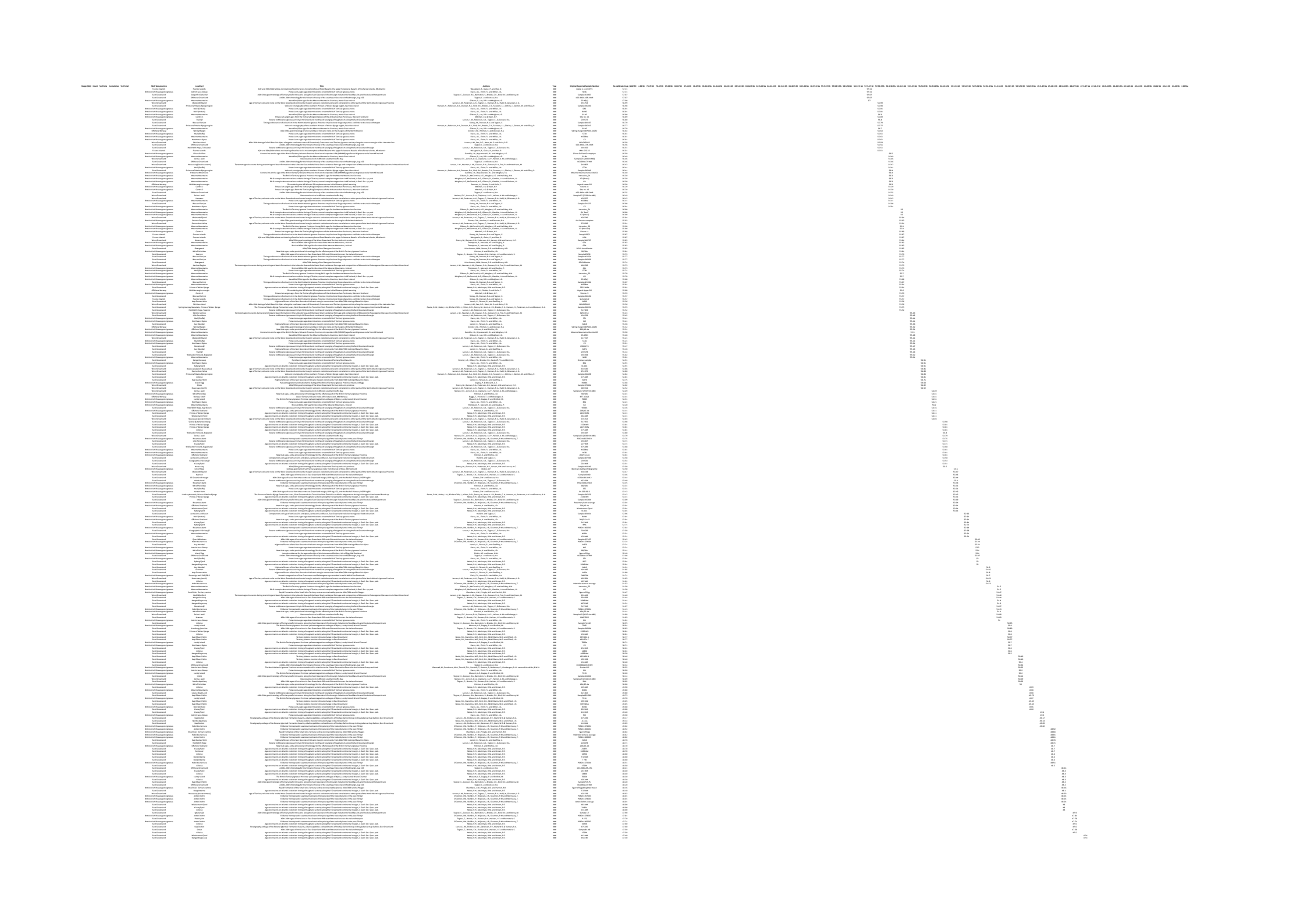

APPENDIX L

NIRE borehole logs (Lonmin)